AD_____

Award Number: DAMD17-99-1-9149

TITLE: The Role of Molybdenum Hydroxylase Generated Free Radicals in Alcohol Induced Breast Cancer

PRINCIPAL INVESTIGATOR: Richard M. Wright, Ph.D.
James L. McManaman, Ph.D.

CONTRACTING ORGANIZATION: University of Colorado Health Sciences Center
Denver, Colorado 80045-0508

REPORT DATE: September 2002

TYPE OF REPORT: Final

PREPARED FOR: U.S. Army Medical Research and Materiel Command
Fort Detrick, Maryland 21702-5012

REPORT DOCUMENTATION PAGE

Form Approved
OMB No. 074-0188

1. AGENCY USE ONLY (Leave blank)	2. REPORT DATE	3. REPORT TYPE AND DATES COVERED
	September 2002	Final (1 Sep 99 - 31 Aug 02)

4. TITLE AND SUBTITLE
The Role of Molybdenum Hydroxylase Generated Free Radicals in Alcohol Induced Breast Cancer

5. FUNDING NUMBERS
DAMD17-99-1-9149

6. AUTHOR(S)
Richard M. Wright, Ph.D.
James L. McManaman, Ph.D.

7. PERFORMING ORGANIZATION NAME(S) AND ADDRESS(ES)
University of Colorado Health Sciences Center
Denver, Colorado 80045-0508

E-Mail: richard.m.wright@uchsc.edu

8. PERFORMING ORGANIZATION REPORT NUMBER

9. SPONSORING / MONITORING AGENCY NAME(S) AND ADDRESS(ES)
U.S. Army Medical Research and Materiel Command
Fort Detrick, Maryland 21702-5012

10. SPONSORING / MONITORING AGENCY REPORT NUMBER

11. SUPPLEMENTARY NOTES
Original contains color plates. All DTIC reproductions will be in black and white.

12a. DISTRIBUTION / AVAILABILITY STATEMENT
Approved for Public Release; Distribution Unlimited

12b. DISTRIBUTION CODE

13. ABSTRACT ***(Maximum 200 Words)***

Alcohol consumption by women is an important risk factor for breast cancer (BC) found to promote BC through reactive oxygen species (ROS) induced carcinogenesis. Our experiments revealed that alcohol dehydrogenase (ADH), aldehyde oxidase (AOX), and xanthine oxidoreductase (XOR) are expressed and regulated in breast tissues. Mammary gland XOR and AOX were efficient sources of ROS using the products of alcohol breakdown. The human gene for XOR was activated in mammary glands and mammary epithelial cells by cytokines and hormones known to mediate mammary gland development, and activation was accompanied ROS generation. XOR was found to be an inducible source of ROS in mammary epithelial cells. Conversion of XOR from D-form to O-form is necessary for the formation of ROS by XOR, and we discovered an important structural determinant of the conversion. The human AOX gene was also expressed in mammary epithelial cells and its gene was activated by transcription factors known promote alcohol metabolism. The potential for AOX and XOR to generate ROS in the mammary gland and ultimately to promote BC was strengthened by the observation that both genes are activated in mammary glands and in mammary epithelial cells to produce ROS from the products of alcohol breakdown.

14. SUBJECT TERMS
breast cancer, oxygen radicals, xanthine oxidase, aldehyde oxidase, DNA damage, carcinogenesis, alcohol consumption

15. NUMBER OF PAGES
80

16. PRICE CODE

17. SECURITY CLASSIFICATION OF REPORT	18. SECURITY CLASSIFICATION OF THIS PAGE	19. SECURITY CLASSIFICATION OF ABSTRACT	20. LIMITATION OF ABSTRACT
Unclassified	Unclassified	Unclassified	Unlimited

Table of Contents

INTRODUCTION

Alcohol consumption by women is one of several important risk factors for breast cancer (BC) that may promote BC through reactive oxygen species (ROS) induced carcinogenesis. Alcohol metabolism is known to produce ROS, and epithelial carcinoma of the breast is associated with high levels of hydroxyl radical (.OH) modified DNA, point mutations, single strand nicks, and chromosome rearrangement. Furthermore, ROS modification of DNA can produce the mutations and DNA damage found in many types of BC. ROS damage to breast DNA can be potentiated by accumulating iron and in conjunction with the diminished antioxidant defenses in breast tissue with advancing age thereby exacerbate the risk for ROS induced breast cancer. Our preliminary studies revealed that alcohol dehydrogenase (ADH), aldehyde oxidase (AOX), and xanthine oxidoreductase (XOR) are expressed and regulated in breast tissues. Mammary gland XOR and AOX were efficient sources of the ROS, hydrogen peroxide and superoxide anion. Furthermore, XOR and AOX were found to generate ROS in two ways from alcohol metabolism: by a*cetaldehyde* consumption and by an *intrinsic NADH oxidase* activity of XOR and AOX. We proposed that: (1) expression of ADH, XOR and/or AOX in breast tissue provides the enzymes that generate ROS; (2) metabolism of alcohol produces acetaldehyde and NADH which can both be substrates for XOR and/or AOX and thereby result in ROS formation; and (3) ROS generated by XOR or AOX can induce the carcinogenic mutations and DNA damage found in breast cancer. The presence of elevated iron and diminished antioxidant status in breast tissue with greater age have provided additional support for the role of ROS in breast carcinogenesis.

BODY

Our Original Technical Objectives Were The Following:

To characterize ROS production by XOR and AOX purified from mouse mammary glands.

Much of our effort over the period of this grant was devoted to characterizing the ROS generating enzymes XOR and AOX from rat and mouse mammary glands, and this has resulted in numerous publications (References 29,32,33,35,37). This enzymology component has focused largely on XOR which was purified and characterized in the mammary gland. Nonetheless, both enzymes will utilize acetaldehyde as an efficient substrate for ROS formation. In addition, expression and regulation of XOR in mammary gland has been analyzed. Importantly, we have observed that XOR in the mammary gland is subject to regulation by lactogenic hormones and several cytokines and growth factors. Regulation of XOR expression was recently published (33,35). Characterization of mammary gland AOX was complicated by the observation that *AOX is encoded by a multi-gene family (AOX1-4) that exhibits marked tissue specific expression.* This work will be presented in review form in 2003 with support from this grant noted. Characterization of the AOX1 gene expression and regulation progressed significantly throughout the period of support of this grant. Importantly, AOX1 is evidently the dominant AOX expressed in mammary tissue. Furthermore, we discovered that in humans most AOX genes have been reduced by sequence drift to become pseudogenes. While this may simplify some aspects of this analysis, it also suggests that rodent models of human disease may significantly differ from "real" human disease. As described below expression analysis of AOX and XOR has suggested that each enzyme may be uniquely regulated in the mammary gland and therefore responsible for ROS generation at different times and under different circumstances.

To determine the contribution of XOR and AOX to the damage and modification of DNA, specific proteins, and lipids in cultured mouse mammary epithelial cells and in whole mouse mammary glands.

We began the studies directed at ROS mediated damage to mammary cells by first measuring ROS generation after activation of cells in culture. These experiments derived from those initiated in the last specific aim because they reflected the activation of XOR by additional mechanisms. We have measured the ROS sensitive fluorescence indicator dichlorofluorescene-diacetate (DCFH) in epithelial cells following activation by several cytokines thought to activate XOR or AOX. Presently, we find IL-1 inducible DCFH fluorescence can be inhibited in epithelial cells by allopurinol, an inhibitor of XOR. Thus XOR dependent ROS generation can be induced in epithelial cells by IL-1. This will have significant impact on the course of our experiments because the mammary gland and mammary epithelial cells are highly responsive to IL-1, and these data suggest that one consequence of this sensitivity is the generation of potentially cytotoxic ROS.

A vital aspect of the work supported by this grant concerned the conversion of XOR from D-form to O-form. XOR is synthesized as a dehydrogenase (XD) that is a poor source of ROS inasmuch as its reducing substrate is NAD+. It can be converted into O-form by several mechanisms and in this form will utilize molecular oxygen as a reducing substrate to generate ROS. We were concerned with several aspects of the conversion process. One of these concerned the structural mechanisms of conversion and this was recently published (37,38). We were also concerned with the biological basis of conversion in general, and have discovered that some cytokine combinations will both activate XOR expression and convert the enzyme in vivo to nearly 100% O-form. This data are in preparation for publication at the present moment (39). Importantly, they suggest a link to inflammation as a process that can both activate XOR expression and promote conversion to O-form.

Alcohol metabolism is anticipated to modulate gene expression in epithelial cells and possibly expression of those genes important for alcohol breakdown and ROS generation. Accordingly, we have initiated analyses of the promoter regions for human, mouse, and rat XOR and human AOX1. Promoters for each of these genes have been cloned and fused to reporter genes and used to transfect epithelial cells in tissue culture. Presently these studies indicate that XOR is subject to very complex regulation in epithelial cells. Transcription can be induced from promoter fusions by (a) lactogenic hormones, (b) IL-1, (c) IL-6, and (d) hypoxic growth. AOX is also subject to complex transcriptional activation. Its basal promoter is activated by Sp1/Sp3 transcription factors and the gene is sensitive to activation by several cytokines and growth factors. Importantly, in the mammary epithelium, AOX can be transcriptionally activated by TGF-beta and EGF, two growth factors with great significance to development in the mammary gland. Furthermore, regulation in the mammary gland is opposite to that occurring in lung epithelium. However, these studies do confirm induction of AOX and XOR gene expression in the mammary epithelium by cytokine and growth factors known to have important affects on the mammary gland, known to be affected by alcohol metabolism, and known to be primary cytokines mediating tissue inflammation. *These observations suggest a possible link to inflammation as a mechanism for marked elevation in ROS production in the mammary gland.*

To determine whether the metabolism of alcohol contributes to DNA and protein damage and modification resulting from the action of XOR and AOX.

Two pertinent aspects of this work have been the major foci of our efforts. First, it has become clear that the biological dynamics of XOR in the mammary gland are intimately involved with its capacity to convert from D-form to O-form and as a result considerable research effort has been invested in analysis of some of these basic regulatory processes. In particular, the dynamic relocalization of XOR to the plasma membrane following hormone stimulation has been described in detail and prepared for publication as the following manuscript (38).

The second area of focus has revolved around analysis of expression of rat and human XOR in mammary epithelial cells. Our present data reveal that XOR gene expression is highly regulated by several cytokines that clearly identify XOR as an acute phase gene. In particular, cytokine combinations that are most frequently associated with tissue inflammation were found to be potent and synergistic activators of XOR gene expression in mammary epithelial cells. Furthermore, the same cytokine combinations found to activate XOR gene expression were found to potentiate conversion from D-form to O-form as well. Importantly, little evidence could be garnered for activation of XOR gene expression by the products of alcohol metabolism. *While the enzymes can use these products as substrates for ROS production, the genes will be activated by indirect mechanisms, possibly reflecting the dynamic shifts in cytokine production induced by alcohol metabolism.* As a result, studies have been initiated to determine the role of inflammation itself in breast cancer and the possible potentiation of ROS production during alcohol metabolism by inflammation and inflammatory mediators.

KEY RESEARCH ACCOMPLISHMENTS

- We have purified XOR and AOX from mammary gland tissue in rats and mice and have extensively characterized XOR by enzymological criteria resulting in numerous publications.
- We have detected ROS generation by XOR in epithelial cells using cytokine induced DCFH fluorescence.
- We have analyzed the structural and biological determinants of conversion of D-form XOR to O-form XOR resulting in key publications.
- We have identified mouse and human mammary epithelial cells that express the ROS generators XOR and AOX in cell culture (HC-11 and HB-4a.) where expression of these enzymes has been analyzed extensively.
- We have cloned, sequenced, and characterized promoter domains for human, mouse, and rat XOR and human AOX and have analyzed mechanisms of transcriptional regulation in mammary epithelial cells. Importantly, these data reveal activation of these genes by cytokine mediators of inflammation suggesting a potentially vital link between BC and inflammation.

REPORTABLE OUTCOMES

1. Mammary gland and mammary epithelial cells in culture express genes responsible for ROS generation. Importantly, genes for both XOR and AOX were found to be activated in mammary glands and mammary epithelial cells.

2. The human XOR gene, encoding the ROS generating enzyme xanthine oxidoreductase, is activated in mammary epithelial cells by cytokines and hormones known to have significant affects in mammary gland development. Activation by cytokines was accompanied ROS generation that could be inhibited by XOR specific inhibitors. Thus, XOR has been found to be an inducible source of ROS in epithelial cells.

3. The human AOX gene, encoding an enzyme highly related to XOR and capable of significant ROS generation was also found to be expressed in mammary epithelial cells. Furthermore, its gene was found to be activated by a group of transcription factors, the Sp family, known to be important for mammary gland development and to be of particular significance for alcohol metabolism.

4. Analysis of genes and mechanisms of gene expression for human, mouse, and rat XOR and human AOX have revealed activation of these genes by cytokine mediators of inflammation suggesting a potentially vital link between BC and inflammation.

CONCLUSIONS

The potential for AOX and XOR to contribute to ROS generation in the mammary gland and ultimately to BC has been strengthened by the work supported by this grant. Both genes are activated in mammary glands and in mammary epithelial cells. Both enzymes can utilize the products of alcohol metabolism to generate hydrogen peroxide and superoxide radical. Activation of each gene is distinct, therefore it is likely that they contribute to ROS generation at different times and following different stimulation. In the mammary gland XOR is regulated by lactogenic hormones and inflammatory cytokines suggesting a potential link to mammary gland inflammation. Furthermore, structural and biological mechanisms for conversion of XOR from D-form to O-form have been described that underlie the capacity of XOR to promote ROS formation. Thus, the argument that that either AOX or XOR may contribute to ROS generation in the mammary gland during alcohol metabolism has been strengthened and a potentially vital link between ROS generation and mammary gland inflammation has been identified as well.

REFERENCES PUBLISHED AS A DIRECT RESULT OF SUPPORT FROM THIS GRANT

29. **Wright, R.M.,** McManaman, J.L., and Repine,J.R.: Alcohol induced breast cancer - a proposed mechanism. **Free Radical Biology & Medicine 26: 348-354, 1999.**

30. **Wright, R.M.,** Clayton, D.A., Riley, M.G., McManaman, J.L., and Repine, J.E. cDNA cloning, sequencing, and characterization of male and female rat aldehyde oxidase (rAOX1). Differences in redox status may distinguish male and female forms of AOX. **J. Biol. Chem. 274:2888-2998, 1999.**

31. Faust-Chan, L-R., Hybertson, B., Flores, S., **Wright, R.M.,** and Repine J.R.: Initiation and tolerance to acute lung injury. A Tin-Yang mechanism involving interleukin-1. **Chest 116:102S-103S, 1999.**

32. McManaman, J.L., Neville, M.C., and **Wright, R.M**. Mouse mammary gland xanthine oxidoreductase: purification, characterization, and regulation. **Arch. Biochem. Biophys. 371: 308-316, 1999.**

33. McManaman, J.L., Hanson, L., Neville, M.E., and **Wright, R.M**.: Lactogenic hormones regulate xanthine oxidoreductase and beta casein levels in mammary epithelial cells by distinct mechanisms. **Arch. Biochem. Biophys. 373: 318-327, 2000.**

34. **Wright, R.M.,** Riley, M.G., Weigel, L.G., Ginger, L.A., Costantino, D.A., and MacManaman, J.L. Activation of the human aldehyde oxidase (hAOX1) promoter by tandem, cooperative Sp1/Sp3 binding sites. **DNA and Cell Biology 19: 459-474, 2000.**

35. McManaman, J.L., Palmer, C., and **Wright, R.M.** Secretory differentiation regulates expression and cellular localization of xanthine oxidoreductase in mammary glands. **(Accepted August, 2002).**

36. **Wright, R.M.,** Ginger, L.A., McManaman, J.L., and Repine, J.E.: Characterization of a second locus for aldehyde oxidase (AOX) in humans: AOX gene duplication at chromosome 2q32.3-2q33.1 **(In preparation, 9/2002**).

37. McManaman, J.L. and Bain, D.L. Structural and conformational analysis of the oxidase to dehydrogenase conversion of xanthine oxidoreductase. **J. Biol. Chem. 277: 21261-21268, 2002.**

38. Wu CC, Howell KE, Neville MC, Yates JR 3rd, McManaman JL. Proteomics reveal a link between the endoplasmic reticulum and lipid secretory mechanisms in mammary epithelial cells. **Electrophoresis 21:3470-82, 2000.**

39. **Wright, R.M.**, Ginger,L.A., Kosila, N., Elkins, N.N., McManaman, J.L., and Repine, J.E. Xanthine oxidoreductase (XOR) is induced *in vivo* in differentiating alveolar macrophages by interleukin-1 and interferon-γ which promote lung epithelial cell apoptosis by XOR dependent mechanisms. **(Submitted September, 2002).**

Free Radical Biology & Medicine, Vol. 26, Nos. 3/4, pp. 348–354, 1999

0891-5849/99/$–see front matter

ELSEVIER

PII S0891-5849(98)00204-4

Original Contribution

ALCOHOL-INDUCED BREAST CANCER: A PROPOSED MECHANISM

RICHARD M. WRIGHT, JAMES L. MCMANAMAN, and JOHN E. REPINE

*Webb–Waring Antioxidant Research Institute and University of Colorado Health Sciences Center, 4200 East 9th Avenue, Denver, CO, USA

(*Received* 1 *May* 1998; *Revised* 21 *July* 1998; *Accepted* 21 *July* 1998)

Abstract—Alcohol consumption increases the risk for breast cancer in women by still undefined means. Alcohol metabolism is known to produce reactive oxygen species (ROS), and breast cancer is associated with high levels of hydroxyl radical (•OH) modified DNA, point mutations, single strand nicks, and chromosome rearrangement. Furthermore, ROS modification of DNA can produce the mutations and DNA damage found in breast cancer. Alcohol dehydrogenase (ADH) and xanthine oxidoreductase (XOR) are expressed and regulated in breast tissues and aldehyde oxidase (AOX) may be present as well. Mammary gland XOR is an efficient source of ROS. Recently, hepatic XOR and AOX were found to generate ROS in two ways from alcohol metabolism: by a*cetaldehyde* consumption and by the *intrinsic NADH oxidase* activity of both XOR and AOX. The data obtained suggests that: (1) expression of ADH and XOR or AOX in breast tissue provides the enzymes that generate ROS; (2) metabolism of alcohol produces acetaldehyde and NADH that can both be substrates for XOR or AOX and thereby result in ROS formation; and (3) ROS generated by XOR or AOX can induce the carcinogenic mutations and DNA damage found in breast cancer. Accumulation of iron coupled with diminished antioxidant defenses in breast tissue with advancing age provide additional support for this hypothesis because both result in elevated ROS damage that may exacerbate the risk for ROS-induced breast cancer. © 1998 Elsevier Science Inc.

Keywords—Free radical, Xanthine oxidase, Aldehyde oxidase, DNA damage, Breast cancer, Carcinogenesis, Alcohol consumption

INTRODUCTION

Although alcohol consumption has been recognized to increase the incidence of breast cancer in women, no underlying biochemical mechanism has been proposed. We hypothesize herein that reactive oxygen species (ROS) generated from the combined action of alcohol dehydrogenase (ADH) and xanthine oxidoreductase (XOR) mediate alcohol-induced damage to DNA contributing to carcinogenesis and breast cancer.

Alcohol consumption increases the risk for breast cancer

Breast cancer is the result of a complex, multi-stage process [1] in that hereditary susceptibility [2,3], age [3], estrogen metabolism [4–6], tobacco smoke [7] and alcohol consumption constitute recognized risk factors. Recent studies confirm the significant association between alcohol consumption and breast cancer. Analysis of 322,467 women, including 4,335 cases of invasive breast cancer evaluated for up to 11 years, revealed a 41% increase in the incidence of breast cancer by alcohol consumption, and this association was dose dependent up to a dose of 30–60 g alcohol/day [8]. This observation is consistent with several previous studies that revealed an increased risk for breast cancer by alcohol consumption ranging from 20–89% [9–15].

Alcohol metabolism produces ROS

Ethanol can be converted to acetate by a simple, two step reaction involving the combined activities of ADH, that produces acetaldehyde, and the molybdenum hydroxylase enzymes, XOR and/or aldehyde oxidase (AOX), that produce acetate from acetaldehyde. Both

Address correspondence to: R. M. Wright, University of Colorado Health Sciences Center, 4200 East 9th Avenue, Campus Box C-322, Denver, CO 80262, USA; Tel: 303-315-4593; Fax: 303-315-3776; E-Mail: richard.m.wright@uchsc.edu.

XOR and AOX can generate ROS. Although acetaldehyde also can be metabolized by aldehyde dehydrogenase (ALDH) to produce acetate, this reaction does not form ROS. In the following discussion, we have used the term "reactive oxygen species" to denote three partial reduction products of oxygen: the superoxide anion ($O_2^{\bullet -}$), hydroxyl radical ($^{\bullet}OH$), and hydrogen peroxide (H_2O_2). Metabolism of alcohol has been recognized to produce ROS during acute alcohol toxicity of the liver that has been directly associated with increased ROS damage to DNA leading to DNA modification and strand breakage [16]. Importantly, considerable evidence has been marshaled to indicate that oxidative injury resulting from alcohol toxicity of the liver and pancreas is mediated by ROS generated from the combined activity of XOR and AOX [16–19]. We suggest that a similar process may contribute to the development of breast cancer.

Breast cancer is associated with high levels of $^{\bullet}OH$ modified DNA

DNA from invasive ductal carcinoma of the breast contains extensive $^{\bullet}OH$ modifications that include $^{\bullet}OH$ adducts of adenine, guanine, cytosine, as well as single and double strand breaks [20–22]. $^{\bullet}OH$ modification in breast cancer DNA was elevated between 8 and 17 fold over normal tissue DNA [20] and as many as one base lesion in 46 normal bases has been reported [21]. Furthermore, $^{\bullet}OH$ is of paramount concern for breast carcinogenesis because $^{\bullet}OH$, but not $O_2^{\bullet -}$ or H_2O_2 [23] can modify DNA to produce several $^{\bullet}OH$ adduction products, base deletions, single strand and double strand breaks [20–27]. Importantly, $^{\bullet}OH$ modified DNA has been directly linked to the progression of human breast cancer and provides excellent prognostic information on the progression of breast cancer [22].

Considerable evidence supports a role for alcohol metabolism in carcinogenesis that invokes direct toxicity of acetaldehyde [28–36]. However, acetaldehyde toxicity alone fails to account for the spectrum of DNA alterations found in breast cancer, and in particular, fails to account for the generation of transition and transversion mutations, single and double strand breaks, and $^{\bullet}OH$ modified DNA. We propose that the presence of a highly efficient enzyme system that can further metabolize acetaldehyde may significantly elevate the risk for ROS damage in breast tissues, and these data would be consistent with a reduction in the incidence of breast cancer by diets enriched in antioxidants [37–39].

THE XOR HYPOTHESIS

Our hypothesis is shown schematically in Fig. 1. We propose that: (1) expression of ADH and XOR in breast tissue provides enzymes that generate ROS; (2) metabolism of alcohol produces acetaldehyde and NADH that can both be substrates for XOR and thereby result in ROS formation; and (3) ROS generated by XOR can induce the carcinogenic mutations and DNA damage found in breast cancer tissue. The following discussion provides evidence for each of these points. Furthermore, the role of elevated iron and diminished breast antioxidant status with greater age provide additional support for this hypothesis.

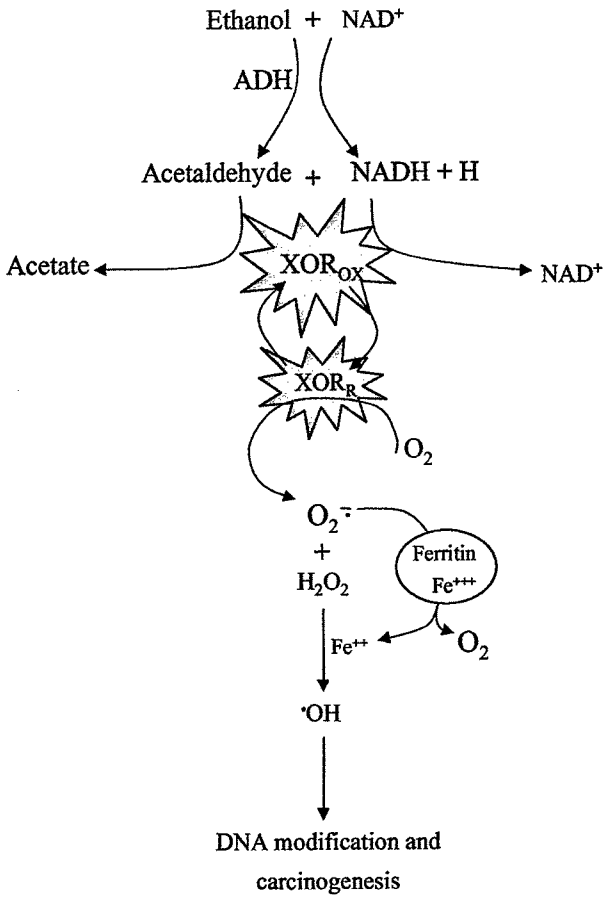

Fig. 1. The XOR hypothesis. The action of ADH on ethanol in the breast produces acetaldehyde and NADH both of which can be substrates for XOR. Reduction of XOR by either acetaldehyde or NADH results in ROS formation when XOR is subsequently oxidized by molecular oxygen. The resulting superoxide anion and hydrogen peroxide can participate in Fenton chemistry yielding hydroxyl radical, the primary ROS that produces DNA damage and mutation.

ADH and XOR are expressed in breast tissues

An explicit condition of the present hypothesis is that ADH and XOR or AOX must be present in breast tissues in sufficient abundance to promote ROS formation from alcohol. ADH is expressed in breast tissue. Although most abundant in the liver, ADH activity has been mea-

sured in normal human breast specimens where it was found to yield 23.8 (SD ± 1.6) IU/gram of tissue. ADH levels were not markedly altered by carcinoma when compared to adjacent normal tissue [40].

XOR is also expressed in breast tissue. XOR is derived from the breast by native secretory processes [41] and is routinely prepared from bovine or human milk where it constitutes a large proportion of the total protein mass [42,43]. XOR has been localized by immunohistochemical methods to secretory epithelial cells of the bovine mammary gland [44,45]. Human and mouse mammary epithelial cells in tissue culture also express XOR protein and XOR activity [46–48]. When induced by lactation, XOR comprises between 1–2% of the total mammary gland protein mass [47]. Furthermore, significant levels of XOR are expressed in the non-lactating mammary tissue [47]. Thus, XOR has the potential to comprise a substantial proportion of total breast protein. Although the presence of XOR in breast tissue is also unambiguous, we have been unable to detect substantial levels of AOX activity, protein, or gene expression in mouse mammary glands [49]. Thus, although either XOR or AOX could contribute to ROS burden in the human breast, XOR may be the more important enzyme.

Alcohol consumption may induce both ADH and XOR genes by a common mechanism. ADHs comprise a complex class of genes, ADH1-ADH6, that fall into three enzymatic classes. Class I ADHs, ADH1-ADH3, are most pertinent to alcohol metabolism [50]. Class I ADH genes can be induced at the level of transcription by chronic alcohol administration [51]. Genes encoding XOR are induced 40–80 fold by pregnancy and lactation [47,48]. Regulation of XOR expression may be controlled by STAT factors 3 and 5 that appear to mediate mammary gland development [52,53], and potential STAT factor binding sites can be found in XOR promoters. However, further analysis of XOR promoter sequences also suggests the potential for coordinate regulation with ADH. Transcription factors mediating class I ADH activation include C/EBP, USF, Sp1, NF1, and HNF [50]. Strikingly, promoter sequences for human, rat, and mouse XOR genes also contain recognition sites for C/EBP, USF, Sp1, and HNF [54–57]. These findings support the intriguing possibility that ADH and XOR genes may share some common modes of induction that are possibly related to alcohol consumption.

XOR can generate ROS in two ways from alcohol metabolism

Recent biomedical interest in the molybdenum hydroxylase enzymes has revolved around their capacity to generate ROS that have been linked to numerous human diseases [58–60]. Alcohol dependent ROS generation by breast XOR could proceed by two independent mechanisms: metabolism of acetaldehyde and NADH. Thus, it may be of considerable significance that the action of ADH on alcohol stoichiometrically produces NADH. The mechanism of ROS generation by XOR and AOX is now well understood [61,62]. H_2O_2 and $O_2^{\bullet -}$ are generated directly from substrate reduced enzymes when diatomic oxygen acquires reducing equivalents from a reduced flavin site. Rapid, two electron reduction produces H_2O_2, although kinetically slower univalent reduction produces $O_2^{\bullet -}$ [61,62]. $^{\bullet}OH$ is not a direct product of enzyme catalysis [23,63], however it can be produced secondarily in the Haber-Weiss reaction by interaction with iron or copper in vitro or in vivo [24,64].

Acetaldehyde metabolism. XOR can undergo conversion from an NAD^+ dependent "D-form" to an oxygen dependent "O-form." Conversion appears to be a tightly regulated event in the mammary gland as the D-form predominates in the tissue although nearly all of the enzyme in milk is in the O-form [47]. It was long held that ROS generation was a unique property of the O-form. However, recent analysis of D- to O-form conversion indicates that conversion per se is not necessary for ROS generation by XOR [62]. Preparation of XOR from bovine milk entirely in the D-form indicates that the D-form enzyme can react with oxygen to produce ROS at one third the rate of the O-form in the absence of NAD^+ [65]. Because D-form XOR has a strong preference for NAD^+ over oxygen as an oxidizing substrate, the relative availability of NAD^+ or oxygen could become an important determinant of ROS generation by XOR [65]. Although XOR has been defined by its capacity to oxidize xanthine to produce uric acid, XOR can also use numerous other compounds as substrates [61]. Because acetaldehyde is a substrate for both the D- and O-forms of XOR, ROS generation by XOR during acetaldehyde metabolism could be a significant source of ROS in breast tissue.

NADH oxidase activity of XOR. The nature of molybdenum hydroxylases in human breast tissue is complicated by reports that XOR in human milk is catalytically inactive toward conventional substrates [43,66]. However, the molybdenum hydroxylase enzymes, AOX and XOR, also possess kinetically efficient intrinsic NADH oxidase activities [17,23,65,66]. XOR has a K_m for NADH of 2.8 μM, in contrast to its K_m for acetaldehyde that has been reported to be from 100 μM to 16 mM depending on the source [61]. Also, the catalytic rate constant for NADH oxidation by XOR in the presence of oxygen is comparable to that for xanthine utilization and reflects comparably efficient V_{max} for both substrates [65,66]. Thus, NADH would be a more efficient sub-

strate for XOR than would acetaldehyde in tissues expressing this enzyme. The NADH oxidase activity of both molybdenum hydroxylase enzymes also generates ROS [17,23,65,66]. Moreover, the ROS injury sustained during alcohol toxicity of the liver appears to operate entirely through the combined NADH oxidase activities of XOR and AOX and injury appears to be mediated by an iron dependent process [16–18]. Although human XOR possesses low catalytic activity toward purine substrates it has efficient NADH oxidase activity [43,65,66]. We suggest that NADH may be an important, but largely overlooked, substrate for XOR in the breast and that the intrinsic NADH oxidase activity of XOR may also generate ROS in the breast.

ROS modification of DNA can produce the mutations found in breast cancer

In the absence of contaminating metals, DNA is resistant to H_2O_2 to a concentration of at least 10 mM [23]. Addition of only picograms of ferrous iron is sufficient to convert H_2O_2 into $^{\bullet}OH$ and induce DNA modification and single strand cleavage [24,26,64]. Thus, $^{\bullet}OH$ is considered to be the ROS species that induces DNA modification and strand breakage. Although singlet oxygen (O_2^1), an energetically activated form of diatomic oxygen, can also induce the modifications considered here, it probably has little relevance to alcohol toxicity [67,68] and is not produced by the molybdenum hydroxylase enzymes.

Hydroxyl radical induces numerous modifications to DNA [20,23–27] including single base deletions, base ring opening (largely adenine and guanine) [21] single and double strand breakage, and adduction of bases to form chiefly 5-OH-cytosine, 8-OH-guanine, and 8-OH-adenine, although many other sites of $^{\bullet}OH$ attack have been identified [69]. Single strand breakage, for example, would be estimated to represent no more than 10% of the hydroxylation events [20,26,27,69]. Thus, no single measure of oxidative DNA damage fully represents the extent of DNA modification.

Metabolically derived oxygen-based ROS can be mutagenic [70]. However, not all of the hydroxylation events on DNA have proved to be mutagenic. For example, base ring opening has not been linked to mutagenesis, and single or double strand cleavage may be more involved in chromosome deletion and rearrangement. Interest has centered, however, on 8-OH-deoxyguanosine (8-OH-dG) as an indicator of oxidatively modified DNA that can be mutagenic [68,71]. 8-OH-dG is a common and easily measured modification that is markedly elevated in breast cancer [20–22]. G::C to T::A transversion mutations have been specifically linked to 8-OH-dG in post replication cells [68,71], and current focus on 8-OH-dG reflects its great abundance in oxidatively modified DNA. 5-OH-deoxy cytosine can also be mutagenic, producing C::G to T::A transition mutations [72].

Oxidative DNA modification is most likely random, and specific genetic targets for ROS generated mutations in carcinogenesis of the breast have not been characterized. However, a number of somatic mutations have been identified in breast cancer [73]. These include transversion mutations of p53, BRCA1, and BRCA2. These key genes have been linked to breast cancer progression [74–77] and the mutations found in them can be produced by ROS [74]. Although the direct link between alcohol-induced ROS modification of DNA and mutation of these genes remains to be established, they should be considered important candidates for alcohol-induced carcinogenesis because mutations in these genes could be responsible for tumor initiation as well as tumor progression.

FURTHER SUPPORT FOR THE XOR MEDIATED ROS HYPOTHESIS OF BREAST CANCER

Iron accumulation may potentiate ROS damage to breast DNA

Iron can catalyze conversion of H_2O_2 into $^{\bullet}OH$, the primary ROS responsible for damage to DNA. Iron has been recognized to potentiate carcinogenesis in several different organ systems and is an important risk factor for breast cancer [78,79,80]. For reasons not fully understood, iron accumulates in intracellular complexes with ferritin storage protein as a function of age. Thus, males and females reveal progressive iron accumulation with age that is especially enhanced in post-menopausal women [81] whose incidence of breast cancer is increased.

Importantly, serum and breast ferritin levels are substantially elevated in breast carcinoma [82,83] and have been directly linked to mammary carcinogenesis through ROS [83]. It has been suggested that elevated ferritin/iron complexes may supply the unusual needs for iron during proliferation of mammary tissue in normal or breast carcinoma cells. However, the need for iron in mammary gland cell growth may also substantially contribute to an unusual risk for ROS mediated injury.

Diminished antioxidant defenses in breast tissue may enhance ROS damage to DNA

All cells are subjected to a constant barrage of metabolically derived ROS either from enzyme sources, of which the molybdenum hydroxylases are only one example, or from mitochondrial electron transport [84].

Intracellular defenses against this oxidative onslaught are numerous with a primary role attributable to the enzymes superoxide dismutase (SOD), catalase (CAT), and the glutathione (GSH) redox system [85]. The presence of both efficient ROS scavenging systems and ROS generating enzymes has enabled the view of an oxidant/antioxidant balance composed of these opposing elements. Disruption of this balance by excessive ROS generation or diminished ROS scavenging capacity will predispose the cell to oxidative injury.

Levels of both SOD and CAT in mammary glands from rodents and humans decline with age [86,87,88], as do the levels of GSH in human mammary glands [89,90]. Furthermore, in mammary carcinoma tissues from humans and mice CAT levels are even more markedly diminished [86,87]. The combination of age associated diminished ROS scavenging and a potent mechanism for ROS generation could promote excessive ROS injury of the breast. We would argue that diminishing levels of catalase with age in conjunction with naturally elevated iron stores places mammary cells at unusual risk for alcohol-induced ROS damage to DNA contributing to mammary carcinogenesis.

DISCUSSION

We have proposed an explicit model for alcohol-induced ROS generation that depends on the combined activities of ADH and XOR. The direct action of cytochrome p450 2E1 on ethanol in the mammary gland may be an additional source of carcinogenic ROS [91,92]. Although the role of ROS in carcinogenesis is still being defined, the amelioration of several cancers, including breast cancer, by antioxidants underscores the importance of confirming this mechanism. Alcohol derived ROS could contribute to several stages in breast cancer development. For example, alcohol derived ROS could act at an early stage of mutagenesis leading to tumor initiation and breast cancer, at later stages of progression and transformation to a cancer phenotype, or perhaps affect cell proliferation. We have focused on the role played by ROS in DNA modification and carcinogenesis. However, potential effects on proteins such as the redox sensitive transcription factors AP-1 and NF-κB may also play important roles in transformation.

Improved understanding of the causes of breast cancer could lead to improved diagnosis and treatment. The realization that ROS may participate in the development of breast cancer suggests that removing potentially carcinogenic ROS may have therapeutic value. Treatment with ROS scavenging antioxidants, inhibition of critical ROS generating enzymes like XOR, reduction of iron intake, and reduced alcohol consumption by women in the higher age dependent risk categories could significantly modulate the incidence of breast cancer.

Acknowledgements — Supported by grants from the National Institutes of Health (HL52509 and HL45582), The Muscular Dystrophy Association, and The Robert and Helen Kleberg Foundation.

REFERENCES

[1] Russo, J.; Calaf, G.; Sohi, N.; Tahin, Q.; Zhang, P. L.; Alvarado, M. E.; Estrada, S.; Russo, I. H. Critical steps in breast carcinogenesis. *Ann. N.Y. Acad. Sci.* **698:**1–17; 1993.

[2] Wolman, S. R.; Dawson, P. J. Genetic events in breast cancer and their clinical correlates. *Oncogenesis* **2:**277–291; 1991.

[3] Colditz, G. A.; Willett, W. C.; Hunter, D. J.; Stampfer, M. J.; Manson, J. J.; Hennekens, C. H.; Rosner, B. A.; Speizer, F. E. Family history, age, and risk of breast cancer. *J. Am. Med. Assoc.* **270:**338–343; 1993.

[4] Liehr, J. G. Dual role of oestrogens as hormones and pro-carcinogens: tumor initiation by metabolic activation of oestrogens. *Eur. J. Cancer Prevention* **6:**3–10; 1997.

[5] Sipe, H. J.; Jordan, S. J.; Hana, P. M.; Mason, R. P. The metabolism of 17-β-estradiol by lactoperoxidase: a possible source of oxidative stress in breast cancer. *Carcinogenesis* **15:**:2637–2643; 1994.

[6] Nutter, L. M.; Wu, Y. Y.; Ngo, E. O.; Sierra, E. E.; Gutierrez, P. L.; Abul-Hajj, Y. J. An *o*-quinone form of estrogen produces ROS in human breast cancer cells: correlation with DNA damage. *Chem. Res. Tox.* **7:**:23–28; 1994.

[7] Morabia, A.; Bernstein, M.; Heritier, S.; Khatchatrian, N. Relation of breast cancer with passive and active exposure to tobacco smoke. *Amer. J. Epidiol.* **143:**918–928; 1996.

[8] Smith-Warner, S. A.; Spiegelman, D.; Yaun, S. S.; Brandt, P. A.; Folsom, A. R.; Goldbohm, R. A.; Graham, S.; Holmberg, L.; Howe, G. R.; Marshall, J. R.; Miller, A. B.; Potter, J. D.; Speizer, F. E.; Willett, W. C.; Wolk, A.; Hunter, D. J. Alcohol and breast cancer in women. *J. Amer. Med. Assoc.* **279:**535–540; 1998.

[9] Singletary, K. Ethanol and experimental breast cancer. *Alcohol. Clin. Exp. Res.* **21:**334–339; 1997.

[10] Swanson, C. A.; Coates, R. J.; Malone, K. E.; Gammon, M. D.; Shoenberg, J. B.; Brogan, D. J.; McAdams, M.; Potischman, N.; Hoover, R. N.; Brinton, L. A. Alcohol consumption and breast cancer risk among women under age 45 years. *Epidemiology* **8:**231–237; 1997.

[11] Longnecker, M. P. Alcoholic beverage consumption in relation to risk of breast cancer: meta-analysis and review. *Cancer Causes Control* **5:**73–82; 1994.

[12] Rosenberg, L.; Metzger, L. S.; Palmer, J. R. Alcohol consumption and risk of breast cancer: a review of the epidemiologic evidence. *Epidemiol. Rev.* **15:**133–144; 1993.

[13] van den Brandt, P. A.; Goldbohm, R. A.; van't Veer, P. Alcohol and breast cancer: results from the Netherlands Cohort Study. *Am. J. Epidemiol.* **141:**907–915; 1995.

[14] Friedenreich, C. M.; Howe, G. R.; Miller, A. B.; Jain, M. G. A cohort study of alcohol consumption and risk of breast cancer. *Am. J. Epidemiol.* **137:**512–520; 1993.

[15] Gapstur, S. M.; Potter, J. D.; Sellers, T. A.; Folsom, A. R. Increased risk of breast cancer with alcohol consumption in post-menopausal women. *Am. J. Epidemiol.* **136:**1221–1231; 1992.

[16] Rajasinghe, H.; Jayatilleke, E.; Shaw, S. DNA cleavage during ethanol metabolism: role of superoxide radicals and catalytic iron. *Life Sci.* **47:**807–814; 1990.

[17] Mira, L.; Maia, L.; Barreira, L.; Manso, C. F. Evidence for ROS generation due to NADH oxidation by aldehyde oxidase during ethanol metabolism. *Arch. Biochem. Biophys.* **318:**53–58; 1995.

[18] Shaw, S.; Jayatilleke, E. The role of cellular oxidases and catalytic iron in the pathogenesis of ethanol induced liver injury. *Life Sci* **50:**2045–2052; 1992.

[19] Nordback, I. H.; Olson, J. L.; Chako, V. P.; Cameron, J. L.

Detailed characterization of experimental acute alcoholic pancreatitis. *Surgery* **117:**41–49; 1994.
[20] Malins, D. C.; Haimanot, R. Major alterations in the nucleotide structure of DNA in cancer of the female breast. *Cancer Res.* **51:**5430–5432; 1991.
[21] Malins, D. C.; Holmes, E. H.; Polissar, N. L.; Gunselman, S. J. The etiology of breast cancer: characteristic alterations in ˙OH radical induced DNA base lesions during oncogenesis with potential for evaluating incidence risk. *Cancer* **71:**3036–3043; 1993.
[22] Malins, D. C.; Polissar, N. L.; Gunselman, S. J. Progression of human breast cancers to the metastatic state is linked to ˙OH radical induced DNA damage. *Proc. Natl. Acad. Sci. USA* **93:** 2557–2563; 1996.
[23] Wright, R. M.; Weigel, L. K.; Repine, J. E. Aldehyde oxidase generates deoxyribonucleic acid single strand nicks in vitro. *Redox Report* **1:**349–355; 1995.
[24] Lubec, G. The ˙OH radical: from chemistry to human disease. *J. Invest. Med.* **44:**324–346; 1996.
[25] Brawn, K.; Fridovich, I. DNA strand scission by enzymatically generated oxygen radicals. *Arch. Biochem. Biophys.* **206:**414–419; 1981.
[26] Kukielka, E.; Cederbaum, A. I. DNA strand cleavage as a sensitive assay for the production of ˙OH radicals by microsomes: role of cytochrome P4502E1 in the increased activity after ethanol treatment. *Biochem. J.* **302:**773–779; 1994.
[27] Takeuchi, T.; Nakajima, M.; Morimoto, K. Relationship between the intracellular reactive oxygen species and the induction of oxidative DNA damage in human neutrophil-like cells. *Carcinogenesis* **17:**1543–1548; 1996.
[28] Shaw, S.; Eng, J.; Jayatilleke, E. Ethanol induced ROS injury to the hepatocyte glucagon receptor. *Alcohol* **12:**273–277; 1995.
[29] Grattagliano, I.; Vendemiale, G.; Didonna, D.; Errico, F.; Bolognino, A.; Pistone, A.; Cofano, M.; Signorile, A.; Ciannamea, F.; Altomare, E. Oxidative modification of protein in chronic alcoholics. *Bollettino Soc. Ital. Biol Speriment* **71:**189–195; 1995.
[30] Li, C. J.; Nanji, A. A.; Siakotos, A. N.; Lin, R. C. Acetaldehyde modified and 4-hydroxynonenal modified proteins in the livers of rats with alcoholic liver disease. *Hepatology* **26:**650–657; 1997.
[31] Nicholls, R.; de Jersey, J.; Worrall, S.; Wilce, P. Modification of proteins and other biological molecules by acetaldehyde: adduct structure and functional significance. *Int. J. Biochem.* **24:**1899–1906; 1992.
[32] Worrall, S.; deJersey, J.; Shanley, B. C.; Wilce, P. A. Detection of stable acetaldehyde modified proteins in the livers of ethanol fed rats. *Alcohol and Alcoholism* **26:**437–444; 1991.
[33] Kenney, W. C. Acetaldehyde adducts of phospholipids. *Alcholism Clin. Exp. Res.* **6:**412–416; 1982.
[34] Lambert, B.; Andersson, B.; Bastlova, T.; Hou, S. M.; Hellgren, D.; Kolman, A. Mutations induced in the HPRT gene by three urban air pollutants: acetaldehyde, benzo[a]pyrene diolepoxide, and ethylene oxide. *Environ. Health Perspect.* **4:**135–138; 1994.
[35] He, S. M.; Lambert. B. Acetaldehyde induced mutation at the hprt locus in human lymphocytes in vitro. *Environ. Mol. Mutagen.* **16:**57–63; 1990.
[36] Fang, J. L.; Vaca, C. E. Detection of DNA adducts of acetaldehyde in peripheral white blood cells of alcohol abusers. *Carcinogenesis* **18:**627–632; 1997.
[37] Troll, W. Prevention of cancer by agents that suppress oxygen radical formation. *Free Radic. Res. Comm.* **12:**751–757; 1991.
[38] Byers, T.; Perry, G. Dietary carotenes, vitamin C, and vitamin E as protective antioxidants in human cancers. *Ann. Rev. Nutr.* **12:**139–159; 1992.
[39] Dwyer, J. T. Diet and nutritional strategies for cancer risk reduction. *Cancer* **72:**1024–1031; 1993.
[40] Saleem, M. M.; al-Tamer, Y. Y.; Skursky, L.; Al-Habbal, Z. Alcohol dehydrogenase activity in human tissues. *Biochem. Med.* **31:**1–9; 1984.
[41] Ishii, T.; Aoki, N.; Noda, A.; Adachi, T.; Nakamura, R.; Matsuda, T. Carboxy terminal cytoplasmic domain of mouse butyrophilin specifically associates with a 150 kDa protein of mammary epithelial cells and milk fat globule membrane. *Biochem. Biophys. Acta* **1245:**285–292; 1995.
[42] Waud, W. R.; Brady, F. O.; Wiley, R. D.; Rajagopalan, K. V. A new purification procedure for bovine milk xanthine oxidase: effects of proteolysis on the subunit structure. *Arch. Biochem. Biophys.* **169:**695–701; 1975.
[43] Abadeh, S.; Killacky, J.; Benboubetra, M.; Harrison, R. Purification and partial characterization of xanthine oxidase from human milk. *Biochem. Biophys. Acta* **1117:**25–32; 1992.
[44] Kooij, A.; Frederiks, W. M.; Gossrau, R.; van Noorden, C. J. F. Localization of xanthine oxidoreductase activity using the tissue protectant polyvinyl alcohol and final electron acceptor teranitro BT. *J. Histochem. Cytochem.* **39:**87–93; 1991.
[45] Jarasch, E. D.; Grund, C.; Bruder, G.; Heid, H. W.; Keenan, T. W.; Franke, W. W. Localization of xanthine oxidase in mammary gland epithelium and capillary endothelium. *Cell* **25:**67–82; 1981.
[46] Powell, D.; Benboubtra, M.; Newey, S.; Harrison, R. Xanthine oxidase activity and subcellular localization in human mammary epithelial cells. *Biochem. Soc. Trans.* **616S:**23; 1995.
[47] McManaman, J. L.; Wright, R. M.; Shellman, V.; Repine, J. E. Purification and characterization of the properties and expression of xanthine dehydrogenase in mouse mammary glands. Submitted.
[48] Kurosaki, M.; Zanotta, S.; Calzi, M. L.; Garattini, E.; Terao, M. Expression of xanthine oxidoreductase in mouse mammary epithelium during pregnancy and lactation: regulation of gene expression by glucocorticoids and prolactin. *Biochem. J.* **319:**801–810; 1996.
[49] Wright, R. M.; McManaman, J. L.; Repine, J. E. Unpublished observations.
[50] Edenberg, H. J.; Brown, C. J. Regulation of human alcohol dehydrogenase genes. *Pharmacogenetics* **2:**185–196; 1992.
[51] Sze, P. Y. The permissive effect of glucocorticoids in the induction of liver alcohol dehydrogenase by ethanol. *Biochem. Med.* **14:**156–161; 1975.
[52] Wakao, H.; Gouilleux, F.; Groner, B. Mammary gland factor (MGF) is a novel member of the cytokine regulated transcription factor gene family and confers the prolactin response. *EMBO J.* **13:**2182–2191; 1994.
[53] Philip, J.; Burdon, T. G.; Watson, C. J. Differential activation of STATs 3 and 5 during mammary gland development. *FEBS Lett.* **396:**77–80; 1996.
[54] Xu, P.; Huecksteadt, T. P.; Hoidal, J. R. Molceular cloning and characterization of the human xanthine dehydrogenase gene (XDH). *Genomics* **34:**173–180; 1996.
[55] Cazzaniga, G.; Terao, M.; Schiavo, PL.; Galbiati, F.; Segalla, F.; Seldin, M. F.; Garattini, E. Chromosomal mapping, isolation, and characterization of the mouse xanthine dehydrogenase gene. *Genomics* **23:**390–402; 1994.
[56] Chow, C. W.; Clark, M.; Rinaldo, J.; Chalkley, R. Identification of the rat xanthine dehydrogenase/oxidase promoter. *Nucleic Acids Res.* **22:**1846–1854; 1994.
[57] Wright, R. M.; Repine, J. E. The human molybdenum hydroxylase gene family: co-conspirators in metabolic ROS generation and disease. *Biochem. Soc. Trans.* **25:**799–804; 1997.
[58] Kurose, I.; Higuchi, H.; Kato, S.; Miura, S. W.; Ishii, H. Ethanol induced oxidative stress in the liver. *Alchol. Clin. Exp. Res.* **20:**77A–85A; 1996.
[59] Moriwaki, Y.; Yamamoto, T.; Higashino, K. Distribution and pathophysiologic role of molybdenum containing enzymes. *Histology Histopath.* **12:**513–24; 1997.
[60] Granger, D. N.; Korthuis, R. J. Physiologic mechanisms of postischemic tissue injury. *Ann. Rev. Physiol.* **57:**311–332; 1995.
[61] Hille, R.; Massey, V. Molybdenum containing hydroxylases: xanthine oxidase, aldehyde oxidase, and sulfite oxidase. In: Spiro, T.G., ed. *Molybdenum enzymes.* New York: J. Wiley & Sons; 1985:444–518.
[62] Nishino, T. The conversion of xanthine dehydrogenase to xanthine oxidase and the role of the enzyme in reperfusion injury. *J. Biochem.* **116:**1–6; 1994.

[63] Britigan, B. E.; Pou, S.; Rosen, G. M.; Lilleg, D. M.; Buettner, G. R. Hydroxyl radical is not a product of the reaction of xanthine oxidase and xanthine. *J. Biol. Chem.* **265:**17533–17538; 1990.
[64] Mello-Filho, A. C.; Meneghini, R. In vivo formation of single strand breaks in DNA by hydrogen peroxide is mediated by the Haber-Weiss reaction. *Biochem. Biophys. Acta* **781:**56–63; 1984.
[65] Harris, C. M.; Massey, V. The reaction of reduced xanthine dehydrogenase with molecular oxygen. *J. Biol. Chem.* **272:**8370–8379; 1997.
[66] Sanders, S. A.; Eisenthal, R.; Harrison, R. NADH oxidase activity of human xanthine oxidoreductase: generation of superoxide anion. *Eur. J. Biochem.* **245:**541–548; 1997.
[67] Akker, E-v-d.; Lutgerink, J. T.; Lafleur, M. V. M.; Joenje, H.; Retel, J. The formation of one-G deletions as a consequence of singlet oxygen induced DNA damage. *Mut. Res.* **309:**45–52; 1994.
[68] Ribeiro, D. T.; Oliveira, R. C. D.; Mascio, P. D.; Menck, C. F. M. Singlet oxygen induces predominantly G to T transversions on a single stranded shuttle vector replicated in monkey cells. *Free Radic. Res.* **21:**75–83; 1994.
[69] Wagner, J. R.; Hu, C. C.; Ames, B. N. Endogenous oxidative damage of deoxycytidine in DNA. *Proc. Natl. Acad. Sci. USA* **89:**3380–3384; 1992.
[70] Gille, J. J. P.; van Berkel, C. G. M.; Joenje, H. Mutagenicity of metabolic oxygen radicals in mammalian cultures. *Carcinogenesis* **15:**2695–2699; 1994.
[71] Toyokuni, S.; Mori, T.; Dizdaroglu, M. DNA base modification in renal chromatin of Wistar rats treated with a renal carcinogen, ferric nitriloacetate. *Int. J. Cancer* **57:**123–128; 1994.
[72] Feig, D. I.; Sowers, L. C.; Loeb, L. A. Reverse chemical mutagenesis: identification of the mutagenic lesion resulting from reactive oxygen species mediated damage to DNA. *Proc. Natl. Acad. Sci. USA* **91:**6609–6613; 1994.
[73] Callahan, R.; Cropp, C. S.; Merlo, G. R.; Liscia, D. S.; Cappa, A. P. M.; Lidereau, R. Somatic mutations and human breast cancer. *Cancer* **69:**1582–1588; 1992.
[74] Hussain, S. P.; Aguilar, F.; Amstad, P.; Cerutti, P. Oxy-radical induced mutagenesis of hotspot codons 248 and 249 of the human p53 gene. *Oncogene* **9:**2277–2281; 1994.
[75] Elledge, R. M.; Fuqua, S. A. W.; Clark, G. M.; Pujol, P.; Allred, D. C. The role and prognostic significance of p53 gene alterations in breast cancer. *Breast Cancer Res. Treat.* **27:**95–102; 1993.
[76] Merlo, G. R.; Venesio, T.; Taverna, D.; Marte, B. M.; Callahan, R.; Hynes, N. E. Growth suppression of normal mammary epithelial cells by wild-type p53. *Oncogene* **9:**443–453; 1994.
[77] Brody, L. C.; Biesecker, B. B. Breast cancer: the high risk mutations. *Hosp. Practice* **15:**:59–80; 1997.
[78] Reizenstein, P. Iron, ROS and cancer. *Med. Oncol. Tumor Pharmacother.* **8:**229–233; 1991.
[79] Elliott, R. L.; Elliott, M. C.; Wang, F.; Head, J. F. Breast carcinoma and the role of iron metabolism. *Ann. N.Y. Acad. Sci.* **698:**159–166; 1993.
[80] Thompson, H. J.; Kennedy, K.; Witt, M.; Juzefyk, J. Effect of dietary iron deficiency or excess on the induction of mammary carcinogenesis by *1*-methyl-*1*-nitrosourea. *Carcinogenesis* **12:** 111–114; 1991.
[81] Giler, S.; Moroz, C. The significance of ferritin in malignant disease. *Biomedicine* **28:**203–206; 1978.
[82] Marcus, D. M.; Zinberg, N. Measurement of serum ferritin by radioimmunoassay: results in normal individuals and patients with breast cancer. *J. Nat. Cancer Inst.* **55:**791–795; 1975.
[83] Wyllie, S.; Liehr, J. G. Release of iron from ferritin storage by redox cycling of stilbene and steroid estrogen metabolites: mechanism of induction of ROS damage by estrogen. *Arch. Biochem. Biophys.* **346:**180–186; 1997.
[84] Guidot, D. M.; McCord, J. M.; Wright, R. M.; Repine, J. E. Absence of electron transport restores growth of a manganese superoxide dismutase deficient *S. cerevisiae* in hyperoxia: evidence for electron transport as a major source of superoxide generation in vivo. *J. Biol. Chem.* **268:**26699–26703; 1993.
[85] Sun, Y. ROS, antioxidant enzymes, and carcinogenesis. *Free Radic. Biol. Med.* **8:**583–599; 1990.
[86] el Bouhtoury, F.; Keller, J. M.; Colin, S.; Parache, R. M.; Dauca, M. Peroxisomal enzymes in normal and tumoral human breast. *J. Path.* **166:**27–35; 1992.
[87] Punnonen, K.; Ahotupa, M.; Asaishi, K.; Hyoty, M.; Kudo, R.; Punnonen, R. Antioxidant enzyme activities and oxidative stress in human breast cancer. *J. Cancer Clin. Oncol.* **120:**374–377; 1994.
[88] Ishii, K.; Zhen, L. X.; Wang, D. H.; Funamori, Y.; Ogawa, K.; Taketa, K. Prevention of mammary tumorigenesis in acatalasemic mice by vitamin E supplementation. *Jap. J. Cancer Res.* **87:**680–684; 1996.
[89] Buser, K.; Joncourt, F.; Altermatt, H. J.; Bacchi, M.; Oberli, A.; Cerny, T. Breast cancer: pretreatment drug reisitance parameters in tumor tissue and their correlation with clinical and prognostic characteristics. *Ann. Oncol.* **8:**335–341; 1997.
[90] Kumar, K.; Thangaraju, M.; Sachdanandam, P. Changes observed in antioxidant systems in the blood of postmenopausal women with breast cancer. *Biochem. Int.* **25:**371–380; 1991.
[91] Bell, L. C.; Guengerich, F. P. Oxidation kinetics of ethanol by human cytochrome P450 2E1. *J. Biol. Chem.* **272:**29643–29651; 1997.
[92] Hellmold, H.; Lamb, J. G.; Wyss, A.; Gustafsson, J. A.; Warner, M. Developmental and endocrine regulation of P450 isoforms in rat breast. *Mol. Pharm.* **48:**630–638; 1995.

ABBREVIATIONS

ADH—alcohol dehydrogenase
AOX—aldehyde oxidase
GSH—glutathione
H_2O_2—hydrogen peroxide
$O_2^{\bullet -}$—superoxide anion
$^{\bullet}OH$—hydroxyl radical
XOR—xanthine oxidoreductase

Archives of Biochemistry and Biophysics
Vol. 373, No. 2, January 15, pp. 318–327, 2000
doi:10.1006/abbi.1999.1573, available online at http://www.idealibrary.com on IDEAL®

Lactogenic Hormones Regulate Xanthine Oxidoreductase and β-Casein Levels in Mammary Epithelial Cells by Distinct Mechanisms[1]

J. L. McManaman,*,[2] L. Hanson,† M. C. Neville,† and R. M. Wright‡
*Department of Biochemistry and Molecular Genetics, †Department of Physiology, and ‡Webb-Waring Institute for Antioxidant Research, University of Colorado Health Sciences Center, Denver, Colorado 80262

Received August 2, 1999

Xanthine oxidoreductase (XOR) is a prominent component of the milk lipid globule, whose concentration is selectively increased in mammary epithelial cells during the transition from pregnancy to lactation. To understand how XOR expression is controlled in the mammary gland, we investigated its properties and regulation by lactogenic hormones in cultured HC11 mammary epithelial cells. XOR was purified as the NAD^+-dependent dehydrogenase by benzamidine–Sepharose chromatography and was shown to be intact and to have biochemical properties similar to those of enzyme from other sources. Treating confluent HC11 cells with prolactin and cortisol produced a progressive, four- to fivefold, increase in XOR activity, while XOR activity in control cells remained constant. Elevated cellular XOR activity was correlated with increased XOR protein and was due to both increased synthesis and decreased degradation of XOR. Prolactin and cortisol increased XOR protein and mRNA in the presence of epidermal growth factor, which blocked the stimulation of β-casein synthesis by these hormones. Further, hormonal stimulation of XOR was inhibited by genistein (a protein tyrosine kinase inhibitor) and by PD 98059 (a specific inhibitor of the MAP kinase cascade). These findings indicate that lactogenic hormones stimulate XOR and β-casein expression via distinct pathways and suggest that a MAP kinase pathway mediates their effects on XOR. Our results provide evidence that lactogenic hormones regulate milk protein synthesis by multiple signaling pathways. © 2000 Academic Press

Key Words: **xanthine oxidase; affinity chromatography; development; cell culture; hormonal regulation.**

Xanthine oxidoreductase (XOR)[3] is an important metabolic enzyme; in vertebrates it catalyzes the oxidation of wide variety of organic compounds and is responsible for the conversion of xanthine to uric acid, the rate-limiting step in purine degradation (1, 2). XOR is a member of the molybdenum hydroxylase family of proteins. It is composed of two identical 150-kDa subunits, which contain binding sites for molybdopterin, iron, and flavin cofactors. The enzyme has been isolated from a variety of sources, and biochemical and genetic studies have shown that its general catalytic properties, cofactor requirements, and primary structure have been phylogenetically conserved (1, 3). Despite its general importance in cellular metabolism, XOR may have distinct tissue specific functions. It is found at relatively high concentrations in milk from numerous species, including humans (4). The enzyme in milk is associated predominantly with secreted lipid globules and it appears to be a major protein constituent (~14% of the total protein) of the membrane surrounding milk lipid globules (4). Although it is a cytoplasmic protein in most cells, immunocytochemical studies have shown that XOR localizes to the apical plasma membrane of milk-secreting cells in lactating bovine mammary glands (5). These observations are

[1] This work was supported by NIH Grants HL 45582-05A2 and HL 52509-03, NCI Cancer Core Grant CA46934, and the Robert and Helen Kleberg Foundation.

[2] To whom correspondence should be addressed. Fax: (303) 315-8215.

[3] Abbreviations used: XOR, xanthine oxidoreductase; XO, xanthine oxidase; XD, xanthine dehydrogenase; SDS, sodium dodecyl sulfate; PMSF, phenylmethylsulfonyl fluoride; DCIP, dichloroindophenol; DMSO, dimethyl sulfoxide; PAGE, polyacrylamide gel electrophoresis; CBB, Coomassie brilliant blue; NBT, nitroblue tetrazolium; PVDF, polyvinylidene difluoride.

0003-9861/00 $35.00

difficult to reconcile with a purely metabolic role for XOR and have led to proposals that XOR may play distinct roles in milk or milk secretion (6).

Expression of XOR in mouse mammary glands is tightly regulated and correlates with the ability of mammary tissue to secrete milk (7, 8). During the reproductive cycle the activity, protein, and mRNA levels of XOR in mouse mammary tissue undergo multiphasic changes. These changes are specific to the mammary gland and correlate with the differentiation of mammary epithelial cells that occurs during lactogenesis and with alterations in the functional status of the mammary gland (7, 8). Developmental studies have also shown that XOR mRNA increases severalfold during the later part of pregnancy and again at birth but then remains relatively constant during lactation until the weaning period, when it returns to prepregnancy levels (8). XOR activity and protein also increase during pregnancy, but in contrast to mRNA, their levels continue to increase after parturition until approximately day 15 of lactation and then decline as weaning commences (8). These observations suggest that lactogenic hormones regulate mammary XOR expression and that mechanisms of regulation are complex and may involve multilevel effects on transcriptional, translational, and posttranslational processes.

Lactogenic hormones have been shown to increase XOR expression in cultured mammary epithelial cells (9–11); however, the mechanism(s) mediating this effect remain poorly defined. In addition, the enzyme from human and goat milk is mostly inactive toward traditional purine substrates (4, 12). This observation suggests that mammary epithelial cells are capable of synthesizing and/or secreting significant amounts of enzyme with reduced catalytic activity. At present little is known about the properties of enzyme from cultured cells or the percentage of the enzyme that is catalytically active. To address these issues we characterized the effects of prolactin and cortisol on the expression of XOR in the HC11 mouse mammary epithelial cell line. HC11 cells are a clonal derivative of the COMMA-1D cell line (13) and have proven to be an important model for understanding hormonal regulation of mammary epithelial cell differentiation and milk protein gene expression (14–16). Our studies show that lactogenic hormones regulate XOR expression in HC11 cells by multiple mechanisms and provide evidence for both pre- and posttranslational control of XOR levels in mammary epithelial cells. In addition, we show that most of the hormonally induced XOR is catalytically active toward xanthine, its traditional purine substrate, and that its kinetic and biochemical properties are similar to those of tissue-derived enzyme. Finally we provide evidence that lactogenic hormones utilize different intracellular signaling pathways to regulate XOR and β-casein expression in HC11 cells.

MATERIALS AND METHODS

Materials. [^{35}S]Methionine was purchased from Amersham Corp. Benzamidine–Sepharose, benzamidine, BCIP (bromochloroindoyl phosphate), NBT (nitroblue tetrazolium), and cortisol were purchased from Sigma Chemical Co. Fetal calf serum was obtained from Gemini Bioproducts (Carlsbad, CA) and RPMI media was obtained from the University of Colorado Health Sciences Center's Cancer Center Media and Serum Core Facility. Genistein was purchased from Calbiochem-Novachem Corp. and PD 98059 was purchased from New England Biolabs, Inc. Prolactin was kindly provided by Dr. A. F. Parlow at NIDDK's National Pituitary Program. Rabbit antibodies to bovine XOR were a generous gift from Dr. Lance Terada (Dallas, Texas). Anti-casein antibodies were generated in rabbits using mouse casein. HC11 mammary epithelial cells were obtained from Dr. Jeffery Rosen (Houston, Texas) and were used with the permission of Dr. Bernd Groner (Frieburg, Germany).

Cell culture and hormone treatment. HC11 cells were grown to confluency in RPMI 1640 medium containing 2 mM glutamine, 5 μg/ml bovine insulin, 10 ng/ml mouse EGF (basal medium) supplemented with 8% heat-inactivated fetal calf serum. At confluence, approximately 5 days after plating, the cells were washed and incubated for the indicated times in serum-free basal medium with and without 10 μg/ml prolactin and 1 μM cortisol (lactogenic hormones). Culture medium was changed daily and fresh lactogenic hormones were added with each medium change.

Preparation of cell extracts and assay of XOR activity. Cells were lysed on ice in 0.3 ml/well of lysis buffer (50 mM Tris, 150 mM NaCl, 1% NP-40, 1 mM phenylmethylsulfonyl fluoride (PMSF), 2 mM leupeptin, 1 mM EDTA, pH 8). Insoluble material was removed by centrifugation and total XOR activity (both oxidase and dehydrogenase activities) was assayed by the reduction of dichloroindophenol (DCIP) using xanthine as a substrate (17). Each extract (20 μl) was assayed in duplicate in 80 μl of substrate solution (0.15 mM xanthine, 0.025 mM DCIP, 10% (v/v) DMSO, 1.0 mM EDTA, 0.1% (v/v) catalase in 50 mM Tris, pH 8) in the absence and presence of 500 μM allopurinol. The rate of reduction of DCIP was monitored at 595 nm using a kinetic microplate reader (Molecular Devices, Menlo Park, CA). XOR activity was normalized to cellular protein as previously described (17). Enzymatic activity specifically associated with either XD (xanthine: NAD^+ oxidoreductase activity) or XO (xanthine: O_2 oxidoreductase activity) was calculated as the allopurinol-sensitive rate of aerobic formation of uric acid from xanthine in the presence (XD) or absence (XO) of 0.6 mM NAD^+. The ratio of XD to XO activities (D/O) was calculated as described previously (17).

Labeling HC11 cells with [^{35}S]methionine and measurement of [^{35}S]methionine labeled XOR. Confluent cells were washed and incubated in methionine-free culture media at 37°C, 5% CO_2 for 4 h. The medium was then changed to basal medium containing [^{35}S]methionine (10 μCi/well) and the cells were incubated in the presence and absence of prolactin and cortisol for 16 h at 37°C, 5% CO_2. Labeled cells were washed three times in RPMI and extracted with 0.3 ml/well of lysis buffer. Lysates from three wells were pooled, centrifuged to remove insoluble material, and assayed for total protein and XOR activity as described above. Total [^{35}S]methionine-labeled protein was determined by trichloroacetic acid (TCA) precipitation. [^{35}S]methionine-labled XOR was determined by incubating equal volumes of the lysate with either 10 μl of rabbit anti-XO antisera or 10 μl of preimmune rabbit sera (18) at 4°C for 2 h. Immuncomplexes were bound to protein-A Sepharose, washed three times with lysis buffer, solubilized by boiling in 50 μl of sample buffer, and analyzed by SDS–polyacrylamide gel electrophoresis (PAGE) on 7% acrylamide gels. The gels were dried and the amount

of [^{35}S]methionine-labeled XOR quantified using a Phosphorimager and ImageQuant software (Molecular Dynamics).

Determination of XOR turnover. Confluent HC11 cells were cultured in the presence of prolactin and cortisol for 8 days and then pulsed with [^{35}S]methionine for 16 h as described above. The cells were washed with RPMI to remove excess [^{35}S]methionine and then incubated in basal medium with and without prolactin and cortisol. At the specified times the cells were extracted in lysis buffer and [^{35}S]methionine-labeled XOR was immunoprecipitated and quantified by SDS–PAGE and phosphorimaging as described above. Total [^{35}S]-labeled protein was determined by TCA precipitation and scintillation counting.

Purification of [^{35}S]methionine-labeled XOR by benzamidine–Sepharose chromatography. HC11 cells were cultured for 8 days with or without prolactin and cortisol and proteins were labeled with [^{35}S]methionine for 16 h as described above. The cells were then washed three times in RPMI and homogenized in 0.1 M glycine, 0.1 M NaCl, pH 9 (GS9). The homogenates were clarified by centrifugation, and applied directly to 2-ml columns of benzamidine–Sepharose preequilibrated in GS9. The columns were washed with three volumes of GS9 and eluted with 25 mM benzamidine in GS9 as previously described (17).

Western blot analysis. Samples were separated by SDS–PAGE in 10% acrylamide gels and electrophoretically transferred to nitrocellulose membranes in 10 mM Caps (3-cyclohexylamino-1-propansulfonic acid), 10% methanol, pH 11. The membranes were blocked in 3% gelatin overnight at room temperature, washed twice with TBS (25 mM Tris, 138 mM NaCl, 3 mM KCl, pH 8) containing 0.1% Tween-20 (TBS–Tween), and incubated with rabbit antibodies to either XOR (7) or mouse casein at 1/1000 dilution for 2 h at room temperature. Immunoreactive bands were detected using ExtrAvidin reagents (Sigma) and bromochloroindoyl phosphate/nitroblue tetrazolium substrate (19). Casein antibody specificity was established by Western blot and sequence analysis of mouse milk proteins (data not shown).

Isolation and quantification of mRNA. RNA was isolated from cultured HC11 cells using Trizol Reagent (GibcoBRL, Grand Island, NY). Each well of a six-well plate was washed twice with 1 ml of PBS. Cells from three wells were lysed in 1000 μl of Trizol and held at room temperature for 5 min; 200 μl of chloroform was added and the extracts were vortexed and held for 2 min at room temperature. After centrifugation at 13,000 rpm for 15 min, the aqueous phase was transferred to new tubes and 500 μl of isopropanol was added. Mixtures were vortexed and stored at −70°C for 30 min. Nucleic acids were pelleted at 4°C, 13,000 rpm, for 15 min and pellets were washed in 75% ethanol. Pellets were dried to completion in the air and dissolved in 80 μl of water. DNA was removed by Dnase I treatment (20) at 37°C for 1 h. RNA was extracted with phenol: chloroform:isoamylalcohol and recovered by precipitation in isopropanol. RNA pellets were washed in 75% ethanol, dried, and suspended in water.

Random primed reverse transcription (RT) was carried out with 1.0 μg of RNA and mouse Maloney Leukemia Virus reverse transcriptase using the Advantage RT for PCR Kit (K1402) from Clontech Laboratories (Palo Alto, CA). Reactions were incubated at 42°C for 60 min and enzyme was denatured at 94°C for 5 min. Samples were then brought to 100 μl with water. Then 100-μl Polymerase chain reactions were conducted by mixing 10 μl of diluted RT reaction, 4 μl of each primer (10 μM), 8 μl of dNTP mix (10 mM), 30 μl of 3.3× buffer, 5 μl of magnesium acetate (25 mM), 38 μl of water, and 10 μl of rTth DNA polymerase (Perkin–Elmer Applied Biosystems, Foster City, CA). PCR conditions were first established to be in a linear response range for RNA input and amplification cycles. Final reaction conditions were as follows: 94°C for 5 min (1 cycle), 94°C for 30 s, 60°C for 2 min (10 cycles decreasing temperature by 1°C to 55°C), 94°C for 30 s, 55°C for 2 min (25 cycles), 55°C for 7 min (1 cycle). Products were held at 4°C until analysis on 2% agarose gels. Gels were stained with ethidium bromide, photographed, and used in Southern blot analysis for quantitation. Alternatively, PCRs were amplified in the presence of 50 μCi of [α^{32}P]dCTP; reaction products were resolved by polyacrylamide gel electrophoresis and bands were visualized by phosphorimaging and quantified using ImageQuant software.

RESULTS

Lactogenic Hormones and EGF Stimulate XO Activity in HC11 Cells

Incubating HC11 cells in media containing insulin, EGF, and the lactogenic hormones, prolactin and cortisol (PC), produced a time-dependent increase in their XOR activity. Figure 1 shows that the XOR activity (activity/mg of cellular protein) in confluent cells incubated with PC increased approximately 1.5-fold after 3 days, 3-fold after 6 days, and 5-fold after 10 days. In the absence of PC the mean XOR activity remained relatively constant over the 10-day culture period. In previous studies EGF was found to inhibit lactogenic-hormone induction of β-casein in HC11 cells (21). The inset in Fig. 1 shows that, in agreement with these earlier results, EGF blocked PC stimulation of β-casein synthesis in our cultures as well. In contrast, the data in Table I show that EGF enhances the effects of prolactin and cortisol on XOR activity. These results suggest that the processes by which lactogenic hormones induce β-casein production in HC11 cells are distinct from those by which they increase XOR activity.

Increased XOR Activity Is the Result of Increased XOR Protein Synthesis

To clarify the mechanisms by which lactogenic hormones increase XOR activity, we first investigated the effects of prolactin and cortisol on *de novo* XOR synthesis in HC11 cells cultured in the presence of EGF. Cellular proteins were pulse-labeled with [^{35}S]methionine and labeled XOR was purified by benzamidine–Sepharose affinity chromatography, which selectively isolates catalytically active XOR (17), or by immunoprecipitation, which isolates total XOR. Figure 2 shows the purification of XOR from extracts of control and PC-treated cells by benzamidine–Sepharose chromatography. XOR activity from both control and PC-treated cells bound to benzamidine–Sepharose and was specifically eluted by 25 mM benzamidine (Figs. 2A and 2B). The purified enzyme had a K_m for xanthine of 1.7 μM and its D to O ratio was 3.3, indicating that it was purified as the NAD$^+$-dependent dehydrogenase (XD form) of XOR (22).

SDS–PAGE and phosphorimaging analysis of the [^{35}S]-labeled proteins eluted by benzamidine (insets in Figs. 2A and 2B) showed that the fractions from PC-treated cells containing the highest XOR activity were

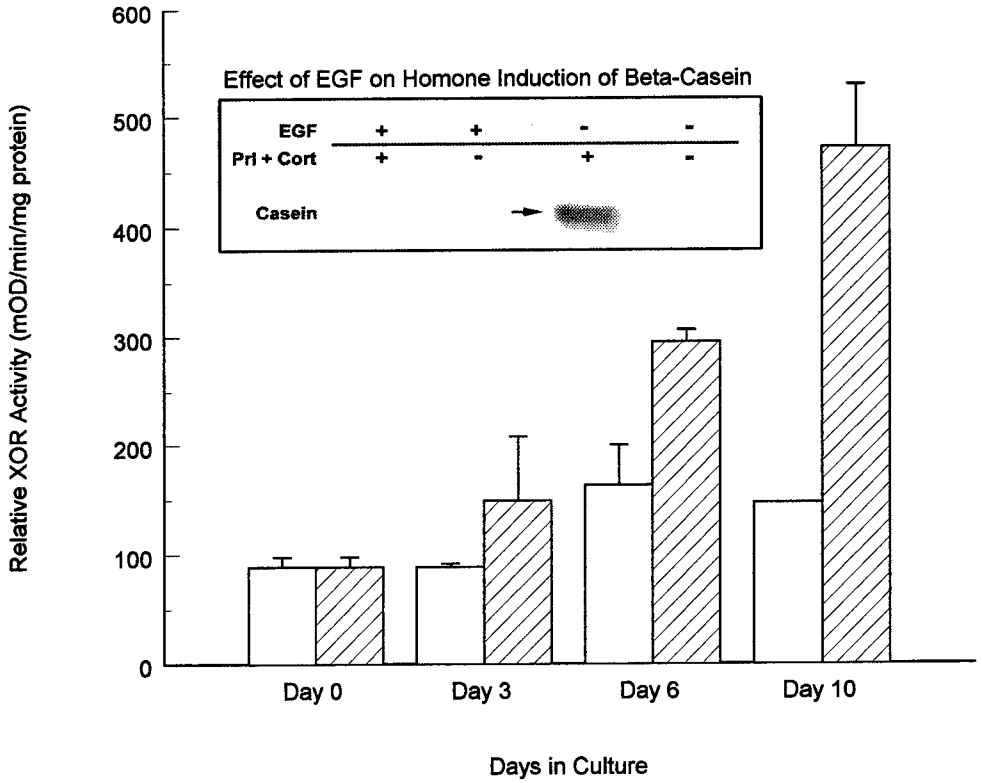

FIG. 1. Prolactin and cortisol increase XOR activity in HC11 cells in the presence of EGF. The relative activity of XOR is shown in confluent HC11 cells incubated in the presence (crosshatched bars) or absence (open bars) of prolactin and cortisol for the indicated times. HC11 cells were grown to confluency as described under Materials and Methods and then placed in serum-free medium containing insulin and EGF with or without prolactin and cortisol, as indicated. XOR activity is expressed as the allopurinol-sensitive rate of oxidation of xanthine/mg of cellular protein. Each value is the mean ± SD for triplicate culture wells. The inset shows the effects of EGF on the induction of β-casein by prolactin and cortisol. Confluent HC11 cells were incubated with or without prolactin and cortisol, as described above, in serum-free medium containing insulin and EGF (lanes 1 and 2) or in media containing insulin alone for 6 days. Cell extracts were analyzed for β-casein by SDS–PAGE and Western blotting with an anti-mouse casein antibody and an alkaline phosphatase-labeled secondary antibody. The arrow shows the position of mouse milk β-casein.

enriched in a band that comigrated with the intact 150-kDa subunit of purified bovine XOR (arrows) and reacted to anti-XOR antibodies (inset box, Fig. 2B). XOR protein was detectable by Western blotting in fractions from PC-treated cells with the greatest XOR activity (inset, Fig. 2B) but could not be detected in the most active fractions from control cells (data not shown). Thus, increased XOR synthesis appeared to be correlated with increased amounts of total XOR protein. The relative amounts of newly synthesized XOR protein in fractions isolated from control and PC-treated cells were estimated from the intensity of the [^{35}S]methionine-labeled XOR bands in the phophorimager analysis and are plotted (closed triangles) in Fig. 2. The data show good correspondence between XOR activity and [^{35}S]methionine-labeled XOR protein in these fractions. The XOR activity in benzamidine-eluted fractions from PC-treated HC11 cells was 5.5 times that of control cells in duplicate experiments. The total amount of [^{35}S]methionine-labeled XOR isolated from PC-treated cells, on the other hand, was 3.9

TABLE I

Effects of EGF on the Ability of Prolactin and Cortisol to Increase XOR Activity in HC11 Cells

Culture time (days)	Relative increase in XOR activity (% control)	
	EGF/minus medium	EGF/plus medium
3	89 ± 2	170 ± 30
6	162 ± 25	320 ± 12
10	220 ± 40	467 ± 75

Note. The effect of prolactin and cortisol (PC) on XOR activity in HC11 cells was examined in confluent HC11 cells incubated in serum-free medium supplemented with insulin and EGF (EGF/plus medium) or with insulin alone (EGF/minus medium) for 3, 6, or 10 days. XOR activity (rate of xanthine oxidation/mg of cellular protein) was determined in the cell lysates using the xanthine/DCIP assay (see Materials and Methods). The relative stimulation of XOR activity by PC was determined by normalizing XOR activity in PC-treated cultures to the activity in the corresponding control cultures and is shown as the percentage of control XOR activity. The values represent the mean ± SD for three separate experiments.

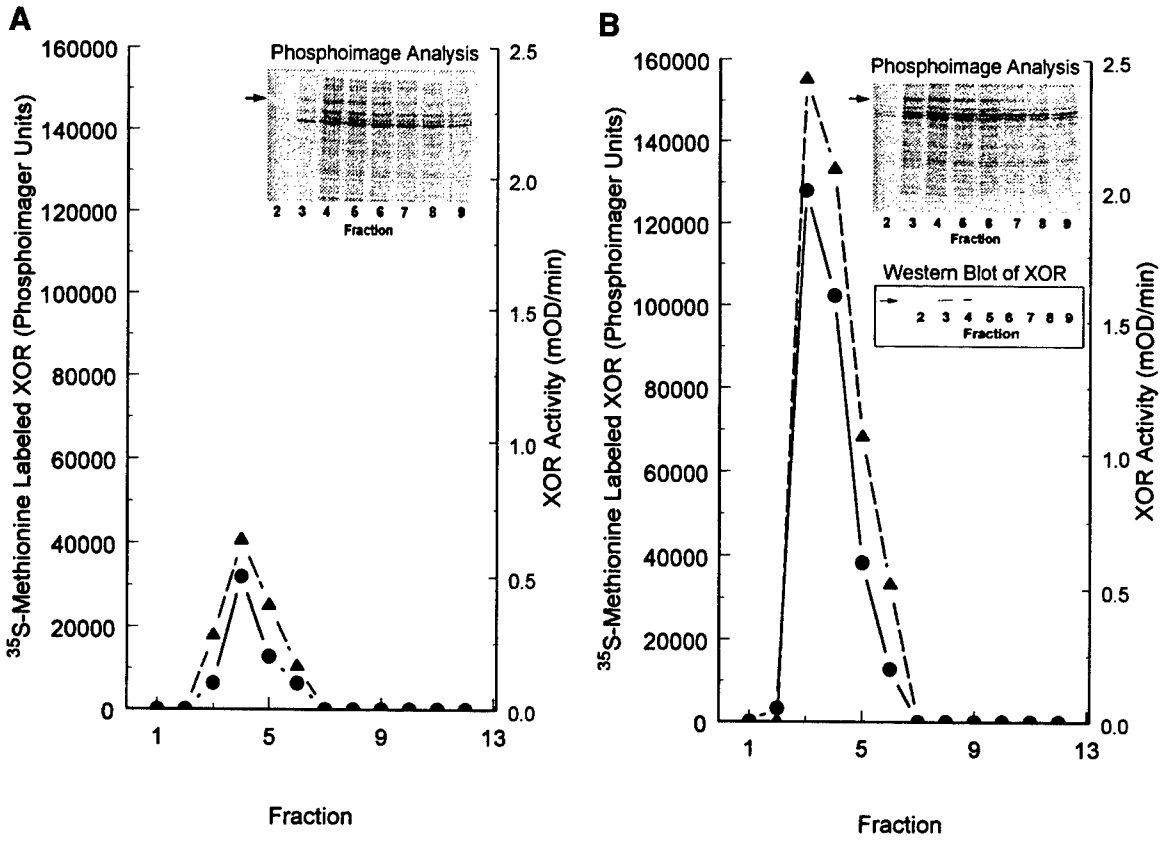

FIG. 2. Benzamidine–Sepharose purification of [^{35}S]methionine-labeled XOR. Confluent cultures of HC11 cells were incubated in serum-free medium containing insulin and EGF in the absence (A) or presence (B) of prolactin and cortisol (PC) for 8 days, as described in the legend to Fig. 1, and then pulsed with [^{35}S]methionine for 16 h. The cells were extracted and XOR purified by benzamidine–Sepharose chromatography (see Materials and Methods). The relative levels of XOR activity (●) and [^{35}S]methionine-labeled XOR (▲) in the fractions eluted by 25 mM benzamidine are shown. XOR activity was determined using the xanthine/DCIP assay and is expressed as the relative rate of xanthine oxidation. [^{35}S]Methionine-labeled proteins in the benzamidine-eluted fractions were examined by SDS–PAGE and phosphorimaging (insets A and B). The relative amount of [^{35}S]-labeled XOR in these fractions (arrows in the phosphorimage analyses) was quantified using ImageQuant software (Molecular Devices) and is expressed as relative phosphorimager units per fraction. A Western blot of XOR protein in the benzamidine-eluted fractions from PC-treated cells is shown in the box in B. The arrows in each inset show the position of migration of intact, purified, bovine milk XOR.

times that isolated from control cells in the same experiments. Because benzamidine–Sepharose chromatography selectively purifies only catalytically active and intact XOR (17) it was possible that HC11 cells contained significant amounts of inactive and/or partially degraded XOR. To investigate this possibility [^{35}S]methionine-labeled XOR was immunoprecipitated and analyzed by SDS–PAGE (Fig. 3). A single radioactive protein band, which comigrated with purified intact XOR subunits (arrow), was specifically precipitated from extracts of control and PC-treated cells using antibodies to XOR. In contrast, no bands were precipitated using preimmune sera. Quantitation of [^{35}S]methionine-labeled XOR in the immunoprecipitates showed that PC-treated HC11 cells had an average of 3.6 ± 0.1 times (N = 4) more newly synthesized XOR than control cells. The total amount of [^{35}S]methionine-labeled protein in PC-treated cells was similar to that of control cells (1.05 ± 0.1 times; N = 4) and the composition of the labeled proteins appeared to be identical (Fig. 3B). No XOR synthesis was detected when HC11 cells were incubated with 30 μM cycloheximide for 4 h prior to pulsing with [^{35}S]methionine and 82% ± 2.5% (N = 2) of the basal and PC-stimulated XOR synthesis was blocked by 10 μM cycloheximide. Thus, lactogenic hormones appear to be directly affecting the synthesis of XOR in HC11 cells.

Prolactin and Cortisol Decrease XOR Turnover

Together, the benzamidine–Sepharose and immunoprecipitation findings indicate that most of the newly synthesized XOR in HC11 cells is intact and catalytically active. However, in both cases the stimulation of XOR synthesis did not completely account for the increased XOR activity. To determine if lactogenic hormones also affected XOR degradation, we next investigated the effects of prolactin and cortisol on XOR

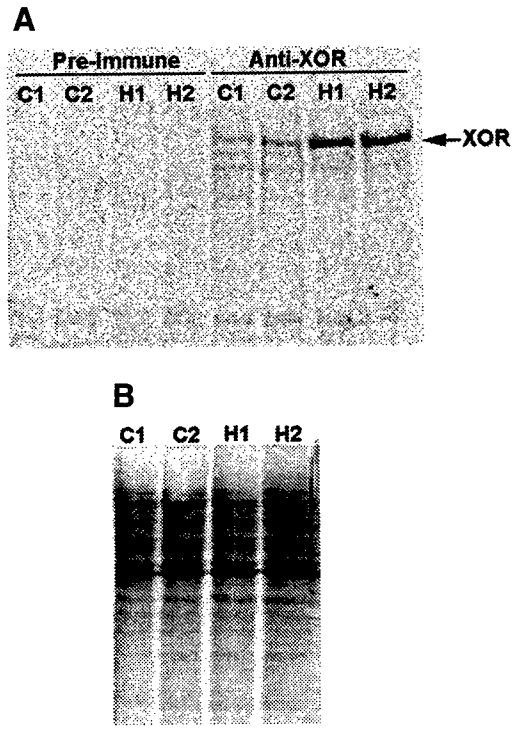

FIG. 3. Immunoprecipitation of [^{35}S]methionine-labeled XOR. Duplicate plates of confluent HC11 cells were incubated in serum-free media containing insulin and EGF with (H1 and H2) or without (C1 and C2) prolactin and cortisol for 8 days and pulsed with [^{35}S]methionine for 16 h. The cells were then extracted and immunoprecipitated with anti-XOR antibodies or with preimmune serum. Immunoprecipitated XOR (A) and total labeled proteins (B) were analyzed by SDS–PAGE and phosphorimaging. The migration position of immunoprecipitated XOR is shown relative to purified, intact, bovine XOR (arrow in A).

turnover in HC11 cells. The amount of XOR remaining in control and PC-treated cells was determined 24 and 48 h after pulse-labeling proteins with [^{35}S]methionine. Figure 4 shows that the rate of loss [^{35}S]methionine-labeled XOR from both control and hormone-treated cells appears to follow first-order kinetics. In control cells the average half-time ($t_{1/2}$) for XOR degradtion was 33 h (N = 2), in agreement with previous estimates of the turnover rate ($t_{1/2}$ = 28.3 h) for XOR in Swiss 3T3 cells (18). In contrast, the average $t_{1/2}$ for XOR degradation in PC-treated cells was 59 h (N = 2), nearly double that of control cells. The loss of total [^{35}S]methionine protein also followed first-order kinetics with an average $t_{1/2}$ (22 h) that was the same for control and PC-treated cells. These results show that lactogenic hormones increase XOR activity in HC11 cells by both increasing synthesis and decreasing the turnover of XOR.

Prolactin and Cortisol Increase XOR mRNA Levels

The next question to be addressed was whether the increased synthesis of XOR could be attributed to increased levels of XOR mRNA. Figure 5A shows a Southern blot of products obtained following RT-PCR of XOR mRNA in confluent HC11 cells cultured in the presence or absence of prolactin and cortisol for 24, 48, and 96 h. The blot shows relatively little effect of the hormones on XOR mRNA until the 4th day of culture. Quantitation of the relative amount of XOR mRNA in control cells showed that the steady-state levels of XOR mRNA did not change significantly over the 4-day time course. However, XOR mRNA in hormone-treated cells was slightly elevated by day 2 of culture and was 3.3 ± 0.2 times the control level by the 4th day of culture. Thus, there also appears to be a 2- to 3-day lag in the ability of PC to elevate XOR mRNA levels in HC11 cells. To determine if this lag is specific for XOR, we investigated the effects of prolactin and cortisol on the steady-state mRNA levels of lactoferrin (another secreted mammary gland protein), β-actin (a common cellular protein), and aldehyde oxidase (another member of the molybdenum hydroxylase gene family (3). Figure 5B shows that prolactin and cortisol increased Lf mRNA levels in HC11 with a similar lag period but did not affect the steady-state mRNA levels of β-actin or aldehyde oxidase. Thus, these effects of prolactin and cortisol appear to be specific for milk proteins.

Lactogenic Hormones Stimulate XOR Expression by a MAP Kinase-Dependent Pathway

The observation that prolactin and cortisol increase XOR, but not β-casein, in HC11 cells grown in the presence of EGF suggested that lactogenic hormones might use different signaling pathways to regulate XOR and β-casein expression. To investigate this possibility we examined the effects of kinase inhibitors on the stimulation of XOR activity by prolactin and cortisol. Figure 6A shows that genistein, a specific protein tyrosine kinase inhibitor (23), blocked the PC-induced increase in XOR activity. This effect was dose dependent and the effective concentration range agreed with values previously reported for genistein (24, 25). Genistein had the opposite effect on XOR activity in control cells, in which incubation with this compound produced a significant dose-dependent increase in XOR activity. Treatment with genistein, however, did not alter XOR activity *in vitro* or affect the appearance or number of HC11 cells at any concentration (data not shown). Similar effects of genistein on the basal and prolactin-induced orinthine decarboxylase activity in primary cultures of mouse epithelial cells have been reported (24). Thus, the inhibitory effects of genistein on XOR activity appear to reflect selective interference with the actions of prolactin and cortisol and not a general toxic effect of this compound.

Previous studies have shown that lactogenic hormones can activate p42 MAP kinase in HC11 cells (26).

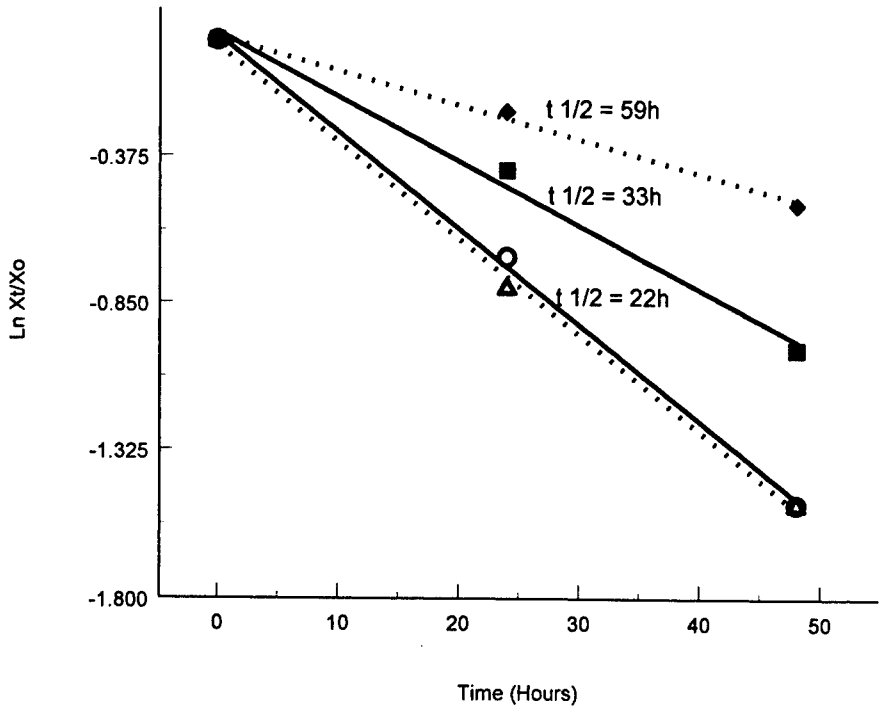

FIG. 4. Prolactin and cortisol decrease the turnover rate of XOR. The effects of prolactin and cortisol on the turnover rates of XOR and total protein were determined in confluent HC11 cells by pulse-chase analysis (see Materials and Methods). Logarithms of the ratio of [^{35}S]XOR remaining at the indicated times to the initial amount of [^{35}S]XOR in the cultures is plotted as function of chase time for cells incubated in the presence (◆) or absence (■) of prolactin and cortisol. The ratio of labeled total protein is plotted similarly for cells incubated in the presence (△) or absence (○) of prolactin and cortisol. The calculated turnover half-times for XOR and total protein are shown.

However, inhibiting MAP kinase activation with PD 98059 (a specific inhibitor of MEK 1/2—the upstream activator of p42 and p44 MAP kinase—27) did not interfere with lactogenic hormone induction of β-casein expression (26). To determine the involvement of MAP kinase activation in the effects of PC on XOR levels, HC11 cells were incubated with PC in the presence and absence of PD 98059 and assayed for XOR activity. Figure 6B shows that PD 98059 effectively blocked the ability of PC to increase XOR levels in HC11 cells. This effect was dose-dependent and the effective concentration range was between 20 and 50 μM. In contrast to genistein, PD 98059 did not alter XOR activity in control cells (Fig. 6B). PD 98059 also did not affect the appearance of HC11 cells, and it did not interfere with the enzymatic activity of purified XOR (data not shown). Thus, the decrease in XOR activity does not appear to be due to nonspecific effects on HC11 cells or to direct interference with the enzymatic activity of XOR.

Table II shows that PD 98059 also blocked the increase in *de novo* XOR synthesis brought about by prolactin and cortisol but did not affect basal XOR synthesis. In the absence of PD 98059, prolactin and cortisol increased XOR synthesis threefold over control cultures, whereas in the presence of 50 μM PD 98059, XOR synthesis was increased only 23%. In contrast,

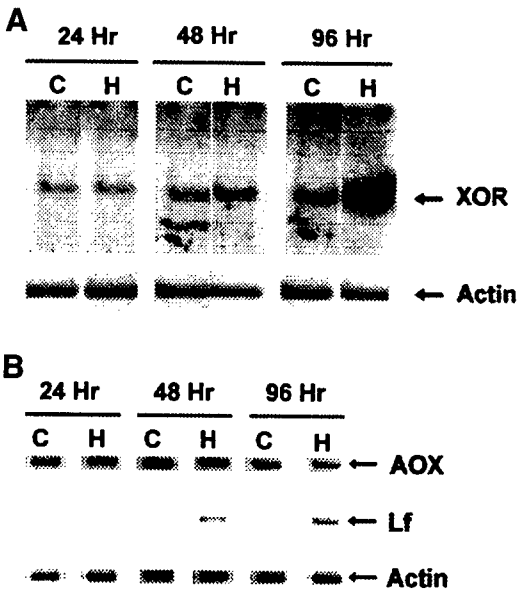

FIG. 5. Prolactin and cortisol selectively increase the steady-state mRNA levels of XOR. Confluent HC11 cells were incubated in serum-free media containing insulin and EGF in the presence (H) or absence (C) of prolactin and cortisol for 24, 48, and 96 h and mRNA levels were analyzed by RT-PCR and Southern blotting. (A) Results of phosphorimager analysis of Southern blots of XOR and β-actin (Actin) mRNA. (B) Results of phosphorimager analysis of Southern blots of aldehyde oxidase (AOX), lactoferrin (Lf), and β-actin (Actin) mRNA.

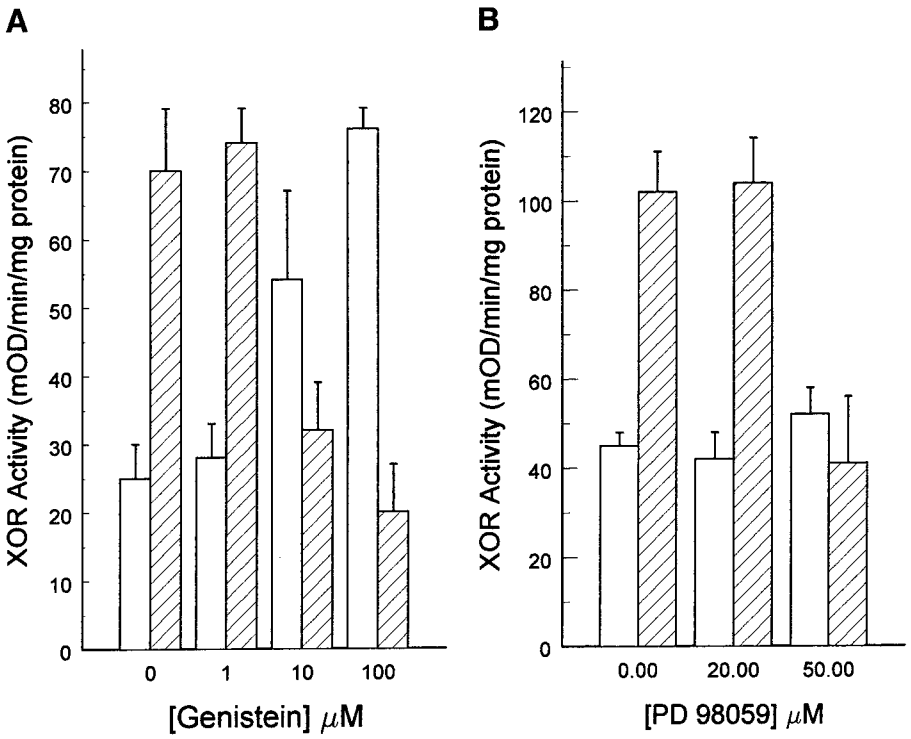

FIG. 6. Genistein and PD 98059 block the effects of prolactin and cortisol on XOR expression. The relative amounts of XOR activity in control (open bars) and lactogenic hormone-treated (hatched bars) cultures are shown for HC11 cells incubated with the indicated concentrations of genistein (A) and PD 98059 (B). XOR activity is expressed as the allopurinol-sensitive rate of xanthine oxidation/mg cellular protein. The values are means ± SD for triplicate culture wells. Similar results were obtained in two experiments.

the level of [^{35}S]methionine incorporation into XOR in control cultures was similar in the presence and absence of PD 98059. In addition, 50 μM PD 98059 did not interfere with [^{35}S]methionine incorporation into total protein (data not shown). Thus, the effect of PD 98059 on XOR synthesis appears to be due to a specific inhibition of the actions of prolactin and cortisol and not to a general reduction in XOR synthesis or nonspecific interference with protein synthesis by HC11 cells. Together, these results provide evidence that the effects of prolactin and cortisol on XOR synthesis are mediated by activation of the MAP kinase pathway and involve the activation of a specific protein tyrosine kinase or kinases.

TABLE II

PD 98059 Blocks the Effect of Prolactin and Cortisol on XOR Synthesis

Treatment conditions	[^{35}S]Methionine-labeled XOR
Control cells	1500 ± 230
PC-treated cells	4843 ± 515
Control cells + PD 98059	1724 ± 313
PC-treated cells + PD 98059	2130 ± 346

Note. The relative amounts of [^{35}S]methionine-labeled XOR in HC11 cells are shown for control and hormone-treated cells that were incubated with and without 50 μM PD 98059 for 6 days. Cells were pulsed with [^{35}S]methionine for 16 h and [^{35}S]methionine-labeled XOR was isolated by immunoprecipitation. The amount of [^{35}S]methionine-labeled XOR was determined by phosphorimaging analysis after SDS–PAGE. The values are average ± range for duplicate assays.

DISCUSSION

The lactogenic combination of the hormones prolactin and cortisol is known to play a prominent role in the functional development of the mammary gland and the expression of milk proteins (28, 29). However, the cellular mechanisms that mediate the actions of these hormones appear to be complex and remain poorly defined (29, 30). In the present study we investigated the effects of prolactin and cortisol on XOR activity in the HC11 mammary epithelial cell line. Our results show that these hormones increase XOR by increasing the accumulation of XOR mRNA, stimulating XOR synthesis, and decreasing XOR turnover. These effects are consistent with *in vivo* studies of XOR during mammary development, in which increases in XOR mRNA and protein were documented during lactogenesis and lactation in mouse mammary glands (7–9), and provide evidence that prolactin and cortisol are physiologically important regulators of XOR expression in mammary

tissue. Although it is well established that prolactin and glucorticoids can regulate transcription of milk proteins (29–31), our finding that these hormones slowed the turnover of XOR suggests that they also affect the level of specific milk proteins by nongenetic mechanisms. This possibility is supported by the observation that XOR activity and protein levels in mouse mammary glands continue to increase during lactation, while the level of XOR mRNA remained constant (8). Similar, nongenetic effects of lactogenic hormones on β-casein levels in primary cultures of mouse mammary epithelial cells have also been reported (32). Given the need for increased milk production to support neonatal growth, such mechanisms may play an important role in maintaining milk protein levels.

β-Casein induction in HC11 cells by lactogenic hormones has been the subject of extensive study (30, 33–35). In our study we found that the combination of prolactin and cortisol also induced the expression of lactoferrin and β-casein, but they did not affect the expression of common, nonsecreted, cellular proteins (β-actin and aldehyde oxidase). Thus, the increased expression of XOR in HC11 cells appears to be a specific lactogenic response to prolactin and cortisol, rather than a general affect of these hormones on cellular metabolism. Moreover, because XOR and AOX are closely related members of the molybdenum hydroxylase family, with similar structural and functional properties (3), it is unlikely that the increased expression of XOR is due to selective effects of lactogenic hormones on molybdenum hydroxylase gene expression in general.

Recent studies of XOR in human and goat milk indicate that mammary epithelial cells can synthesize and secrete significant amounts of catalytically deficient enzyme (4, 12). Our results, however, show that the properties of newly synthesized XOR in HC11 cells are similar to those of the highly active enzyme from lactating mouse mammary glands (7). Immunoprecipitation of metabolically labeled XOR demonstrated that, in both control and hormone-treated cells, the enzyme was composed of single species on SDS–PAGE with the same molecular weight as intact purified XOR from bovine milk. In addition, both the basal and the hormone-induced XOR activities could be extracted by benzamidine–Sepharose affinity chromatography and there was good correspondence in the purification of xanthine oxidizing activity and metabolically labeled XOR subunits. Furthermore, the purified enzyme from HC11 cells had a K_m for xanthine that agreed with that reported for purified XOR from rodent tissue (17, 36). Thus, most of the enzyme in HC11 cells appears to be intact and capable of oxidizing purine substrates and to possess biochemical and kinetic properties that are similar to purified XOR from other sources (1, 7, 17, 36). Finally, XOR has been shown to function as an oxidase (XO: E.C. 1.1.3.22) or as a dehydrogenase (XD: E.C. 1.1.3.204), depending on the oxidation state of its cysteine thiols (37). Our study shows that the predominant form of the purified enzyme from HC11 cells was XD, which indicates that XOR exists primarily in the reduced form in HC11 cells. This finding is consistent with our previous studies demonstrating that XD is the predominant tissue form of XOR in the lactating mouse mammary gland (7).

Although prolactin and cortisol enhance the expression of both β-casein and XOR in HC11 cells, evidence presented in this study suggests that the mechanisms that mediate these effects may be different. EGF inhibits the ability of prolactin and cortisol to stimulate β-casein expression, whereas it modestly promotes the effects of these hormones on XOR levels. The induction of β-casein by lactogenic hormones is mediated by the JAK2/STAT5 intracellular signaling pathway (29). In the presence of EGF, the lactogenic hormone activation of STAT5 and its subsequent interaction with the β-casein promoter are blocked (29). However, the molecular basis for this inhibition is unknown and EGF stimulation has also been shown to promote nuclear translocation and activation of STAT5 binding to other DNA regulatory elements (38, 39). Thus, both positive and negative interactions between the EGF and the STAT5 pathways appear to be possible. While additional studies will be required to establish the nature of the interactions between the EGF and the lactogenic hormone signaling pathways, our results suggest that there may be differences in the signaling processes that mediate the effects of lactogenic hormones on β-casein and XOR expression. One possible difference is the MAP kinase pathway. Lactogenic hormones activate both the JAK/STAT5 and the MAP kinase pathways in HC11 cells (26, 29); however, lactogenic hormone induction of β-casein expression is independent of MAP kinase activation (26). In contrast, our results showed that inhibitors of MAP kinase activation blocked lactogenic hormone stimulation of XOR synthesis. Thus, while lactogenic hormone regulation of β-casein expression appears to involve the selective activation of the JAK/STAT pathway, the MAP kinase pathway appears to play a significant role in regulation of XOR expression by these hormones.

In summary, our study provides evidence that prolactin and cortisol increase XOR levels in mammary epithelial cells by coordinately increasing the *de novo* synthesis and decreasing the degradation rate of XOR. Increased *de novo* synthesis of XOR is associated with increased steady-state levels of XOR mRNA and appears to be a specific lactogenic response. Although additional studies will be required to fully delineate the cellular and genetic mechanisms by which lactogenic hormones regulate XOR expression, our results

suggest that they are mediated by a tyrosine kinase- and MAP kinase-dependent signaling pathway.

ACKNOWLEDGMENTS

The authors thank Jennifer Richer, Carol Lang, and Joe McCord for helpful discussions and critical reading of the manuscript.

REFERENCES

1. Bray, R. C. (1975) *in* The Enzymes (Boyer, P. D., Ed.), 3rd ed., pp. 299–419, Academic Press, New York.
2. Stryer, L. (1988) Biochemistry, 3rd ed., Freeman, New York.
3. Wooton, J. C., Nicolson, R. E., Cock, J. M., Walters, D. E., Burke, J. F., Doyle, W. A., and Bray, R. C. (1991) *Biochim. Biophys. Acta* **1057,** 157–185.
4. Keenan, T. W., and Patton, S. (1995) *in* Handbook of Milk Composition (Jensen, R. G., Ed.), pp. 5–50, Academic Press, New York.
5. Jarasch, E. D., Grund, C., Bruder, G., Heid, H. W., Keenan, T. W., and Franke, W. W. (1981) *Cell* **25,** 67–82.
6. Mather, I. H., and Keenan, T. W. (1998) *J. Mam. Gland Biol. Neoplasia* **3,** 259–273.
7. McManaman, J. L., and Wright, R. M. (1999) *Arch. Biochem. Biophys.* **371,** 308–316, 1999.
8. McManaman, J. L., Monks, J., Wright, R. M., and Neville, M. C. Submitted for publication.
9. Kurosaki, M., Zanotta, S., Calzi, M. L., Garattini, E., and Terao, M. (1996) *Biochem. J.* **319,** 801–810.
10. Ringo, D. L., and Rocha, V. (1983) *Exp. Cell Res.* **147,** 216–210.
11. Hayden, T. J., Brennan, D., Quirke, K., and Murphy, P. (1991) *J. Dairy Res.* **58,** 401–409.
12. Abadeh, S., Killacky, J., Benboubetra, M., and Harrison, R. (1992) *Biochem. Biophys. Acta* **117,** 25–32.
13. Ball, R. K., Friis, R. R., Schoenenberger, C. A., Doppler, W., and Groner, B. (1988) *EMBO J.* **7,** 2089–2095.
14. Doppler, W., Groner, B., and Ball, R. K. (1988) *Proc. Natl. Acad. Sci. USA* **86,** 104–108.
15. Merlo, G. R., Graus-Porta, D., Cella, N., Marte B. M., Taverna, D., and Hynes, N. E. (1996) *Eur. J. Cell Biol.* **70,** 97–105.
16. Chammas, R., Taverna, D., Cella, N., Santos, C., and Hynes, N. E. (1994) *J. Cell Sci.* **107,** 1031–1040.
17. McManaman, J. L., Shellman, V., Wright, R. M., and Repine, J. E. (1996) *Arch. Biochem. Biophys.* **332,** 135–141.
18. Terada, L. S., Piermattei, D., Shibao, G. N., McManaman, J. L., and Wright, R. M. (1997) *Arch. Biochem. Biophys.* **348,** 163–168.
19. Harlow, E., and Lane, D. (1988) Antibodies: A Laboratory Manual, Cold Spring Harbor Laboratory Press, Cold Spring Harbor, NY.
20. Ausubel, F. M., Brent, R., Kingston, R. E., Moore, D. D., Seidman, J. G., Smith, J. A., and Struhl, K. (1993) Current Protocols in Molecular Biology, Wiley, New York.
21. Schmitt-Ney, M., Happ, B., Hofer, P., Hynes, N. E., and Groner, B. (1992) *Mol. Endo.* **6,** 1988–1997.
22. Waud, W. R., and Rajagopalan, K. V. (1976) *Arch. Biochem. Biophys.* **172,** 354–364.
23. Akiyama, T., Ishida, J., Nakagawa, S., Ogawara, H., Watanabe, S-I., Itoh, N., Shibuya, M., and Fukami, Y. (1987) *J. Biol. Chem.* **262,** 5592–5595.
24. Fan, G., and Rillema, J. A. (1992) *Mol. Cell. Endocrinol.* **83,** 51–55.
25. Gouilleux, F., Wakao, H., Mundt, M., and Groner, B. (1994) *EMBO J.* **13,** 4361–4369.
26. Wartmann, M., Cella, N., Hofer, P., Groner, B., Liu, X., Hennighausen, L., and Hynes, N. E. (1996) *J. Biol. Chem.* **271,** 31863.
27. Alessi, D. R., Cuenda, A., Cohn, P., Dudley, D. T., and Saltiel, A. R. (1995) *J. Biol. Chem.* **270,** 27489–27494.
28. Topper, Y., and Freeman, C. S. (1981) *Physiol. Rev.* **60,** 1049–1056.
29. Groner, B., and Gouilleux, F. (1995) *Curr. Opin. Genet. Dev.* **5,** 587–594.
30. Groner, B., Altiok, S., and Meier, V. (1994) *Mol. Cell. Endocrinol.* **100,** 109–114.
31. Rosen, J. M., Rodgers, J. R., Couch, C. M., Bisbee, C. A., David-Inouye, Y., Campbell, S. M., and Yu-Lee, L. Y. (1986) *Ann. N. Y. Acad. Sci.* **478,** 63–76.
32. Nagamatsu, Y., and Oka, T. (1983) *Biochem. J.* **212,** 507–515.
33. Altiok, S., and Groner, B. (1998) *Biochem. Soc. Symp.* **63,** 115–131.
34. Goodman, H. S., and Rosen, J. M. (1990) *Mol. Endocrinol.* **4,** 1661–1670.
35. Raught, B., Liao, W. S., and Rosen, J. M. (1995) *Mol. Endocrinol.* **9,** 1223–1232.
36. Terao, M., Cazzaniga, G., Ghezzi P., Bianchi, M., Falciani, F., Perani P., and Garattini, E. (1992). *Biochem. J.* **283,** 863–870.
37. Waud, W. R., and Rajagopalan, K. V. (1976) *Arch. Biochem. Biophys.* **172,** 365–379.
38. Ruff-Jamison, S., Chen, K., and Cohen, S. (1995) *Proc. Natl. Acad. Sci USA* **92,** 4215–4218.
39. Richer, J., Lang, C., Manning, N., Owen, G., Powell, R., and Horwitz, K., (1998) *J. Biol. Chem.* **273,** 31317–31326.

Archives of Biochemistry and Biophysics
Vol. 371, No. 2, November 15, pp. 308–316, 1999
Article ID abbi.1999.1432, available online at http://www.idealibrary.com on IDEAL®

Mouse Mammary Gland Xanthine Oxidoreductase: Purification, Characterization, and Regulation[1]

J. L. McManaman,*[,2] M. C. Neville,† and R. M. Wright‡

*Department of Biochemistry and Molecular Genetics, †Department of Physiology, and ‡Webb-Waring Institute for Antioxidant Research, University of Colorado Health Sciences Center, Denver, Colorado 80262

Received June 17, 1999, and in revised form July 28, 1999

Xanthine oxidoreductase (XOR) has been purified from lactating mouse mammary tissue and its properties and developmental expression have been characterized. XOR was purified 80-fold in two steps using benzamidine–Sepharose affinity chromatography. The purified enzyme had a specific activity of 5.7 U/mg and an activity to flavin ratio of 192. SDS–polyacrylamide gel electrophoresis showed that it was composed of a single (150 kDa) band and N-terminal sequence analysis verified that it was intact mouse XOR. Isoelectric focusing showed that purified XOR was composed of three catalytically active, electrophoretic variants with p*I* values of 7.55, 7.65, and 7.70. The majority of the XOR activity in both pregnant and lactating mammary glands was shown to exist as NAD+-dependent dehydrogenase (XD form), while the enzyme in freshly obtained mouse milk exits as O2-dependent oxidase (XO form). The activity and protein levels of XOR selectively increased in mammary tissue during pregnancy and lactation. The time course of these increases was biphasic and correlated with the functional maturation of the mammary gland. These results indicate that XOR may have novel, mammary gland-specific functions, in addition to its role in purine metabolism. © 1999 Academic Press

Key Words: **molybdenum hydroxylases; xanthine oxidase; mammary gland; affinity purification; isoforms; enzyme properties; developmental changes.**

Xanthine oxidoreductase (XOR)[3] is a member of the molybdenum hydroxylase family of proteins (1). The enzyme is a 300,000-kDa dimer composed of identical subunits. Each subunit consists of 1333–1358 amino acids, depending on the species, and contains binding sites for molybdopterin, iron, and flavin cofactors (1, 2). In mammals, XOR can exist in two intraconvertible enzymatic forms: a dehydrogenase (XD; EC 1.1.3.204) which utilizes NAD^+ as an electron acceptor and an oxidase (XO; EC 1.2.3.22) which utilizes O_2 as an electron acceptor (2). Both enzymatic forms are identical in size, subunit composition, and cofactor requirements and are capable of oxidizing a wide range of substrates (1). In the organisms studied to date XD appears to be the primary gene product and the predominant form of the enzyme in mammalian tissues (3, 4). At present, the cellular mechanisms that regulate the relative tissue levels of the XD and XO forms of XOR have not been defined. However, XD can be converted to XO in a reversible process by sulfhydryl oxidation or in an irreversible process by proteolytic action (3). Although it is unclear if the XD and XO forms of the enzyme serve distinct biological roles, differences have been detected in their structural and kinetic properties (3). In addition, high levels of the XO form have been associated with tissue injury and certain diseases (5, 6) and are believed to contribute to oxidative damage of cells through the generation of cytotoxic oxygen metabolites (H_2O_2; O_2^- and OH^-) (5). The XD form, on the other hand, may be an important component in the defense

[1] This work was supported by NIH Grants HL 45582-05A2 and HL 52509-03 and NCI Cancer Core Grant CA46934 and the Robert and Helen Kleberg Foundation.

[2] To whom correspondence and reprint requests should be addressed. Fax (303) 315-8215. E-mail: jim.mcmanaman@UCHSC.edu.

[3] Abbreviations used: XOR, xanthine oxidoreductase; XO, xanthine oxidase; XD, xanthine dehydrogenase; PMSF, phenylmethylsulfonyl fluoride; DCIP, dichloroindophenol; CBB, Coomassie brilliant blue; PVDF, polyvinylidene difluoride; DTT, dithiothreitol; MLG, milk lipid globules; MLGM, milk lipid globule membrane; IEF, isoelectric focusing; AFR, activity to flavin ratio.

0003-9861/99 $30.00

against oxygen radical damage through its role in the synthesis of uric acid, a potent antioxidant (7).

One of the primary biological functions of XOR in mammals is purine degradation where the enzyme catalyzes the rate-limiting step in the oxidation of xanthine and hypoxanthine to uric acid (8). Biochemical and genetic studies of XOR from phylogenetically diverse species have shown that there has been a general conservation of the catalytic properties, cofactor requirements, and primary structure of the enzyme during evolution (2). Although such a high degree of conservation is consistent with the general importance of this enzyme in purine metabolism, its tissue and cell expression patterns suggest that it may also have additional, tissue-specific functions distinct from its common role in purine metabolism (9).

One of the richest sources of XOR is bovine milk (10). The enzyme in bovine milk exists exclusively in the XO form and is found primarily in milk lipid globules (MLG). XOR comprises as much as 13% of the total MLG protein and appears to be tightly associated with the cytoplasmic surface of the plasma membrane that surrounds these structures (10). At present, the functional significance of such high levels of the XO form of the enzyme in MLGs is unclear, and the basis for the association of XOR with milk lipid globule membranes is unknown. Immunocytochemical (9) and histochemical studies (11) showed that detectable amounts of XOR were found only in the milk-producing alveolar epithelial cells in lactating bovine mammary tissue and that the enzyme appeared to be concentrated at the apical surface of these cells (9). These observations suggest that the levels of XOR in mammary tissue are regulated by cell-specific processes and that it may have mammary or milk-specific functions. However, its role in the mammary gland remains unknown, due in part to a lack of information about the properties of the enzyme from mammary tissue and its regulation during the reproductive cycle.

Earlier studies of XOR expression in mouse mammary tissue suggested that XOR may play a role in mammary gland differentiation (12–14), but the details of its development during the reproductive cycle were not fully established. Further, XOR has not been purified from mammary tissue and the properties of mammary XOR have not been investigated. In addition, studies of XOR from human and goat milk have shown that the enzyme from these species is inactive toward traditional purine substrates (10). Thus, there may be species-dependent differences in the properties of XOR. To address these issues and the potential role of XOR in mammary gland development we (i) purified XOR from lactating mouse mammary glands, (ii) characterized the properties of the purified enzyme and investigated the catalytic form of XOR in mammary tissue and milk, and (iii) characterized the development of XOR in mouse mammary glands throughout the reproductive cycle. Our studies demonstrate that mouse mammary gland XOR is a highly active enzyme composed of three major isoforms and that it comprises a relatively large amount of the soluble protein in lactating mouse mammary glands. Our studies also indicate that the expression of XOR in mammary gland development is a complex process regulated by the reproductive stage and is associated with the functional maturation of the mammary gland.

EXPERIMENTAL PROCEDURES

Materials. CD-1 mice were obtained from Charles River Inc. and maintained as a breeding colony in the Animal Resource Center of the University of Colorado Health Sciences Center. Benzamidine–Sepharose, xanthine, and dichloroindophenol (DCIP) were obtained from Sigma Chemical Co. Ampholines, nitrocellulose membranes, and molecular weight markers were obtained from Bio-Rad. Hyperbond polyvinylidene difluoride (PVDF) membranes were obtained from Beckman Inc. Antisera to bovine XOR were generously provided by Dr. Lance Terada (Dallas, TX).

Preparation of mammary gland extracts and purification of XOR. XOR was purified from mammary glands of lactating CD-1 mice by affinity chromatography on benzamidine–Sepharose (15). Fourth and fifth mammary glands were removed from animals on the 12th to 13th days of lactation. The glands were dissected free of connective tissue, finely minced, and washed several times to remove milk. The glands were then blotted dry, weighed, and homogenized in 3 vol of ice-cold 0.1 M NaH_2PO_4, pH 7, containing 0.4 mM EDTA, 100 μM PMSF, 1 mM salicylate (PEPS) using a Dounce homogenizer. Homogenates were centrifuged for 30 min at 28,000*g*. The supernatant was removed, treated with fresh PMSF, and placed in a 65°C water bath for 10 min. Insoluble material was removed by centrifugation, and solid ammonium sulfate was added to the supernatant (HS) to a final concentration of 60% saturation. After 30–60 min on ice precipitated proteins (60-P) were removed by centrifugation, resuspended in a minimal volume of PEPS, and desalted by chromatography on Sephadex G-50(M) equilibrated in 0.1 M glycine, 0.1 M NaCl, pH 9 (GS9). The desalted extract was applied to a 5- to 7-ml column of benzamidine–Sepharose equilibrated in GS9. The column was washed with 3 column volumes of GS9 and XOR was eluted with 25 mM benzamidine in GS9 as previously described (15). The specific activity of XOR refers to the units (μmol uric acid/min) of xanthine:O_2 oxidoreductase activity at room temperature/mg protein (see below).

Isolation of milk lipid globule membranes. Milk lipid globules were isolated by the addition of sucrose to fresh whole bovine milk (obtained locally) to a final concentration of 5% (w/v). An equal volume of TBS (25 mM Tris, 138 mM NaCl, 3 mM KCl, pH 7.4) was carefully layered on top of this solution and the mixture was centrifuged at 2500*g* for 30 min at ambient temperature. The cream layer was removed, diluted with TBS, and churned in a Waring blender at low speed until butter curds formed. The curds were removed by straining through cheesecloth and milk lipid globule membranes were isolated from the buttermilk by centrifugation at 125,000*g* for 60 min at 4°C. The remaining triglycerides and the supernatant were removed and the membrane pellet was suspended in 50 mM Tris, 1 mM EDTA, pH 7.5 (TE buffer) using brief sonication. The membrane suspension was then washed by two cycles of centrifugation at 100,000*g* for 1 h at 4°C and resuspended by sonication in TE buffer. The protein concentration of resuspended membranes ranged from 2 to 4 mg/ml.

Enzyme and protein assays. The combined activities of xanthine oxidase and xanthine dehydrogenase in mammary gland extracts were assayed by the reduction of DCIP using xanthine as a substrate as described previously (15). Briefly, XOR activities were measured at room temperature in substrate solution containing 0.15 mM xanthine, 0.025 mM DCIP, 10% (v/v) dimethyl sulfoxide, 1.0 mM EDTA, 0.1% (v/v) catalase in 50 mM Tris, pH 8. Assays were performed in microtiter plates by monitoring the rate of DCIP reduction at 595 nm on a kinetic microplate reader (Molecular Devices, Menlo Park, CA). Relative activity values were calculated as the allopurinol-sensitive rates of DCIP reduction per milligram of protein in the homogenates. Enzymatic activity specifically associated with either XD (xanthine: NAD^+ oxidoreductase activity) or XO (xanthine:O_2 oxidoreductase activity) was calculated as the allopurinol-sensitive rates of aerobic formation of uric acid from xanthine in the presence and absence of 0.6 mM NAD^+ and the ratio of XD to XO activities (XD/XO) was calculated according to Waud and Rajagopalan (3) as described previously (15). Protein was quantified using the bicinchoninic acid method (16).

Conversion of XD to XO. XOR was converted to XD by incubation with 2 mM DTT for 1 h at room temperature. The DTT was removed by dialysis or gel filtration on Sephadex G-25 prior to adding milk lipid globule membranes (MLGMs). MLGMs were incubated with allopurinol (50 μM) to inactivate membrane-associated XOR and subjected to two cycles of centrifugation at 100,000*g* for 45 min to remove remaining allopurinol. The membranes were resuspended in TE, added to XD to final concentration of 10% (v/v), and incubated at room temperature with gentle mixing. A portion of the suspension was heated in a boiling water bath for 20 min prior to incubation with XD. At the indicated times XD and XO activities were determined as described above.

Electrophoretic analyses. SDS–polyacrylamide gel electrophoresis (SDS–PAGE) and isoelectric focusing analyses (IEF) of XOR were conducted as described previously (15). Protein bands were detected by staining the gels with Coomassie brilliant blue (CBB) and prestained molecular weight marker proteins (Kaleidoscope Standards, Bio-Rad) were used to estimate protein molecular weights. Native isoelectric focusing of purified XOR was conducted at 15°C for 1700 V-h in 5% acrylamide gels containing pH 3 to 10 ampholines. Protein was detected by silver staining and enzymatically active XOR isoforms were detected by staining with xanthine/nitroblue tetrazolium (15). IEF of XOR under denaturing conditions was conducted at 20°C for 1700 V-h in 5% acrylamide gels containing 4 M urea. Purified XOR was incubated in 8 M urea containing 2 mM DTT, 0.1% NP-40 at 60°C for 30 min prior to analysis. IEF pH gradients were determined by measuring the pH values in sequential adjacent 1-mm sections of the focused gel, and protein bands were visualized by staining with CBB.

Western blots. Samples were separated by SDS–PAGE in 7% acrylamide gels and electrophoretically transferred to nitrocellulose membranes at 90 V for 30 min in Caps buffer, pH 11. The membranes were blocked in 3% gelatin overnight at room temperature, washed twice with TBS, pH 8, containing 0.1% Tween 20 (TBS–Tween), and incubated overnight at 4°C with 1/500 dilution of rabbit antibodies affinity purified against a 71-kDa C-terminal fragment of bovine XOR according to Madara *et al.* (17). Immunoreactive bands were detected using ExtrAvidin reagents (Sigma) and bromochloroindoyl phosphate/nitroblue tetrazolium substrate (18) or with [^{125}]I-Protein A (Amersham Inc.). Immunoreactive bands were quantified using a Phosphoimager and ImageQuant software (Molecular Dynamics).

Protein sequence determination. N-terminal amino acid sequence analyses were performed by automated Edman degradation of proteins after electrophoretic transfer to PVDF (19). Analyses were performed at the University of Colorado Cancer Center's Protein Chemistry Core Facility using an Applied Biosystems Model 477A automated protein sequencing instrument equipped with an in-line Model 120 HPLC.

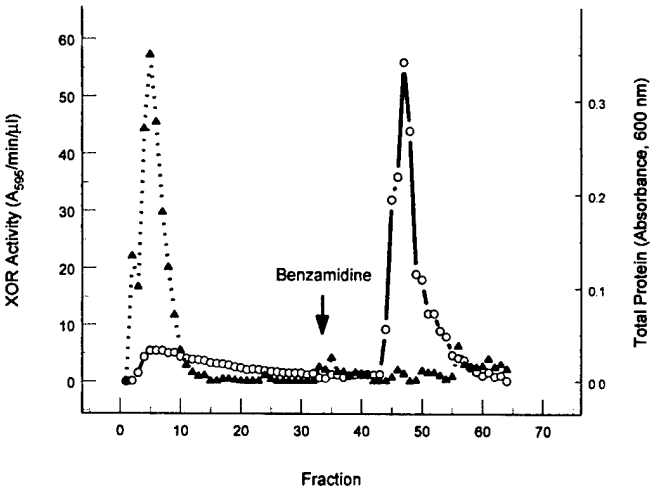

FIG. 1. Affinity purification of XOR from mouse mammary glands. The desalted 60-P fraction obtained from an extract of 12-day lactating mouse mammary glands was subjected to chromatography on benzamidine–Sepharose as described under Experimental Procedures. The levels of protein (dashed line, solid triangles) and XOR activity (solid line, open circles) are shown for individual fractions. The column was eluted with 25 mM benzamidine starting at the arrow.

RESULTS

Purification of mouse mammary gland XOR. XOR was purified from extracts of lactating mouse mammary glands by ammonium sulfate precipitation and affinity chromatography on benzamidine–Sepharose. The elution profiles of protein and XOR activity from benzamidine–Sepharose are shown in Fig. 1. The majority of the protein eluted in the flowthrough and wash fractions, while most of the XOR activity bound to the column and was eluted by 25 mM benzamidine. The enzymatic activities in the flowthrough and benzamidine-eluted fractions were verified as XOR by inhibition with allopurinol (data not shown). A representative purification of XOR is shown in Table I. The average purification of XOR from the heat-treated supernatant by ammonium sulfate fractionation and benzamidine–Sepharose was 80 ± 6-fold. The purified enzyme had an average specific activity of 5.7 ± 0.8 U/mg which is comparable to highly purified enzyme preparations from other sources. In addition, purified XOR had an A_{280}/A_{450} ratio of 4.5 and an activity to flavin ratio (AFR) of 192 indicating that it was free of contaminating proteins and inactive enzyme forms.

Properties of mouse mammary gland XOR. The relative degree of purification achieved by benzamidine–Sepharose chromatography and the purity of XOR ob-

TABLE I

Purification of XOR from Lactating Mouse Mammary Glands

Purification step	Protein (mg)	Specific activity (units/mg)	AFR	Fold purification
Heat-treated SPN	144	0.07	7	1
60% ammonium sulfate pellet	47.5	0.21	9	3
Benzamidine–Sepharose pool	1	5.2	192	74

Note. XOR was purified from six inguinal glands obtained from lactating mice on L12–L13. Protein and enzyme activity measurements and the calculations of specific activity and AFR are described under Experimental Procedures. The fold purification refers to the relative increase in specific activity at each step in the purification.

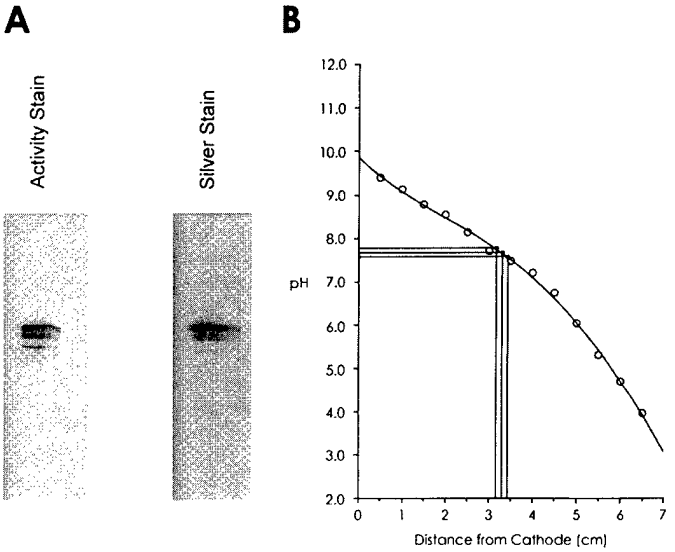

FIG. 3. Isoelectric focusing analysis of affinity-purified mouse mammary gland XOR. (A) Purified XOR was subjected to IEF using pH 4–10 amopholines. Adjacent lanes then were analyzed for XOR activity or for total protein by silver staining. (B) Determination of p*I* values for urea-denatured XOR isoforms. Purified XOR was denatured in 8 M urea and subjected to IEF using pH 4–10 ampholines in acrylamide gels containing 4 M urea. The pH values of the gel (open circles) and the migration positions of XOR isoforms (closed circles) are plotted as a function of the distance from the cathode.

tained by this procedure are illustrated in Fig. 2. This figure shows that purified XOR (lane I) contained a single protein species of approximately 150 kDa. The N-terminal amino acid sequence of this band was TRT-TVDELVFFVNGKKVVEKNADPE which is identical to AA 2–26 of the sequence deduced from mouse XD cDNA (20) and verifies that the purified enzyme was

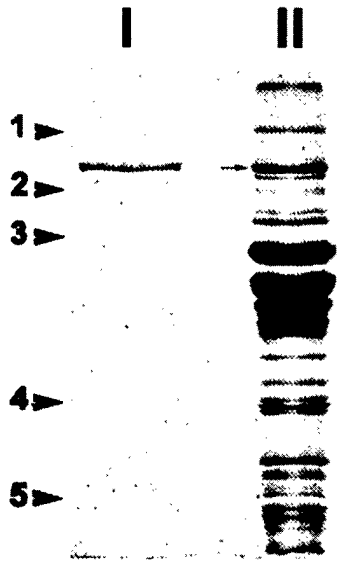

FIG. 2. Electrophoretic analysis of purified mouse XOR. Coomassie blue staining patterns are shown for affinity-purified mouse mammary gland XOR (lane I) and the 60% ammonium sulfate precipitate of mammary gland extracts from 12-day lactating mice (lane II). The migration positions of molecular weight standards (Kaleidoscope prestained standards, Bio-Rad) are shown by numbered arrowheads on the left. 1, myosin (205 kDa); 2, β-galactosidase (119 kDa); 3, bovine serum albumin (85 kDa); 4, carbonic anhydrase (41.8 kDa); 5, soybean trypsin inhibitor (31.8 kDa). The arrow indicates the band in the 60-P fraction that was sequenced.

intact except for missing its N-terminal methionine. Figure 2 also shows that the 60% ammonium sulfate precipitate of mammary gland extracts (lane II) is enriched in a band at approximately 150 kDa that comigrates with purified XOR. Amino acid sequence analysis of this protein gave a single sequence that was identical to the N-terminal sequence obtained for purified mouse XOR and verifies that XOR is a major protein in the 60-P fraction.

The isoform composition of purified mouse mammary gland XOR was investigated by IEF under both nondenaturing and denaturing conditions. To compare the IEF pattern of XOR enzymatic activity with the staining pattern of total XOR protein, duplicate samples of purified XOR were loaded onto adjacent lanes and subjected to IEF under nondenaturing conditions. After focusing, one lane was stained for activity while the other was stained for protein by silver staining. Figure 3A shows that IEF resolved purified XOR into three major protein bands and that each protein band exhibited enzymatic activity. To obtain accurate p*I* values for XOR isoforms, affinity-purified XOR was denatured in 8 M urea and subjected to equilibrium IEF in urea-containing gels. Figure 3B is a plot of the relative migration of the urea-denatured XOR isoforms at 20°C as a function of the pH gradient of the gel. The average

TABLE II

Ratio of XD to XO in Mammary Tissue and Milk

Reproductive stage	Mammary gland XD/XO (%XD)	Milk XD/XO (%XD)
Virgin	7 ± 3 (88%)	NA
12-Day pregnant	6.5 (87%)	NA
7-Day lactating	2.3 ± 0.7 (70%)	0.09 (9%)
15-Day lactating	4 ± 1.1 (80%)	0.11 (10%)
22-Day lactating	2.2 ± 0.6 (69%)	NA

Note. The relative amounts of XD and XO in mammary gland extracts and milk are shown at selected stages of the reproductive cycle. The relative amounts of XD and XO in each extract are expressed as XD/XO values. The percentage of the enzyme in the XD form at each stage is shown in parentheses. XD/XO values for mammary glands are average values ± SD from individual assays of three separate mouse mammary glands. The XD/XO values for milk are single assays.

p*I* values of the XOR isoforms determined from this plot were 7.55 ± 0.01, 7.65 ± 0.02, and 7.70 ± 0.02.

Because no effort was made to prevent oxidation during purification, the ratio of the dehydrogenase to oxidase activities (XD/XO) of purified XOR was 0.05 which indicates that XO was the principal enzymatic form of XOR obtained after purification. However, incubating the purified enzyme with 5 mM DTT at room temperature for 2 h increased its XD/XO ratio to 3.2. Thus, as with XOR from other mammalian sources, the enzyme purified from mouse mammary glands can be converted from the XO form to the XD form by thiol active compounds (3). Previous studies have demonstrated that the predominant form of XOR in bovine milk is XO (21), whereas XD appears to be the predominant form of the enzyme in undamaged mammalian tissues (2, 3). Given the high rate of milk production in lactating mice it was uncertain which enzyme form would predominate in mammary tissue. It was also unclear whether the enzyme form of XOR in fully lactating mammary tissue differed from that found in nonlactating mammary tissue. Table II shows the ratio of XD to XO activity (XD/XO) in mammary gland extracts at various stages of the reproductive cycle. Although XD is the major form of XOR in mammary tissue at all stages of the reproductive cycle, the relative proportion of the XD form was higher in the mammary glands of virgin and pregnant animals. In contrast, 90% of the enzyme in fresh mouse milk (treated with protease inhibitors and assayed within 5 min of milking) was XO. The preponderance of the XO form in fresh milk does not appear to simply reflect the inability of lower levels of reducing equivalents in milk to maintain XOR in the XD form, since several hours were required for complete air oxidation of purified XD to XO in the absence of reducing agents (see below). These results suggest that the rapid appearance of XO in milk is a specific process regulated by its association with milk lipid globule membranes. This possibility was investigated by determining the effect of washed MLGMs on the conversion of purified XD to XO. Figure 4 shows that in the absence of MLGMs relatively little of the purified XD (XD/XO = 2.3) was converted to XO after 90 min at room temperature. In contrast, the addition of MLGMs to purified XD resulted in its complete conversion to XO within 5 min. Boiling MLGMs prior to their addition to XD abolished their ability to catalyze the conversion of XD to XO as shown by similar XD to XO conversion rates for untreated XD and XD incubated with boiled MLGMs (Fig. 4). Thus, MLGMs appear to possess enzyme activity capable of catalyzing the conversion of XD to XO and the kinetics of this process are consistent with the rapid appearance of XO in milk.

Changes in XOR levels during the reproductive cycle. Earlier studies demonstrated that the enzyme activity and protein levels of XOR in lactating mouse mammary tissue are substantially greater than those in virgin mammary tissue (12–14). However, the time course by which these changes occur was not fully delineated. To better characterize how XOR levels change during mammary gland development we determined the relative levels of XOR activity and immunoreactive protein in the mammary tissue of virgin, preg-

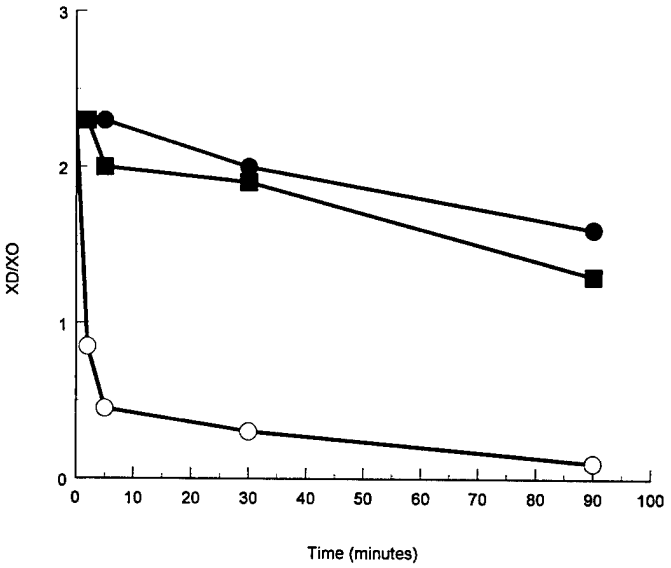

FIG. 4. Effect milk lipid globule membranes on XD to XO conversion. The conversion of XD to XO is shown as a function of incubation time in 50 mM Tris, 1 mM EDTA, pH 8 (●), or in 50 mM Tris, 1 mM EDTA, pH 8, containing isolated bovine milk lipid globule membranes (○) or isolated lipid globule membranes that were boiled for 20 min (■). The initial XD/XO ratio was 2.3 and corresponds to 70% of the XOR in XD form.

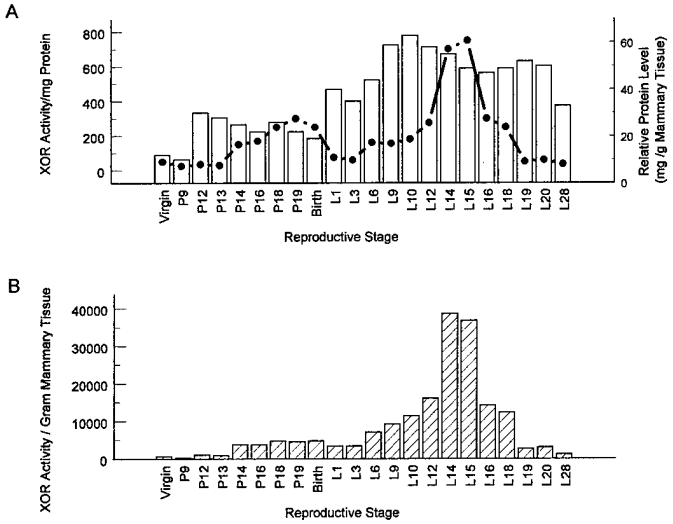

FIG. 5. Changes in the relative activity of XOR in mouse mammary glands during the reproductive cycle. (A) The relative activity of XOR (mOD/min/mg protein: solid circle) in mammary gland extracts and the relative protein content (mg protein/wet wt of mammary gland in grams: open bar) of mouse mammary glands are plotted as a function of reproductive stage. (B) The amount of XOR activity (mOD/min)/g of mammary tissue is shown as a function of reproductive stage. Relative XOR activities refer to allopurinol-sensitive rates determined using the xanthine/DCIP assay.

nant, and lactating mice at multiple time points throughout the reproductive cycle. Figure 5 shows the change in XOR activity in mouse mammary tissue during the reproductive cycle. In Fig. 5A, relative XOR activity is expressed per milligram of mammary gland protein and is compared with the amount of soluble protein per gram of mammary tissue at various reproductive stages. The results show that the relative XOR activity in mammary glands began to increase on about day 14 of pregnancy (P14) and reached an initial peak around birth. After parturition the relative XOR activity of the glands decreased slightly initially but then increased again and peaked at approximately day 15 of lactation (L15) before returning to virgin levels by L19–L20. The decline in the relative XOR activity that occurs at parturition does not appear to be due to a decrease in enzyme levels but rather to marked increases in the synthesis of the major milk proteins (e.g., β-casein, α-lactalbumin) that occurs at the onset of lactation. As shown in Fig. 5B, if the levels of XOR activity are normalized per gram of mammary tissue they remained relatively constant between P14 and L6. To verify the reproducibility of the time course of XOR development and determine the average increase in XOR during the reproductive cycle, we measured the relative XOR activities in mammary tissue from multiple animals at selected stages of the reproductive cycle. As shown in Table III there appears to be relatively little interanimal variability in the time course of XOR development. The average relative XOR activity increased nearly fourfold over the levels in virgin tissue by P15 and more than ninefold over virgin levels by L14 and had returned to near virgin levels by L19.

The increase in the relative XOR activity in mouse mammary tissue during pregnancy and lactation was accompanied by increased amounts of XOR protein. Figure 6 shows a representative Western blot of XOR in extracts of mouse mammary glands at various periods of the reproductive cycle. The primary immunoreactive band at all stages was the 150-kDa subunit of XOR, although weaker staining lower molecular weight bands (near the 71-kDa marker) were observed in some extracts (Fig. 6, lanes e and g). Thus, mammary gland XOR appears to be mostly intact throughout the reproductive cycle. Prior to P14 it was difficult to detect XOR by Western blotting, but between P14 and P18 there was a steady increase in the amount of XOR immunoreactivity in mammary gland extracts. The average amount of immunoreactive XOR in mammary tissue from P16 to P18 mice was 4.5 ± 1.1-fold ($N = 3$) greater than that found in virgin mouse mammary tissue. Between P18 and L6 there was relatively little change in XOR immunoreactivity; however, by L15–L16 it had increased an additional 2.1 ± 0.2-fold ($N = 3$) over P18 values resulting in an overall increase of 9.5-fold over the levels in virgin mammary tissue. In both pregnant and lactating mouse mammary tissue

TABLE III

Changes in Mammary Gland XOR Specific Activity during the Reproductive Cycle

Reproductive stage	Average relative XOR activity (avg ± SD)	Relative increase in XOR activity (% of virgin values)
Virgin	43 ± 14	100
12-Day pregnant	52 ± 7	121
15-Day pregnant	164 ± 11	381
Birth	216 ± 16	502
2-Day lactating	82 ± 8	191
10-Day lactating	191 ± 30	440
14-Day lactating	400 ± 111	930
16-Day lactating	315 ± 45	730
19-Day lactating	68 ± 20	158

Note. The change in the relative XOR activity in mouse mammary glands during the reproductive cycle is shown. XOR activity is shown as the average relative XOR activity in extracts of mouse mammary tissue at selected stages of the reproductive cycle. Relative XOR values refer to allopurinol-sensitive xanthine oxidation rates per milligram of protein. Xanthine oxidation rates were determined using DCIP as an electron acceptor (see Experimental Procedures). Each value is the mean ± SD of three separate tissue extracts. The relative increase in XOR activity is shown as the percentage increase over the average relative XOR values in virgin glands.

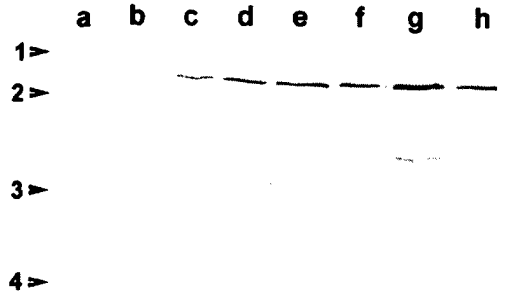

FIG. 6. Changes in the levels of XOR immunoreactive protein in mouse mammary glands during the reproductive cycle. The relative levels of XOR in extracts of mammary glands from mice at various stages of the reproductive cycle were investigated by immunoblot analysis using affinity-purified anti-XOR antibodies. Prior to SDS–PAGE, mammary gland extracts were concentrated by precipitation in 60% ammonium sulfate; precipitated protein was redissolved in 25 mM Hepes, pH 7.5. Each lane contains 25 μg protein. a, virgin; b, P14; c, P16; d, P18; e, L1; f, L6; g, L16; h, L19. Immunoreactive bands were detected with [^{125}]I-Protein A. The migration positions of molecular weight standards (Kaleidoscope prestained standards, Bio-Rad) are shown by numbered arrowheads on the left. 1, myosin (205 kDa); 2, β-galactosidase (119 kDa); 3, bovine serum albumin (85 kDa); 4, carbonic anhydrase (41.8 kDa).

XOR was found only in alveolar epithelial cells by immunofluorescence microscopy (data not shown). Thus, the changes in XOR content in the gland appear to reflect selective increases in the amount of XOR in milk-secreting cells.

DISCUSSION

In this study we characterized the biochemical properties and development of mouse mammary gland XOR. XOR was purified as a highly active enzyme by affinity chromatography on benzamidine–Sepharose. The average specific activity of the purified enzyme was comparable to highly purified XOR from other sources (15, 22, 24) and was significantly greater than the values reported for the enzyme isolated from human milk (23). In addition, the AFR of our XOR preparation was close to the theoretical maximum (200) predicted for XOR (1). Thus, it also appears to be free of inactive enzymatic forms.

SDS–PAGE and amino acid sequence analyses verified that our preparation of XOR was structurally intact and homogenous. However, IEF analysis, under both native and urea-denaturing conditions, showed that it exhibited a significant amount of charge heterogeneity. Isoelectric variants of bovine milk XOR have been demonstrated previously by two-dimensional gel electrophoresis using protein staining and immunological detection methods (9, 25) and enzymatically active XOR isoforms have been identified in partially purified preparations of bovine milk XOR by isoelectric focusing (15, 25). However, the number of isoforms reported for bovine milk XOR has been variable (9, 25), and the basis for the isoforms is unclear since these studies were performed on XOR preparations of variable purity, structural integrity, and catalytic activity. Consequently, the contribution that intact, but enzymatically inactive forms of the enzyme such as those found in human milk (27) made to the apparent charge heterogeneity reported for XOR in these preparations was unclear. Similarly, it was unclear if isoelectric variants detected by enzymatic activity were due to distinct forms of XOR or to the presence of partially degraded, but catalytically active enzyme (15). In the present study we have demonstrated that charge heterogeneity exists in highly purified preparations of mouse mammary gland XOR that are free of inactive enzyme forms and are structurally intact. Moreover, we documented that each isoform was catalytically active and that the relative activity of each isoform was proportional to its silver-staining intensity. Thus, charge heterogeneity does not appear to be due to the presence of inactive, or partially degraded, forms of XOR. Similar isoelectric variants were observed for urea-denatured XOR and the experimentally determined p*I* values (7.55, 7.65, and 7.70 at 20°C) are in close agreement with the p*I* (7.62) calculated[4] from the amino acid sequence deduced from the cDNA of mouse XD (20). Since XOR appears to be a single-copy gene (28), these findings suggest that XOR isoforms are due to minor posttranslational modifications of a single gene product.

The observation that crude mammary gland extracts contained sufficient quantities of XOR to permit detection by Coomassie blue staining and N-terminal sequence analysis suggests that the enzyme is a major soluble protein of lactating mouse mammary glands. Our purification studies showed that the isolation of homogenous, high-specific-activity XOR from lactating mouse mammary tissue required only an 80-fold purification. Combined with a typical recovery of XOR activity of 50–60% this result suggests that XOR represents about 2% of the total soluble protein in lactating mammary tissue, which agrees with the estimated level (1% of the soluble protein) of XOR in lactating bovine mammary tissue (29). The biological significance of high cellular levels of XOR in lactating mammary glands is unknown. However, recent findings that the enzyme from human milk exhibits low catalytic activity toward traditional reducing substrates, such as xanthine and hypoxanthine (23, 27), suggest that purine metabolism may not be the principal role of XOR in mammary tissue.

[4] R. D. Appel, A. Bairoch, and D. F. Hochstrasser (1994) *Trends Biochem. Sci.* **19,** 258–260.

The predominant enzymatic form of XOR in mouse mammary tissue is dehydrogenase (XD). In virgin tissues and throughout lactation the majority (70–90%) of XOR in mouse mammary tissue exists in the XD form. In contrast, nearly all of the XOR in mouse milk exists in the XO form. Thus, the enzymatic properties of the intracellular form of XOR are distinct from those of the secreted form. At present, the basis for this difference is unknown. Although XD can be converted to XO by air oxidation or by partial proteolysis, it is unlikely that either of these processes is responsible for the preponderance of XO in mouse milk. In our study the relative activities of the XD and XO forms were measured within 5 min of collecting milk and at this time 90% of the enzyme existed as XO. In contrast, there appeared to be relatively little conversion of XD to XO in mammary tissue extracts exposed to air 30 to 40 min before assay. In addition, we found that several hours are required for complete oxidation of purified XD to XO in solutions exposed to air. Thus, it is unlikely that short exposure to air can account for the high levels of XO in milk. It is also unlikely that the XO form in mouse milk was generated by proteolytic conversion of XD to XO, as milk was treated with protease inhibitors, and the XOR in milk lipid globules was shown to be intact by SDS–PAGE and N-terminal amino acid sequence analyses (data not shown). These results raise the possibility that conversion of the XD to the XO form is a specific process that occurs relatively rapidly and may be associated with formation and/or secretion of MLG. This possibility is supported by our observation that milk lipid globule membranes are capable of catalyzing the conversion of XD to XO and by XO-specific histochemical studies (11) showing large amounts of XO in bovine milk lipid globules but relatively little XO in the milk-secreting epithelial cells of the bovine mammary gland. Coupled with immunocytochemical studies demonstrating that XOR is enriched on the apical plasma membrane of lactating bovine epithelial cells (9), these observations suggest that XD to XO conversion is associated with milk lipid secretion.

Previous studies documenting increased expression of XOR in mouse mammary glands during late pregnancy led to suggestions that it may play a role in mammary gland differentiation (12–14). The differentiation of alveolar epithelial cells into milk-secreting cells typically begins during the latter part of pregnancy (30). During this period there is increased expression of milk-specific proteins (e.g., casein) and the enzymes involved in the synthesis of milk components (30, 31). However, the synthetic and secretory capabilities of mammary epithelial cells continue to develop during lactation (30, 31). In mice, milk production and the levels of many of the key enzymes involved in the synthesis of milk components continue to increase, as nursing demands increase, until about the 15th day of lactation (32). Subsequently there is a rapid decline in milk production and milk protein levels as nursing demands decrease during the weaning period (32). Our results show that XOR protein and activity levels in the lactating mammary gland increase during both lactogenesis and lactation and decline during the weaning process. Thus, the levels of XOR appear to be correlated with changes in the functional status of the mammary gland. These observations suggest that XOR may be of functional importance to the lactating mammary gland and are consistent with the proposed involvement of XOR in the secretion of milk lipids (33).

REFERENCES

1. Bray, R. C. (1975) *in* The Enzymes, Vol. 12B, 3rd ed., pp. 299–419, Academic Press, New York.
2. Hille, R., and Nishino, T. (1995) *FASEB J.* **9,** 995–1003.
3. Waud, W. R., and Rajagopalan, K. V. (1976) *Arch. Biochem. Biophys.* **172,** 365–379.
4. Krenitsky, T. A., and Tuttle, J. V. (1978) *Arch. Biochem. Biophys.* **185,** 370–375.
5. Cross, C. E. (1987) *Ann. Internal Med.* **107,** 526–545.
6. Southorn, P. A., and Powis, G. (1988) *Mayo Clin. Proc.* **63,** 390–408.
7. Hilliker A. J., Duyf, B., Evans, D., and Phillips, J. P. (1992) *Proc. Natl. Acad. Sci. USA* **89,** 4343–4347.
8. Stryer, L. (1988) *in* Biochemistry, 3rd ed., Freeman, New York.
9. Jarasch, E. D., Grund, C., Bruder, G., Heid, H. W., Keenan, T. W., and Franke, W. W. (1981) *Cell* **25,** 67–82.
10. Keenan, T. W., and Patton, S. (1995) *in* Handbook of Milk Composition, Academic Press, NY.
11. Frederiks, W. M., and Marx, F. J. (1993) *Histochem. Cytochem.* **41,** 667–670.
12. Ringo, D. L., and Rocha, V. (1983) *Exp. Cell Res.* **147,** 216–210.
13. Hayden, T. J., Brennan, D., Quirke, K., and Murphy, P. (1991) *J. Dairy Res.* **58,** 401–409.
14. Kurosaki, M., Zanotta, S., Calzi, M. L., Garattini, E., and Terao, M. (1996) *Biochem. J.* **319,** 801–810.
15. McManaman, J. L., Shellman, V., Wright, R. M., and Repine, J. E. (1996) *Arch. Biochem. Biophys.* **332,** 135–141.
16. Smith, P. K., Krohn, R. I., Hemanson, G. T., Mallial, A. K., Gartner, J. H., Provenzano, M. D., Fujimoto, E. K., Goeke, N. M., Olson, B. J., and Klenk, D. C. (1985) *Anal. Biochem.* **150,** 76–85.
17. Madara, P. J., Banghart, L. R., Jack, L. J., Neira, L. M., and Mather, I. H. (1988) *Anal. Biochem.* **187,** 246–250.
18. Harlow, E., and Lane, D. (1988) Antibodies: A Laboratory Manual, Cold Spring Harbor Laboratory Press, Cold Spring Harbor, NY.
19. Matsudaira, P. (1987) *J. Biol. Chem.* **262,** 10035–10038.
20. Terao, M., Cazzaniga, G., Ghezzi, P., Bianchi, M., Falciani, F., Perani, P., and Garattini, E. (1992) *Biochem. J.* **283,** 863–870.
21. Battelli, M. G., Lorenzoni, E., and Stirpe, F. (1973) *Biochem. J.* **131,** 191–198.
22. Nishino, T., Nishino, T., and Tsushima, K. (1981) *FEBS Lett.* **131,** 369–372.
23. Abadeh, S., Killacky, J., Benboubetra, M., and Harrison, R. (1992) *Biochem. Biophys. Acta* **1117,** 25–32.

24. Carpani, G., Racchi, M., Ghezzi, P., Terao, M., and Garattini, E. (1990) *Arch. Biochem. Biophys.* **279,** 237–241.
25. Sullivan, C. H., Mather, I. H., Greenwalt, D. E., and Madara, P. J. (1982) *Mol. Cell Biochem.* **44,** 13–22.
26. Mather, I. H., Tamplin, C. B., and Irving, M. G. (1980) *Eur. J. Biochem.* **110,** 327–336.
27. Brown, A-M., Benboubetra, M., Ellison, M., Powell, D., Reckless, J. D., and Harrison, R. (1995) *Biochem. Biophys. Acta* **1245,** 248–254.
28. Chow, C. W., Clark, M., Rinaldo, J., and Chalkley, R. (1994) *Nucleic Acids Res.* **22,** 1846–1854.
29. Bruder, G., Heid, H. W., Jarasch, E-D., and Mather, I. H. (1983) *Differentiation* **23,** 218–225.
30. Tucker, A. (1994) *in* The Physiology of Reproduction (Knobil, E., and Neill, J. D., Eds.), Raven Press, New York.
31. Topper, Y. J., and Freeman, C. S. (1980) *Physiol. Rev.* **60,** 1049–1106.
32. Shipman, L. J., Docherty, A. H., Knight, C. H., and Wilde, C. J. (1987) *Q. J. Exp. Physiol.* **72,** 303–311.
33. Mather, I. H., and Keenan, T. W. (1998) *J. Mamm. Gland Biol. Neoplasia* **3,** 259–273.

THE JOURNAL OF BIOLOGICAL CHEMISTRY
Vol. 277, No. 24, Issue of June 14, pp. 21261–21268, 2002
Printed in U.S.A.

Structural and Conformational Analysis of the Oxidase to Dehydrogenase Conversion of Xanthine Oxidoreductase*

Received for publication, January 25, 2002, and in revised form, March 13, 2002
Published, JBC Papers in Press, March 25, 2002, DOI 10.1074/jbc.M200828200

James L. McManaman‡§ and David L. Bain¶

From the ‡Department of Physiology and Biophysics and ¶Department of Pharmaceutical Sciences, University of Colorado Health Sciences Center, Denver, Colorado 80262

Xanthine oxidoreductase (XOR) is a 300-kDa homodimer that can exist as an NAD^+-dependent dehydrogenase (XD) or as an O_2-dependent oxidase (XO) depending on the oxidation state of its cysteine thiols. Both XD and XO undergo limited cleavage by chymotrypsin and trypsin. Trypsin selectively cleaved both enzyme forms at Lys^{184}, while chymotrypsin cleaved XD primarily at Met^{181} but cleaved XO at Met^{181} and at Phe^{560}. Chymotrypsin, but not trypsin, cleavage also prevented the reductive conversion of XO to XD; thus the region surrounding Phe^{560} appears to be important in the interconversion of the two forms. Size exclusion chromatography showed that disulfide bond formation reduced the hydrodynamic volume of the enzyme, and two-dimensional gel electrophoresis of chymotrypsin-digested XO showed significant, disulfide bond-mediated, conformational heterogeneity in the N-terminal third of the enzyme but no evidence of disulfide bonds between the N-terminal and C-terminal regions or between XOR subunits. These results indicate that intrasubunit disulfide bond formation leads to a global conformational change in XOR that results in the exposure of the region surrounding Phe^{560}. Conformational changes within this region in turn appear to play a critical role in the interconversion between the XD and XO forms of the enzyme.

Xanthine oxidoreductase (XOR)[1] plays an important function in vertebrate metabolism by catalyzing the oxidation of xanthine to uric acid, the rate-limiting step in purine degradation (1). Native XOR is a 300,000-dalton dimer composed of identical and catalytically independent subunits. Each subunit consist of 1333–1358 amino acids, depending on the species, and contains binding sites for molybdopterin, iron, and flavin co-factors (2, 3). The genes and full-length coding regions for XOR from mammals, chickens, insects, and fungi have been described (4–10). Analysis of these cDNAs has shown that the amino acid sequence of XOR is highly conserved across the phylogenetic spectrum. The enzymes from rats, mice, humans, and cattle exhibit ~90% identity, while the chicken and *Drosophila* enzymes exhibit, respectively, 70 and 52% identity with mammalian enzymes (3).

In mammals, XOR can exist in two enzymatic forms: a dehydrogenase (XD; EC 1.1.3.204) which utilizes NAD^+ as an electron acceptor and an oxidase (XO; EC 1.1.3.22) which utilizes O_2 as an electron acceptor (11, 12). Both enzymatic forms are the product of the same gene and are identical in size, subunit composition, and co-factor requirements (2, 3). To date, XD appears to be the predominant enzyme form in freshly prepared mammalian tissues (11–13); however, it is often isolated in the XO form during purification (2). It is unclear if XD and XO serve distinct biological roles. High levels of the XO have been associated with tissue injury and certain diseases (14, 15) and are thought to contribute to oxidative damage of cells through the generation of cytotoxic oxygen metabolites (H_2O_2 and O_2^-) (14). The XD form, on the other hand, may be an important component in the defense against oxygen radical damage through its role in the synthesis of uric acid, a potent antioxidant (16).

The cellular mechanism(s) that regulate the relative tissue levels of the XD and XO forms of XOR are poorly defined. XD can be converted to XO in a reversible process by heating or oxidation of cysteine thiols to form disulfide bonds (11, 17). The oxidative conversion of XD to XO has been shown to be associated with the oxidation of selected cysteines (17), loss of NAD^+ binding affinity (3), alterations in redox and kinetic properties (18, 19), and conformational changes at the flavin-binding site (20, 21). However, specific protein domains involved in these changes have not been identified, and the underlying molecular basis of the redox-mediated XD to XO conversion is still uncertain. In addition, it is unclear to what extent conformational changes within the flavin-binding site reflect larger changes in the global conformation of XOR and whether such changes are necessary for the conversion of XD to XO. XD can also be irreversibly converted to XO by proteolysis (6, 11, 17). Recent crystallographic studies have shown that proteolysis of XD leads to structural alterations near the flavin cofactor domain (22). However, the crystallographic structure of intact XO generated by cysteine oxidation has not been solved, and thus it is unclear how similar the structure of disulfide-bonded XO is to proteolyzed XO. In the present study we have used peptide mapping, chromatography, and two-dimensional gel electrophoresis to identify differences in the solution conformations of XD and XO and to investigate the role conformation changes play in the XD to XO conversion.

EXPERIMENTAL PROCEDURES

Materials—XOR (2.5–3.1 IU/mg) isolated from bovine milk in the oxidase form (XO) according to Waud *et al.* (23) was a generous gift from Dr. Joseph McCord (Webb-Waring Antioxidant Research Institute, University of Colorado Health Sciences Center). Sequencing grade trypsin

* This work was supported by National Institutes of Health Grants HL 45582-05AZ and P01CHD38129. Microsequencing was performed at the UCHSC Cancer Center's Protein Chemistry Core Laboratory supported by Grant CA46934 from the NCI, National Institutes of Health. The costs of publication of this article were defrayed in part by the payment of page charges. This article must therefore be hereby marked "*advertisement*" in accordance with 18 U.S.C. Section 1734 solely to indicate this fact.

§ To whom correspondence should be addressed: Dept. of Physiology and Biophysics, University of Colorado Health Sciences Center, 4200 E. 9th Ave., Denver, CO 80262. Tel.: 303-315-7093; Fax: 303-315-8110; E-mail: jim.mcmanaman@uchsc.edu.

[1] The abbreviations used are: XOR, xanthine oxidoreductase; XO, xanthine oxidase; XD, xanthine dehydrogenase; BS3, bis(sulfosuccinimidyl) suberate; DTT, dithiothreitol; SEC, size exclusion chromatography; HPLC, high pressure liquid chromatography.

and chymotrypsin were purchased from Boehringer-Ingleheim Inc. BS3 (bis(sulfosuccinimidyl) suberate) was purchased from Pierce. Polyvinylidene difluoride membranes (Hyperbond) were purchased from Beckman Instruments Inc. Centricon ultrafiltration membranes were purchased from Amicon Inc. Other chemicals and reagents were obtained from either Sigma or Fischer Scientific.

Preparation of XD and Determination of XD and XO Isoforms—Purified XO was converted to XD by incubation with 5–10 mM DTT at room temperature for 1–2 h (17). The enzyme was then cooled to 4 °C and subjected to ultrafiltration at 4 °C using Centricon 10,000-Da cutoff membranes to remove DTT. Enzymatic activity specifically associated with either XD (xanthine:NAD^+ oxidoreductase activity) or XO (xanthine:O_2 oxidoreductase activity) was calculated as the allopurinol-sensitive rates of aerobic formation of uric acid from xanthine in the presence (XD) or absence (XO) of 0.6 mM NAD^+, and the ratio of XD to XO activities (D/O) was calculated according to Waud and Rajagopolan (12) as described previously (24). Total XOR activity (both XD and XO activities) was routinely assayed by the reduction of dichloroindophenol using xanthine as a substrate (xanthine/dichloroindophenol assay) as described previously (24). Total protein was quantified using the bicinchoninic acid method (25).

Protease Digestion—XOR (5–20 μg) in the XD or XO form was incubated at room temperature (25 °C) with 1/20 (w/w) chymotrypsin or trypsin in 50 mM Tris, 150 mM NaCl, pH 8, for 90 min. The reaction was stopped by the addition of phenylmethylsulfonyl fluoride. The samples were then assayed for enzyme activity and/or processed for SDS-PAGE analysis as described below.

Electrophoretic Analyses in One and Two Dimensions—Electrophoresis was performed using a mini-Protean II gel apparatus (Bio-Rad) with 0.75-mm spacers. For one-dimensional electrophoresis samples were diluted with an equal volumes of 2× concentrated SDS-PAGE sample buffer (0.125 M Tris, 4% SDS, 20% glycerol, 10% 2-mercaptoethanol, pH 6.5), heated for 3 min at 95 °C, and separated by electrophoresis in 10% acrylamide gels containing 0.1% SDS at room temperature. For two-dimensional electrophoresis samples were diluted with equal volumes of 2× concentrated SDS-PAGE sample buffer without 2-mercaptoethanol, heated for 3 min at 95 °C, and subjected to electrophoresis in 10% acrylamide gels as described above. When the tracking dye reached the bottom of the gel, electrophoresis was stopped and the protein-containing lanes were excised and prepared for electrophoresis in the second dimension by incubation in 3 ml of SDS-PAGE sample buffer containing 5% 2-mercaptoethanol for 1 h at 60 °C. After reduction the lanes were layered on top of the second dimension gel (10% acrylamide, 0.1% SDS) perpendicular to the direction of electrophoresis. Gaps were sealed with melted agarose (1%) containing 2% SDS, 50 mM DTT. After electrophoresis protein bands were detected by silver staining (26).

Chemical Cross-linking Studies—XO was cross-linked by reaction with a 50-fold molar excess of BS3 in phosphate-buffered saline, pH 7.5, according to the manufacturer's instructions.

Protein Sequence Determination—N-terminal amino acid sequence analyses were performed by automated Edman degradation of proteins electroblotted to polyvinylidene difluoride (27) using an Applied Biosystems Inc. model 477A automated protein sequencing instrument equipped with an in-line model 120 HPLC.

Size Exclusion-HPLC Analysis—HLPC-size exclusion chromatography (HPLC-SEC) analysis was performed on a Beckman System Gold Instrument using a 7.8 × 600-mm SEC-3000 column (Phenomenex Inc.) equilibrated in phosphate-buffered saline, pH 7.5. Chromatography was performed at room temperature at a flow rate of 1 ml/min. The elution of protein and enzyme activity were monitored at 220 nm using an online UV detector and (where indicated by collecting fractions) using an electronically activated fraction collector (Gilson, FC 203B) that was synchronously integrated to sample injection. Determination of XD and XO retention times was performed using a 25-μl injection loop and sample protein concentrations of 1 mg/ml. XO was converted to XD by incubation with 10 mM DTT at room temperature for at least 1 h prior to analysis. Mean retention times of each enzyme form were determined from a minimum of five HPLC-SEC analyses. The SEC properties of cross-linked XO were determined using a 100-μl injection loop. Eluted protein was collected into 0.3-ml fractions. XO activity was determined using the xanthine/dichloroindophenol assay. The electrophoretic characteristics of the cross-linked protein were determined by SDS-PAGE analysis and silver staining as described above.

RESULTS

XD and XO Have Different Proteolytic Digestion Patterns—Differences in the environment surrounding the flavin co-factor

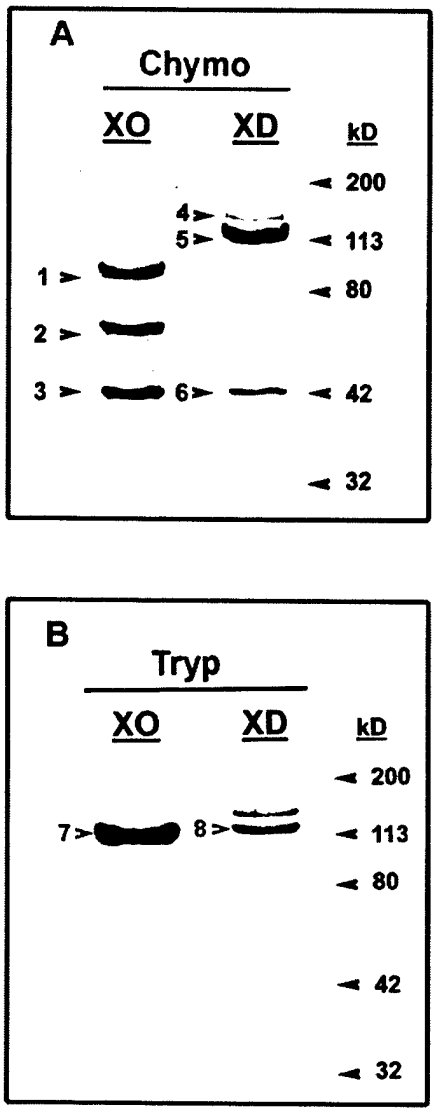

FIG. 1. **Trypsin and chymotrypsin digestion patterns of XD and XO.** XD (D/O = 7) and XO (D/O < 0. 1) were incubated with trypsin or chymotrypsin at 25 °C at an enzyme to protease ratio of 20/1 for the indicated times. The reaction was stopped with phenylmethylsulfonyl fluoride, and the digestion pattern was analyzed by SDS-PAGE using a 10% acrylamide gel. *A* shows the chymotrypsin digestion patterns of XD and XO. *B* shows the trypsin digestion patterns of XD and XO. The migration positions of molecular weight marker proteins (Kalidoscope standards, Bio-Rad) are shown on the *right* in each panel.

binding regions of XD and XO have been reported previously (20, 21). To determine whether these differences reflect broader structural changes we investigated the trypsin and chymotrypsin digestion patterns of both catalytic forms (Fig. 1). Chymotrypsin cleavage of XO (D/O = 0.1; 90% XO form) generated three major cleavage products with estimated molecular weights on SDS-PAGE of 85,000 (band 1), 64,000 (band 2), and 44,000 fragments (band 3). In contrast, chymotrypsin cleavage of XD (D/O = 7.1; 88% XD form) yielded a single major product with an estimated molecular weight of 125,000 (band 5) and minor amounts of a 44,000 fragment (band 6). Trypsin cleavage of either isozyme of XOR generated a single 125-kDa fragment (Fig. 1*B*, bands 7 and 8). In agreement with earlier studies (6, 11, 17) neither chymotrypsin nor trypsin digestion affected total XOR activity or altered the apparent molecular weights of the isozymes (data not shown).

The identities of the cleavage sites were determined by N-terminal sequencing and comparing the experimentally deter-

TABLE I

Identification of trypsin and chymotrypsin cleavage sites

The N-terminal sequences of peptide fragments generated by incubation of XD and XO with trypsin or chymotrypsin are shown with their corresponding positions within XOR and their cleavage sites.

Enzyme form	Protease	Fragment size	N-terminal sequence	Corresponding position in XOR	Cleavage position
XO	Trypsin	125 kDa (Band 7)	KDHTVTL	Lys^{185}-Leu^{191}	Lys^{185}
XO	Chymotrypsin	85 kDa (Band 1)	QEVPNGQ	Gln^{561}-Gln^{567}	Phe^{560}
XO	Chymotrypsin	64 kDa (Band 2)	TADELVFF	Thr^{2}-Phe^{9}	NA
XO	Chymotrypsin	44 kDa (Band 3)	NQKKDHT	Asn^{182}-Thr^{188}	Met^{181}
XD	Trypsin	125 kDa (Band 8)	KDHTVTL	Lys^{185}-Leu^{191}	Lys^{184}
XD	Chymotrypsin	125 kDa (Band 5)	NQKKDHT	Asn^{182}-Thr^{188}	Met^{181}

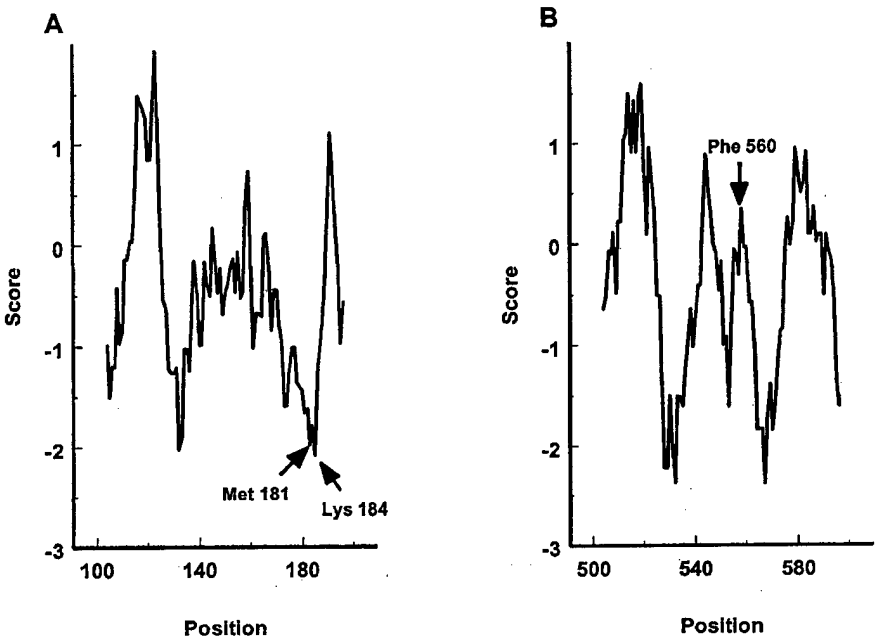

FIG. 2. **Hydropathy profile of regions surrounding Met^{181} and Phe^{560} of bovine XOR.** Kyte and Doolittle hydropathy profiles of bovine XOR from Val^{101}–Phe^{201} (*A*) and from Gly^{502}–Asn^{601} (*B*). The hydropathy profiles are based on the amino acid sequence deduced from bovine XOR cDNA (7). The locations of trypsin and chymotrypsin cleavage sites are indicated in each panel.

mined sequences to the deduced sequence of bovine XD cDNA (7). Table I shows the sequences of the first 7 amino acids of the major XD and XO cleavage products, the position of these sequences within the enzyme, and the corresponding cleavage site. The N-terminal sequences of the 125-kDa fragments (bands 7 and 8) generated by trypsin digestion of XD or XO correspond to Lys^{185}–Leu^{191} and are consistent with cleavage of both enzyme forms at Lys^{184}. The sequence of the 125-kDa fragment (band 5) generated by chymotrypsin digestion of XD corresponds to Asn^{182}–Thr^{188} and is consistent with cleavage at Met^{181}. Based on the deduced amino acid sequence of bovine XD the calculated molecular mass values for peptide fragments from Asn^{182} to Val^{1331} (the C terminus of bovine XD) and Lys^{185}–Val^{1331} are 127,225 and 126,854 kDa, respectively (28). These values are in good agreement with SDS-PAGE size estimates (~125 kDa) for the major fragments generated by trypsin digestion of XD or XO and chymotrypsin digestion of XD, and indicate that these fragments contain the C terminus of XOR.

The N-terminal sequence of the 85-kDa fragment (band 1) generated by chymotrypsin digestion of XO corresponds to Gln^{561}–Gln^{567} and is consistent with cleavage at Phe^{560}. The sequence of the 64-kDa fragment (band 2) corresponds to the N terminus of purified XOR (Thr^{2}–Phe^{7}). The sizes of the 64- and 85-kDa fragments by SDS-PAGE agree reasonably well with the predicted molecular masses of the N-terminal (Thr^{2}-Phe^{560}; 61,678 daltons) and C-terminal (Gln^{561}–Val^{1331}; 84,829 daltons) peptide fragments generated by cleavage at Phe^{560}. These results suggest that the 64- and 85-kDa fragments are primary products of chymotrypsin digestion of XO. The sequence of the first 7 amino acids of the 44-kDa fragment (band 3) corresponds to Asn^{182}–Thr^{188} and is consistent with cleavage at Met^{181}. The size of this fragment agrees with that predicted for a peptide fragment from Asn^{182} to Phe^{560} (42,413 daltons) and suggests that the 44-kDa fragment is generated by cleavage of the 64-kDa fragment at Met^{181}. Hydropathy analysis (28) of the amino acid sequences surrounding the cleavage sites (Fig. 2) shows that Met^{181} and Lys^{184} lie in a hydrophilic region, while Phe^{560} is in a relatively hydrophobic region of XOR. These results demonstrate that native XD and XO possess distinct solution conformations characterized, in part, by exposure of a hydrophobic region containing Phe^{560} in the XO form.

XD and XO Possess Different Hydrodynamic Properties—To determine whether the conformational differences in XD and XO represented global changes in their conformations we investigated their hydrodynamic properties by size exclusion chromatography. Fig. 3 shows the elution properties of XD (D/O = 6.2) and XO (D/O < 0.1) during HPLC-SEC at pH 7.5. Both forms of the enzyme eluted as single peaks (the small amount of absorbance at later retention times in the XD sample is due to DTT used to prepare XD) and appeared to be homogenous in composition. However, the average retention time of XO (17.52 ± 0.11 min; n = 6) was longer than that of XD (17.13 ± 0.07 min; n = 5). These results indicate that disulfide bond reduction leads to a significant change in the frictional coefficient of XOR and is consistent with an increase in the hydrodynamic volume of the enzyme. The nature of the disulfide bonds within XO was investigated by two-dimensional peptide mapping of chymotrypsin-digested XO under nonreduced and reduced conditions.

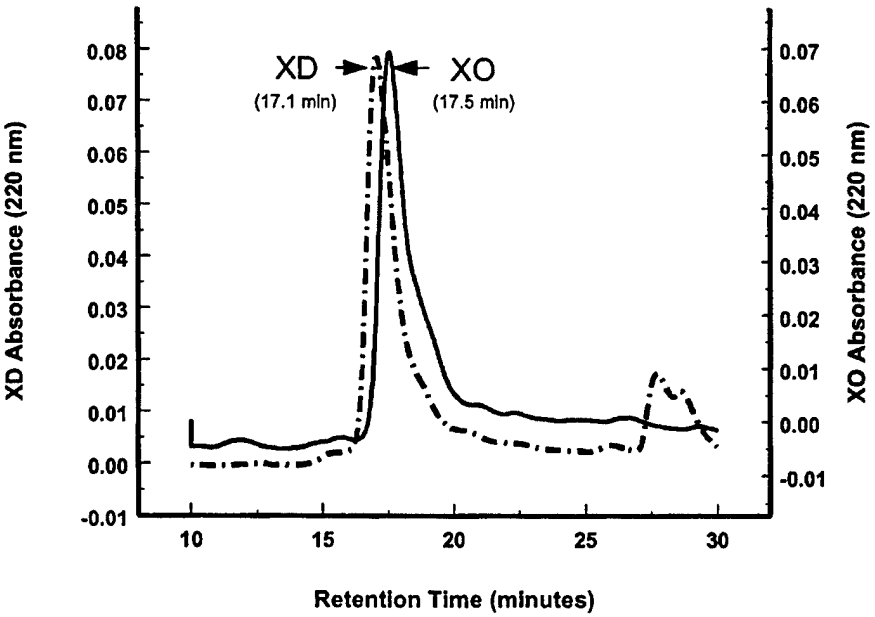

FIG. 3. **Size exclusion chromatography analysis of XD and XO.** Samples of XD (D/O = 6.2) and XO (D/O < 0.1), each containing 20 μg of protein, were analyzed by HPLC-SEC in phosphate-buffered saline, pH 7.5, using a 7.8 × 600-mm SEC-3000 column (Phenomenex, Inc.). Eluting material was monitored at 220 nm. The *dashed* and *solid lines* show representative chromatograms of XD and XO, respectively. The mean retention times of XD (17.13 ± 0.07 min; $n = 5$) and XO (17.52 ± 0.11 min; $n = 6$) were significantly different; $p < 0.01$.

Organization of Disulfide Bonds in XO—A representative two-dimensional peptide map of chymotrypsin-digested XO is shown in Fig. 4*A*. The digested enzyme was denatured in SDS in the absence of reducing agents and subjected to SDS-PAGE under nonreducing (first dimension) and reducing (second dimension) conditions. In addition to residual intact XO at 145 kDa, prominent bands at 85, 64, and 44 kDa were observed to lie on the diagonal indicated by *arrowheads*. Additional bands were also observed to the right of the diagonal at 64 and 44 kDa. The lack of significant staining to the left of the diagonal indicates that there are few, if any, disulfide bridges between undigested XO subunits or between the 85-, 64-, and 44-kDa fragments generated by chymotrypsin digestion. The presence of groups of bands spreading horizontally to the right of the 64- and 44-kDa bands indicates the existence of electrophoretic heterogeneity within these fragments. Since the first dimension was carried out in SDS under nonreducing conditions and fragments within each group have the same size, this observation suggests that this heterogeneity is due to disulfide bond-mediated conformational differences within these fragments. To verify that the electrophoretic heterogeneity within the 64- and 44-kDa fragments is the result of disulfide bonding, XO was first digested with chymotrypsin and then incubated with 5 mM DTT prior to two-dimensional peptide mapping. Fig. 4*B* shows that under these conditions the 85-, 64-, and 44-kDa fragments appear as tight bands on the diagonal (*arrowheads*), and there is no evidence of electrophoretic heterogeneity associated with these fragments.

Cross-linking Prevents Thiol-mediated Conversion of XO to XD—To determine whether a conformational switch is required for the conversion of XO to XD we investigate the effects of cross-linking on the conversion process. Table II shows the effects of cross-linking XO with the amine-specific reagent BS3 on the ability of DTT to convert XO to XD as indicated by an increase in the D/O ratio. The initial D/O values of cross-linked and non-cross-linked (control) enzyme were <0.1. After incubating with 10 mM DTT for 2 h the D/O of control XO increased to nearly 4, whereas the D/O value of the cross-linked enzyme was still less than 0.1. BS3 did not react with cysteine thiols or interfere with the ability of DTT to reduce XO cysteine thiols (data not shown). Moreover it did not interfere with the XD activity of enzyme that was reduced prior to adding cross-linking reagent (Table II). Thus, the inability of DTT to convert BS3 cross-linked XO to XD does not appear to be due to a specific interference of BS3 with XD enzymatic activity or its reaction with cysteine thiols.

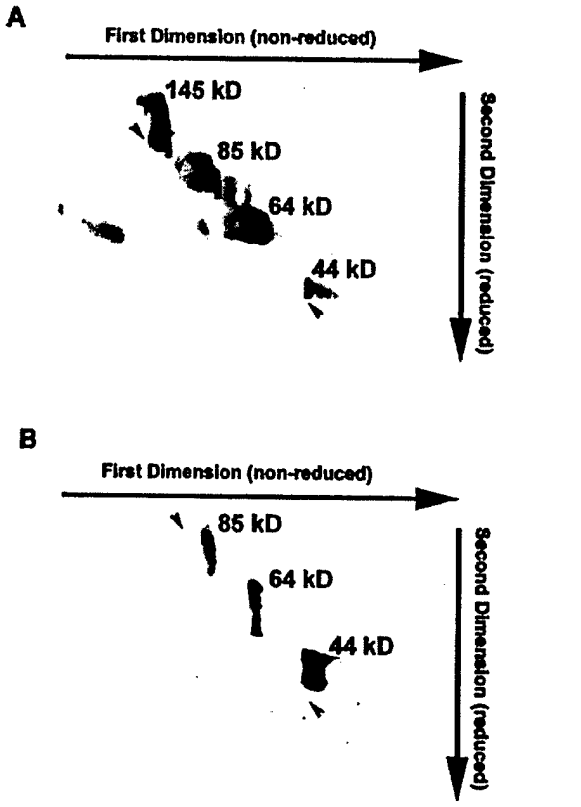

FIG. 4. **Two-dimensional electrophoresis of chymotrypsin-digested XO.** XO was digested with chymotrypsin (20/1) at room temperature and then analyzed by two-dimensional electrophoresis under nonreducing conditions (first dimension) and reducing conditions (second dimension). *A*, shows the two-dimensional electrophoresis pattern of XO incubated with chymotrypsin for 1 h. *B*, two-dimensional electrophoresis of XO incubated with chymotrypsin for 2 h and then with 5 mM DTT for 2 h. Protein fragments were detected by silver staining. The orientation of electrophoresis in each dimension is shown at the *top* and *right side* of each gel. The size of each band is shown on its *right*. The *arrowheads* indicate the position of the diagonal.

The nature of the BS3 cross-linked enzyme was characterized by HPLC-SEC and SDS-PAGE. The majority of the cross-linked enzyme eluted with the same retention time as native

TABLE II

The effect of cross-linking on the conversion of XO to XD by DTT

Equal amounts of XO (starting D/O = 0.1) were incubated with or without BS3 at pH 7.5 as detailed under "Experimental Procedures." After stopping the cross-linking reaction the samples were incubated with 10 mM DTT and their xanthine oxidation rates were determined in the presence and absence of NAD^+. A separate sample of XO was converted to XD prior to the addition of BS3. The rates of xanthine oxidation are shown as the relative increase in absorbance at 295 nm (mOD) per min. D/O values were calculated as described under "Experimental Procedures."

Treatment	Rate (−) NAD (A295 × 1000/min)	Rate (+) NAD (A295 × 1000/min)	D/O
DTT reduced XO	5.5	27	3.9
BS3 x-linked XO reduced with DTT	10	11.3	<0.1
DTT reduced XO X-linked with BS3	1.5	10.9	6.2

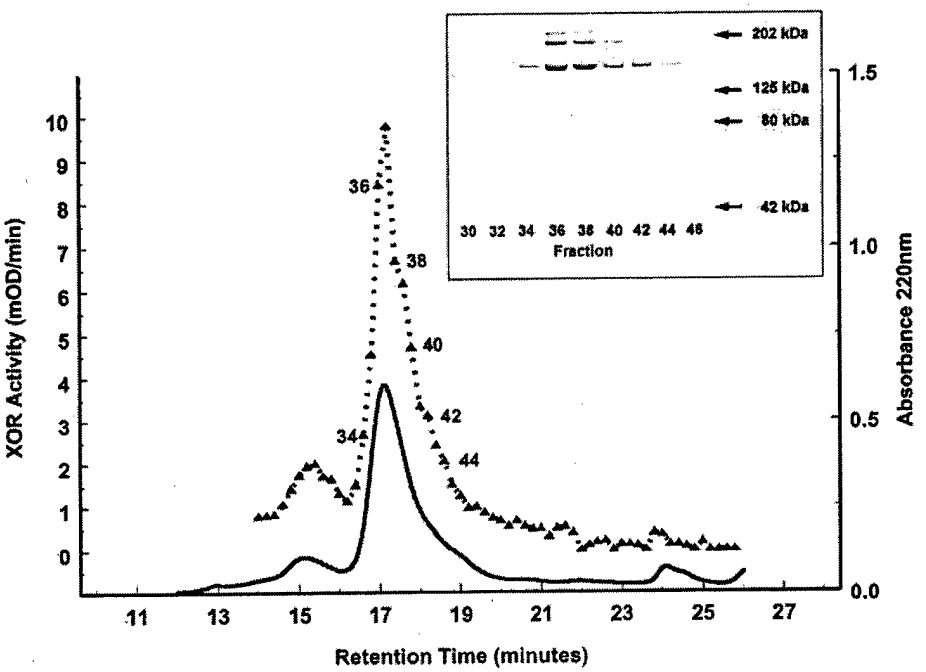

FIG. 5. **Size exclusion chromatography of cross-linked XO.** XO (50 μg; D/O = 0.1) was cross-linked with BS3 and analyzed by HPLC-SEC in phosphate-buffered saline, pH 7.5. Fractions were collected every 0.3 min starting 12 min after injection. The elution of protein (*solid line*) and XO activity (*dotted line* with *triangles*) are shown as a function of column retention time. The *inset* shows the SDS-PAGE and silver stain analysis of selected fractions across the peak. The *numbers* adjacent to the XO activity profile indicate the fractions assayed by SDS-PAGE. The elution of protein was monitored at 220 nm and the elution XOR activity was monitored using the xanthine/dichloroindophenol assay ("Experimental Procedures") and is shown as the relative rate of xanthine oxidation/min per 20-μl aliquot.

XO (Fig. 5). SDS-PAGE analysis of cross-linked XO (Fig. 5, *inset*) showed that it was composed of bands between 180 and 200 kDa as well as bands near the top of the gel and at ~150 kDa. The results demonstrate that cross-linking primarily occurs within, and/or between, individual XO subunits and that there is relatively little cross-linking between enzyme molecules or formation of large cross-linked enzyme aggregates. Therefore, cross-linking also does not appear to influence the assembly state of the enzyme. Together these results suggest that cross-linking with BS3 prevents a conformational change that is necessary for the reductive conversion of XO to XD.

Cleavage of XO at Phe^{560} Prevents Conversion to XD—Since exposure of the region containing Phe^{560} is a distinct feature of the XO conformation we tested the possibility that alterations to this region by proteolytic cleavage would interfere with conversion to XD by thiol reduction. Fig. 6 shows the effects of trypsin and chymotrypsin digestion on the ability of DTT to convert XO to XD (Fig. 6*A*) and on the conversion of XD to XO (Fig. 6*B*). XO digested with trypsin for up to 2 h could still be converted to XD by incubation with 5 mM DTT for 1 h; however, digestion with chymotrypsin for as little as 30 min completely prevented conversion. In contrast, neither chymotrypsin nor trypsin digestion led to significant conversion of XD to XO. Since chymotrypsin and trypsin cleave XO and XD at proximal sites (Met^{181} and Lys^{184}, respectively) within their N-terminal regions it is unlikely that cleavage within this region is responsible for the failure of DTT to convert chymotrypsin-cleaved XO to XD. Conversely, the selective cleavage at XO at Phe^{560} by chymotrypsin suggests that structural alterations within this region are responsible for the inability of XO to be converted to XD by DTT reduction.

DISCUSSION

It is well established that mammalian XOR can be reversibly converted from an NAD^+-dependent dehydrogenase to an O_2-dependent oxidase by oxidation of cysteine thiols to disulfide bonds (11, 12). The present study demonstrates that the conversion of XD to XO involves a global conformational change that is coupled to a reduction in the apparent hydrodynamic size of XOR. The conformational change was mapped to a specific region surrounding Phe^{560} and was shown to be a necessary step in the conversion process.

Although the specific activities of our preparations indicate that 30–50% of the purified enzyme is catalytically inactive (2), evidence from the literature and from the present studies suggests that active and inactive XOR molecules possess similar structures and undergo equivalent conformational changes. First, catalytically inactive forms are present in many highly purified and physically homogenous XOR preparations (2). The inactive forms appear to result from specific alterations of the

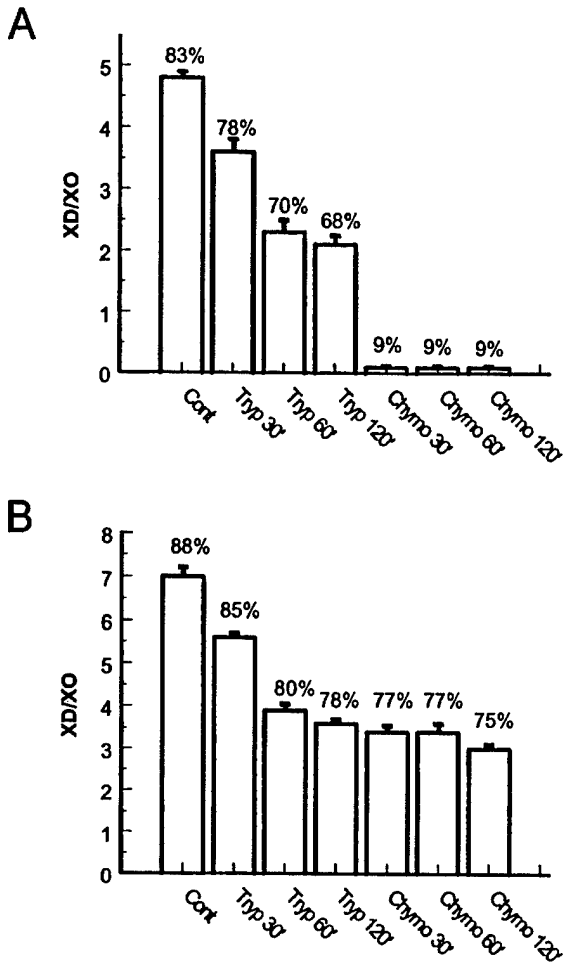

FIG. 6. **Effects of trypsin and chymotrypsin digestion of interconversion of XD and XO.** *A* shows the effects of trypsin and chymotrypsin digestion on the conversion of XO to XD by DTT. XO was incubated with trypsin or chymotrypsin at room temperature for the indicated times, at a ratio of enzyme to protease of 20/1. The reactions were stopped with phenylmethylsulfonyl fluoride, and the samples were then incubated with 5 mM DTT for 1 h at room temperature and assayed for XD and XO activities as described under "Experimental Procedures." The control sample shows the D/O of undigested XO that was incubated with 5 mM DTT for 1 h. The total XOR activity (D + O) in control and protease-digested samples averaged 17.1 ± 2 μmol of uric acid/ml/min. *B* shows the effects of trypsin and chymotrypsin digestion on the conversion of XD to XO. XD (D/O = 7) was incubated with trypsin or chymotrypsin at room temperature for the indicated times. The reactions were stopped with phenylmethylsulfonyl fluoride and the samples were assayed for XD and XO activities. The control sample shows the D/O of undigested XD incubated at room temperature for 2 h. The total XOR activity (D + O) in control and protease-digested samples averaged 15.4 ± 2.8 μmol of uric acid/ml/min. In both *A* and *B* the mean D/O values (*bars*) of duplicate samples are shown as a function of digestion time for each protease. The *values above* each *bar* show the percentage of the enzyme in the XD form.

molybdopterin cofactor (2) and not from alterations in the structural properties of the protein. Second, the hydrodynamic and electrophoretic properties of our purified XOR preparations demonstrate that the enzyme is intact and is composed of a relatively homogenous population of molecules. Size exclusion chromatography of the XD and XO isoforms also indicates that there is a uniform response to thiol reduction of XO. Third, the precise proteolytic patterns observed for both the XD and XO isoforms indicate that within a given isoform population the overall conformations are relatively homogenous.

The limited and highly selective cleavage of XD and XO by trypsin and chymotrypsin is consistent with previous proteolysis studies of rat and bovine XOR (6, 29) and with subtilisin cleavage of chicken XD (8) and indicates that the native conformations of both isoforms are highly ordered and that homologous forms of avian and mammalian XOR have similar structural domains. Trypsin selectively cleaved the bovine XD and XO isoforms at Lys^{184}. The absence of significant amounts of additional trypsin cleavage products indicates this region is highly accessible in the native conformations of both enzyme forms and that the degree of local segmental motion within this region is significantly greater than that of other regions of the enzyme (30, 31). Chymotrypsin selectively cleaved XD and XO at an adjacent site in this region (Met^{181}). The close proximity of the Met^{181} and Lys^{184} sites combined with earlier findings that trypsin cleaves rat liver XD at Lys^{185} (6) and subtilisin cleaves chicken liver XD at a homologous site (Lys^{248}) suggests that flexible structural properties are a general feature of this region in both mammalian and avian XOR molecules. Comparison of the amino acid sequences of mammalian and avian enzymes shows that Lys^{184} and Met^{181} are located in a highly conserved, hydrophilic region of the enzyme at the boundary between the iron-sulfur and flavin domains (8, 10, 22).

In contrast to the high susceptibility of Met^{181} and Lys^{184} to proteolytic attack in both XD and XO isoforms, Phe^{560} is cleaved by chymotrypsin only when it is in the XO form. Hydropathy analysis shows that Phe^{560} is in a relatively hydrophobic region of the enzyme that would be expected to exhibit reduced solvent exposure under physiological conditions. The observation that this site becomes accessible to chymotrypsin only after XD is converted to XO therefore suggests that disulfide bond formation produces significant structural changes within this region of XOR. Based on sequence alignment comparisons of XOR family members (32) and crystallographic studies of bovine XD (22), the Phe^{560} site appears to be in an unstructured region near the boundary of the flavin and molybdopterin domains. Thus, disulfide bond formation appears to produce conformational changes that delineate the extent of the flavin-binding region of XOR. Furthermore, size exclusion analysis indicates that disulfide bond formation reduces the hydrodynamic size of XOR. These results extend previous observations (20, 21) of conformational changes within the flavin-binding site following thiol oxidation-dependent conversion of XD to XO by demonstrating that the conversion involves specific structural alterations and global changes in the hydrodynamic properties of XOR.

The pattern of chymotrypsin digestion of bovine milk XD is different from that previously reported for rat liver XD (11). In this earlier study, chymotrypsin cleavage of XD generated significant amounts of 64- and 44-kDa fragments. However, the D/O value of enzyme used in these studies was 1.3; thus their preparation appeared to contain significant amounts of the XO form. In addition, the digestion was carried out at 37 °C, which potentially leads to local unfolding (30) and has been reported to result in the conversion of XD to XO (17). Therefore, the basis for the difference in chymotrypsin cleavage pattern may reside in the relative XD/XO composition of the sample and/or temperature-dependent conformational changes, rather than actual differences in the conformations of the rat and bovine enzymes. This conclusion is supported by the similarity of the chymotrypsin cleavage pattern of chicken XDH at 25 °C (33) to that reported here for bovine XDH. Since avian XOR exists only in the XDH form (8) and contains a region that is highly homologous to that surrounding Phe^{560} of bovine XOR (8), it is likely that the inaccessibility of the Phe^{560} region to chymotrypsin is a general feature of the XDH isoform.

Initial studies of the XD to XO conversion suggested that the cysteine residues affecting the dehydrogenase activity of XOR were located in the cysteine-rich N-terminal region (6, 17).

However, recent studies of rat liver XOR have led to the proposal that Cys^{535} and Cys^{992} are involved in the conversion through the formation of disulfide bonds between these residues (34). Our two-dimensional electrophoresis results provide evidence of significant disulfide bond formation within the N-terminal region of XOR (the 44- and 64-kDa fragments) but not between residues located in the C-terminal fragment (the 85-kDa band, which contains Cys^{992}) and N-terminal fragment (the 64-kDa band, which contains Cys^{535}). Since these residues are conserved in all mammalian enzymes studied to date, our data suggest the Cys^{535} and Cys^{992} form disulfide bonds with as yet unidentified Cys residues in the 64- and 85-kDa regions, respectively.

The basis of the disulfide bond heterogeneity in the N-terminal region of XO is unknown. However, milk XO appears to be formed by the action of a membrane-bound sulfhydryl oxidase during the secretion process (13, 35). If the conformation of XD leads to clustering of cysteine residues it is possible that this enzyme might catalyze formation of disulfide bonds within groups of closely associated cysteine residues resulting from the generation of XO molecules with different disulfide bond combinations and consequently different conformations and electrophoretic mobilities. The formation and rearrangement of disulfide bond isomers by folding catalysts such as protein-disulfide isomerase are known to occur during the folding of nascent proteins and are part of the process of generating proper native conformations (36). A similar process may occur in the conversion of XD to XO during milk secretion and lead to the formation of disulfide bond isomers of XO.

Two lines of evidence from the present study demonstrate that the conversion of XO to XD is dependent on specific structural changes associated with disulfide bond reduction. The first is that cross-linking XO prevents the reductive conversion of XO to XD. Cross-linking did not interfere with XOR activity, and the majority of the cross-linking was intramolecular and occurred without major changes in the conformation of XO. Thus it appears that the inability of DTT to convert cross-linked XO to XD is not due to alterations in substrate utilization or artifactual intermolecular interactions between cross-linked XOR dimers. The second is that selective cleavage of XO at Phe^{560} prevents conversion to XD by DTT. Because trypsin and chymotrypsin cleave XO at nearby sites in the N-terminal region but only chymotrypsin cleavage prevents conversion to XD, it appears that structural changes within the region around Phe^{560} are critical for the conversion process. As yet it is unclear if cleavage at Phe^{560} alone or a combination of cleavage at Phe^{560} and Met^{181} is required to prevent reductive conversion of XO to XD. However, time course studies indicate that Phe^{560} cleavage occurs first and that cleavage at this site correlates with the inhibition of the XO to XD conversion.[2] Support for the importance of the region surrounding Phe^{560} comes from observations that modification of Cys^{535} of rat liver XOR converts XD to XO (34) and from crystallographic data that show that this region is disordered in intact bovine XD and proteolyzed bovine XO and constitutes a linking segment between the flavin and molybdopterin domains (22). Our results do not support earlier conclusions, based on proteolytic digestion of rat XOR, that alterations within the cysteine-rich N-terminal region by cleavage at Lys^{185} are responsible for the XD to XO conversion (6, 17). As indicated above, technical differences, especially the use of elevated temperatures for proteolytic digestion experiments, may be the basis for this discrepancy. In fact, more recent studies of rat liver XOR have shown that cleavage at Lys^{185} does not induce the D to O conversion of rat XOR (34). Together with evidence from recent investigations of the role of cysteine residues in the XD to XO conversion (34), the results from our study indicate that the XD-XO interconversion requires a conformational switch in the region surrounding Phe^{560}. Alterations that affect the structure of this region, such as proteolysis, decouple this switch and interfere with the interconversion process.

Although the conversion of XD to XO represents a pathologically important event due to increased production of cytotoxic reactive oxygen species by the XO form (37), the biological importance of the conformational change associated with the conversion is less established. A potential physiological function of this conformational change is in milk lipid secretion. It has been known for nearly a century that XOR is highly enriched in cow's milk (2). Numerous studies have documented that the primary form of the milk enzyme is XO (11, 13, 38), and it has been demonstrated that XOR is a major protein constituent of the membrane that surrounds lipid globules in milk (39). Immunofluorescence studies have shown that XOR is selectively associated with the apical plasma membrane in lactating cattle (40), and histochemical evidence suggests that the membrane-associated form is XO (41). We recently demonstrated that the primary form of XOR in mouse mammary tissue is XD, that rapid conversion of the XD form to the XO form occurs during milk secretion, and that membranes surrounding milk lipid globules contain an enzyme capable of converting XD to XO (13). Thus, it is possible that the conformational changes associated with the XD to XO conversion, in particular the exposure of the hydrophobic region around Phe^{560}, are important in the association of XOR with the apical membrane in mammary epithelial cells and may play a role in milk lipid secretion. Electron microscopic studies have shown that the proteins on the inner surface of milk fat globule membranes are structurally organized into highly ordered hexagonal arrays (42). It will be interesting to determine whether changes in the conformation of XOR contribute to the organization of these structures.

Acknowledgments—We thank Drs. Richard Wright and Margaret Neville for helpful discussions and critically reading the manuscript.

REFERENCES

1. Stryer, L. (1988) *Biochemistry,* 3rd Ed., W. H. Freeman and Co., New York
2. Bray, R. C. (1975) in *The Enzymes* (Boyer, P. D., ed) Third Ed., Vol. XII, pp. 299–419, Academic Press, New York
3. Hille, R., and Nishino, T. (1995) *FASEB J.* **9,** 995–1003
4. Ichida K., Amaya, Y., Noda, K., Minoshima, S., Hosoya, T., Sakai, O., Shimizu, N., and Nishino, T. (1993) *Gene (Amst.)* **133,** 279–284
5. Terao, M., Cassaniga, G., Ghezzi, P., Bianchi, M., Falciani, F., Perani, P., and Garattini, E. (1992) *Biochem. J.* **283,** 863–870
6. Amaya, Y., Yamazaki, K-I., Sato, M., Noda, K., Nishino, T., and Nishino, T. (1990) *J. Biol. Chem.* **265,** 14170–14175
7. Bergland, L., Rasmussen, J. T., Andersen, M. D., Rasmussen, M. S., and Petersen, T. E. (1996) *J. Dairy Sci.* **79,** 198–204
8. Sato, A., Nishino, T., Noda, K., Amaya, A., and Nishino, T. (1995) *J. Biol. Chem.* **270,** 2818–2826
9. Lee, C. S., Curtis, D., McCarron, M., Love, C., Gray, M., Bender, W., and Chovnick, A. (1987) *Genetics* **116,** 67–73
10. Glatigny, A., and Scazzocchio, C. (1995) *J. Biol. Chem.* **270,** 3534–3560
11. Stirpe, F., and Della Corte, E. (1969) *J. Biol. Chem.* **244,** 3855–3863
12. Waud, W. R., and Rajagopalan, K. V. (1976) *Arch. Biochem. Biophys.* **172,** 354–364
13. McManaman, J. L., Neville, M. C., and Wright, R. M. (1999) *Arch. Biochem. Biophys.* **371,** 308–316
14. Cross, C. E. (1987) *Ann. Intern. Med.* **107,** 526–545
15. Southorn, P. A., and Powis, G. (1988) *Mayo Clin. Proc.* **63,** 390–408
16. Becker, B. F. (1993) *Free Radic. Biol. Med.* **14,** 615–631
17. Waud, W. R., and Rajagopalan, K. V. (1976) *Arch. Biochem. Biophys.* **172,** 365–379
18. Saito, T., and Nishino, T. (1989) *J. Biol. Chem.* **264,** 10015–10022
19. Hunt, J., and Massey, V. (1992) *J. Biol. Chem.* **267,** 21479–21485
20. Massey, V., Schopfer, L. M., Nishino, T., and Nishino, T. (1989) *J. Biol. Chem.* **264,** 10567–10573
21. Saito, T., Nishino, T., and Massey, V. (1989) *J. Biol. Chem.* **264,** 15930–15935
22. Enroth, C., Eger, B. T., Okamoto, K., Nishino, T., Nishino, T., and Pai, E. F. (2000) *Proc. Natl. Acad. Sci. U. S. A.* **97,** 10723–10728
23. Waud, W. R., Brady, F. O., Wiley, R. D., and Rajagopalan, K. V. (1975) *Arch. Biochem. Biophys.* **169,** 695–701

[2] J. L. McManaman, unpublished observations.

24. McManaman, J. L., Shellman, V., Wright, R. M., and Repine, J. E. (1996) *Arch. Biochem. Biophys.* **332,** 135–141
25. Smith, P. K., Krohn, R. I., Hemanson, G. T., Mallial, A. K., Gartner, J. H., Provenzano, M. D., Fujimoto, E. K., Goeke, N. M., Olson, B. J., and Klenk, D. C. (1985) *Anal. Biochem.* **150,** 76–85
26. Wray, W., Boulikas, T., Wray, V. P., and Hancock, R. (1981) *Anal. Biochem.* **118,** 197–203
27. Matsudaira, P. (1987) *J. Biol. Chem.* **262,** 10035–10038
28. Appel, R. D., Bairoch, A., and Hochstrasser, D. F. A. (1996) *Trends Biochem. Sci.* **19,** 258–260
29. Nagler, L. G., and Vartanyan, L. S. (1976) *Biochim. Biophys. Acta* **427,** 78–90
30. Fontana, A., Fassina, G., Vita, C., Dalzoppo, D., Zamai, M., and Zambonin, M. (1986) *Biochemistry* **25,** 1847–1851
31. Hubbard, S. J. (1998) *Biochim. Biophys. Acta* **1382,** 191–206
32. Ramao, M. J., and Huber, R. (1998) *Struct. Bonding* **90,** 69–95
33. Coughlan, M. P., Betcher-Lange, S. L., and Rajagopalan, K. V. (1979) *J. Biol. Chem.* **254,** 10694–10699
34. Nishino, T., and Nishino, T. (1997) *J. Biol. Chem.* **272,** 29859–29864
35. Clare, D. A., Blakistone, B. A., Swaisgood, H. E., and Horton, H. R. (1981) *Arch. Biochem. Biophys.* **211,** 44–47
36. Gilbert, H. F. (1997) *J. Biol. Chem.* **272,** 29399–29402
37. McCord, J. M. (1985) *N. Engl. J. Med.* **312,** 159–163
38. Nakamura, M., and Yamazaki, I. (1982) *J. Biochem.* (*Tokyo*) **92,** 1279–1286
39. Mather, I. H., and Keenan, T. W. (1998) *J. Mam. Gland Biol. Neoplasia* **3,** 259–273
40. Jarasch, E. D., Grund, C., Bruder, G., Heid, H. W., Keenan, T. W., and Franke, W. W. (1981) *Cell* **25,** 67–82
41. Fredricks, W. M., and Marx, F. J. (1993) *Histochem. Cytochem.* **41,** 667–670
42. Bucheim, W. (1982) *Naturwissenschaften* **69,** 505–507

Electrophoresis 2000, *21*, 3470–3482

Christine C. Wu[1]
Kathryn E. Howell[1]
Margaret C. Neville[2]
John R. Yates III[3*]
James L. McManaman[4]

[1]Department of Cellular and Structural Biology
[2]Department of Physiology, University of Colorado Health Sciences Center, Denver, CO, USA
[3]Department of Molecular Biotechnology, University of Washington, Seattle, WA, USA
[4]Department of Biochemistry, University of Colorado Health Sciences Center, Denver, CO, USA

Proteomics reveal a link between the endoplasmic reticulum and lipid secretory mechanisms in mammary epithelial cells

The synthesis and secretion of lipids by mammary epithelial cells is a highly ordered process that involves several distinct steps. Triacylglycerols are synthesized in the endoplasmic reticulum and incorporated into microlipid droplets which coalesce into cytoplasmic lipid droplets. These are vectorially transported to the apical plasma membrane where they are secreted into the milk surrounded by a membrane bilayer. The origin of this membrane as well as the mechanism by which cytoplasmic lipid droplets form and become surrounded by membrane is poorly understood. Proteomic analysis of the protein composition of milk fat globules and cytoplasmic lipid droplet has revealed that the endoplasmic reticulum is not only involved in the synthesis of the lipid but also potentially contributes to the membrane component of milk fat globules. The proteins identified suggest possible mechanisms of multiple steps during this process. Completion of the proteome of milk fat globule membranes and cytoplasmic lipid droplets will provide the necessary reporter molecules to follow and dissect the mechanisms of the sorting and ultimate secretion of cytoplasmic lipid droplets.

Keywords: Proteomics / Lipid droplet secretion / Milk fat globule membranes / Endoplasmic reticulum / Mass spectrometry

EL 4111

1 Introduction

Mammary epithelial cells utilize two distinct pathways for the secretion of milk constituents. Soluble proteins, as well as water, lactose and some minerals, are secreted using the exocytic pathway involving the endoplasmic reticulum (ER), Golgi complex, and secretory vesicles [1]. Lipids, primarily triacylglycerols, are thought to accumulate into microlipid droplets which are released from the ER into the cytosol surrounded by a protein and nonbilayer polar lipid coat [2]. Molecules of this coat have been proposed to play a role in the aggregation of lipid into droplets, the release of the microlipid droplet from the ER, fusion steps into the cytoplasmic lipid droplets (CLDs), and subsequent fusion with the apical plasma membrane [2]. CLDs are secreted from the apical surface of the cell enveloped within a membrane bilayer. To date, the molecular events comprising most of this complex lipid secretory pathway remain unknown.

Lipid secretion in the mammary epithelial cell is unique. The most distinct difference between the mammary epithelial cell and other cell types containing lipid droplets (*e.g.*, hepatocytes, adipocytes) is that mammary CLDs are secreted from the apical surface of the cell surrounded by a membrane bilayer, the milk fat globule membrane (MFGM). Ultrastructural analysis has led to competing hypotheses about the mechanism of secretion and the origin of the membrane bilayer. The most widely accepted view is that CLDs are gradually enveloped by the apical plasma membrane in a budding process [3, 4]. In this hypothesis, the MFGM is derived solely from the apical plasma membrane. A second scenario is that lipid secretion results from the progressive fusion of Golgi-derived secretory vesicles that surround the CLDs within the cytoplasm [5, 6]. This process would lead to a membrane entirely composed of secretory vesicle components. A third view is that secretory vesicles associated with CLDs fuse with each other and the apical membrane [6, 7] to yield a composite membrane derived from both the vesicles and the apical plasma membrane.

Correspondence: Dr. Kathryn E. Howell, Department of Cellular and Structural Biology, University of Colorado Health Sciences Center, 4200 E. 9th Ave B-111, Denver, CO 80262, USA
E-mail: kathryn.howell@uchsc.edu
Fax: +303-315-4729

Abbreviations: ADPH, adipophilin; **BTN**, butyrophilin; **CLD**, cytoplasmic lipid droplet; **EM**, electron microscopy; **ER**, endoplasmic reticulum; **ERP**, endoplasmic reticulum protein; **FABP**, fatty acid binding protein; **FAS**, fatty acid synthase; **MFG(M)**, milk fat globule (membrane); **TER**, transitional ER; **WAP**, whey acidic protein; **XDH/XO**, xanthine oxidoreductase

* Present address: Department of Cell Biology, The Scripps Research Institute, La Jolla, CA, USA

0173-0835/00/1616-3470 $17.50+.50/0

Another unique feature of lipid secretion in mammary epithelial cells is the vectorial transport of CLDs from the basal region of the cell to the apical membrane for secretion [3]. Microtubules have previously been analyzed and quantitated ultrastructurally in lactating mammary epithelial cells. Most were oriented perpendicular to the apical plasma membrane and concentrated in the apical and medial portions of the cell cytoplasm [8]. These microtubules were found in close contact with secretory vesicles, and treatment with colchicine was found to inhibit exocytosis as well as to suppress milk fat globule secretion [9, 10]. Specific molecules involved in the interaction between the cytoskeleton and secretory vesicles and CLDs remain unknown, and although CLDs are covered by a protein coat, the protein composition is largely undefined.

Only eight of the major protein components of the MFGM have been identified and studied in detail: mucin 1 (MUC-1), xanthine oxidoreductase (XDH/XO), periodic acid Schiff III (PASIII), CD36, butyrophilin (BTN), adipophilin (ADPH), periodic acid Schiff 6/7 (PAS6/7), and fatty acid binding protein (FABP) [11]. Based on biochemical, cytochemical, and developmental studies of the mammary gland and milk fat globules (MFGs), BTN, XDH/XO, and ADPH are proposed to mediate binding of CLDs to the apical plasma membrane [3]. However, there are at least four distinct steps required for the production and secretion of CLDs. (i) Lipids accumulate and are released as microlipid droplets from the ER into the cytoplasm where they coalesce into CLDs. (ii) CLDs are vectorially transported to the apical plasma membrane. (iii) CLDs dock with the apical plasma membrane. (iv) Fusion occurs, resulting in the secretion of CLDs from the apical surface surrounded by a membrane bilayer. Therefore, it is reasonable to assume that there must be multiple other proteins involved in the entire process and that some of these proteins will be present in the MFGM.

Proteomic analysis of cell organelles has been used to identify endogenous proteins and dissect the molecular mechanisms underlying their functions [12–14]. In this study, we present the first installment of the MFGM and the CLD proteomes. 2-D master maps were prepared from MFGMs isolated from milk and CLDs fractionated from mammary gland and liver. Protein spots excised from these gels were identified using reversed-phase LC coupled with tandem mass spectrometry (MS/MS) [15]. Our results suggest that: (i) mammary CLDs differ from liver CLDs in protein composition; (ii) mammary CLDs are intimately associated with membrane-like structures which contain components originating from the ER. (iii) A subset of the proteins present in the MFGM are also present in the mammary CLDs, suggesting that the membranes and adherent proteins associated with the CLDs are involved in the secretory process. Taken together, we propose that the ER may not only contribute the enzymes for lipid synthesis, but also provide some of the molecules required for the vectorial transport and subsequent fusion of the CLD with the apical plasma membrane.

2 Materials and methods

2.1 Isolation of MFGs and MFGMs

Milk was collected from CD1 mice on day 12 of lactation (L12). MFGs were isolated according to Patton and Huston [16]. Briefly, freshly collected warm milk was adjusted to 10% w/v sucrose. Ten volumes of PBS was layered on top of the milk solution and centrifuged at 1500 × *g* for 20 min at room temperature. The floated MFGs were collected with a spatula and resuspended in five volumes of ice-cold PBS. MFGMs were isolated by physical agitation [11]. Briefly, the MFG sample was churned in a Dounce homogenizer until no further clumping of lipid was observed (~ 20 strokes). The suspension was centrifuged at 100 000 × *g* for 1 h at 4°C. Pelleted MFGMs were collected from the bottom of the tube and either washed 1 × in ice-cold PBS by repeating the homogenization and centrifugation step or immediately analyzed.

2.2 Fractionation of CLDs and cytosol

Inguinal mammary glands and livers were removed from the same L12 mice previously milked. The mammary glands were washed in ice-cold PBS to remove the milk present. Both the glands and the livers were minced finely and lightly homogenized using a Polytron PT 10/35 (Brinkmann, Westbury, NY, USA) in 100 mM KH_2PO_4/K_2HPO_4, pH 6.8, 5 mM $MgCl_2$, and 1 μg/mL each of proteolytic inhibitors chymostatin, leupeptin, antipain, and pepstatin. All subsequent sucrose solutions were prepared in this buffer. The homogenate was subjected to low-speed centrifugation (3000 × *g* for 10 min at 4°C) and the resulting postnuclear supernatant (PNS) was loaded in the middle of a sucrose step gradient (1.3 M, 0.86 M, PNS, 0.25 M) and centrifuged at 100 000 × *g* for 1 h at 4°C. The cytosol was collected from the PNS step between the 0.25 M/PNS interface and the PNS/0.86 M interface. The lipid droplets were collected from the top of the gradient and washed 0–3 times as follows. The CLDs were gently resuspended in ten volumes of 0.25 M sucrose in a Dounce homogenizer (~ 5 strokes), floated with centrifugation at 100 000 × *g* for 2 h at 4°C, and recollected from the surface of the solution.

2.3 2-D gel electrophoresis

20–50 μg protein were precipitated using methanol and chloroform [17] for analysis on silver-stained gels. 1–2 mg

protein were precipitated for preparative Coomassie Brilliant Blue R-250 stained gels used for subsequent identification by MS. Precipitated proteins were solubilized in 8 M urea, 4% CHAPS, 1 M thiourea, 83 mM dithioerythritol, 18 mM Trizma base, 0.4% carrier ampholytes pH 3.5–10 (BDH, Poole, UK), and 0.0025% bromophenol blue. Isoelectric focusing was performed using Immobiline dry strips (nonlinear pH range from 3.5–10; Pharmacia, Uppsala, Sweden). The dry strips were rehydrated with the solubilized protein sample by in-gel reswelling [18] and were electrophoresed for 14 h. The second dimension was run on a 9–16% polyacrylamide SDS gel using a Bio-Rad Protean XII cell (Bio-Rad, Hercules, CA, USA). Silver staining was performed according to SWISS-PROT 2-D PAGE procedures [18]. All gels were scanned using a flatbed scanner, and the resulting images were analyzed by the Melanie II software (Bio-Rad).

2.4 In-gel digestion of 2-D spots

In-gel digests of Coomassie blue-stained 2-D spots were performed as described [19]. Briefly, spots were excised with a scalpel and washed in 100 mM NH_4HCO_3 for 10 min. Proteins were reduced with 3 mM DTT/100 mM NH_4HCO_3 for 20 min at 60°C. After cooling to room temperature, iodoacetamide was added to 6 mM final concentration and incubated in the dark for 20 min at room temperature. The aqueous solution was discarded, and the gel slice was washed in 50% acetonitrile/100 mM NH_4HCO_3 for 20 min. The gel slice was cut into 1 mm^3 pieces and transferred into new 0.5 mL low adhesion Optimum® tubes (Life Science Products, Denver, CD, USA). Gel pieces were dehydrated with the addition of 100% acetonitrile for 15 min. The solvent was removed, and the gel pieces were dried. Gel pieces were reswelled with 0.2 μg modified trypsin (Roche Molecular Biochemicals)/ 25 mM NH_4HCO_3 overnight at 37°C. The supernatant was removed and placed into new 0.5 mL Optimum® tubes. Peptides were extracted from the gel pieces with 100 μL 60% acetonitrile/0.1% TFA for 20 min. The supernatant was removed and added to the previous extract. This extraction was repeated twice. The pooled extract was lyophilized to dryness and reconstituted in 10 μL 5% formic acid immediately before analysis by MS.

2.5 Identification of protein peptides by MS/MS

Peptide samples were centrifuged for 10 min at 15 000 rpm in a microfuge to remove any particulate matter. Samples were then loaded onto a 100 μm fused-silica column with a 5 μm tip. Flow rates were adjusted to ~ 300 nL/min on an HP1100 pump and positioned in front of the heated capillary opening on a Finnigan LCQ (San Jose, CA, USA). Peptides were eluted with an acetonitrile gradient from 98% buffer A/2% buffer B to 40% buffer A/ 60% buffer B where buffer A is 5% acetonitrile/0.5% acetic acid and buffer B is 80% acetonitrile/0.5% acetic acid. Spectra were analyzed using Sequest software [20–22]. Positive identifications were made with the criteria of three separate spectra of high correlation scores. Factors included in the calculation of the correlation score are part of the Sequest software and are discussed elsewhere [22].

2.6 Electron microscopy (EM)

For thin sections, 1 mm^3 tissue pieces were fixed in 2% glutaraldehyde/2% sucrose/100 mM sodium cacodylate, pH 7.35, overnight at 4°C. The tissue was postfixed in 2% OsO_4 in 0.8% potassium ferrocyanide buffered with 100 mM sodium cacodylate, pH 7.35. The tissue blocks were washed with water, dehydrated with increasing EtOH steps (50, 75, 90, 98, 100%), and embedded in Spurr's resin. Sections were post-stained in 5% uranyl acetate in MeOH and Reynold's lead citrate. For negatively stained images, CLDs isolated from mammary epithelial cells and liver were deposited onto formvar-coated copper grids and air-dried. The samples were stained with 2% phosphotungstic acid for 30 s and air-dried again. Samples were imaged using a Phillips CM10 microscope.

3 Results

3.1 Isolation of MFGMs

MFGs were floated from fresh mouse milk collected from lactation day 12 (L12) mice. The MFGMs were separated from the lipid droplet by agitation and subsequently isolated by centrifugation. Analytical (silver-stained) 2-D gels were prepared. Figure 1 shows a comparison between (A) 50 μg total milk and (B) 25 μg MFGM. Major proteins present in both the milk and MFGM samples are boxed. Of the 18 major proteins present in both samples, seven were de-enriched in the isolated MFGMs and later identified by tandem MS/MS as major skim milk or serum proteins, *i.e.*, transferrin, albumin, α-1-protease inhibitor, α-casein, β-casein, ε-casein, and whey acidic protein (WAP). As expected, these proteins were less abundant in the isolated membrane fraction because most of the skim milk proteins would have been separated from the MFGs during the initial float and subsequently diluted away into the supernatant above the membrane pellet during centrifugation [11]. Sixty-five protein spots were enriched in the MFGM and are circled. Clearly, there are a large number of proteins present in the MFGM sample. We have identified some of these proteins using MS/MS and the implications of these identifications will be discussed later in this section.

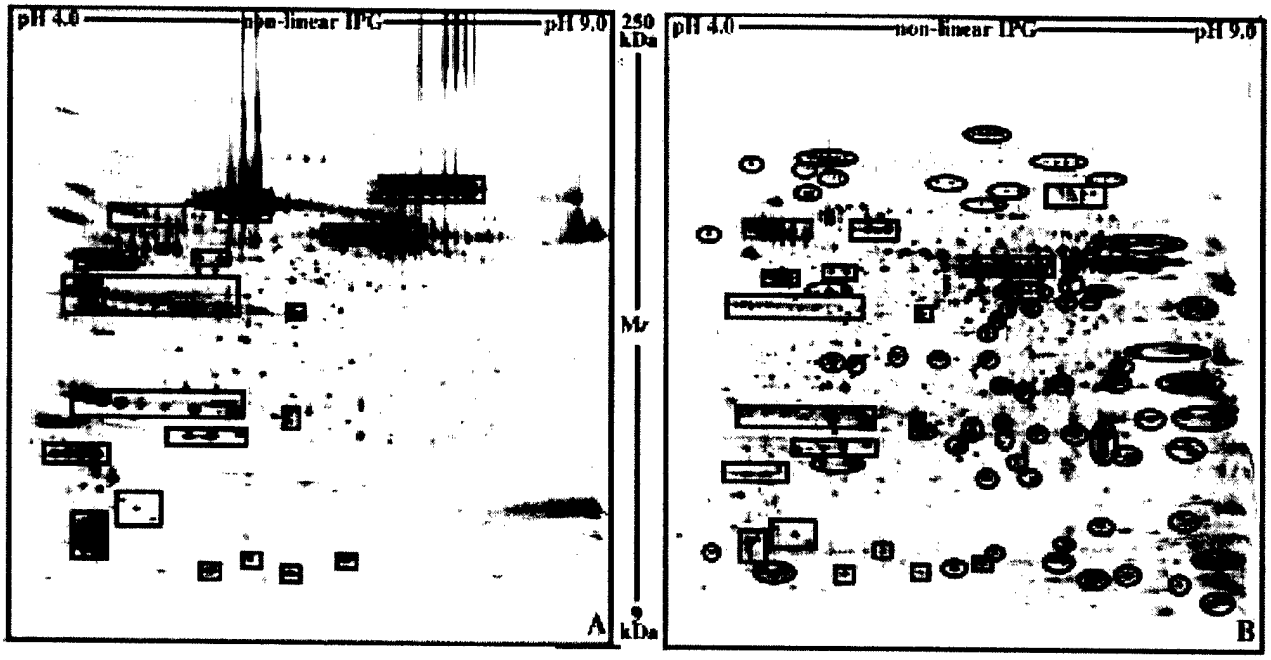

Figure 1. Comparison of the protein composition of total mouse milk and MFGMs by 2-D gel electrophoresis. (A) 50 μg whole milk; (B) 25 μg MFGMs. Silver-stained protein spots present in both samples are boxed. Protein spots enriched in the MFGM sample are circled.

3.2 EM of lactating mammary epithelial cells

Thin sections were prepared from Spurr's embedded lactating mouse mammary glands. The micrographs in Figs. 2A and B show lipid droplets in the apical portion of a mammary epithelial cell. MFGs are present within the alveolar lumen (open star) in Fig. 2A. In addition, a small CLD, almost completely surrounded by membrane, is in the process of being released from the cell surface (closed star). An important observation is that there appears to be very little cytoplasmic component between the lipid droplet and the membrane. The CLD in Fig. 2A (arrow) is observed to be surrounded by vesicles of varying sizes and shapes (large arrowheads). Seen more clearly in a different cell photographed at a slightly higher magnification in Fig. 2B, the vesicle membrane occasionally deforms the surface of the lipid droplet. This observation has been reporeted by others and suggests that there is some physical interaction between the vesicle and the lipid droplet [5]. Frequently, casein micelles are present in the lumen of the surrounding vesicles (small arrowheads). Because casein stains well with osmium, it is visualized using standard EM methods and provides a convenient marker for analysis of secretory compartments. The presence of the casein micelles has supported the hypothesis that these vesicles are Golgi-derived secretory granules. Though there have been no *bona fide* Golgi proteins identified to date, it has been hypothesized that these vesicles are involved in the secretion of CLDs and that the apical plasma membrane is not the sole membrane involved in the secretory process [5].

3.3 Fractionation of mammary and liver CLDs

To investigate the nature of the association between the vesicles and the lipid droplets, CLDs were prepared by cell fractionation from the inguinal mammary glands of the same L12 mice from which the milk was obtained for the MFGM analysis. The isolated CLD samples were negatively stained with phosphotungstic acid and visualized by EM. The micrograph in Fig. 3A shows that the isolated mammary CLDs (arrows) are intimately associated with a variety of flattened membrane-like structures (arrowheads). This sample was washed three times to reduce the presence of membranes that may have bound nonspecifically during the fractionation protocol. There was no apparent change in the amount or appearance of the membranes associated with the CLDs during or after the three washes (unwashed CLDs are not shown).

It was possible that membranes could have remained nonspecifically associated to the CLDs through strong hydrophobic interactions even after multiple washes. Therefore, CLDs were isolated from the livers of the same L12 mice from which the mammary glands and milk were obtained. Liver CLDs are not known to be secreted and

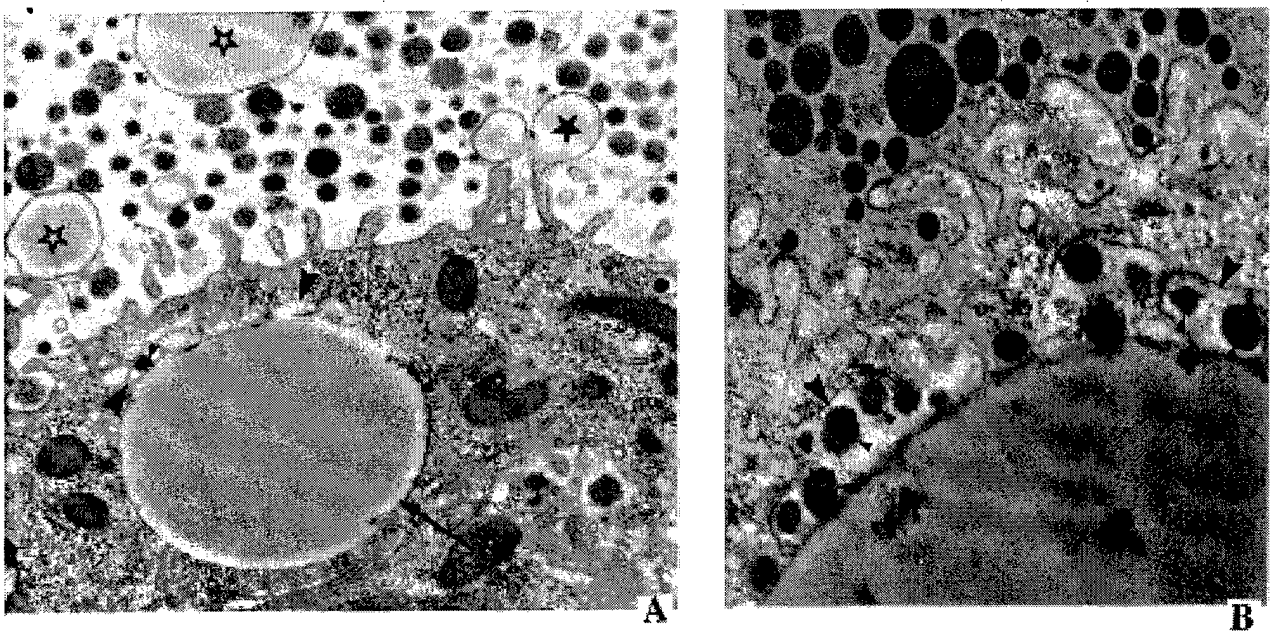

Figure 2. Electron micrographs of CLDs in the apical region of mouse mammary epithelial cells. (A) 600 × magnification; (B) 10 000 × magnification. Symbols: large arrowheads (vesicles associated with the CLDs), small arrowheads (vesicles containing casein micelles), arrow (CLD), open star (secreted MFG), and closed star (CLD in the process of being secreted).

provide an ideal control. If the membranes were associated with the mammary CLDs by nonspecific interactions occurring during the fractionation protocol, then the liver CLDs would be expected to also have membranes bound to their surfaces. Figure 3B shows that there were no detectable membrane structures associated with the unwashed liver lipid droplets isolated in parallel with the mammary CLDs.

3.4 Comparison of mammary and liver CLDs and cytosol

To analyze the protein compositions of the liver and mammary CLDs, analytical (silver-stained) 2-D gels were prepared from both and are shown in Fig. 4B and D, respectively. In addition, 2-D gels were prepared from liver and mammary cytosols to identify major cytosolic proteins (Fig. 4A and C, respectively). Major proteins present in the liver CLDs are boxed (Fig. 4B). These boxed locations are transposed onto the liver cytosol map (Fig. 4A) for comparison. Many of the proteins present in the liver CLDs are either greatly de-enriched or are not at all present in the liver cytosol. Proteins corresponding to the boxed spots in the liver CLDs (Fig. 4B) are also boxed in the mammary CLDs (Fig. 4D). These boxed locations are transposed onto the mammary cytosol map (Fig. 4C) for comparison. Major proteins present in the mammary CLDs but not present in the liver CLDs are circled (Fig. 4D) and the circled locations are transposed onto the mammary cytosol map (Fig.4C) for comparison. As in the liver, many of the proteins present in the mammary CLDs are either greatly de-enriched or are not present at all in the mammary cytosol. The mammary CLDs contain three times more protein spots (84) than the liver CLDs (27) indicating that mammary CLDs are significantly more complex than the liver CLDs. Interestingly, all proteins present in the liver CLDs are also present in the mammary CLDs (boxed spots). These proteins most likely represent some of the basic machinery required for the biogenesis of CLDs. Two of these spots were later identified by MS/MS and found to be ADPH and FABP, two previously characterized MFGM proteins. ADPH has been shown to associate with lipid droplets in many cell types [11], and FABP is thought to function in the transport of fatty acids required for the accretion of lipid droplets in the cytoplasm [11].

3.5 Comparison of MFGM and CLDs by protein identification

An important finding was that many of the spots from the MFGM 2-D map (Figs. 1B, 5A) were identical to the spots on the mammary CLD 2-D map (Figs. 4D, 5B) while there were few matches to the liver CLD 2-D map (Figs. 4B,

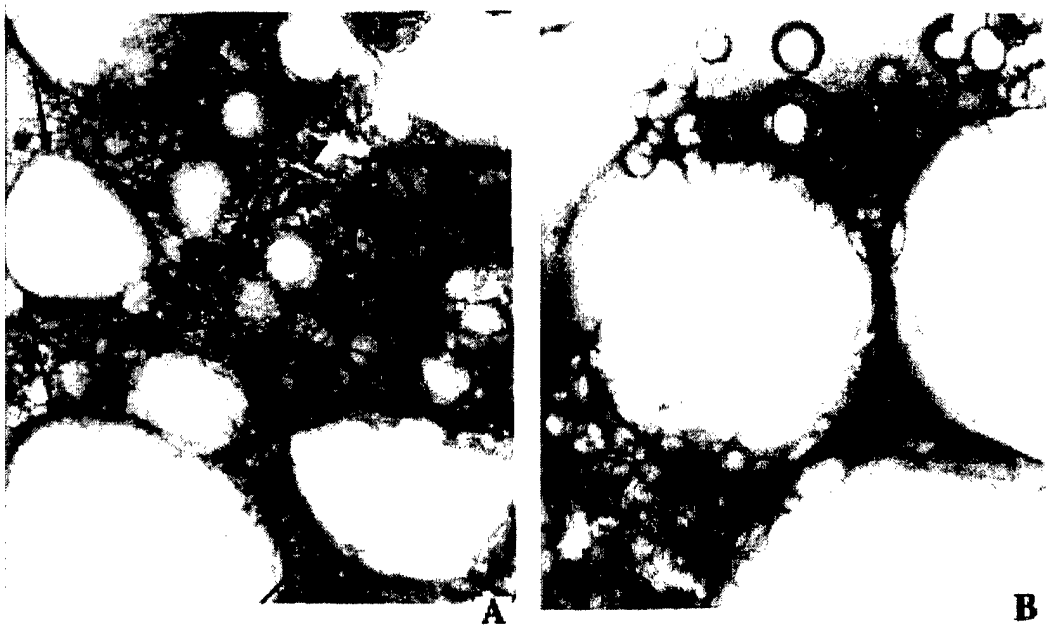

Figure 3. Electron micrographs of negatively stained isolated mouse mammary and liver CLD fractions. (A) Mammary CLDs (washed three times; (19 000 × magnification); (B) liver CLDs (unwashed; 19 000 × magnification). Symbols: arrowheads (membrane-like structures) and arrows (CLDs).

5C). To gain insight into the origin of the membranes surrounding the secreted CLDs, 2-D gel spots were excised from preparative (Coomassie-stained) 2-D gels, and the proteins were identified using reversed-phase LC coupled to MS/MS. Map identification numbers are used to label the spots on these 2-D maps (Figs. 5A, B and C). Protein identifications of the labeled spots are presented in Table 1. All proteins listed in the table were present in the MFGM fraction, and their presence or absence in the mammary and liver CLD fractions is indicated. Of the 29 proteins identified, 19 were also found in the mammary CLDs. Only four were found in the liver CLDs, two of which were the same two major serum proteins (albumin and transferrin) also found in the mammary CLDs. These serum proteins were found in high abundance in the mammary and liver cytosols, presumably due to the rupturing of organelles of the secretory pathway during the homogenization of the tissue and the nonspecific adsorption during the fractionation protocol. The other two proteins found in the liver CLDs were ADPH and FABP, as previously mentioned. An interesting observation was that three isoelectric variants and one truncated form of ADPH were found in MFGMs. However, only the two more basic variants as well as the truncated form were found in mammary CLDs. These same two were found in liver CLDs, but the truncated form was not (Fig. 5, # GM_C). Variable forms of these proteins may be functionally significant.

4 Discussion

4.1 Enrichment of samples analyzed and interpretation of protein identifications

The issue of contamination must be addressed whenever subcellular or secreted fractions are analyzed, especially when using a sensitive technique like 2-D gel electrophoresis coupled to MS/MS. The MFGMs were enriched from the milk expressed by groups of four L12 mice. Multiple mice were used to control for variation among animals. Because the membranes are isolated from milk, there is likely to be little contamination from cytoplasmic lipid droplets or any cellular organelles. The most likely contaminant would be cytosol. Cytoplasmic "crescents" (cytoplasmic inclusions between the lipid droplet and the membrane of the MFG) have been found in varying amounts in the MFGs, depending on the species of animal milked [1]. However, mouse MFGs contain very little cytoplasm, and, in fact, actin is significantly de-enriched in the MFGM fraction compared to the cytosol (data not shown). Nevertheless, contaminants are expected both from milk proteins and cytosol and have been reported by others to be found in their MFGM preparations [11]. In this study, minor amounts of skim milk proteins (α-casein, β-casein, ε-casein, and WAP) and serum proteins (albumin, transferrin, apo A-IV, and apo E/J, fibrinogen γ) were identified in the isolated MFGM fraction.

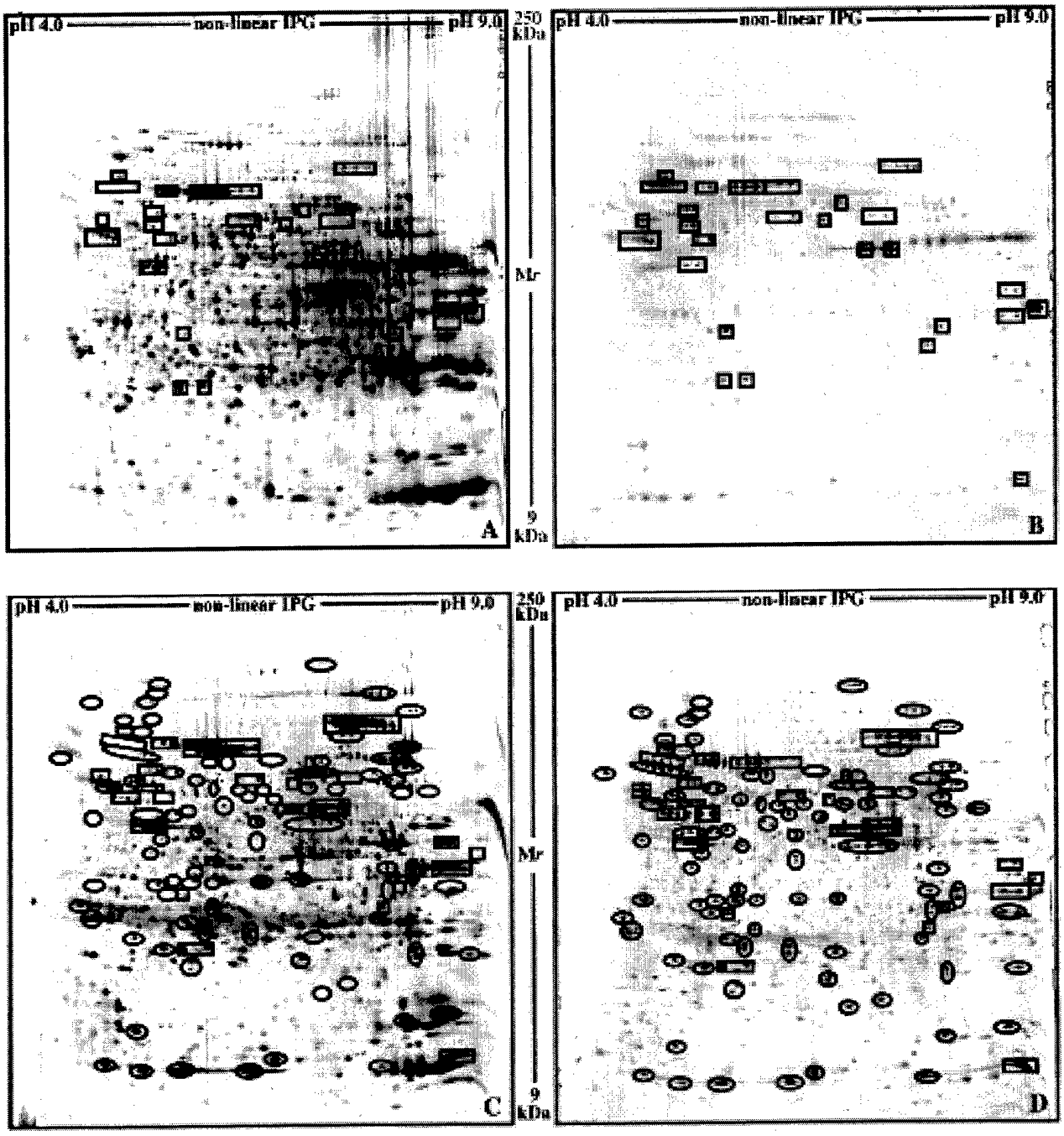

Figure 4. Comparison of the protein composition of mouse mammary and liver CLDs with mouse mammary and liver cytosol by 2-D gel electrophoresis. (A) 40 μg liver cytosol; (B) 20 μg liver CLDs; (C) 40 μg mammary cytosol; (D) 20 μg mammary CLDs. Silver-stained protein spots present in gel (B) are boxed. These boxed locations have been transposed onto gel (A) and gel (C). Silver-stained spots enriched in gel (D) as compared to gel (B) are circled. These circled locations have been transposed onto gel (C).

Mammary CLDs were prepared from the inguinal mammary glands from groups of four L12 mice. The major contaminant to be considered here would be the CLDs from cells other than the mammary epithelial cell, most notably the adipocyte. However, at this stage in development of the mammary gland, most of the cells in the gland are epithelial cells [23]. By immunofluorescence and EM, there are few detectable adipocytes (data not shown). In

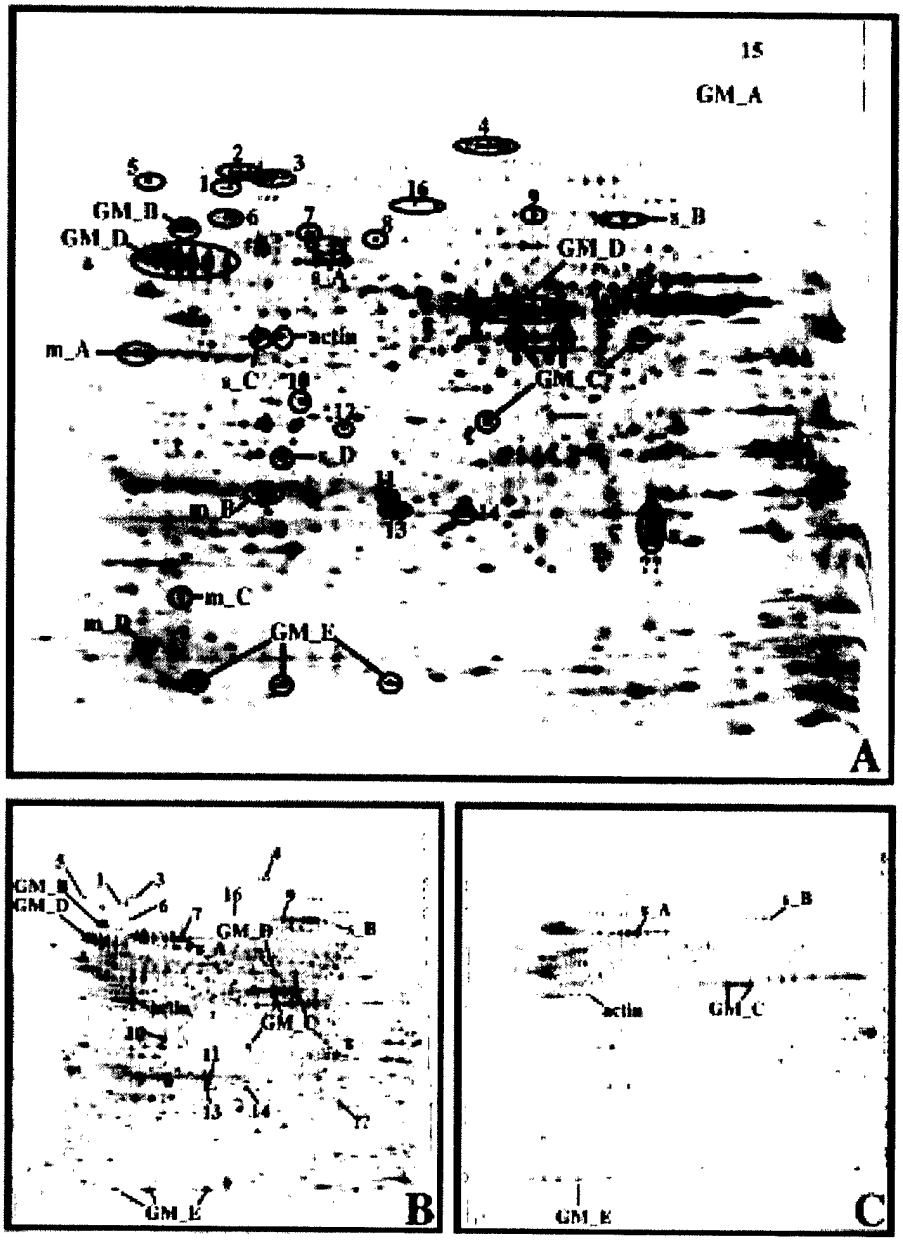

Figure 5. 2-D MFGM master map indicating the locations of the protein spots identified by MS/MS. Mammary and liver CLD maps are included for comparison of identified proteins. Proteins corresponding to # 15 and # GM_A are labeled at the top right corner of the master map. These spots could not be visualized on these 2-D gels. However, they are present in the sample and were identified by MS/MS in bands excised from a 1-D lane run on the edge of the 2-D gel during the second dimension.

the isolation procedure, milk was first washed from the intact mammary glands. The mammary glands were lightly homogenized, followed by the floatation of CLDs on a sucrose step gradient. The isolated CLDs were washed three times, and the fractions were monitored by EM for composition. Importantly, skim milk proteins were not detected in the mammary CLD fraction (Table 1). This implies that the washing of the gland prior to fractionation was adequate. As expected, the major contaminants of this preparation were serum proteins. However, it is clear that many proteins present in the mammary CLDs were not present in the cytosol (circled spots in Fig. 4C and D; Table 1). Liver CLDs were prepared using the same method and, like the mammary CLDs, contained small amounts of serum proteins (boxed spots in Fig. 4A and B; Table 1).

Our controls suggest that proteins identified to be present in both the MFGM and the mammary CLDs are specific and will be discussed in the following sections. The fact that they were isolated and identified from cell homogenates and secreted milk argues strongly that the data are not artifactual. In addition, the liver provides an extremely convincing control. The cytosolic contaminants in the

Table 1 Protein identification by MS[a)]

Map ID#	Identification (abbreviation)	MFGM	Mam. CLD	liver CLD	Mol. mass (kDa)	p*I*
1	TER ATPase	+	+	–	89.3	5.13
2	Fibrinogen γ	+	–	–	99.2	5.57
3	Gephyrin	+	+	–	79.8	5.29
4	Pyruvate carboxylase	+	+	–	129.6	6.57
5	ERP99	+	+	–	91.2	4.91
6	Dynein intermediate chain	+	+	–	68.3	5.16
7	Hsp 70	+	+	–	70.0	6.37
8	Cholesterol esterase	+	–	–	65.8	6.30
9	Motor protein	+	+	–	79.7	6.71
10	TIF32/RPG1	+	+	–	40.1	6.10
11	ER carboxylesterase	+	+	–	30.9	6.31
12	Heterotrimeric G protein β	+	–	–	37.3	6.19
13	ERP29	+	+	–	28.9	6.37
14	Peroxiredoxin IV	+	+	–	28.3	6.50
15	FAS	+	–	–	272.0	5.96
16	Gelsolin	+	+	–	80.8	6.43
MFGM proteins						
GM_A	XDH/XO	+	+[b)]	–[b)]	146.8	8.00
GM_B	BTN	+	+	–	65.0	5.11
GM_C	ADPH	+	+	+	59.2	6.60, 6.75, 6.95
	ADPH (truncated)				40.0	6.53
GM_D	Periodic acid Schiff 6/7 (PAS 6/7)	+	+	–	51.2 65.0	6.55–6.80 4.90–5.50
GM_E	FABP	+	+	+	14.8	5.68, 6.00, 6.31
Milk proteins						
m_A	α-Casein	+	–	–	35.6	4.98
m_B	β-Casein	+	–	–	25.3	5.82
m_C	ε-Casein	+	–	–	16.9	5.26
m_D	WAP	+	–	–	14.7	4.70
Serum proteins						
s_A	Albumin	+	+	+	68.7	6.20
s_B	Transferrin	+	+	+	76.3	6.94
s_C	Apolipoprotein A-IV (ApoA-IV)	+	–	–	49.2	5.86
s_D	Apolipoprotein E/apolipoprotein J (ApoE/ApoJ)	+	–	–	33.2/ 51.5	5.82/ 5.33

a) All protein identifications were by MS/MS unless otherwise indicated.
b) Presence/absence of this protein in the CLD sample was by 1-D immunoblot.

CLD fractions isolated from both tissue types were found to be the same (albumin and transferrin; Table 1), suggesting that proteins present in only mammary CLDs, but not liver CLDs, are specific.

4.2 ER membrane, lumenal proteins and cytosolic proteins may play a role in the formation of the CLDs

The following proteins were identified in both MFGMs and mammary CLDs, but not liver CLDs. These proteins are proposed to play a role in the first step of lipid secretion (Fig. 6).

ERP99 (# 6) is a type I transmembrane glycoprotein enriched in the rough endoplasmic reticulum [24]. The ERP99 oligosaccaride is endoglycosidase H-sensitive, and the glycan was shown by HPLC to be the trimmed form, $Man_8GlcNAc_2$. Therefore, it is presumed to cycle between the ER and the *cis*-Golgi. ERP99 is anchored in the membrane on the *N*-terminal domain, and 75% of the *C*-terminal portion of the protein is exposed on the cytoplasmic face of the ER [25]. From pulse chase experiments in MOPC-315 plasmacytoma cells, ERP99 remained localized to the ER [26]. Synthesis of the protein is upregulated 3- to 10-fold when cells are actively

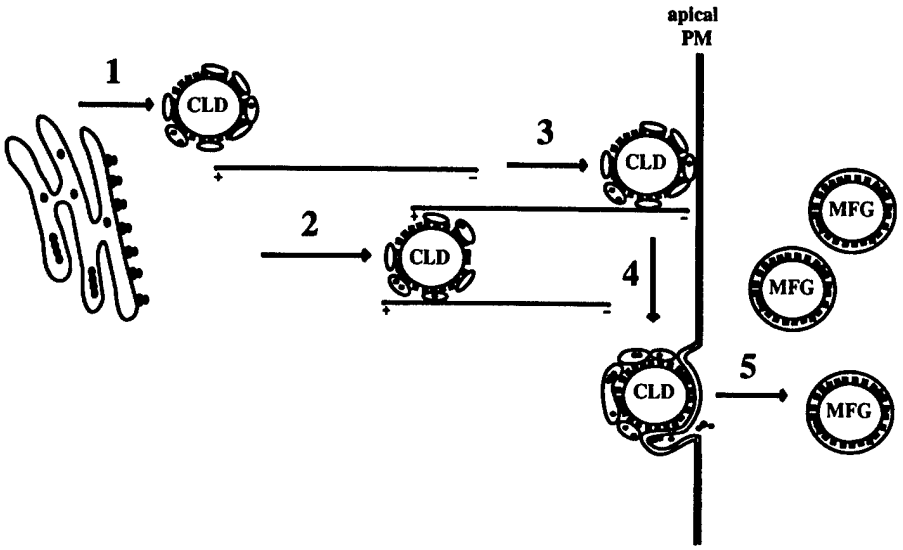

Figure 6. Schematic of five proposed steps involved in lipid droplet secretion in the mammary epithelial cell. (1) Assembly of lipid, protein coat, and vesicles onto the CLDs (2) Attachment of CLDs on to microtubules. (3) Vectorial transport of CLDs to the apical plasma membrane. (4) Fusion events at the apical plasma membrane. (5) Secretion of MFG into the lumen of the alveolus.

secreting [24], suggesting that it may play a role in secretion [27]. ERP99 may be useful as a marker for CLD-associated membranes.

ERP29 (# 13) is a soluble, lumenal ER protein retained in the ER by a variant retention motif, KEEL. ERP29 has homology to protein disulfide isomerase (PDI), but it lacks the characteristic calcium-binding motif of PDI. The expression of ERP29 is upregulated in response to increased secretion but not stress-induced by tunicamycin and calcium ionophores [28]. Therefore, it has been proposed that ERP29 is primarily involved in secretory events [29].

TER ATPase (# 1) is a cytosolic protein (p97) found in a complex with its cofactor p47. It interacts with *N*-ethylmaleimide sensitive fusion protein (NSF) and soluble NSF attachment protein (α-SNAP) to mediate fusion in depletion and add-back cell-free membrane fusion assays using liposomes and microsomes [30]. More recently, p97 was found to regulate the assembly of transitional ER (tER). Depletion of p97 inhibited tER assembly while readdition of purified p97 promoted reconstitution [31].

TIF32/RPG1 (#10) is the 100 kDa subunit (Rpg1p) of the translation initiation factor 3 core complex and is associated with the cytoskeleton. By immunofluorescence microscopy, Rpg1p colocalized with microtubules [32]. In nocodazole-treated samples, the microtubule staining pattern was abrogated. Also, Rpg1p coimmunoprecipitates with α-tubulin as well as intact mibrotubules [32]

Peroxiredoxin IV (# 14) is a new member of a family of enzymes that plays a role in protecting free thiol groups on proteins against oxidative damage [33]. Peroxiredoxin IV (PRxIV) is the secretable form of the enzyme. However, it is largely localized to the ER based on colocalization with calreticulin [33]. PRxIV has a glutathione-dependent peroxidase activity in addition to its thioredoxin-dependent activity and is proposed to play a protective role against oxidative damage by scavenging reactive oxygen species [33].

ER carboxylesterase (# 11) is a resident protein of the ER lumen. In yeast, ER carboxylesterase uses the HDEL retention signal to maintain its localization [34]. It has been shown to be involved in a process leading to the synthesis of luminal triacylglycerols [35].

Hsp70 (# 7) is a member of a family of chaperone proteins that bind to nascent polypeptide chains and partially folded intermediates to prevent their aggregation and misfolding [36].

Pyruvate carboxylase (# 4) is a member of the biotin-dependent carboxylases. It plays a crucial role in gluconeogenesis and lipogenesis by catalyzing the formation of oxaloacetate in response to increased Ca^{2+} levels [37, 38]. It is localized primarily to the cytoplasm [37].

The following two proteins were only found in MFGMs and not in either of the CLD fractions. These will not be discussed further.

Cholesterol esterase (bile salt activated lipase; # 8) is a secreted enzyme involved in the hydrolysis of triglycerides [39]. This enzyme is present in milk and facilitates fat and vitamin absorption and triglyceride hydrolysis in the intestine of the infant [40].

Fatty acid synthase (FAS) (# 15) is a cytosolic protein found to be in a complex with other proteins and lipids in the mammary epithelial cell cytoplasm [41]. This complex was found to contain butyrophilin, xanthine dehydrogenase/oxidase, and a group of small GTP-binding proteins that included ADP-ribosylation factor [41]. This complex interacts with the ER and lipid droplets [41]. FAS was found in MFGMs. FAS is expected to be present in the mammary CLD sample. However, its staining pattern on the 2-D gels (a large faint smear) was not consistent enough to get a positive identification.

A possible mechanism for step 1 (Fig. 6) of lipid secretion is the following. Vesicles enriched with a select group of ER proteins bud from the ER associated with microlipid droplets. Homotypic fusion catalyzed by ER ATPase mediates the fusion of microlipid droplets in the cytoplasm. These fusion events result in the formation of a CLD coated with proteins and large membrane-bound compartments.

4.3 Cytoskeletal components may play a role in vectorial movement of CLDs to the apical plasma membrane

The following proteins were found both in MFGMs and mammary CLDs, but not liver CLDs. These proteins are proposed to play a role in the second and third steps in lipid secretion (Fig. 6).

Dynein intermediate chain (# 6) is the cargo binding component of the minus end-directed microtubule motor complex which plays a role in maintaining the integrity, intracellular location, and function of the Golgi complex [42]. The ATPase which functions as the microtubule motor is localized within the large globular head of the dynein heavy chain, and several classes of light chains are thought to participate in a regulatory role [43]. Traditionally, secretory granules have been thought to utilize the traditional microtubule plus end-targeting motor, the kinesin complex, from the Golgi complex to the cell periphery. However, in the pancreatic acinar cell, targeting of zymogen granules to the apical surface requires an intact microtubule system with the microtubule minus ends close to the apical plasma membrane. Purified zymogen granules were found to be associated with the dynein intermediate and heavy chain but not with kinesin motor components [44]. Immunofluorescence studies showed a zymogen-like distribution for dynein and dynactin in the apical cytoplasm, and a calreticulin staining pattern for kinesin and kinectin in the basal portion of the cell. In addition, secretory granules of nonpolarized chromaffin cells, shown to use the traditional microtubule plus end-targeting motor from the Golgi complex to the cell periphery, were not found to be associated with dynein or dynactin [44].

Motor protein (# 9) is a novel human motor protein found in the heart [45]. To date, its function remains unclear.

Gelsolin (# 16) is a Ca^{2+} and polyphosphoinositide 4,5-bisphosphate (PIP_2)-regulated actin filament severing and capping protein that is implicated in actin remodeling [46]. In response to increased Ca^{2+} and H^+ levels, gelsolin is stimulated to sever actin filaments, after which it remains attached to the barbed end of the filament as a cap. The actin network then remains disassembled because the short actin filaments can no longer attach to one another [47].

Gephyrin (# 3) is a peripheral membrane protein found to be involved in membrane protein-cytoskeletal interactions. Specifically, it binds with high affinity to polymerized microtubules and is thought to anchor inhibitory glycine receptors to the subsynaptic microtubules [48]. Gephyrin interacts with profilin, an actin binding protein that stimulates actin polymerization.

Dynein intermediate chain, motor protein, gelsolin, and gephyrin were all found in both MFGMs and mammary CLDs. The dynein intermediate chain binds membrane vesicles to the heavy chain motor protein, which binds microtubules and functions by hydrolyzing ATP. However, an alternative scenario is that the identified novel motor protein replaces dynein motor protein and functions to link the CLD to the cytoskeleton. The dynein motor is traditionally thought to act as a minus end-directed or "retrograde" motor. As in pancreatic acinar cells, microtubules in the mammary epithelial cell may be oriented with the minus end at the periphery of the cell and the dynein complex would be required for the delivery of cargo to the apical surface. A possible mechanism for steps 2 and 3 (Fig. 6) of the lipid secretion model is the following. The dynein intermediate chain, already associated with its CLD/membrane cargo, bind to one of two possible motors, which moves along the microtubule towards the minus end at the apical plasma membrane. Once at the apical plasma membrane, the actin cytoskeleton is severed by the associated gelsolin to allow for direct contact between the CLDs and the plasma membrane, or "docking". The gephyrin present may be involved in the initial tethering step. These interactions would complement the interaction between XDH/XO and BTN, which has been proposed to be the "docking" mechanism of CLDs [3]. Alternatively, actin reorganization could occur through the interaction of gephyrin with profilin. Once the initial contact has been made, TER ATPase could mediate further fusion events between vesicles and/or the plasma membrane in step 4 (Fig. 6).

4.4 Release or scission of the MFGs into the lumen of the mammary alveolus

Trimeric G protein β (# 12) is the 37 kDa subunit of a complex composed of three subunits (α, β, γ). Trimeric G proteins are classically known to be involved as modulator or transducer in various transmembrane signaling systems. However, it has also been shown to modulate the exocytosis of secretory granules in prancreatic beta-cells by transient phosphorylation of a histidine residue by a GTP-specific protein kinase [49]. In this study, trimeric G protein β was only found in the MFGMs and not in either CLD

fraction. G-proteins could play a regulatory role in step 5 (Fig. 6) involving the release of the CLDs covered with a membrane composed of proteins originating from ER and plasma membrane, as well as those of other intracellular compartments.

4.5 Conclusion

Using a proteomics approach, we have successfully identified some of the major proteins in MFGMs and mammary CLDs. By performing this type of global analysis, we utilized a nonbiased method for the discovery of specific molecules involved in a unique secretory function. This knowledge provides us with a preliminary set of tools with which to dissect the complexity involved in the secretion of lipids in mammary epithelial cells. Our results provide evidence of the following: (i) mammary CLDs differ from liver CLDs in protein composition; (ii) mammary CLDs are intimately associated with membrane-like structures which contain components originating from the ER; (iii) a subset of the proteins present in MFGMs are also present in mammary CLDs, suggesting that the membranes and adherent proteins associated with CLDs are involved in the secretory process. Functional questions are currently being addressed on a select subset of the proteins identified in this study. Future progress on the MFGM and CLD proteomes will provide the identities of even more molecules involved in the mechanism of lipid secretion, and the ultimate completion of the proteomes will definitively address the specific origin of MFGMs.

We would like to thank Dr. Ian Mather for his expedient and generous donation of purified bovine BTN protein, guinea pig MFGs, and BTN antibodies, and also for his invaluable comments, suggestions, and encouragement. We would also like to thank Jimmy Erg for his expertise and guidance using Sequest software. This work was supported by NIH grants # R37 HD19547 (Margaret C. Neville) and # RO1 GM42629 (Kathryn E. Howell).

Received March 4, 2000

5 References

[1] Mather, I. H., Keenan, T. W., in: Mepham, T. B., (Ed.), *Biochemistry of Lactation*, Elsevier, Amsterdam 1983, pp. 231–283.

[2] Ghosal, D., Shappell, N. W., Keenan, T. W., *Biochim. Biophys. Acta* 1994, *1200*, 175–181.

[3] Mather, I. H., Keenan, T. W., *J. Mam. Gland Biol. Neoplasia* 1998, *3*, 259–273.

[4] Keenan, T. W., Patton, S., in: Jensen, R. G. (Ed.), *Handbook of Milk Composition*, Academic Press, San Diego, CA 1995, pp. 5–49.

[5] Wooding, F. B., *J. Cell Sci.* 1973, *13*, 221–235.

[6] Wooding, F. B., *J. Cell Sci.* 1971, *9*, 805–821.

[7] Kralj, M., Pipan, N., Methka, K., Nada, P., *Biol. Cell* 1992, *76*, 288–293.

[8] Nickerson, S. C., Keenan, T. W., *Cell Tissue Res.* 1979, *202*, 303–312.

[9] Patton, S., *J. Dairy Sci.* 1976, *59*, 1414–1419.

[10] Patton, S., Stemberger, B. H., Knudsen, C. M., *Biochim. Biophys. Acta* 1977, *499*, 404–410.

[11] Mather, I. H., *J. Dairy Sci.* 2000, *83*, 203–247.

[12] Taylor, R. S., Fialka, I., Jones, S. M., Huber, L. A., Howell, K. E., *Electrophoresis* 1997, *18*, 2601–2612.

[13] Rabilloud, T., Kieffer, S., Procaccio, V., Louwagie, M., Courchesne, P. L., Patterson, S. D., Martinez, P., Garin, J., Lunardi, J., *Electrophoresis* 1998, *19*, 1006–1014.

[14] Scianimanico, S., Pasquali, C., Lavoie, J., Huber, L. A., Gorvel, J. P., Desjardins, M., *Electrophoresis* 1997, *18*, 2566–2572.

[15] Yates III, J. R., Morgan, S. F., Gatlin, C. L., Griffin, P. R., Eng, J. K., *Anal. Chem.* 1998, *70*, 3557–3565.

[16] Patton, S., Huston, G. E., *Lipids* 1986, *21*, 170–174.

[17] Wessel, D., Flügge, U. I., *Anal. Biochem.* 1984, *138*, 141–143.

[18] Pasquali, L., Fialka, I., Huber, L. A., *Electrophoresis* 1997, *18*, 2573–2581.

[19] Shevchenko, A., Keller, P., Scheiffele, P., Mann, M., Simons, K., *Electrophoresis* 1997, *18*, 2591–2600.

[20] Gatlin, C. L., Kleemann, G. R., Hays, L. G., Link, A. J., Yates III, J. R., *Anal. Biochem.* 1998, *263*, 93–101.

[21] Dongre, A. R., Eng, J. K., Yates III, J. R., *Trends Biotechnol.* 1997, *15*, 418–425.

[22] Yates III, J. R., Carmack, E., Eng, J. K., in: Celis, J. E. (Ed.), *Cell Biology: A Laboratory Handbook*, Academic Press, San Diego, CA 1998, pp. 539–546.

[23] Hollmann, K. H., in: Larson, B. L., Smith, V. R. (Eds.), *Lactation I*, Academic Press, New York 1974, pp. 3–95.

[24] Lewis, M. J., Mazzarella, R. A., Green, M., *J. Biol. Chem.* 1985, *260*, 3050–3057.

[25] Mazzarella, R. A., Green, M., *J. Biol. Chem.* 1987, *262*, 8875–8883.

[26] Lewis, M. J., Turco, S. J., Green, M., *J. Biol. Chem.* 1985, *260*, 6926–6931.

[27] Koyasu, S., Nishida, E., Miyata, Y., Sakai, H., Yahara, I., *J. Biol. Chem.* 1989, *264*, 15083–15087.

[28] Demmer, J., Zhou, C., Hubbard, M. J., *FEBS Lett.* 1997, *402*, 145–150.

[29] Hubbard, M. J., McHugh, N. J., Carne, D. L., *Eur. J. Biochem.* 2000, *267*, 1945–1957.

[30] Otter-Nilsson, M., Hendriks, R., Pecheur-Huet, E. I., Hoekstra, D., Nilsson, T., *EMBO J.* 1999, *18*, 2074–2083.

[31] Paiement, J., Roy, L., Hendriks, R., Lavoie, C., Gushue, J., Chevet, E., Pelletier, A., Morre, D. J., *ASCB abstract 1739*, 1999.

[32] Hasek, J., Kovarik, P., Valasek, L., Malinska, K., Schneider, J., Kohlwein, S. D., Ruis, H., *Cell Motil. Cytoskel.* 2000, *45*, 235–246.

[33] Okado-Matsumoto, A., Matsumoto, A., Fujii, J., Taniguchi, N., *J. Biochem. (Tokyo)* 2000, *127*, 493–501.

[34] Medda, S., Proia, R. L., *Eur. J. Biochem.* 1992, *206*, 801–806.

[35] Abo-Hashema, K. A., Cake, M. H., Power, G. W., Clarke, D., *J. Biol. Chem.* 1999, *274*, 35577–35582.

[36] Fink, A. L., *Physiol. Rev.* 1999, *79*, 425–449.

[37] Kraus-Friedmann, N., Feng, L., *Metabolism* 1996, *45*, 389–403.

[38] Attwood, P. V., *Int. J. Biochem. Cell Biol.* 1995, *27*, 231–249.

[39] Bruneau, N., Lombardo, D., Bendayan, M., *J. Histochem. Cytochem* 2000, *48*, 267–276.

[40] Mechref, Y., Chen, P., Novotny, M. V., *Glycobiology* 1999, *9*, 227–234.

[41] Keon, B. H., Ankrapp, D. P., Keenan, T. W., *Biochim. Biophys. Acta* 1994, *1215*, 327–336.

[42] Roghi, C., Allan, V. J., *J. Cell. Sci.* 1999, *112*, 4673–4685.

[43] King, S. M., *Biochim. Biophys. Acta* 2000, *1496*, 60–75.

[44] Kraemer, J., Schmitz, F., Drenckhahn, D., *Eur. J. Cell Biol.* 1999, *78*, 265–277.

[45] Icho, T., Ikeda, T., Matsumoto, Y., Hanoaka, F., Kaji, K., Tsuchita, N., *Gene* 1994, *144*, 301–306.

[46] Sun, H. Q., Yamamoto, M., Mejillano, M., Yin, H. L., *J. Biol. Chem.* 1999, *274*, 33179–33182.

[47] Cooper, J. A., Schafer, D. A., *Curr. Opin. Cell Biol.* 2000, *12*, 97–103.

[48] Prior, P., Scmitt, B., Grenningloh, G., Pribilla, I., Multhaup, G., Beyreuther, K., Maulet, Y., Werner, P., Langosch, D., Kirsch, J., *Neuron* 1992, *8*, 1161–1170.

[49] Kowluru, A., Seavey, S. E., Rhodes, C. J., Metz, S. A., *Biochem. J.* 1996, *313*, 97–107.

THE JOURNAL OF BIOLOGICAL CHEMISTRY
Vol. 274, No. 6, Issue of February 5, pp. 3878–3886, 1999
Printed in U.S.A.

cDNA Cloning, Sequencing, and Characterization of Male and Female Rat Liver Aldehyde Oxidase (rAOX1)

DIFFERENCES IN REDOX STATUS MAY DISTINGUISH MALE AND FEMALE FORMS OF HEPATIC AOX*

(Received for publication, September 24, 1998, and in revised form, November 24, 1998)

Richard M. Wright‡, Daniel A. Clayton, Mary G. Riley, James L. McManaman§, and John E. Repine

From The Webb-Waring Antioxidant Research Institute and Department of Medicine, and §Department of Biochemistry, Biophysics, and Genetics, The University of Colorado Health Sciences Center, Denver, Colorado 80262

Molecular characterization of male and female rat liver aldehyde oxidase is reported. As described for the mouse liver, male and female rat liver expressed kinetically distinct forms of aldehyde oxidase. Our data suggest that the two forms arise as a result of differences in redox state and are most simply explained by expression of a single gene encoding aldehyde oxidase in rats. In support of this argument we have sequenced cDNAs from male and female rat liver. We examined mRNA expression by Northern blot analysis with RNA from males and females, from several tissues, and following androgen induction. Purified rat liver enzyme from males or females revealed a single 150-kDa species consistent with cDNA sequence analysis. Both male and female forms were reactive to the same carboxyl-terminal directed antisera. $K_{m(app)}$ values obtained in crude extracts of male or female rat liver and post-benzamidine-purified aldehyde oxidase differed substantially from each other but could be interconverted by chemical reduction with dithiothreitol or oxidation with 4,4′-dithiodipyridine. Our data indicate that a single gene is most likely expressed in male or female rat liver and that the kinetic differences between male and female rat liver aldehyde oxidases are sensitive to redox manipulation.

Aldehyde oxidase (AOX)[1] is a member of the molybdenum cofactor containing enzymes. Native AOX is routinely prepared as a homodimer of 300 kDa. Each 150-kDa subunit contains two iron-sulfur centers, an FAD, and the molybdenum-pterin cofactor (MoCo) (1–3). AOX (EC 1.2.3.1) catalyzes the oxidation of a wide range of aldehydic compounds, purines, quinoliniums, and numerous pharmacologic agents. While substrate specificity for AOX is very broad, and wide species variation in substrate specificity exists, the general catalytic reaction takes the form of hydroxyl transfer from water to an aldehyde creating the cognate acid. For example, conversion of benzaldehyde to benzoic acid is a very efficient reaction for AOX from most species. Conversion of *N*-1-methyl nicotinamide (NMN) to the 2- or -4-pyridone has been used as a standard definition of AOXs, although it is usually a kinetically less efficient reaction than benzaldehyde oxidation.

AOX is of interest both for its role in drug metabolism and as a source of the reactive oxygen species (ROS), hydrogen peroxide, and the superoxide anion, that have been related to numerous human pathologies. The human gene encoding AOX has been linked to a rare form of amyotrophic lateral sclerosis, although it is unknown if AOX encodes the amyotrophic lateral sclerosis locus itself (4–6). ROS are generated from AOX in an oxidative half-reaction following reduction of the enzyme by substrate. The FeS, FAD, and MoCo cofactors comprise an internal electron transfer chain in which electrons are passed from the active site molybdenum center to the FeS centers and finally to FAD. Partial reduction of oxygen at the the reduced FAD site produces ROS. Unlike the related enzyme xanthine dehydrogenase (XDH), AOX does not utilize NAD^+ as a cofactor and therefore AOX does not undergo the classical "D-form" to "O-form" conversion characteristic of XDH (7).

Two distinct AOX activities have been reported for mouse liver (8). Hepatic AOX from male and female mice differed in K_m and V_{max} for use of the substrate, benzaldehyde. The male enzyme exhibited a K_m of 40 μM while the female enzyme had a K_m of 115.4 μM. The male V_{max} was 423.7 nmol/min/mg of protein and the female enzyme was 203.0 nmol/min/mg of protein. Furthermore, male and female mouse AOX enzymes were dramatically regulated by testosterone. Treatment of female mice with testosterone proprionate (TP) converted both K_m and V_{max} values to the male pattern (8). Previous work had shown that castration resulted in the loss of a male pattern with conversion to a female pattern and TP supplementation restored the male-specific pattern of AOX expression (9). This observation was consistent with early reports of androgenic regulation of mouse hepatic AOX (10, 11). More recently, regulation of mouse hepatic AOX by testosterone was found to be mediated by growth hormone (12) where, again, growth hormone supplementation was found to convert K_m and V_{max} of the female-specific pattern to a male-specific pattern. Nonetheless, when male and female hepatic AOXs were purified to homogeneity they revealed a single band of 150 kDa on SDS-PAGE analysis and a single active band on native PAGE (8). How the differences between male and female hepatic AOXs were generated remained unclear.

* This work was supported in part by National Institutes of Health Grants HL52509 and HL45582, The Muscular Dystrophy Association, and the Robert and Helen Kleberg Foundation. The costs of publication of this article were defrayed in part by the payment of page charges. This article must therefore be hereby marked "*advertisement*" in accordance with 18 U.S.C. Section 1734 solely to indicate this fact.

The nucleotide sequence(s) reported in this paper has been submitted to the GenBank™/EBI Data Bank with accession number(s) AF110477 and AF110478.

‡ To whom correspondence should be addressed. The Webb-Waring Antioxidant Research Institute and The University of Colorado Health Sciences Center, Dept. of Medicine, 4200 East 9th Ave., Denver, CO 80262. Tel.: 303-315-4593; Fax: 303-315-3776; E-mail: richard.m.wright@uchsc.edu.

[1] The abbreviations used are: AOX, aldehyde oxidase; XDH, xanthine dehydrogenase; NMN, *N*-methyl nicotinamide; DTT, dithiothreitol; 4,4′-DTDP, 4,4′-dithiodipyridine; PAGE, polyacrylamide gel electrophoresis; ROS, reactive oxygen species; AOX-NT, anti-AOX antisera for the amino-terminal decapeptide; AOX-CT, anti-AOX antisera for the carboxyl-terminal decapeptide; MoCo, molybdenum-pterin cofactor; PCR, polymerase chain reaction; TP, testosterone proprionate; nt, nucleotide; RACE, rapid amplification of cDNA.

TABLE I
Oligonucleotides used for amplification of male and female rat AOX1

3′-RATRACE	5′CCCGGGGAATTCCTGCAGGTCGAC(T30)VN-3′
3′-RATUTR	5′-CCCGGGGAATTCCTGCAGGTCGACGCGTTCTGTAGTTGTTGAGCCAATCC-3′
MAO4RAT1	5′-CTGGAGTACATTAAAGTACCAGAATG-3
MAO4RAT2	5′-GTATTTCACCTTCAAGAATTTGATC-3′
FORINRAO	5′-GTTAGGATCAGAGGCTCCAAGTCTCGG-3′
REVINRAO	5′-CCGAGACTTGGAGCCTCTGATCCTAAC-3′
3′-IVS10	5′-GACTGGGCACAGACTGCTTTTGATG-3′
3′-IVS11	5′-CATCAAAAGCAGTCTGTGCCCAGTC-3′
IVS22	5′-CCGAGCTGCTCTTCTACGTGAACG-3′
RAT5	5′-CATCTCCTTCCTGAAATTCTGCCGATCC-3′
RAT6	5′-CCCGTGAGTCGGAGGTTCTTCCTCAGG-3′
3′-RREND	5′-CCCGGGGAATTCCTGCAGGTCGACTTT-3′

Two distinct AOX activities were also purified from rat liver and identified as NMN oxidases I and II (13, 14). The two activities exhibited different K_m values for the oxidation of NMN to either its 2- or 4-pyridone. These two activities also differed by pH optima, heat stability, and inhibitor sensitivity. NMN oxidases I and II were found to possess distinct kinetic parameters, K_m and V_{max}, for oxidation of several different substrates, including benzaldehyde and NMN. Furthermore, wide variation in K_m has been observed between different species and between individual rat strains (15–17). As was found for mice, rat hepatic AOX could be purified to homogeneity to yield a native enzyme of 300 kDa that resolved into two 150-kDa subunits by SDS-PAGE (13, 14).

AOX genes are widely expressed phylogenetically and in some organisms appear to arise from multigene families. Even the Archae express MoCo enzymes related to AOX (18). Two different AOX cDNA sequences were reported for corn plants that were themselves 83% identical (19). Three cDNA sequences were reported for *Arabidopsis thaliana* (20), and tomato plants may also possess several AOX genes (21). Two AOX genes have been identified in *Drosophila melanogaster*, one encoding AOX and the other encoding the highly related pyridoxal oxidase (PO) which was identified as an AOX (22–24). Sequences for AOX or PO in *Drosophila* have not been reported. Multiplicity in AOX genes was also reported for the mouse where independently segregating loci appeared to encode AOX enzymes with distinct electrophoretic mobilities and these were identified as AOX1 and AOX2 (9). Importantly, the different isozymes appeared to segregate as different AOX genetic loci under differential developmental and androgenic regulation. Human and bovine AOX sequences have been published that are approximately 82% identical, and a small fragment of a mouse AOX sequence was published (5, 25–27). However, second copies of the vertebrate AOX genes have not been cloned or sequenced. Therefore, while at least two or three AOX genes appear to exist in plants and flys, they have not been confirmed by sequence analysis in higher organisms. Furthermore, Southern blot analysis of chromosomal DNA could be interpreted to suggest that only a single AOX gene was present in humans (28).

Molecular characterization of AOX from the rat has not been reported. Because both forms of AOX appeared to be expressed in rat liver, we have examined expression of AOX genes from both male and female rat livers. We have confirmed the existence of two kinetically different forms of AOX in male and female rats. Sequence analysis of the corresponding cDNAs indicates that a single AOX gene is most likely activated in the liver in male and female rats. By Northern blot analysis, male and female rat liver RNA contained a single mRNA species that did not exhibit induction by TP. Purified rat liver AOX from males and females revealed a single 150-kDa band on SDS-PAGE. Present experiments suggest that a primary difference between male and female forms of AOX may lie in their respective redox states.

MATERIALS AND METHODS

RNA Purification and cDNA Synthesis—RNA was prepared from organs of freshly killed Sprague-Dawley rats by quick freezing the tissue in liquid nitrogen followed by extraction in guanidine isothionate and phenol:chloroform:isoamyl alcohol (24:24:1) (29). Frozen tissues were stored at −70 °C until use. Poly(A)$^+$ RNA was prepared by fractionation on oligo(dT)-cellulose (Stratagene, La Jolla, CA). cDNA was prepared by reverse transcription in a final volume of 20 μl as follows. 1.0 μg of poly(A)$^+$ RNA was mixed with diethyl pyrocarbonate-treated water, 1.0 μl of primer oligonucleotide at 20 μM, 1.0 μl of 10 mM deoxyribonucleoside triphosphates (ACGT), 0.5 μl of RNase inhibitor, 1.0 μl of recombinant Moloney murine leukemia virus reverse transcriptase (CLONTECH Laboratories, Palo Alto, CA), and 4.0 μl of 5 × buffer (final conditions: 50 mM Tris-HCl, pH 8.3, 75 mM KCl, 3 mM $MgCl_2$). Reactions were incubated at 42 °C for 60 min and then heated to 94 °C for 5 min to inactivate reverse transcriptase. Prior to use, reactions were diluted to 100 μl and 5 μl was used for PCR amplification. Reverse transcriptase reactions were stored at −70 °C.

3′ and 5′ RACE—A region from the middle of AOX1 was obtained by PCR amplification of reverse transcribed male rat liver poly(A)$^+$ RNA using synthetic oligonucleotides (Life Technologies, Inc., Gaitherburg, MD) derived from a fragment of the mouse liver AOX1 sequence (27). Nucleotides 1,682 through 2,217 were amplified with the oligonucleotides MAO4RAT1 and MAO4RAT2 (Table I) to produce a single 535-base pair fragment that was gel purified, sequenced in its entirety from two directions, and cloned as pMID. The resulting sequence was used to derive the unique sequence oligonucleotides for rat AOX1, FORINRAO, and REVINRAO. 3′ RACE was performed as follows. Male rat liver poly(A)$^+$ RNA was reverse transcribed using the oligonucleotide 3′ RATRACE as a primer for reverse transcriptase. The resulting single strand DNA was amplified by PCR using the oligonucleotides MAO4RAT1 and 3′ RATRACE. A second round of PCR amplification was performed using the 5′ nested oligonucleotide, REVINRAO, and 3′ RATRACE. A single product of 2,180 nt was obtained and sequenced entirely from both directions. This fragment was cloned as p3′ RATRACE and showed 100% identity with the overlap region of pMID. 5′ RACE was performed as follows. Male rat liver poly(A)$^+$ RNA was reverse transcribed using random hexamer oligonucleotides. The resulting single strand DNA was amplified by PCR using the oligonucleotides MAO4RAT2 and IVS22. A second round of PCR amplification was performed using IVS22 and the nested oligonucleotide FORINRAO. A single band of 1,930 nt was obtained, sequenced in its entirety from both directions, and cloned as p5′RATRACE. This sequence revealed 100% identity in the region of overlap with pMID. The extreme 5′ end and upstream region of the male rat AOX1 cDNA was obtained by a modified 5′ RACE as follows. Male rat liver poly(A)$^+$ RNA was reverse transcribed using random hexamer oligonucleotides. RNA was hydrolyzed in sodium hydroxide and the resulting single strand DNA was subjected to two cycles of nested PCR, the first using an adapter ligated oligonucleotide at the 5′ end. Oligonucleotide 3′IVS11 was phosphorylated with polynucleotide kinase in the presence of ATP. Following extraction with phenol:chloroform:isoamyl alcohol and ethanol precipitation the phosphorylated oligonucleotide was treated with dideoxyadenosine triphosphate and terminal transferase from bacteriophage T4 to block elongation from the 3′ end. Blocked, phosphorylated oligonucleotide was then ligated to single strand DNA using bacteriophage T4 RNA ligase in the presence of hexamine cobalt chloride to produce

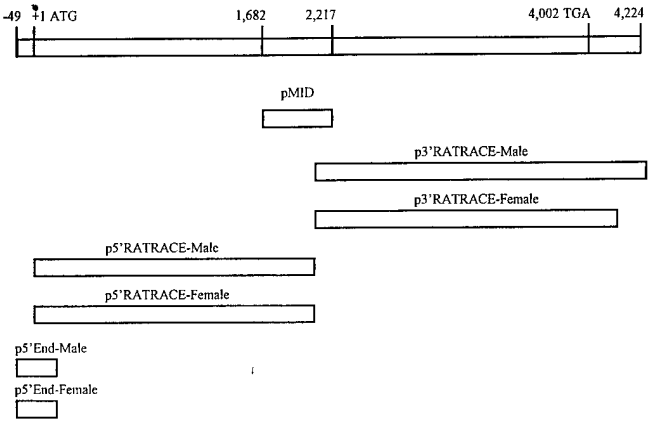

FIG. 1. **PCR amplification, cloning, and sequence strategy for male and female rat AOX1.** The *upper bar* shows the deduced cDNA structure for both male and female rat liver AOX1. PCR amplified and cloned fragments are shown *below*. Note that the 3′ RACE product for the female has been truncated within the untranslated region and does not comprise the entire untranslated region. Each cloned PCR fragment was subjected to DNA sequence analysis using a battery of oligonucleotides designed to encompass approximately 400 nucleotides between oligonucleotide primers. Each fragment was sequenced entirely from both directions. A list of sequence analysis primers and their sequences is available upon request. The assembled cDNA sequences for both male and female rat liver AOX have been deposited in the NCBI gene bank data base.

adapter-ligated single strand DNA. Adapter-ligated single strand-DNA was subjected to first round amplification using the oligonucleotides 3′ IVS11 and RAT5. The resulting PCR products were subjected to a second round of amplification using 3′ IVS11 and the nested primer, RAT6. The resulting 160-base pair DNA was cloned (p5′END-male), sequenced, and showed 100% identity with the overlap region of p5′RATRACE. This sequence was inferred to contain the translation initiation site and 49 nucleotides of 5′-untranslated region because it showed excellent deduced amino acid sequence homology with human and bovine AOX sequences, a single ATG was found to be in-frame with the downstream sequence, and translational termination sequences were observed upstream of this ATG and in the same reading frame.

DNA Sequence Analysis—Direct fluorescence sequence analysis was performed on plasmid DNA or PCR products using oligonucleotide primers designed to yield approximately 400 nt between primers and approximately 100 nt of overlap. A list of sequencing oligonucleotides and their sequences is available upon request. Prior to sequence determination, plasmids were prepared by alkaline lysis (29). PCR products were purified from low melting point agarose by phenol extraction and precipitation in ethanol. Sequences were determined using dideoxynucleotide chain terminating system from Perkin-Elmer Applied Biosystems (Foster City, CA). Reactions used the ABI PRISM™ Dye Terminator cycle sequencing ready reaction kits (Perkin-Elmer). Sequence reactions were fractionated on an ABI PRISM 310 DNA sequencer equipped with a 43-cm microcapillary (Perkin-Elmer). All sequences were determined from both directions and sequence data were compiled manually.

Northern Blot Analysis and Quantitation—Northern blots were run using formaldehyde-agarose gels and 5 μg of poly(A)$^+$ RNA (6, 29). Hybridization probes were isolated from the clones pMID, p3′RATRACE, and p5′RATRACE by PCR amplification and agarose gel electrophoresis. Following isolation in phenol, DNA fragments were labeled by random primed synthesis in the presence of [^{32}P]dATP for use as hybridization probes. High stringency hybridization and washing were conducted as described (6, 29). Following hybridization and autoradiography, each 4,500-nt band was cut from the hybridization filter and counted by liquid scintillation counting for quantitation. The remaining filter was dissociated from residual ^{32}P and rehybridized with a β-actin specific probe. Actin hybridization was also quantitated by excising the bands from the filter and liquid scintillation counting. Each AOX1 hybridization signal was normalized to the corresponding signal for β-actin after correction for background hybridization.

Castration and Hormone Supplementation—Castrated or sham castrated male Sprague-Dawley rats were obtained from Charles Rivers Laboratory (Wilmington, MA) following 1 week of recovery from surgery. Surgery was performed when rats were 4 weeks of age. Rats were maintained at Webb-Waring facilities for 1 additional week of equilibration. Testosterone proprionate was administered at a dose of 50 mg/kg body weight in corn oil by daily subcutaneous injection. Growth hormone was administered at a dose rate of 0.05 IU/100 g of body weight in a buffer composed of 30 mM $NaHCO_3$, 150 mM NaCl, pH 8.25, by subcutaneous injection twice daily. Sham castrated and castrated controls received corn oil injection. Following 10 days of treatment, rats were killed by sodium pentabarbitol administration. Organs were harvested immediately and dropped into liquid nitrogen for subsequent RNA preparation. RNA was analyzed from individual organs with 4 rats in the sham controls, 4 rats in the castrated control group, 5 rats in the castrated and testosterone supplemented group, and 5 rats in the castrated and growth hormone supplemented group.

AOX Activity Assays—AOX activity and initial rate data were determined spectrophotometrically in a 1-ml reaction containing 50 mM potassium phosphate buffer, pH 8.0, NMN at 5 mM or as needed, 10% dimethyl sulfoxide, 250 international units of CAT, 5–50 μM menadione as required, and appropriate levels of purified or partially purified enzyme. Initial rate data were obtained over a 5-min period. Formation of the pyridone of NMN was monitored at 300 nm.

AOX Enzyme Purification and Characterization—AOX enzyme activity was purified from male and female Spraque-Dawley rat livers. After removal of the liver, all procedures were performed at 4 °C or on ice using ice-chilled buffers. Liver sections (10–20 g) were diced, rinsed several times, homogenized, and dounced in 3 volumes of ice-cold 100 mM potassium phosphate, pH 7.5, containing 25 mM benzamidine hydrochloride, .2 mM phenylmethylsulfonyl fluoride, .1 mM EDTA. Homogenates were centrifuged for 1 h at 100,000 × *g*. The supernatant was brought to 5 mM DTT and incubated for 1 h. $MnCl_2$ was then added to the supernatant to a final concentration of 10 mM. The solution was then centrifuged for 5 min at 17,000 × *g* and the pellet was discarded. Dry ammonium sulfate was added with stirring to achieve a final concentration of 30%. The slurry was centrifuged and the pellet discarded. The resulting supernatant was brought to 50% saturation with ammonium sulfate, centrifuged, and the supernatant discarded. The resulting pellet (50% pellet) was resuspended in 1/20 the original volume of potassium phosphate buffer. Acetone fractionation was subsequently achieved using acetone chilled with dry ice. Suspensions were brought to 40% in chilled acetone, centrifuged, and the pellet discarded. Supernatants were brought to 50% in acetone, centrifuged, and the pellets collected. The 50% pellet was resuspended in the original volume of buffer and dry ammonium sulfate was added to achieve a 60% saturation. The pellet was recovered by centrifugation and resuspended in 1/20 of the original volume in 100 mM glycine, pH 9, containing 100 mM NaCl. After resuspension, insoluble debris was removed by centrifugation and the solution was desalted on a 5 × 15-cm Sephadex G-25 column in the above glycine buffer. The desalted solution was loaded onto a 2.5 × 10-cm benzamidine-Sepharose 6B (Pharmacia) column equilibrated in the same buffer. The column was washed with 3 column volumes of buffer and elution was achieved by flushing the column with 500 mM benzamidine hydrochloride. Elution was monitored at 436 nM and the single eluting peak was collected and precipitated with ammonium sulfate at 60% saturation. The pellet was stored at 4 °C for up to 1 day or was resuspended in a minimum volume of 100 mM potassium phosphate, pH 7.5, and dialyzed against the same buffer overnight.

The OD 280/450 ratio was between 5 and 7 for male or female preparations. Specific activity for NMN hydroxylation to the pyridone was 100–250 nmol/min/mg for the female or male enzymes. Both enzyme preparations were inhibited to greater than 95% by inclusion of 50 μM menadione. We observed persistent aggregation of the soluble protein fraction when preparations did not include treatment with DTT early in the fractionation. Aggregation reduced the overall yield of AOX enzyme to less than 0.1% of the starting activity. Reduction of the crude lysate prior to $MnCl_2$ treatment improved the overall yield to 7% of the starting activity. SDS-PAGE analysis of the aggregated proteins suggested no obvious bias for specific aggregated proteins. Furthermore, reduction in 5 mM DTT was significantly more effective in preventing aggregation than was 10 mM cysteine. Reduction of male or female liver extracts permitted purification of both enzymes to homogeneity.

Preparation of Antibody to AOX—The amino-terminal decapeptide comprising the sequence NH_2-DRASELLFYV-COOH and the carboxyl-terminal decapeptide comprising the sequence NH_2-GSYVPWNIPV-COOH were synthesized by Dr. Hans-Richard Rackwitz (German Cancer Research Center, Heidelberg, Germany). Antibody to the synthetic oligo peptides was produced in rabbits by intravenous injection of 20 μg of peptide. Rabbits were boosted with peptide every 2 weeks. The IgG fraction was prepared from serum by ammonium sulfate precipitation following coagulation of the blood and sedimentation. This produced two antisera preparations: AOX-NT (amino-terminal antibody) and

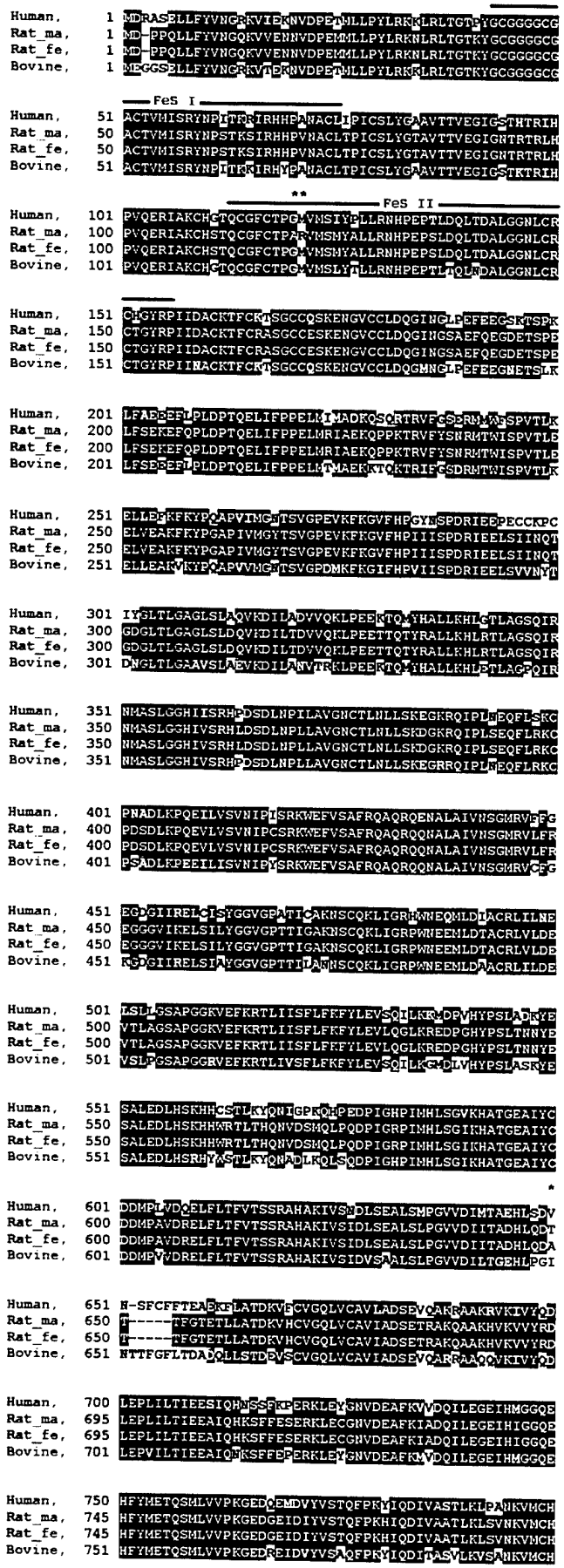

FIG. 2. **Alignment of deduced amino acid sequences.** Amino acid sequences for the four vertebrate AOXs have been aligned by multiple Clustal analysis. Identical amino acids are *boxed* in black and biochemically conserved differences are shown in *gray*. Regions thought to mediate cofactor binding are indicated by the *overline*. Five sites within the large MoCo-binding domain have been identified and are shown individually. The 5 amino acid differences between male and female rat liver AOXs have been indicated with an *asterisk*. The programs ClustalW, Boxshade, and Paint were used to create the figure.

FIG. 2—*continued*

AOX-CT (carboxyl-terminal antibody).

Western Immunoblot Analysis—Protein was electrophoresed on SDS-PAGE and transferred to polyvinylidine difluoride membranes (Bio-Rad). Filters were sliced for staining with Commassie Brilliant Blue or processed for immunoblot analysis. For reaction with antisera, filter strips were blocked with gelatin overnight prior to reaction with pre-immune sera, AOX-NT, or AOX-CT antisera. Antigen-antibody complexes were detected by reaction with alkaline phosphatase streptavidin kit (Bio-Rad).

RESULTS

Different Forms of AOX Exist in Male and Female Rat Livers—AOX enzyme activity was measured in crude extracts of

male and female rat livers. Apparent K_m ($K_{m(app)}$) values were determined from Lineweaver-Burk plots by measuring conversion of NMN to its pyridone. $K_{m(app)}$ for male rat liver AOX was 538.8 μM and $K_{m(app)}$ for the female was 1062.3 μM, consistent with previous reports showing two forms of AOX in livers from rats and different forms of AOX in livers from male and female mice. While no explanation for this difference has been produced, the two AOX genes identified in mice, AOX1 and AOX2, suggested the possibility that two different AOX genes may be expressed in rat liver.

cDNA Sequence Analysis of Male and Female Rat Liver AOX1—Fig. 1 illustrates the PCR amplification strategy used to obtain segments of male rat liver AOX1. DNA sequence of the three PCR products was assembled to produce the male rAOX1 cDNA. RAOX1 comprised 4,304 nucleotides, including 30 nt of polyadenylation, 210 nt of 3′-untranslated region, and 49 nt of 5′-untranslated region. A single open reading frame was identified that encoded a protein of 1,333 amino acids and a deduced mass of 147,009 Da. The deduced male rAOX1 protein exhibited 82% sequence identity with human AOX1 and 81% sequence identity with bovine AOX1. Multiple sequence clustal analysis revealed conservation of co-factor domains corresponding to FeS I, FeS II, FAD, and five small domains within the MoCo binding segment (Fig. 2).

TABLE II
Sequence differences in male and female rat AOX1 clones described here

The differences in cDNA sequence between the male and female rat AOX1 clones are shown. nt-site refers to the specific base changed from male to female using the A of the translational initiator as nucleotide +1. The nature of the base pair changed is shown along with the change, if any, in the deduced amino acid sequence and the corresponding amino acid number. Note, these changes reflect differences between our clones and do not necessarily reflect consistent differences between genders.

No.	nt-Site	Base pair change	Amino acid change	Amino acid site
1	133	G:C–A:T	P–P	
2	405	C:G–G:C	A–G	119
3	408	G:C–T:A	R–M	120
4	1,679	T:A–C:G	L–L	
5	1,994	A:T–G:C	T–A	649
6	2,563	G:C–A:T	L–L	
7	2,872	T:A–C:G	S–S	
8	3,739	G:C–A:T	Q–Q	
9	3,875	C:G–T:A	L–F	1,276
10	3,993	G:C–C:G	R–T	1,315

Female rat liver AOX1 cDNA sequence was obtained using a similar strategy with the exception that a unique sequence oligonucleotide derived from the male sequence, 3′ RATUTR, was used to obtain the 3′ RACE product. Thus, 47 nucleotides of 3′-untranslated region was obtained for the female and this does not include the polyadenylation site (Fig. 1). The assembled cDNA sequence for female rat liver AOX1 encoded a deduced protein of 1,333 amino acids and 146,919 Da. The female cDNA sequence was 99.8% identical to the male sequence and the deduced protein sequence was 99.6% identical to the male sequence. Of the 10 nucleotide differences detected between the male and female rat liver AOX1 cDNA sequences described here, five resulted in changes to the deduced amino acid sequences (Table II). However, while nucleotides 405 and 408 differ between male and female sequences reported here and to the GenBank data base, these variations were also found between individual male clones and therefore do not represent gender differences but differences between individual rats. The full extent of individual variation was not determined and it remains possible that all of the differences observed between the two clones described may be attributed this cause alone.

Expression of Rat AOX1 mRNA—Fig. 3A shows Northern blot analysis of poly(A)$^+$ RNA from male rat liver. Hybridization probes were derived from each of the three male clones, pMID, p5′RATRACE, and p3′RATRACE. The region between nucleotides 1,682 and 2,217 of the male cDNA, corresponding to the pMID hybridization probe, produced hybridization signals at approximately 4,500 and 2,500 nt. Hybridization probes derived from both the p5′RATRACE and p3′RATRACE clones produced predominantly a single band at 4,500 nt with weak hybridization to the band at 2,500 nt. We conclude that the predominant mRNA for rAOX1 detected by Northern blot analysis in males is approximately 4,500 nt, consistent with the cDNA sequence assembled for rAOX1. The unexpected signal at 2,500 nt may represent a cross-reactive species largely localized to the pMID region.

Hybridization probes derived from the p5′RATRACE produced predominantly a single band from both male and female RNA (Fig. 3*B*). This RNA was also estimated to be 4,500 nucleotides in size, and no difference in size or number of hybridizing bands was detected between males and females.

Northern blot analysis of poly(A)$^+$ RNA from several different tissues showed expression of a single 4,500-nt RNA for all tissues examined (Fig. 3*C*). Different tissues did not show variation in either the size or multiplicity of AOX RNAs. Var-

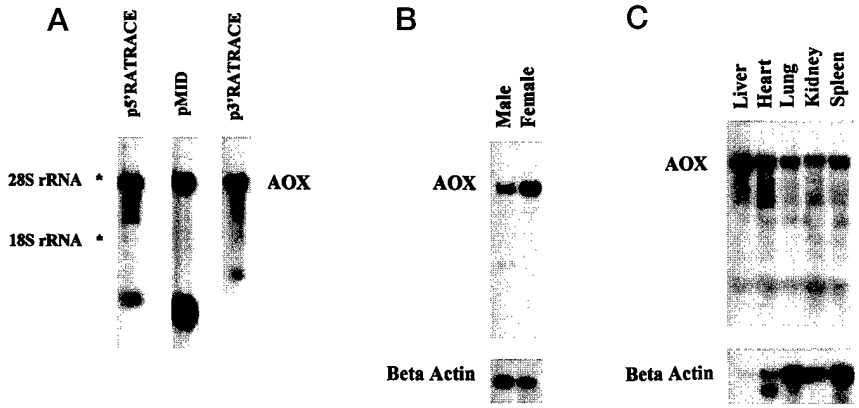

FIG. 3. **Northern blot analysis of rat AOX1 expression.** *A*, each of the three clones used to assemble male rat liver AOX1 was used as a hybridization probe for independent Northern blots of male rat liver poly(A)$^+$ RNA. The major band at 4,500 nt corresponds to the AOX1 mRNA. The band at 2,500 nt that has greater localization to the pMID region of AOX is assumed to represent a cross-reactive species. Although it has not been excluded that this may represent a breakdown product of the larger RNA, it is too small to encode a full-length AOX. *B*, poly(A)$^+$ RNA from male and female rat liver has been analyzed by Northern blot using the p5′RATRACE clone as a hybridization probe. No attempt is made here to indicate a difference in abundance of the AOX mRNA between males and females. *C*, poly(A)$^+$ RNA from several different male rat tissues has been analyzed by Northern blot using the AOX1 insert from p5′RATRACE as a hybridization probe.

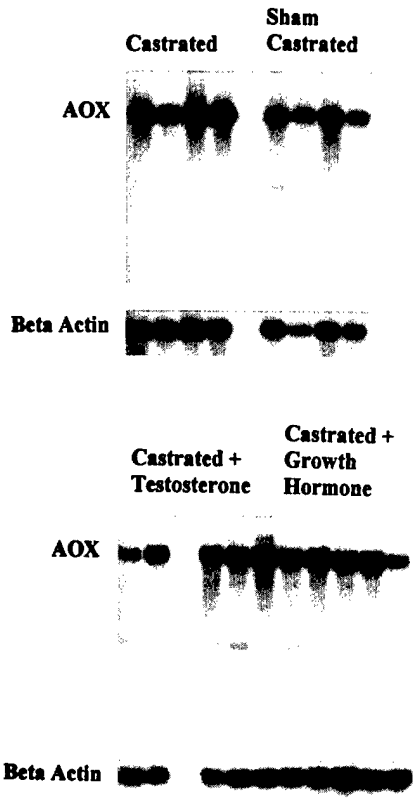

FIG. 4. **Testosterone does not regulate steady state levels of rat hepatic AOX.** Poly(A)$^+$ RNA from individual male rat livers has been analyzed by Northern blot. Individuals from the following four groups have been used: castrated, sham castrated, castrated and testosterone supplemented, castrated and growth hormone supplemented. β-Actin was used as a control to reveal uniform loading of RNA. Blots were first probed with the AOX probe, the corresponding region cut from the filter for counting, and the remaining filter was dissociated of all ^{32}P and rehybridized with the β-actin probe.

iation in the β-actin control precludes drawing firm conclusions at this point concerning relative levels of expression between tissues.

RNA from male rats that had been sham castrated, castrated, castrated and treated with TP, or castrated and treated with growth hormone was analyzed by Northern blot. Fig. 4 shows that steady state RNA levels were only slightly affected by any of these treatments. When hybridization signals were quantitated and normalized to either OD 280 or to β-actin hybridization signal (Table III), we found no statistically significant difference between groups in AOX1 mRNA abundance. These data do not support significant regulation of rat AOX1 mRNA abundance by TP.

AOX Enzyme Purification and Characterization—AOX enzyme activity was purified to homogeneity from male rat livers (Fig. 5*A*). These preparations produced a single band of 150 kDa by SDS-PAGE analysis. We were unable to sequence this protein by direct Edman degradation suggesting that its amino terminus was blocked, as was found for both the rabbit liver and bovine liver AOXs (5, 26). Western immunoblot analysis of partially purified AOX from male and female rat livers revealed excellent reactivity of each enzyme preparation to this synthetic peptide-derived antibody (Fig. 5*B*). Furthermore, reactive proteins from male and female revealed a predominant polypeptide of approximately 150 kDa with no evident difference in size between genders. (Fig. 5*C*).

$K_{m(app)}$ values for oxidation of NMN to its pyridone were determined by analysis of Lineweaver-Burk plots. Fig. 6 and Table IV show these results. As noted above, crude liver extracts from males produced $K_{m(app)}$ of 538.8 and 1062.3 μM for females. Reduction of the crude liver extract with 5 mM DTT shifted $K_{m(app)}$ for males and females. Reduced male rat liver produced $K_{m(app)}$ of 359.9 μM and for the reduced female enzyme $K_{m(app)}$ was 354.5 μM (Fig. 6*B*). Thus, male and female forms of AOX can be converted to a form with indistinguishable $K_{m(app)}$ values by chemical reduction in a crude lysate. Oxidation of the reduced female preparation with 4,4′-DTDP converted $K_{m(app)}$ back to a form similar to that obtained from the untreated female preparations (Fig. 6*B*). Furthermore, AOX purified from female rat liver through the post-benzamidine stage could be reduced with DTT to yield an enzyme with $K_{m(app)}$ of 261 μM. Reoxidation of the reduced enzyme with 4,4′-DTDP converted the $K_{m(app)}$ to 1673 μM (Fig. 6*C*). Thus, the capacity to modulate $K_{m(app)}$ of rat liver AOX was maintained through purification of the enzyme and may therefore reflect an intrinsic property of the enzyme.

TABLE III
Quantitation of RNA hybridization

Hybridizing bands from the Northern blot shown in Fig. 4 were cut from the filters and counted by liquid scintillation counting. Counts from randomly selected regions were averaged and subtracted from each signal to account for background radioactivity. Counts for each AOX signal were then normalized to the β-actin signal derived from the same lane, and the normalized, background subtracted counts were multiplied by 100. The number of animals in each group is shown by the *n*. The mean and standard error of the mean (SE) were calculated for each group. No statistical significance could be established between group means.

Group	*n*	Mean	S.E.
Sham castrated	4	69.0	10.3
Castrated control	4	86.6	11.4
Castrated testosterone	5	82.9	18.3
Castrated growth hormone	5	64.9	13.5

DISCUSSION

In the present work have assembled full-length sequences for AOX cDNAs from male and female rat liver. We examined expression of AOX by Northern blot analysis from males and females, from several tissues, and have examined the effect of androgen regulation. We purified AOX from rat livers of males and females and obtained a single 150-kDa band by SDS-PAGE analysis consistent with the deduced amino acid sequences from males or females of 1,333 amino acids and 147 kDa. Antisera raised against synthetic decapeptides reacted with AOX from males or females. Furthermore, $K_{m(app)}$ values for crude extracts of male or female rat liver and post-benzamidine purified AOX differed substantially but could be interconverted by chemical reduction with DTT or oxidation with 4,4′-DTDP.

The deduced amino acid sequences for male and female rat liver AOX are 81 and 82% identical to human and bovine AOXs and are themselves 99.6% identical. They show excellent conservation in the domains attributed to iron, FAD, and MoCo binding. By this criterion, the rat AOXs clearly belong to the molybdenum iron-sulfur flavoproteins that include AOX, XDH, and XO. Furthermore, the rat AOXs conform to the domain models proposed for XDHs (7, 30, 31). Amino acids critical for catalysis of this class of enzymes are conserved in the rat AOX sequences as they are in most other AOXs and XDHs. In particular, Glu-869 of the Mop enzyme is critical for catalysis and is conserved in nearly all XDHs and AOXs (see Ref. 21 for alignment of several sequences), including the two rat sequences reported here where it is found at amino acid 1265 in MoCo domain 5 (Fig. 2).

We observed that the male and female cDNA sequences were not identical. While several arguments could be advanced to explain the differences, we suggest that the least tenable ar-

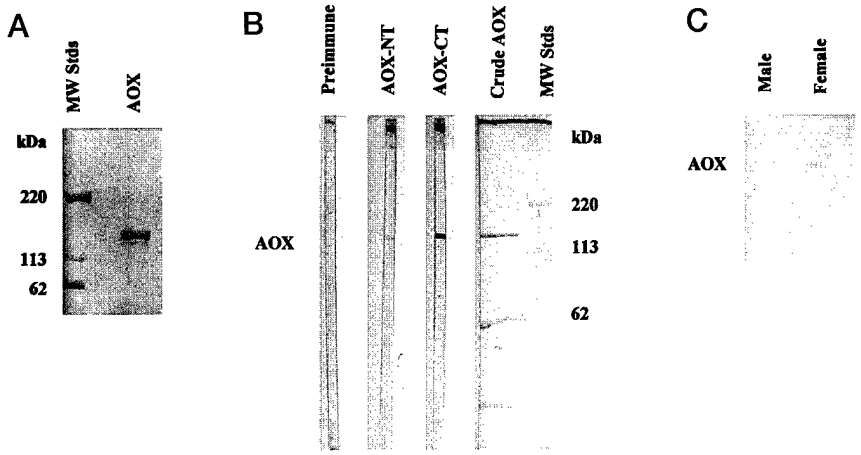

FIG. 5. **Analysis of rat liver AOX1 protein.** *A,* male rat liver AOX was purified to homogeneity from initially reduced extracts as described under "Materials and Methods." Purified AOX was analyzed by SDS-PAGE and stained with Ponceau S prior to subjecting the enzyme to amino-terminal sequence analysis. *B,* antibody was raised against synthetic decapeptides from the amino (*AOX-NT*) and carboxy (*AOX-CT*) termini. AOX was partially purified to retain numerous unrelated proteins, analyzed by SDS-PAGE (*Crude AOX*), and reacted to each antibody as described under "Materials and Methods." Preimmune, AOX-NT, and AOX-CT antisera were used at a 1:500 dilution. *C,* male and female rat liver AOX was purified to homogeneity from initially reduced preparations. Enzymes were analyzed by SDS-PAGE and subjected to Western immunoblot analysis using the AOX-CT antisera. Both male and female preparations migrated with apparent size of 150 kDa and both preparations reacted to the AOX-CT antisera.

gument is for the expression of two different AOX genes in the livers of male and female rats. Nucleotide differences between males and females could arise during PCR amplification, cloning, or sequence analysis since this is also PCR based. The small number of differences observed between male and female sequences could also arise from allelic differences between males and females or simply from individual differences between rats. Sequence analysis of only one additional male cDNA uncovered two of the changes (nt 405 and 408) found between the male and female clones. The minimal number of differences found between males and females coupled with the individual variation already observed suggests that the differences are unlikely to represent expression of alternative genes. Furthermore, sequence polymorphism is a well described phenomenon in *Drosophila* XDH (32–34).

Multiplicity of AOX genes has been established for some organisms (19–24), and in plants these data are supported by multiple cDNA sequences of approximately 80% identity (19, 20). Thus, the observation that mice appear to express two AOX genes in the liver was not surprising (9). However, genetic data derived in the mouse have not been supported yet by corresponding molecular data and few efforts have been made to establish AOX gene copy number in vertebrates. Southern blot analysis of chromosomal DNA failed to reveal second AOX genes in several vertebrates under conditions in which at least 80% identity would have produced hybridization (28).

Northern blot analysis of AOX mRNA from male or female rats, and from several different tissues, demonstrated expression of a single 4,500 nt RNA. We did not observe variation in size or multiplicity of AOX mRNAs in the liver from males or females where kinetically distinct forms of AOX were identified. Furthermore, castration and/or testosterone supplementation resulted in no significant alteration in AOX mRNA abundance and we infer that testosterone does not appear to exert significant regulation of AOX mRNA abundance or form in the rat liver. We did observe surprisingly strong hybridization to an RNA of 2,500 nt that could be localized to the region from +1,682 to +2,217. While the identity of this RNA is unknown, it is too small to encode an AOX of 150 kDa. Thus, RNA analysis supports expression of a single AOX gene in the liver where post-translational events may be important for determining the differences between male and female kinetic variants.

Interestingly, AOX-3 from *A. thaliana* encoded a protein of only 568 amino acids truncated at the amino terminus (20). It must differ from a true AOX because it cannot encode a protein capable of binding the full set of co-factors. AOX-3 from *A. thaliana* showed striking homology to AOX-1 and AOX-2 in the MoCo-binding region, confirming that it is indeed a member of the MH family. Confirmation that vertebrates encode such a protein would be of great interest since it may represent the RNA detected at 2,500 nt.

Since our observations suggested that rats express a single AOX gene in the liver, we examined the possibility that redox status might underlie the differences in male and female variants. We found that partially purified crude extracts of male and female rat liver did indeed reveal different $K_{m(app)}$ variants of AOX. Reduction of crude extracts from males or females with DTT resulted in conversion to a single form. Subsequent reoxidation of the reduced AOX with 4,4′-DTDP resulted in conversion to a more female like $K_{m(app)}$. Reduction or oxidation of post-benzamidine purified AOX also resulted in interconversion between the two extremes of $K_{m(app)}$ suggesting that the variants differed by their intrinsic oxidation state. Since DTT directly reduces protein disulfides to thiols while 4,4′-DTDP forms disulfides from thiols (35–38), we infer that manipulation of thiol oxidation state can interconvert kinetic variants of AOX.

Redox effects on XDH are well known. Conversion between the NAD^+ dependent, D-form, and the oxygen dependent, O-form, is a redox-dependent process reversible by chemical reduction (7, 39, 40). Furthermore, redox effects on XDH have dramatic effects on the kinetic parameters of the enzyme (41). AOX does not have an NAD^+-dependent form of the enzyme, and therefore conversion between D-form and O-form is irrelevant. While cysteine residues critical for D-form to O-form conversion in XDH were not conserved in AOX (42), most of the 41 cysteine residues found in rat liver AOX are conserved with vertebrate XDHs. These cysteine residues would be expected to take part in the same biochemical reactivities as those found in XDH. Since we observed that redox effects on $K_{m(app)}$ were preserved from crude extracts through post-benzamidine-puri-

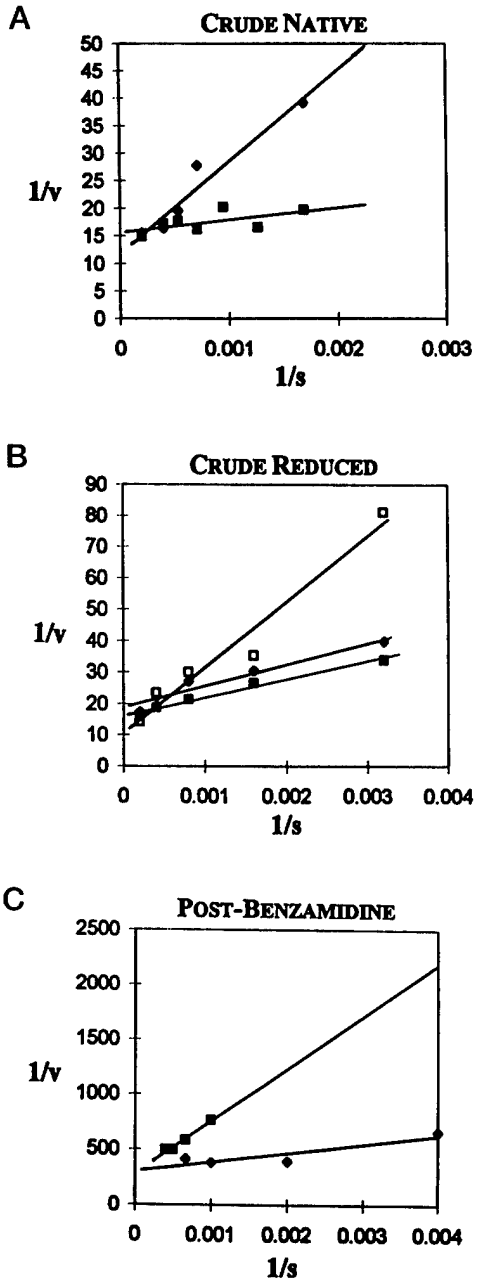

FIG. 6. **Chemical reduction or oxidation abolishes differences in $K_{m(app)}$ between male and female rat liver AOX.** AOX activity was purified from unreduced male and female rat livers through $(NH_4)_2SO_4$ fractionation and either treated with 5 mM DTT or not to produce the crude native or crude reduced preparations. A separate preparation was reduced initially and purified through benzamidine fractionation to produce the post-benzamidine preparation. *A*, Lineweaver-Burk plots were determined for male (*squares*) and female (*diamonds*) preparations using NMN as the oxidizing substrate. *B*, Lineweaver-Burk plots were determined for initially reduced male and female crude extracts. In addition, the reduced female extract was then treated with 1 mM 4,4'-DTDP to reoxidize it (*open squares*) and subjected to Lineweaver-Burk analysis. *C*, female rat liver AOX was purified through benzamidine fractionation from an initially reduced extract. Enzyme was treated with 5 mM DTT or 1 mM 4,4'-DTDP to reduce or oxidize the enzyme. Lineweaver-Burk analysis was then conducted on the reduced (*diamonds*) or oxidized (*squares*) preparations.

fied enzyme and that these effects alone were sufficient to explain the differences between male and female variants, we infer that the different $K_{m(app)}$ variants result not from expression of alternative genes but from redox effects that may act either on AOX itself or on a closely associated protein capable of modulating $K_{m(app)}$ for AOX.

TABLE IV

Effect of reduction and oxidation on $K_{m(app)}$ for crude and purified rat liver AOX

Lineweaver-Burk plots shown in Fig. 6 were fitted by least squares analysis. *$K_{m(app)}$ were determined for each curve and the goodness of fit* r^2 values were determined for each.

		$K_{m(app)}$	r^2
Crude native	Male	371	0.65
	Female	1385	0.94
Crude reduced	Male-red	360	0.98
	Female-red	354	0.94
	Female-reox	1895	0.96
Post-benzamidine	Reduced	261	0.83
	Oxidized	1673	0.97

Our observations can be explained by the activity of the hepatic microsomal monooxygenase. The cystamylating flavin monooxygenase catalyzes oxidation of cysteamine, a thiol, to cystamine, a disulfide, and this reaction provides a significant source of disulfide responsible for maintaining the intracellular thiol:disulfide potential (43, 44). The thiol:disulfide potential is thought to reflect two ratios: the GSH:GSSG ratio and the cysteamine:cystamine ratio. Protein oxidation state depends on overall thiol:disulfide potential. Higher levels of monooxygenase lead to a more oxidizing environment, while reduced monooxygenase levels result in a more reducing environment. Significantly, monooxygenase from mice or rats is regulated by testosterone in precisely the fashion that kinetic variants of AOX are regulated (43). Male rat hepatic monooxygenase levels are lower than female levels. Castration of male rats elevates monooxygenase and leads to elevated cystamine and a more oxidizing cytosol. Testosterone reverses this effect and restores the reducing environment. Furthermore, testosterone treatment of females lowers monooxygenase and elevates cysteamine levels. These observations may explain both the effect of testosterone and the ability to purify kinetically distinct forms of AOX from male and female rats since neither thioltransferase nor glutathione reductase, the two other enzymes establishing thiol:disulfide potential, are regulated by testosterone (43). We posit that AOX is sensitive to the thiol:disulfide potential and that kinetic variants of AOX reflect the intracellular thiol:disulfide potential through thiol modification of AOX. Activity of the monooxygenase could thereby regulate AOX $K_{m(app)}$ by "setting" the thiol:disulfide potential leading to a more oxidized form of AOX in the female or a more reduced form of AOX in the male. This may have direct consequences for ROS generation from AOX since the kinetically less efficient enzyme may bias ROS generation for superoxide anion. This argument does not require expression of a second AOX gene and can account for the failure of testosterone to regulate AOX gene expression in rats despite finding kinetically distinct forms in males and females. AOX thiol modification could also explain both novel electrophoretic variants (9) and the widely variant kinetic characteristics of AOX from different organs and different species (16, 45–47).

Acknowledgments—We thank Drs. Enrico Garrattini and Mineko Terao (Milan, Italy) for discussion of these and other data.

REFERENCES

1. Hille, R., and Massey, V. (1985) in *Molybdenum Enzymes* (Spiro, T. G., ed) pp. 443–518, Wiley-Interscience Publishing Co., New York
2. Wooton, J. C., Nicolson, R. E., Cock, J. M., Walters, D. E., Burke, J. F., Doyle, W. A., and Bray, R. C. (1991) *Biochim. Biophys. Acta* **1057,** 157–185
3. Kisker, C., Schindelin, H., and Rees, D. C. (1997) *Annu. Rev. Biochem.* **66,** 233–267
4. Berger, R., Mezey, E., Clancy K. P., Harta, G., Wright, R. M., Repine, J. E., Brown, M., Brownstein, M., and Patterson, D. (1995) *Somatic Cell Mol. Gen.* **21,** 121–131
5. Wright, R. M., Vaitaitis, G. M., Weigel, L. K., Repine, T. B., McManaman, J. L.,

and Repine, J. E. (1995) *Redox Report* **1,** 313–321
6. Wright, R. M., Weigel, L. K., Varella-Garcia, M., Vaitaitis, G. M., and Repine, J. E. (1997) *Redox Report* **3,** 135–144
7. Nishino, T. (1994) *J. Biochem. (Tokyo)* **116,** 1–6
8. Yoshihara, S., and Tatsumi, K. (1997) *Arch. Biochem. Biophys.* **338,** 29–34
9. Holmes, R. S. (1979) *Biochem. Genet.* **17,** 517–527
10. Huff, S. D., and Chaykin, S. (1967) *J. Biol. Chem.* **242,** 1265–1270
11. Gluecksohn-Waelsch, S., Greengard, P., Quinn, G. P., and Teicher, L. S. (1967) *J. Biol. Chem.* **242,** 1271–1273
12. Yoshihara, S., and Tatsumi, K. (1997) *Biochem. Pharmacol.* **53,** 1099–1105
13. Ohkubo, M., and Fujimura, S. (1982) *Biochem. Int.* **4,** 353–358
14. Ohkubo, M., Sakiyama, S., and Fujimura, S. (1983) *Arch. Biochem. Biophys.* **221,** 534–542
15. Felsted, R. L., and Chaykin, S. (1967) *J. Biol. Chem.* **242,** 1274–1279
16. Beedham, C., Bruce, S. E., Critchley, D. J., Al-Tayib, Y., and Rance, D. J. (1987) *Eur. J. Drug Met. Pharmokin.* **12,** 307–310
17. Sugihara, K., Kitamura, S., and Tatsumi, K. (1995) *Biochem. Mol. Biol. Internat.* **37,** 861–869
18. Bult, C. J., White, O., Olsen, G. J., Zhou, L., Fleischmann, R. D., Sutton, G. G., Blake, J. A., FitzGerald, L. M., Clayton, R. A., Gocayne, J. D., Kerlavage, A. R., Dougherty, B. A., Tomb, J. F., Adams, M. D., Reich, C. I., Overbeek, R., Kirkness, E. F., Weinstock, K. G., Merrick, J. M., Glodek, A., Scott, J. L., Geoghagen, N. S. M., Weidman, J. F., Fuhrmann, J. L., Nguyen, D., Utterback, T. R., Kelley, J. M., Peterson, J. D., Sadow, P. W., Hanna, M. C., Cotton, M. D., Roberts, K. M., Hurst, M. A., Kaine, B. P., Borodovsky, M., Klenk, H. P., Fraser, C. M., Smith, H. O., Woese, C. R., and Venter, J. C. (1996) *Science* **273,** 1058–1073
19. Sekimoto, H., Seo, M., Dohmae, N., Takio, K., Kamiya, Y., and Koshiba, T. (1997) *J. Biol. Chem.* **272,** 15280–15285
20. Hoff, T., Frandsen, G. I., Rocher, A., and Mundy, J. (1998) *Biochim. Biophys. Acta* **1398,** 397–402
21. Ori, N., Eshed, Y., Pinto, P., Paran, I., Zamir, D., and Fluhr, R. (1997) *J. Biol. Chem.* **272,** 1019–1025
22. Dickinson, W. J. (1970) *Genetics* **66,** 487–496
23. Warner, C. K., Watts, D. T., and Finnerty, V. (1980) *Mol. Gen. Genet.* **180,** 449–453
24. Warner, C. K., and Finnerty, V. (1981) *Mol. Gen. Genet.* **184,** 92–96
25. Wright, R. M., Vaitaitis, G. M., Wilson, C. M., Repine, T. B., Terada, L. S., and Repine, J. E. (1993) *Proc. Natl. Acad. Sci. U. S. A.* **90,** 10690–10694
26. Li-Calzi, M., Raviolo, C., Ghibaudi, E., De-Gioia, L., Salmona, M., Cazzaniga, G., Kurosaki, M., Terao, M., and Garattini, E. (1995) *J. Biol. Chem.* **270,** 31037–31045
27. Bendotti, C., Prosperini, E., Kurosaki, M., Garattini, E., and Terao, M. (1997) *Neuro. Rep.* **8,** 2343–2349
28. Terao, M., Kurosaki, M., Demontis, S., Zanotta, S., and Garattini, E. (1998) *Biochem. J.* **332,** 383–393
29. Ausubel, F. M., Brent, R., Kingston, R. E., Moore, D. D., Seidman, J. G., Smith, J. A., and Struhl, K. (1994) *Current Protocols Molecular Biology,* Green Publishing and J. Wiley & Sons, New York
30. Sato, A., Nishino, T., Noda, K., Amaya, Y., and Nishino, T. (1995) *J. Biol. Chem.* **270,** 2818–2826
31. Glatigny, A., and Scazzocchio, C. (1995) *J. Biol. Chem.* **270,** 3534–3550
32. Keith, T. P., Brooks, L. D., Lewontin, R. C., Martinez-Cruzado, J. C., and Rigby, D. L. (1985) *Mol. Biol. Evol.* **2,** 206–216
33. Riley, M. A., Kaplan, S. R., and Veuille, M. (1992) *Mol. Biol. Evol.* **9,** 56–69
34. Comeron, J. M., and Aguade, M. (1996) *Genetics* **144,** 1053–1062
35. Grassetti, D. R., and Murray, J. F., Jr. (1967) *Arch. Biochem. Biophys.* **119,** 41–49
36. Eager, K. R., and Dulhunty, A. F. (1998) *J. Membr. Biol.* **163,** 9–18
37. Cai, S., and Sauve, R. (1997) *J. Membr. Biol.* **158,** 147–158
38. Zheng, S. Y., Xu, D., Wang, H. R., Li, J., and Zhou, H. M. (1997) *Int. J. Biol. Macromol.* **20,** 307–313
39. Waud, W. R., and Rajagopalan, K. V. (1976) *Arch. Biochem. Biophys.* **172,** 354–364
40. Waud, W. R., and Rajagopalan, K. V. (1976) *Arch. Biochem. Biophys.* **172,** 365–379
41. Saito, T., and Nishino, T. (1989) *J. Biol. Chem.* **264,** 10015–10022
42. Nishino, T., and Nishino, T. (1997) *J. Biol. Chem.* **272,** 29859–29864
43. Ziegler, D. M., Duffel, M. W., and Poulsen, L. L. (1980) *Ciba Found. Symp.* **72,** 191–204
44. Tynes, R. E., and Hodgson, E. (1985) *Arch. Biochem. Biophys.* **240,** 77–93
45. Krenitsky, T. A., Neil, S. M., Elion, G. B., and Hitchings, G. H. (1972) *Arch. Biochem. Biophys.* **150,** 585–599
46. Taylor, S. M., Stubley-Beedham, C., and Stell, J. G. P. (1984) *Biochem. J.* **220,** 67–74
47. Beedham, C., Critchley, D. J., and Rance, D. J. (1995) *Arch. Biochem. Biophys.* **319,** 481–490

DNA AND CELL BIOLOGY
Volume 19, Number 8, 2000
Mary Ann Liebert, Inc.
Pp. 459–474

Activation of the Human Aldehyde Oxidase (*hAOX*[1]) Promoter by Tandem Cooperative Sp1/Sp3 Binding Sites: Identification of Complex Architecture in the *hAOX* Upstream DNA that Includes a Proximal Promoter, Distal Activation Sites, and a Silencer Element

RICHARD M. WRIGHT,[1] MARY G. RILEY,[1] LAURA K. WEIGEL,[1] LISA A. GINGER,[1] DAVID A. COSTANTINO,[1] and JAMES L. MCMANAMAN[2]

ABSTRACT

Aldehyde oxidase (AOX) is a member of the molybdenum iron–sulfur flavoproteins and is of interest for its role in clinical drug metabolism and as a source of reactive oxygen species (ROS) potentially involved in human pathology. The ROS derived from AOX contribute significantly to alcohol-induced hepatotoxicity. Therefore, expression of AOX could determine both the susceptibility of certain cells and tissues to clinically important pharmacologic agents and the levels of ROS produced under certain pathophysiological conditions. Although some pharmacologic agents regulate AOX enzyme activity, very little is known about the activation or regulation of the human AOX gene (*hAOX*). In the present study, we sought to identify features in the upstream DNA of *hAOX* that could confer regulation of the gene, to locate and characterize the basal promoter apparatus activating *hAOX*, and to identify transcription factors that could mediate activation or regulation. We transfected promoter fusion constructs into epithelial cells from the lung and the mammary gland that express AOX in cell culture. The *hAOX* gene was found to possess a structurally complex region in the upstream DNA that contained sequences for a proximal promoter, enhancer sites, and silencer elements. In addition, we identified an essential role for the transcription factors Sp1 and Sp3 in the proximal promoter. Unexpectedly, *hAOX* was activated in lung and mammary epithelial cells by indistinguishable mechanisms. These observations reveal a potentially complex mode of *hAOX* gene expression in epithelial cells that is dependent on Sp1 and Sp3 transcription factors.

INTRODUCTION

ALDEHYDE OXIDASE (AOX) is a member of the xanthine oxidase family of molybdenum cofactor-containing enzymes that includes AOX, several aldehyde oxidoreductases (AOR), xanthine oxidase (XO), and xanthine dehydrogenase (XDH). Vertebrate AOX can be prepared in its native state as a homodimer of 300 kDa, and the 150-kDa monomeric subunits contain two iron–sulfur centers, an FAD, and the molybdenum–pterin cofactor (MoCo) (Hille and Massey, 1985; Wooton *et al.*, 1991; Kisker *et al.*, 1997). The AOX (EC 1.2.3.1) functions metabolically to catalyze the oxidation of several aldehydes to their cognate acids via hydroxyl transfer from water. While acetaldehyde is an important physiologic substrate for AOX, purines (Krenitsky *et al.*, 1972), quinoliniums (Taylor *et al.*, 1984), phthalazines (Beedham *et al.*, 1995), and numerous pharmacologic agents that include tamoxifen (Ruenitz and Bai, 1995), famciclovir (Clarke *et al.*, 1995; Rashidi *et al.*, 1997), zonisamide (Sugihara *et al.*, 1996), methotrexate (Fabre *et al.*, 1986), and nicotine (Nakayama *et al.*, 1987) are also important substrates. For example, AOX catalyzes an essential step in the activation of the breast cancer drug, tamoxifen (Ruenitz and

[1]The Webb-Waring Institute and Department of Medicine and [2]Department of Biochemistry, Biophysics, and Genetics, The University of Colorado Health Sciences Center, Denver, Colorado.

Bai, 1995). The enzyme may also serve an important role in development by the synthesis of retinoic acid from retinal (Huang *et al.*, 1999).

Aldehyde oxidase is of further interest as a source of the reactive oxygen species (ROS), hydrogen peroxide (H_2O_2) and superoxide anion ($O_2^{\cdot -}$), that mediate numerous human pathologies and may serve as intracellular signals during oxidative or reductive stress. The ROS derived from AOX are directly implicated in free radical damage to the liver and brain during ethanol metabolism (Shaw and Jayatilleke, 1990, 1992a,b; Shaw *et al.*, 1995; Bondy and Orozco, 1994). Ethanol-dependent ROS generation by AOX could proceed by metabolism of acetaldehyde or NADH, both of which are produced from ethanol by the action of alcohol dehydrogenase (ADH). Because acetaldehyde is a substance for AOX, ROS generation by AOX during acetaldehyde metabolism could be a significant source of ROS in certain tissues. The intrinsic NADH oxidase activity of AOX also generates ROS (Mira *et al.*, 1995; Wright *et al.*, 1995a). Recently, the ROS injury sustained during alcohol toxicity of the liver was shown to operate directly through the combined activities of AOX and XDH (Shaw and Jayatilleke, 1990, 1992a,b; Mira *et al.*, 1995) via an iron-dependent process that suggests a role for hydroxyl radical ($^{\cdot}OH$) in tissue damage (Shaw and Jayatilleke, 1992a; Shaw *et al.*, 1995).

The *AOX* genes and cDNAs from several vertebrates have been cloned and analyzed. Hepatic *AOX* appears to be encoded by a predominantly expressed gene in rats and humans (Wright *et al.*, 1997, 1999; Terao *et al.*, 1998). Sequence variants for hepatic *AOX* have been described (Wright *et al.*, 1997), but these have not been fully characterized. The human *AOX* gene (*hAOX*) encoding the predominant mRNA in the liver was mapped to chromosome 2q32.3-2a33.1 by fluorescence *in situ* hybridization (Berger *et al.*, 1995; Wright *et al.*, 1995b), while rat *AOX* was mapped genetically to chromosome 9 (Kunieda *et al.*, 1999). Mouse *AOX* was mapped to chromosome 1 in a region highly syntenic to human chromosome 2a32-2a33 and rat chromosome 9 (Holmes, 1979). Mammalian *AOXs* are encoded by mRNAs of 4700 to 5100 nt, depending on species (Huang *et al.*, 1999; Wright *et al.*, 1995b, 1999; Calzi *et al.*, 1995), although additional homologous RNAs have been observed in poly(A^+) RNA from several rat and human tissues (Wright *et al.*, 1995b, 1999).

The *hAOX* gene lacks an evident TATA sequence in the upstream DNA (Wright *et al.*, 1997; Terao *et al.*, 1998), and the transcription initiation site found in human liver (Wright *et al.*, 1995b) occurs at a consensus transcriptional initiator (Inr) for mammalian RNA polymerase II, consistent with other TATA-less genes (Javahery *et al.*, 1994). In human liver, the transcription initiation site lies 298 bp upstream of the ATG encoding translation initiation (Wright *et al.*, 1995b), whereas initiation of transcription in cultured HepG2 cells appear to arise from several sites much closer to the translation initiator (Terao *et al.*, 1998).

In contrast to the extensive literature surrounding expression and regulation of XDH, very little is known about the expression and regulation of *AOX* genes. The gene is regulated by tissue type in humans (Wright *et al.*, 1995b), cattle (Calzi *et al.*, 1995), rabbits (Huang *et al.*, 1999), and rats (Wright *et al.*, 1999), with the liver and the lung being the predominant sites of expression. Kidney, pancreas, ovary, prostate, and testes also express AOX. The gene is selectively expressed in human spinal cord microglial cells (Berger *et al.*, 1995) and in some neurons of the mouse brain (Bendotti *et al.*, 1997). Expression has not been detected in heart or skeletal muscle (Huang *et al.*, 1999; Wright *et al.*, 1995b; Calzi *et al.*, 1995). Antigen for AOX was reported to exist in several rodent organs, where it appeared to be localized to the epithelial cells in most of the tissues examined (Moriwaki *et al.*, 1996). Initial analyses of the *hAOX* gene revealed that promoter information exists in the upstream 1500 bp of DNA and that this region can bind transcription factors determining cell- or tissue-specific expression (Wright *et al.*, 1997; Terao *et al.*, 1998).

Because expression of AOX could determine both the susceptibility of certain cells and tissues to clinically important pharmacologic agents and the amounts of ROS produced in specific tissues under certain pathophysiological conditions, it is important to understand the mechanism by which *AOX* genes are expressed and regulated. As an initial step in this analysis, we undertook the present study to identify those features in the upstream DNA of *hAOX* that could confer regulation, to locate and characterize the basal promoter apparatus activating *hAOX*, and to identify transcription factors that could mediate expression or regulation.

MATERIALS AND METHODS

Materials and reagents

Media for cell culture were obtained in powdered form from GIBCO/BRL (Bethesda, MD). Antibodies to Sp family members were obtained from Santa Cruz Biotechnology, Inc. (Santa Cruz, CA). Oligonucleotides were synthesized by GIBCO/BRL or Integrated DNA Technology (Coralville, IA). Luciferase fusion plasmids and the β-galactosidase expression plasmid were obtained from Promega (Madison, WI). The Topo-II T:A cloning vector was obtained from Invitrogen (Carlsbad, CA). O-Nitrophenyl beta-D galactopyranoside, poly dI:dC, and restriction endonucleases were obtained from Roche Molecular Biochemicals (Indianapolis, IN). Most buffers, reagents, and electrophoresis supplies were obtained from Sigma (St. Louis, MO).

Cell culture and transfection

Preliminary experiments were conducted to identify cells expressing *AOX* in culture. Because *AOX* appears to be expressed largely by epithelial cells *in vivo*, we examined numerous cultured epithelial cells from many different organs using an RT-PCR expression assay. The MLE-15 lung epithelial cells (Wikenheiser *et al.*, 1993) and HC-11 mammary gland epithelial cells (Hynes *et al.*, 1990) were found to express *AOX*. The former were grown in modified HITES medium containing RPMI 1640, 3 mM L-glutamine, sodium bicarbonate (2 g/l, pH 7.4; 1× Sigma ITS liquid media supplement (insulin, transferrin, sodium selenite), bovine transferrin 2.5 mg/l, 5 nM hydrocortisone, 5 nM beta-estradiol, 5 mM HEPES, pH 7.4; 1× GIBCO/BRL antibiotic-antimycotic (penicillin G 100 units/ml, streptomycin sulfate 100 μg/ml, amphotericin B 250 ng/ml), and fetal bovine serum to 2%. The HC-11 cells were grown in RPMI 1640 containing 2 mM L-glutamine, sodium bicarbonate

2 g/l, pH 7.4; 1× antibiotic/antimycotic, insulin 5 μg/ml, epidermal growth factor 10 ng/ml, and 10% fetal bovine serum. Cells were maintained at 37°C in 95% air/5% CO_2 and were refed every 2 days and split 1:6 when at or near confluency.

Cells to be transfected were grown to 50% to 70% confluency in six-well plates. Transfections were conducted using the liposome vehicle Transfectam (Promega) essentially as described by the supplier. Test plasmid (5.0 μg) and 1.0 μg of pCMV β-galactosidase plasmid were mixed with Transfectam in 1.0 ml of RPMI 1640/sodium bicarbonate medium (starvation medium). After vortexing, the transfecting solution was applied to cells in two wells of a six-well plate for 2 h. Then, either complete medium or starvation medium was applied without removal of the transfecting solution. Cells were harvested for analysis after 48 h of incubation. Wells were harvested in pairs and analyzed for luciferase activity (Promega CCLR kit) using a BMG Lab Technologies (Durham, NC) Lumistar luminometer. β-Galactosidase activity was assayed by reduction of *o*-nitrophenyl β-D-galactopyranoside and followed spectrophotometrically at 420 nm. The protein content was determined spectrophotometrically using the Lowry assay. Each individual transfection was assayed in quadruplicate for each of these measures. For most analyses reported here, each individual transfection was repeated four or five times; thus, each value reported represents 16 or 20 biochemical assays for each parameter. Luciferase values represent arbitrary light units/unit of β-galactosidase/mg of protein per minute. Means and standard deviations were calculated for each group of 16 or 20 assays, and in most cases, standard deviations were no greater than 10% of the mean value. Comparisons between groups used the Student's *t*-test.

Construction of AOX *promoter/luciferase fusions and upstream deletions*

Twelve in frame fusions with the luciferase coding region were constructed exactly as indicated previously (Wright *et al.*, 1997) for both the pGL3-basic (pGL3-B) and pGL3-enhancer (pGL3-E) parent plasmids (Promega). Briefly, upstream DNA to be cloned in the pGL3 plasmids was amplified by PCR using the PAC 8300 artificial chromosome as a template. The 3′ mutagenic oligonucleotide (AOXCON: 5′-GCAGCTGCCCACGCCCGGTCCATGgGGTGTCCGCGCTGG-3′) was designed to convert the AOX initiating ATG into an *Nco*1 restriction endonuclease cleavage site by changing a single A at −1 to a C (at the base indicated in lowercase). The 5′ PCR oligonucleotide was derived from the upstream DNA sequence (GenBank Accession No. AF010260) and could be cloned at a blunt cloning site in each vector (*Sma*1). We reported 1500 bp of the *AOX* upstream DNA sequence in 1997 but have extended this to more than 2600 bp, as described in the GenBank data base. Figure 1 shows the series of upstream deletion constructs. The A residue of the luciferase initiating ATG is denoted by +1, and all upstream nucleotides are numbered from this site with a negative number. For each reporter plasmid, PCR products were cleaved with *Nco*1 and purified by agarose gel electrophoresis. Bands of the appropriate size were extracted in phenol, precipitated in ethanol, and reconstituted in TE buffer. Host plasmids, pGL3-E or pGL3-B, were cleaved with the restriction endonucleases *Nco*1 and *Sma*1, after which they were likewise purified by agarose gel electrophoresis. Recombinants were constructed by overnight ligation at 12°C in a 20-μl volume and were transformed into SURE cells (Stratagene, La Jolla, CA). Ampicillin-resistant colonies were screened for the appropriate recombinant using colony PCR amplification. Plasmid DNA was prepared from positive colonies by the alkaline lysis method. Recombinant plasmids were confirmed to contain a single copy of the appropriate upstream fragment by a combination of DNA sequence analysis and restriction endonuclease cleavage analysis with *Nco*1 and *Kpn*1. The latter was selected as the second diagnostic enzyme because the *Kpn*1 site lies within the multicloning site of each parent plasmid upstream of *Sma*1. The presence of a single *Kpn*1 site in the *AOX* upstream DNA at −1533 bp provided an additional diagnostic cleavage site for longer constructs. Preliminary experiments revealed weak expression of the *hAOX* promoter in the B series of constructs; therefore, the E series of constructs were used to determine the primary characteristics of the *hAOX* upstream DNA.

DNA sequence analysis

Fluorescence sequence analysis was performed using the dideoxynucleotide chain termination system from Perkin-Elmer Applied Biosystems (Foster City, CA). Reactions used the ABI PRISM™ Dye Terminator cycle sequencing ready reaction kits (Perkin-Elmer). Sequence reactions were fractionated on an ABI PRISM 310 DNA sequencer equipped with a 47-cm microcapillary (Perkin-Elmer). All sequences were determined from both directions, and sequence data were compiled manually. The oligonucleotides used as sequencing primers are available on request.

RNA initiation site

Total RNA was prepared from cultured cells grown to 80%/90% confluency using the Trizol reagent (Life Technologies). The MLE-15 and HC-11 cells were shown to express *AOX* in cell culture by RT-PCR as follows. All RNA samples were treated with DNase I prior to cDNA synthesis. cDNA was prepared by reverse transcription (RT) in a final volume of 20 μl as follows. Total RNA (1.0 μg) was mixed with DEPC-treated water, 1.0 μl of primer oligonucleotide at 20 μM, 1.0 μl of 10 mM deoxyribonucleoside triphosphates (ACGT), 0.5 μl of RNAse inhibitor, 1.0 μl of recombinant Moloney murine leukemia virus reverse transcriptase (Clontech Laboratories, Palo Alto, CA), and 4.0 μl of 5× buffer (final conditions: 50 mM Tris HCl, pH 8.3; 75 mM KCl, 3 mM $MgCl_2$). Reaction mixtures were incubated at 42°C for 60 min and were then heated to 94°C for 5 min to inactivate reverse transcriptase. Prior to use, reactions were diluted to 100 μl, and 5 μl was used for PCR amplification. The RT reaction mixtures were stored at −70°C. Semiquantitative PCRs were determined to be in the linear range of AOX and β-actin product formation for input RNA, input single-strand RT DNA, and the number of amplification cycles. The 5′ RACE was then used to determine the RNA initiation site employed by the AOX–luciferase fusion genes in culture cells. The HC-11 and MLE-15 cells were transfected with pAO-E4, and RNA was harvested 48 h later. The 5′ RACE was performed on total RNA as described previously (Wright *et al.*, 1999) using ALSS-DNA and a primer

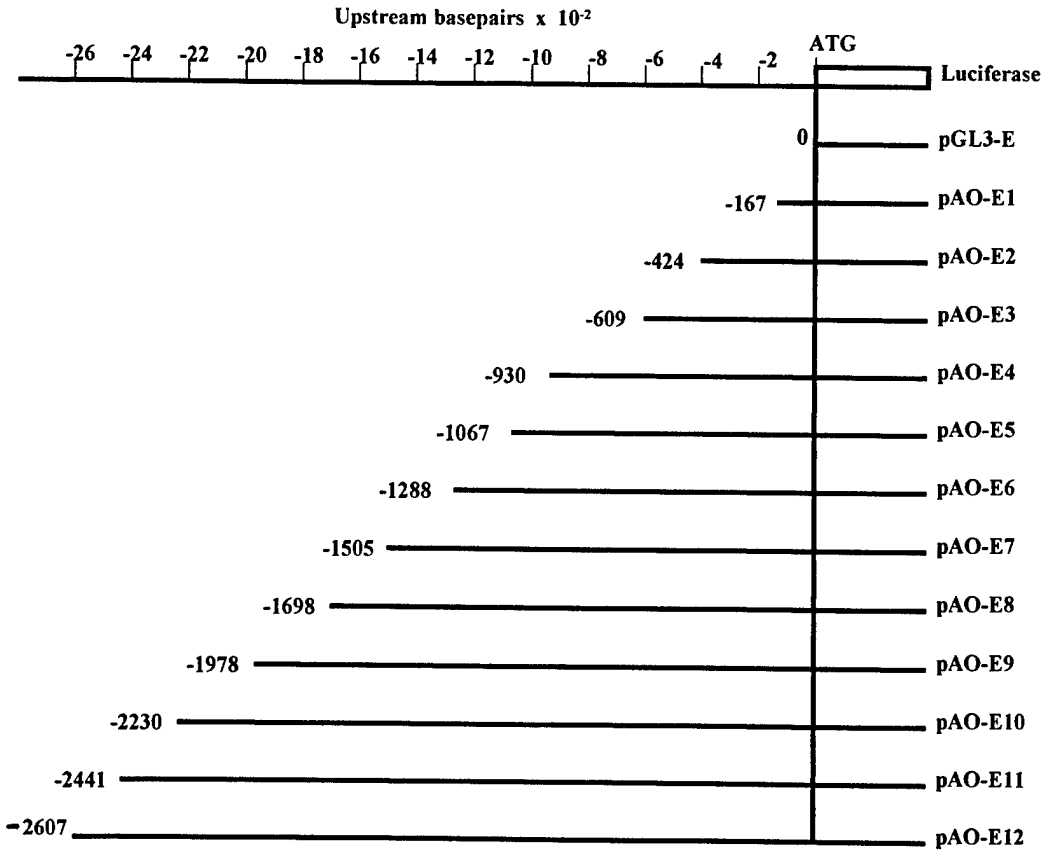

FIG. 1. The *hAOX* promoter–luciferase fusions. Upstream DNA from the *hAOX* gene cloned in PAC 8300 was fused at the initiator methionine of the pGL3-enhancer (pGL3-E) plasmid using the mutagenic oligonucleotide AOXCON to convert the ATG into an *Nco*1 cleavage site. All fusions, therefore, precisely fuse DNA upstream of the *AOX* ATG with the luciferase ATG. Numbering of upstream DNA begins with the first base 5′ of the *AOX* ATG as −1, and the 5′ base of each fusion is listed at the left of each construct. Plasmid pGL3-E is the promoterless parent vector and contains an SV40 enhancer located 3′ of the luciferase gene. Fusions containing sequences that extend up to 2 kb into intron 1 produced diminished activation and have been excluded from the present study.

extension oligonucleotide derived from the luciferase protein-coding region.

Preparation of probes for electrophoretic mobility shift assays

The −1/−167-bp probe corresponding to the *hAOX* proximal promoter (Fig. 2) was prepared from pAO-E1 by restriction endonuclease cleavage with *Nco*1 and *Kpn*1. The appropriate fragment was purified by agarose gel electrophoresis. DNA fragment (500 ng) was end-labeled with bacteriophage T4 DNA polymerase for 5 min at 37°C in a 50-μl reaction mixture containing 50 μCi [α-^{32}P]-dATP; 2 U of T4 DNA polymerase; 500 μM dCTP, dTTP, dGTP; 50 mM Tris, pH 8.0; 5 mM $MgCl_2$, and 5 mM dithiothreitol (DTT). Probe was extracted in (24:24:1) phenol:chloroform:isoamyl alcohol, precipitated in ethanol, and resuspended in TE at 0.5 ng/μl. Double-strand oligonucleotide probes (60 ng) were labeled with 50 μCi of [γ-^{32}P]-ATP by polynucleotide kinase according to the manufacturer's specifications (Roche). Probes were extracted, precipitated, and stored until use at 0.5 ng/μl in TE as described above.

Preparation of nuclei and nuclear proteins

Nuclei were prepared from hypotonically swollen cells by douncing and differential centrifugation following standard methods (Dignam *et al.*, 1983). Proteins were leached from isolated washed nuclei by incubation in 320 mM potassium buffer as described (Dignam *et al.*, 1983). Nuclear preparations were routinely examined microscopically and were estimated to contain >95% nuclei with no more than 5% cellular contamination. Following sedimentation at 10,000 × *g* to remove extracted nuclei, protein solutions were stored at −70°C in high-salt buffer containing 20 mM HEPES, pH 7.9; 1.5 mM $MgCl_2$, 320 mM KCl, 0.2 mM EDTA, 0.2 mM phenylmethylsulfonylfluoride, 0.5 mM DTT, and 25% glycerol.

Electrophoretic mobility shift analysis

The 50-μl EMSA binding reactions without competitors contained 17.8 μg of nuclear protein, 5 μg of poly dI:dC, 0.5 ng of labeled probe, and final reaction buffer composed of 25 mM Tris, pH 7.9; 50 mM KCl, 6.25 mM $MgCl_2$, 0.5 mM DTT, 0.5 mM EDTA, and 10% glycerol. Double-stranded oligonu-

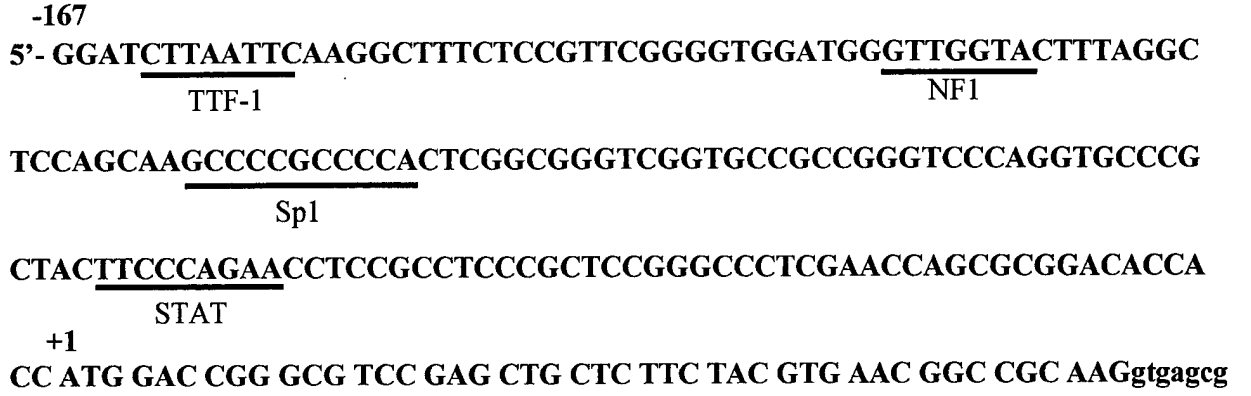

FIG. 2. Sequence features of the *hAOX* proximal promoter. Upstream sequence and sequence of the coding region to intron 1 is shown by uppercase letters. Lowercase letters show the first bases of intron 1 (Wright *et al.*, 1997). Computer-predicted transcription factor binding sites have been identified using the program TRANSFAC, and the core binding domains are underlined. Only those sites showing >95% probability for transcription factor prediction have been indicated.

cleotide competitors were included at 20-, 50-, or 100-fold molar excess as indicated in the figures. Supershift experiments with antisera to Sp1, Sp2, or Sp3 were conducted at a 19.6:1 dilution of antiserum. Preimmune sera were not employed in the present studies because the complete absence of response to the anti-Sp2 antiserum provided an effective nonspecific control. Binding reactions were assembled in the following order: H_2O, buffer, nuclear protein solution, poly dI:dC, competitor oligonucleotide, and labeled probe. Antisera to Sp1, Sp2, or Sp3 were added either 5 min before probe addition or at the end of the binding reaction, 5 min prior to electrophoresis. Binding reactions were conducted at room temperature for 30 min. Following addition of Ficoll dye, 10 μl of binding reaction mixture was electrophoresed on 4% native polyacrylamide gels at 125 V for approximately 4 h. The gels were subsequently dried and exposed to Kodak XAR autoradiographic film.

Competitor oligonucleotides were derived from the *hAOX* proximal promoter (Fig. 2) and correspond to the TTF-1, STAT, and Sp1wt binding sites (Fig. 3). Substitution oligonucleotides were derived from the *hAOX* Sp1wt binding region. Substitutions of the wildtype sequence were made three at a time, span the entire 30 bp of the wildtype sequence and correspond to Sp1a through Sp1j (Fig. 3). The altered triad in each oligonucleotide is underlined. The Sp1 substitution oligonucleotides were used both as competitor oligonucleotides and as individual probes. The B-region substitution oligonucleotides Sp1k and Sp1l were derived from the Sp1wt2 oligonucleotide (Fig. 3) that is shifted 6 bp 3′ relative to Sp1wt.

Construction recombinant plasmids containing Sp1/Sp3 mutations

Substitution mutations were introduced into the Sp1/Sp3 A and B domains of pAO-E1 and pAO-E4 by cassette mutagenesis. Because of constraints in cloning into the pAO-E series of plasmids, the six core nucleotides of each domain were replaced by an *Nde*1 cleavage site that changed the core Sp1 nucleotides from CGCCCC to CATATG (A domain) and GGTGCC to CATATG (B domain). Parent plasmids pAO-E1 and pAO-E4 were amplified by PCR in two separate reactions using *Nde*1 mutagenic primers paired with flanking primers derived from the pGL3-E host vector. DNA fragments of the appropriate size were isolated by gel electrophoresis and cloned in the Topo-II T:A cloning vector (Invitrogen). The resulting clones were cleaved with *Nde*1 and either *Kpn*1 (upstream fragment) or *Apa*1 (downstream fragment). The *Nde*1/*Apa*1 and *Nde*1/*Kpn*1 fragments were ligated, subcloned into Topo-II, and sequenced to confirm the anticipated structure. Subsequently, *Kpn*1/*Apa*1 fragments corresponding to domain A or domain B *Nde*1 substitutions were isolated by gel electrophoresis. The parent plasmids, pAO-E1 and pAO-E4, were cleaved with *Kpn*1 and *Apa*1 and gel purified to isolate hosts lacking the region from the *Kpn*1 site to the *Apa*1 site. The *Kpn*1/*Apa*1 fragments contain-

STAT	GCCCGCTACTTCCCAGAACCTCCGCCTCCC
TTF1	GGATCTTAATTCAAGGCTTTCTCCG
Sp1wt	TCCAGCAAGCCCCGCCCCACTCGGCGGGTC
Sp1a	CAAAGCAAGCCCCGCCCCACTCGGCGGGTC
Sp1b	TCCCATAAGCCCCGCCCCACTCGGCGGGTC
Sp1c	TCCAGCCCTCCCCGCCCCACTCGGCGGGTC
Sp1d	TCCAGCAAGATACGCCCCACTCGGCGGGTC
Sp1e	TCCAGCAAGCCCTTTCCCACTCGGCGGGTC
Sp1f	TCCAGCAAGCCCCGCAAAACTCGGCGGGTC
Sp1g	TCCAGCAAGCCCCGCCCCCTGCGGCGGGTC
Sp1h	TCCAGCAAGCCCCGCCCCACTTTTCGGGTC
Sp1i	TCCAGCAAGCCCCGCCCCACTCGGTTTGTC
Sp1j	TCCAGCAAGCCCCGCCCCACTCGGCGGAAA
Sp1wt2	AAGCCCCGCCCCACTCGGCGGGTCGGTGCC
Sp1k	AAGCCCCGCCCCACTCGGCGGGTCAAAGCC
Sp1l	AAGCCCCGCCCCACTCGGCGGGTCGGTAAA

FIG. 3. Oligonucleotides used in the analysis of the *hAOX* proximal promoter. Only the upper strand of each oligonucleotide is shown. The STAT, TTF-1, and Sp1 sequences were derived from the *hAOX* proximal promoter; Sp1a through Sp1j contain 3-bp substitutions of the wildtype Sp1wt region in *hAOX*, and these are underlined. The Sp1wt2 oligonucleotide is translocated by 6 nt (3′) relative to Sp1wt. Both Sp1k and Sp1l contain substitutions of Sp1wt2 indicated by the underline.

ing the *Nde*1 substitution were then cloned into each deleted parent, creating the substitution mutations M1 (corresponding to the A domain) and M2 (corresponding to the B domain). Thus, four substitution plasmids were generated (pAOE1-M1, pAOE1-M2, pAOE4-M1, and pAOE4-M2), each carrying the substitution CATATG in place of the core Sp1/Sp3 hexanucleotide. The proper structure of each substitution mutation was confirmed by sequence analysis.

Construction of silencer recombinant plasmids

The strong silencer domain lying from −1978 to −2230 was subcloned in the forward direction into four promoter plasmids as follows. The PAC 8300 artificial chromosome containing the 77,000-bp *hAOX* and upstream DNA (Wright *et al.*, 1997) was amplified using the primers PRO18K (5′-ACACA**GGTACC**-CCTCCTGCCCTGGCCCGTTTTCTCTCC-3′) and PRO17N (5′-AACACA**GCTAGC**CCATCTAGGTGGAATA-GAGTTTGAG-3′) that carry, respectively, a *Kpn*1 or an *Nhe*1 restriction endonuclease cleavage site (boldface). A PCR band of approximately 275 bp was obtained and was cleaved sequentially with *Kpn*1 and *Nhe*1; the product was isolated by agarose gel electrophoresis. Recipient plasmids consisted of pGL3-promoter, pGL3-control, pAO-B1, and pAO-E1. Following sequential cleavage with *Kpn*1 and *Nhe*1, the plasmids were purified by agarose gel electrophoresis. Recombinants were ligated overnight and transformed into SURE cells. Positive colonies were identified by PCR colony screen to ensure that only clones with a single insert in the forward orientation were obtained. Correct cloning was confirmed by a combination of DNA sequence analysis and restriction endonuclease cleavage analysis with *Kpn*1, *Nhe*1, and *Nco*1.

RESULTS

Complex architecture of the hAOX *upstream DNA*

We found that several cultured epithelial cells would express *AOX*, including MLE-15 lung epithelial cells and HC-11 mammary gland epithelial cells. Therefore, expression of luciferase from the plasmids pAO-B4, pAO-E4 (with the 5′ terminus at −930), pAO-B12, and pAO-E12 (with the 5′ terminus at −2607) was tested in MLE-15 and HC-11 cells. The MLE-15 cells have been stably transfected with SV40 large T antigen and should greatly stimulate E-series plasmids, whereas HC-11 cells do not express T antigen. The pGL3-B series of enhancerless plasmids exhibited very low expression in both cell types (data not shown), while the presence of an SV40 3′ enhancer in the pGL3-E series of plasmids markedly stimulated expression in both cell types. Furthermore, the additional DNA present in pAO-B12 and pAO-E12, rather than stimulating expression relative to pAO-B4 and pAO-E4, resulted in diminished activity in both cell types. Further experiments were conducted in the E series of plasmids because we could not detect expression from pAO-B12 in either cell type.

The E series luciferase fusion plasmids pAO-E1 through pAO-E12 and the promoterless parent pGL3-E were transfected into MLE-15 and HC-11 cells. The increased luciferase activity observed in MLE-15 cells compared with HC-11 cells was preserved throughout the entire 2607 bp of upstream DNA (Fig. 4A). When luciferase data were normalized to the promoterless parent, pGL3-E, the pattern of activation was essentially identical in the two cell types (Fig. 4B). Several functional domains were identified in the *hAOX* upstream region. First, negative-acting sequences were found from −1288 to −1505 and from 1978 to −2230, with the latter being much more suppressive than the former. Importantly, the addition of sequences 5′ of −2230 restored expression to a fusion plasmid terminating at −2230, as can be seen for clones pAO-E11 and pAO-E12 that terminate, respectively, at −2441 and −2607 (Fig. 4). Second, a strongly positive-acting site was found from −609 to −930 that may represent an upstream enhancer. Third, little change in basal activation in either cell type was found between −167 and −609. Regardless of cell type, the region from −1 to −167 induced 15- to 20-fold activation over the promoterless parent (pGL3-E) that was not statistically different for pAO-E1, pAO-E2, or pAO-E3. Therefore, the −1/−167 region must contain sufficient information to comprise a proximal promoter. Deletions were not constructed 3′ of −167 in order to preserve a potential TTF-1 binding site (see Fig. 2) that was expected to be functional in MLE-15 lung cells but not in HC-11 mammary gland cells.

Identification of an hAOX *proximal promoter*

We had identified a single predominant site for transcription initiation in normal human liver (Wright *et al.*, 1995b) that lies 298 bp upstream of the *AOX* ATG at a consensus Inr (Javahery *et al.*, 1994). However, in cultured HepG2 liver cells, RNA appeared to initiate from two dominant sites at −49 and −56 (Terao *et al.*, 1998). Because the −1/−167 region supported efficient expression of luciferase in HC-11 and MLE-15 cells, we anticipated that the proximal sites would also be functional in these cells. We performed 5′ RACE on total RNA from HC-11 and MLE-15 cells transfected with pAO-E4 (5′ terminus at −930) using an oligonucleotide derived from the luciferase coding region to prime RT. Thus, only RNA derived from the fusion plasmid would be copied. A single major band was obtained and was sequenced to locate the 5′ nucleotide. This sequence was 5′-CCCTCGAACCAGCGCGGACACCAC-CATGG-3′, placing the initiation site used by the fusion plasmids exactly 25 nt upstream of the ATG for translation initiation in both cell lines.

The same transcription factors were determined to bind in the *hAOX* proximal promoter in lung and mammary gland epithelial cells. Nuclear protein complexes from MLE-15 and HC-11 cells that formed with the *hAOX* proximal promoter were indistinguishable when examined by EMSA. Nuclear proteins from each cell produced three complexes with identical mobility in the two cell types (complexes CI, CII, and CIII; Fig. 5). Complexes CI, CII, and CIII were all efficiently blocked by a 100-fold and 50-fold molar excess of either the unlabeled −1/−167 probe itself or the Sp1 region oligonucleotide. Neither the TTF-1 nor the STAT factor oligonucleotide was an effective cold competitor. Cold competition with the Sp1 domain oligonucleotide generated equivalent and simultaneous competition for all three complexes regardless of cell type (Fig. 5A, B).

Antisera against Sp1, Sp2, and Sp3 were employed in EMSA supershift experiments (Fig. 5C, D). Antisera against Sp1 appeared to exert two effects on complexes from both cell types:

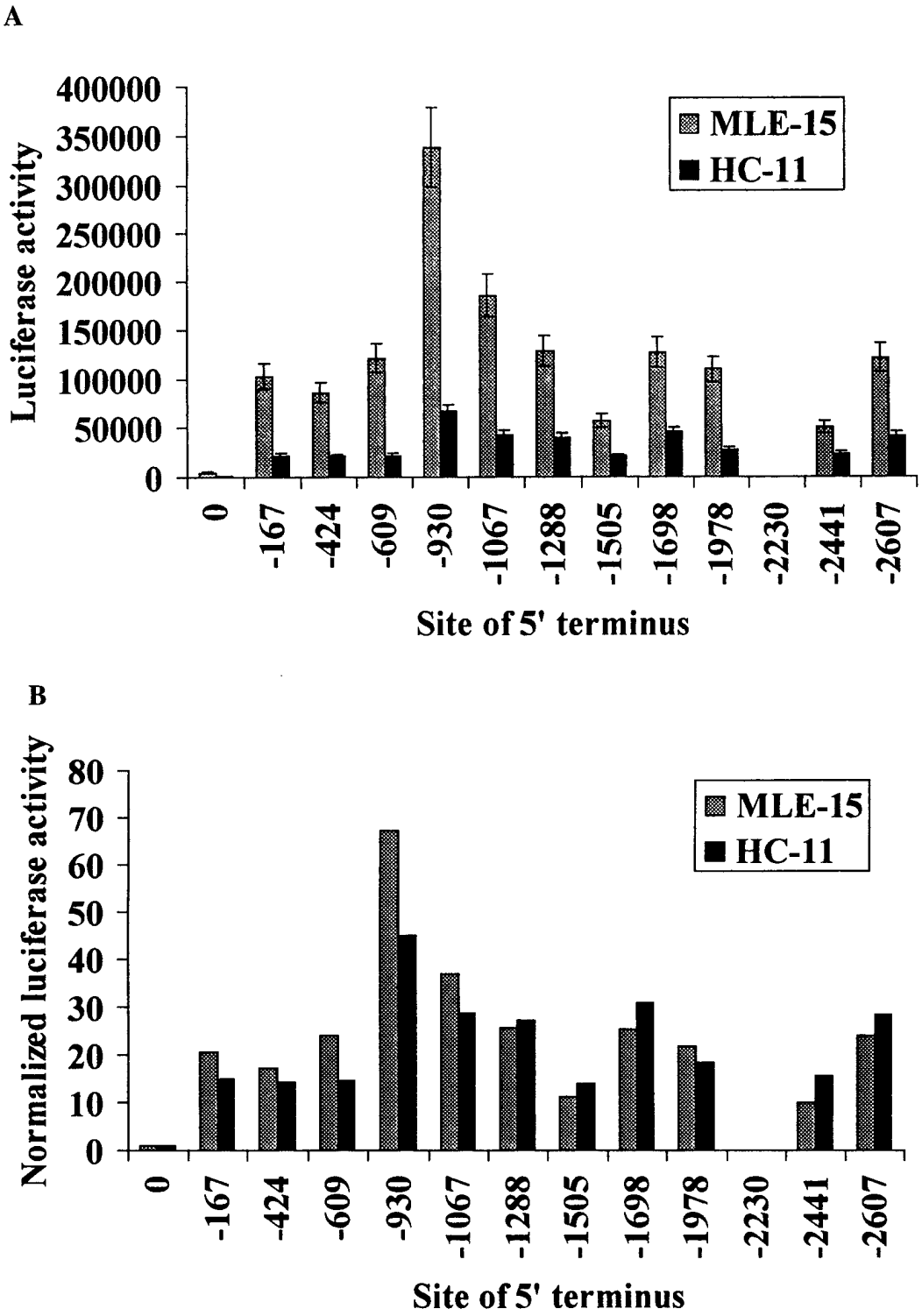

FIG. 4. Complex architecture of the upstream region of *hAOX*. Each of the 12 E-series luciferase fusion plasmids and the parent plasmid, pGL3-E were transfected into MLE-15 and HC-11 cells along with pCMV-β-galactosidase. After 48 h, luciferase activity was determined and normalized to β-galactosidase and protein concentration (**A**). Each transfection was analyzed four times, and five repetitions of the entire transfecting series were performed; thus, each point represents 20 individual assays. Error bars show the standard deviation of the entire 20 assays. (**B**) Data for each transfecting plasmid were then normalized to pGL3-E to determine the degree of stimulation beyond the promoterless parent. Luciferase activity for pAO-E10 (5′ terminus at −2230) was consistently at or below activity of pGL3-E. Site of 5′ terminus identifies the 5′ nucleotide of the deletion (see Fig. 1).

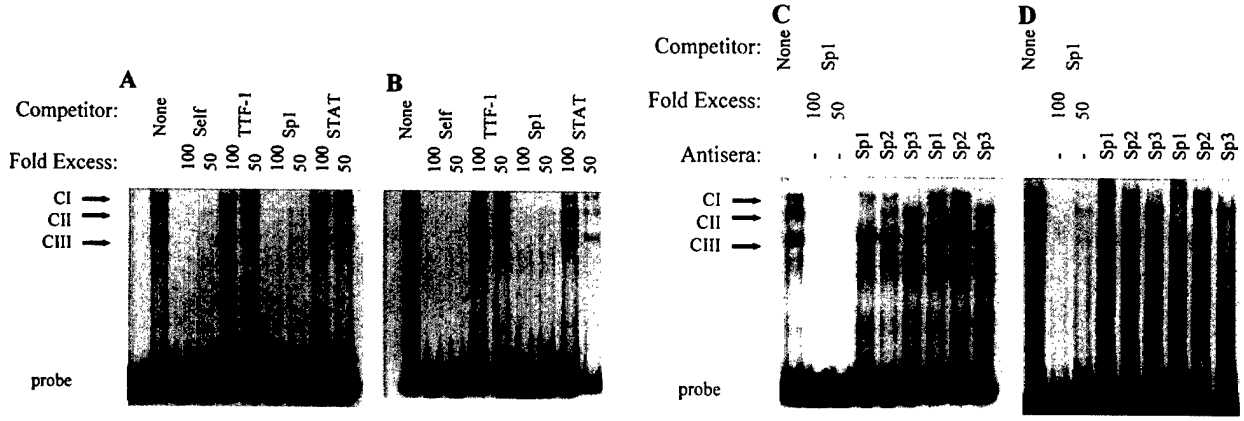

FIG. 5. Identification of Sp1 and Sp3 binding in the *hAOX* proximal promoter in lung and mammary gland epithelial cells. The EMSA was performed using the −1/−167 proximal promoter DNA as end-labeled probe. (**A, C**) MLE-15 cells. (**B, D**) HC-11 cells. Unlabeled competitor oligonucleotides in all panels were present in 100- or 50-fold molar excess. "Self" indicates the −1/−167 proximal promoter DNA. The TTF-1, Sp1, and STAT double-stranded oligonucleotide competitors (**A, B**) were derived from the *hAOX* proximal promoter sequence. (**C**) Part of the STAT 50-fold competition sample was lost prior to electrophoresis. Repetition of this experiment revealed no competition by the STAT oligonucleotide. Supershift EMSAs (**C, D**) were conducted by adding antisera either 5 min before addition of probe (first set of three) or 5 min after a 30-min incubation with probe (second set of three). The complexes formed in unblocked and unshifted nuclear proteins have been designated CI, CII, and CIII.

CII was completely lost, and CI was reduced to approximately 50% of the original band intensity. Antisera against Sp2 exerted no detectable effect on any of these complexes and were hereafter used as a control for nonspecific effects of the antisera. Antisera against Sp3 completely abrogated formation of CI and CII regardless of cell type. The minimal interpretation of these data is that CIII contains Sp3 and not Sp1, CII contains Sp1 and not Sp3, and CI contains Sp3 and perhaps Sp1. Although the binding of additional proteins is not precluded by these observations, Sp1 and Sp3 binding are required for complex formation, as just described.

While all nuclear protein binding in the proximal promoter was efficiently and completely blocked by the Sp1 domain oligonucleotide alone, both Sp1 and Sp3 were required to form the three complexes detected in the *hAOX* proximal promoter. Furthermore, inspection of the Sp1 domain oligonucleotide sequence indicated the presence of two Sp1-related sequences, suggesting that Sp1 or Sp3 could bind to more than one site. As was observed for the 167-bp proximal promoter, three complexes were formed by using the Sp1 domain oligonucleotide as a probe in EMSA analysis, complexes CIV, CV, and CVI, in both MLE-15 and HC-11 cells (Fig. 6). The CV appeared to possess approximately twice the band intensity of CVI. However, by running the PAGE for a longer time, CIV could be clearly separated from CV. All three complexes were completely and efficiently blocked by a 100-fold- or 50-fold excess of cold Sp1 domain oligonucleotide. Antisera to Sp1 eliminated the formation of CIV and may have diminished CV by 50%. Antisera to Sp2 had no detectable effect on complex formation. Antisera to Sp3 precluded formation of both CV and CVI without affecting CIV. These data indicate that CIV contains Sp1 and not Sp3, CV contains Sp3 and may contain Sp1, while CVI contains Sp3 and not Sp1. As noted previously, the binding of additional proteins is not precluded by these data. In addition, neither the STAT nor the TTF-1 domain oligonucleotide produced detectable binding of either MLE-15 or HC-11 nuclear proteins when used as an EMSA probe.

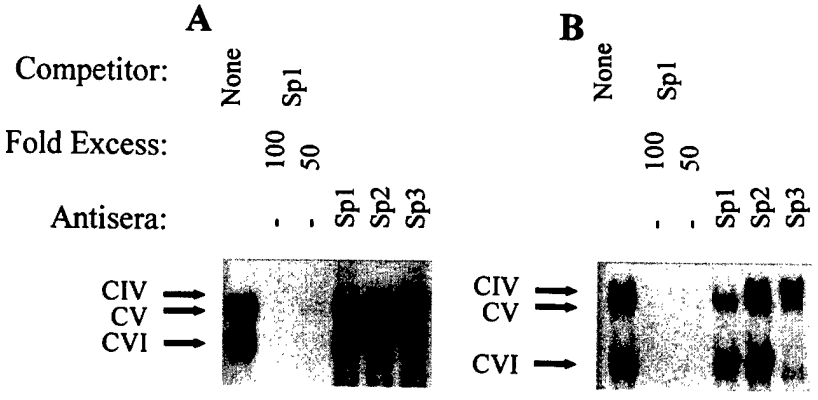

FIG. 6. Identification of Sp1 and Sp3 binding in the Sp1 region with lung and mammary gland epithelial cell nuclear protein. The Sp1wt domain oligonucleotide was end-labeled and used in EMSA of nuclear proteins from MLE-15 (**A**) and HC-11 (**B**) cells. Unlabeled Sp1wt domain oligonucleotide was used as competitor in 100- and 50-fold molar excess. Antisera against Sp1, Sp2, and SP3 were added 5 min before the addition of probe of oligonucleotide. Complexes formed with the unblocked and unshifted nuclear proteins have been designated CIV, CV, and CVI.

Sp1 and Sp3 bind at two adjacent sites in the hAOX proximal promoter

To determine how Sp1 and Sp3 bound in the *hAOX* proximal promoter, substitutions were introduced into the Sp1 domain oligonucleotide, 3 nt at a time and spanning the entire oligonucleotide. Modified oligonucleotides Sp1a through Sp1j were used as cold competitors in EMSA with the −1/−167 probe. In both MLE-15 and HC-11 cells, competition failed in two sites of 6 nt each (Fig. 7A, B). The Sp1e and Sp1f defined binding domain A, in which cold competition failed completely for CI, CII, and CIII simultaneously. The Sp1i and Sp1j formed domain B, in which competition also failed simultaneously for CI, CII, and CIII. Substitutions at Sp1a, Sp1b, Sp1g, and Sp1h had essentially no effect on competition efficiency. The Sp1c and Sp1d exhibited some diminished competition efficiency. However, domains A and B appeared to be important simultaneously to the formation of all three complexes. Analogous data were obtained in both MLE-15 and HC-11 cells when using the Sp1 domain oligonucleotide as a probe (Fig. 7C, D). The Sp1e and Sp1f produced very poor competition, and Sp1i and Sp1j were inefficient competitors. As with the −1/−167 EMSA probe, all complexes formed with the Sp1 domain, oligonucleotide probe (Fig. 7C, D) failed simultaneously and with equivalent efficiency, despite being separated by 9 to 12 nt. For example, the 3-nt substitutions at Sp1f produced an oligonucleotide with essentially no competitive value for Sp1- or Sp3-containing complexes, and markedly reduced competitive value was obtained with Sp1j as well. These data strongly indicate the cooperative nature of binding of both Sp1 and Sp3 to the *hAOX* proximal promoter.

We corroborated these observations by using each substitution oligonucleotide as a probe in EMSA analysis (Fig. 8). In this case, substitutions at Sp1e and Sp1f or Sp1i and Sp1j resulted in failure or diminished capacity of the oligonucleotide to form either Sp1- or Sp3-containing complexes. The CIV, CV, and CVI all failed to form with equivalent efficiency and simultaneously, regardless of cell type. Furthermore, none of the three base substitutions that abrogated Sp1 and Sp3 binding resulted in the formation of any new complexes. Interestingly, substitutions of Sp1b and Sp1g resulted in improved binding of all three complexes. These observations support the significance of domains A and B for Sp1 and Sp3 binding and demonstrate that binding is cooperative.

Refined localization of region B binding

Our data localized Sp1/Sp3 binding to the A and B regions as described above. We suspected that the limits of region B could extend further in the 3′ direction and, therefore, conducted additional competition EMSA using nuclear proteins from HC-11 and MLE-15 cells. Competitor oligonucleotides Sp1k and Sp1l carry 3-bp substitutions of the Sp1wt2 oligonucleotide. Each of these three double-stranded competitors has a 5′ end exactly 6 bp 3′ of the Sp1wt oligonucleotide. Figure 9 shows that substitutions in Sp1k and Sp1l abrogated competitive efficiency relative to Sp1wt2. Thus, region B binding, like region A binding, spans 12 nt, with the most critical sites being the 3′ 6 nt.

Sp1 and Sp3 are essential for activation of the proximal promoter in hAOX

To determine if the Sp1/Sp3 sites identified *in vitro* were functional in transfected cultured cells, we cotransfected HC-11 cells with pAO-E1 and double-stranded phosphorothiolated oligonucleotides as decoys for the Sp1/Sp3 region. The specific decoy corresponded to Sp1wt, and the nonspecific decoy had a random sequence that produced no identity matches when BLAST analyzed through the NCBI DNA sequence database. Figure 10A shows that the phosphorothiolate derivative of Sp1wt blocked expression from pAO-E1 in concentrations from

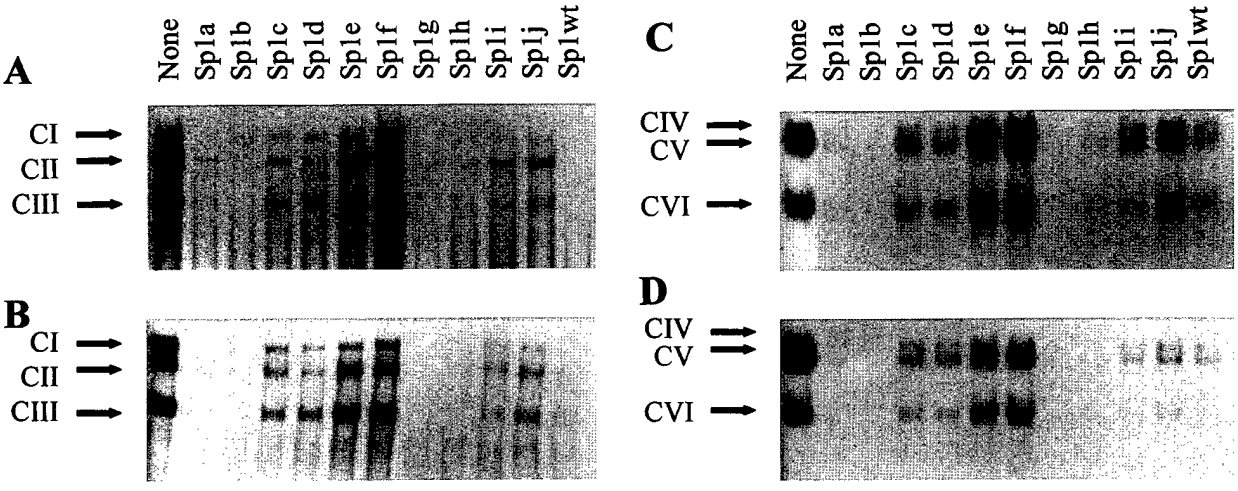

FIG. 7. Identification of critical protein-binding domains in the *hAOX* proximal promoter. (**A, B**) The −1/−167 proximal promoter DNA was used as a probe in competitive EMSA with Sp1-substitution oligonucleotides Sp1a through Sp1j using nuclear proteins from MLE-15 (**A**) and HC-11 (**B**) cells. All competitors were present in 50-fold molar excess. The Sp1 domain oligonucleotide was also used as a probe in competitive EMSA (**C, D**) with Sp1-substitution oligonucleotides and nuclear proteins from MLE-15 (**C**) and HC-11 (**D**) cells. All competitors were present in 50-fold molar excess.

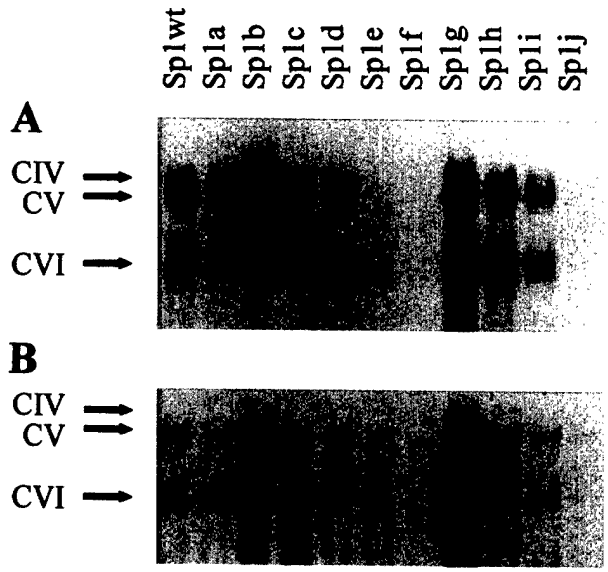

FIG. 8. Cooperativity between the critical binding domains of the *hAOX* proximal promoter. The native Sp1wt domain oligonucleotide and each Sp1-substitution oligonucleotide was end-labeled and used as an individual probe in EMSA with nuclear proteins from MLE-15 (**A**) and HC-11 (**B**) cells. Lanes for Sp1b and Sp1g received the same amount of probe and nuclear protein as all other lanes; these substitutions produced enhanced binding.

30 ng/ml to 100 ng/ml, whereas the nonspecific oligonucleotide had little discernible effect on expression. This result indicates that the Sp1wt domain is essential for expression of the proximal promoter *in vivo*.

To confirm and extend these data, substitution mutations were introduced into pAO-E1 and pAO-E4 by converting domain A and domain B core hexanucleotides into *Nde*1 restriction sites (Fig. 10B). In each case, this action resulted in a 5 of 6 nt substitution. The substitutions correspond to changes known to abrogate Sp1 binding and are similar, but not identical, to those used in competitive EMSA. Figure 10C demonstrates that substitution mutagenesis of domain A in both pAO-E1 and pAO-E4 resulted in nearly complete suppression of luciferase expression. Independent domain B mutagenesis decreased expression 40% and 60% in pAO-E1 and pAO-E4, respectively. This finding confirms that the Sp1/Sp3 sites identified are essential for expression. The M1 mutation was consistently more suppressive than M2, despite their equivalent effect on *in vitro* protein binding. Figure 11 summarizes the structure of the *hAOX* proximal promoter as determined here.

Identification of an upstream silencer

The strongly negative sequence from −1978 to −2230 in the *hAOX* upstream DNA suggested the existence of a silencer element. Sequence analysis revealed no alterations in the *hAOX* DNA from pAO-E10, indicating that the negative activity of pAO-E10 was not the result of mutation or rearrangement during cloning or PCR amplification. To confirm that the negative activity of this region was not the result of defective cloning at some site other than in the *hAOX* DNA, pAO-E10 was cleaved with *Kpn*1, religated, and cloned. This produced a derivative with the 5′ terminus at −1524, a site 19 bp 5′ of the pAO-E7 5′ terminus. Also, pAO-E12 was deleted to −2230 using reverse PCR and recloning to reconstruct pAO-E10 from pAO-E12. The reconstructed pAO-E10 produced luciferase activity in MLE-15 and HC-11 that was essentially indistinguishable from that produced by the original pAO-E10. Furthermore, reconstructing pAO-E7 from pAO-E10 also generated a clone that was expressed in both cells with essentially the same activity as the original pAO-E7. This result confirmed that the activity of pAO-E10 was not artifactual.

To determine if the region between −1978 and −2230 would confer repression independently, it was amplified by PCR, cleaved with *Kpn*1 and *Nhe*1, and subcloned in the forward direction upstream of promoters in pGL3-promoter, pGL3-control, pAO-B1, and pAO-E1 (Fig. 12, top panel). the −1978 to −2230 region repressed activity in each of these clones except the pGL3-promoter plasmid (Fig. 12, bottom panel). Both pGL3 plasmids contain an SV40 promoter; they differ from each other by the absence of a 3′ enhancer in the pGL3-promoter plasmid. The paradoxical activation seen here with incorporation of the −1978/−2230 silencer into the pGL3-promoter is similar to the action of another described silencer that can also serve as an activator depending on its physical location in the reconstructed gene (Shou *et al.*, 1998). Nonetheless, the ability of the *hAOX* −1978/−2230 region to repress activity when placed 5′ of either a foreign promoter or the *hAOX* proximal promoter identifies the silencer function of this domain.

DISCUSSION

The present observations extend our understanding of the *hAOX* gene in several ways. First, we identified epithelial cells

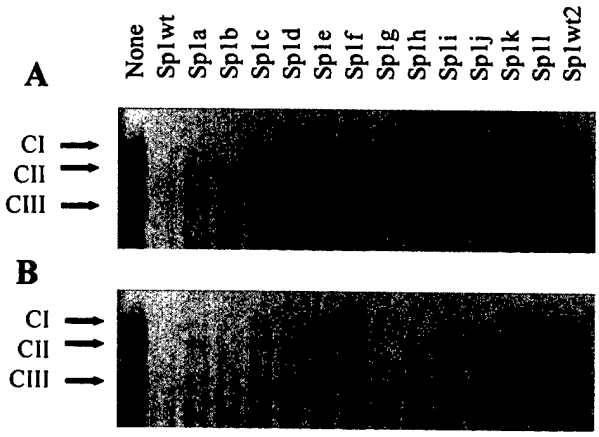

FIG. 9. Improved localization of region B binding. The EMSAs were performed using nuclear proteins from MLE-15 (**A**) and HC-11 (**B**) cells. Competitor oligonucleotides Sp1wt2, Sp1k, and Sp1l were shifted 6 bp in the 3′ direction relative to Sp1wt. All competitor oligonucleotides were present in 50-fold molar excess of the −1/−167 labeled probe. The Sp1wt2 was a less efficient competitor than Sp1wt, reflecting the minor importance of the first 3 bp of Sp1wt for Sp1/Sp3 binding. This can be seen in the reduced efficiency of competition with Sp1a relative to Sp1wt.

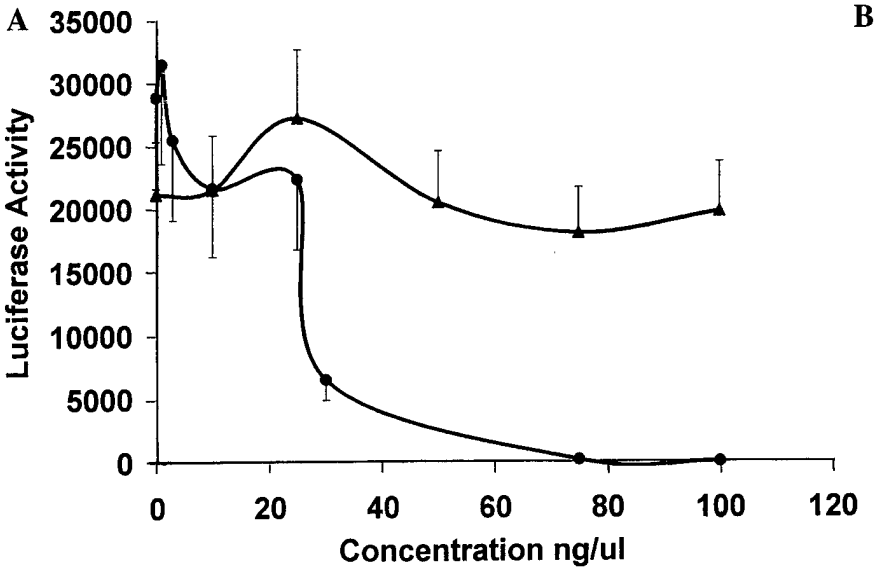

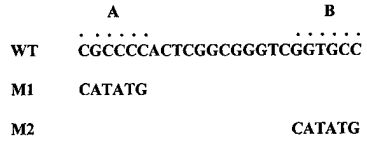

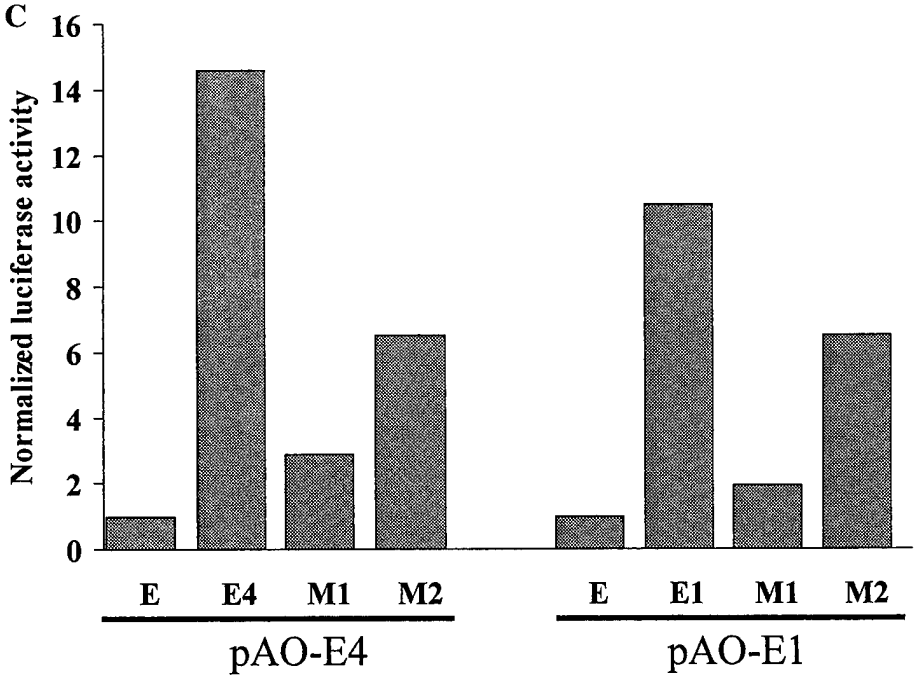

FIG. 10. Functional analysis of the *hAOX* proximal promoter. (**A**) HC-11 cells were cotransfected with pAO-E1, pCMV-β-galactosidase, and double-stranded phosphorothiolate oligonucleotide decoys present in concentrations from 0 to 100 ng/ml. At 48 h after transfection, cells were harvested, and luciferase activity was determined. Triangles show the nonspecific decoy (5′-ACGCATTAGCTATTA CGTACCTAGCATGCA-3′). Circles show the Sp1wt decoy. (**B**) Hexanucleotide substitutions of domain A (M1) and domain B (M2). The M1 and M2 substitution mutations were engineered into both pAO-E1 and pAO-E4 promoter fusion plasmids. (**C**) Results of transfection with M1 and M2 promoter substitution mutations. Six independent transfections were performed for each plasmid, and the data have been normalized to the promoterless parent, pGL3-E. Standard deviations of the un-normalized data were, in each case, <10% of the average value. The pAO-E4 series consists of the plasmids pGL3-E (E), pAO-E4 (E4), pAO-E4M1 (M1), and pAO-E4M2 (M2). The pAO-E1 series consists of pGL3-E (E), pAO-E1 (E1), pAO-E1M1 (M1), and pAO-E1M2 (M2).

from the lung and the mammary gland that express *AOX* in cell culture, consistent with observations demonstrating epithelial expression *in vivo*. Second, we identified a structurally complex region in the upstream region of *hAOX* containing sequences for a proximal promoter, enhancer sites, and a silencer element, indicating the potential for complex regulation of *AOX* gene expression. Third, we identified an essential role for the transcription factors Sp1 and Sp3 in the proximal promoter in the activation in epithelial cells.

An important conclusion from these studies is that lung and mammary gland cells displayed great similarity in the means of *AOX* expression and in the involvement of Sp1 and Sp3 transcription factors in the proximal promoter. We observed essentially no difference in expression between lung and mammary gland cells throughout the 2607 bp of upstream DNA studied here. Sites for the proximal promoter, activation, and silencing were located on the same 5′ deleted clones. The regions between −1288 and −1505 (pAO-E7) and between −1978 and −2230 (pAO-E10) behaved as strongly negative sites in both MLE-15 and HC-11 cells. The domain from −609 to −930 (pAO-E4) behaved as an activation or enhancer region in both cells, and in both cells, little change in expression was detected from −167 to −609 (pAO-E1, pAO-E2, and pAO-E3).

We identified a proximal promoter in the region from −1 to −167 bp. Both MLE-15 and HC-11 cells activated the proximal promoter 15 to 20 fold over the parental plasmid. Therefore, the −1/−167 region contains sequences sufficient for basal activation and transcription initiation. We identified a

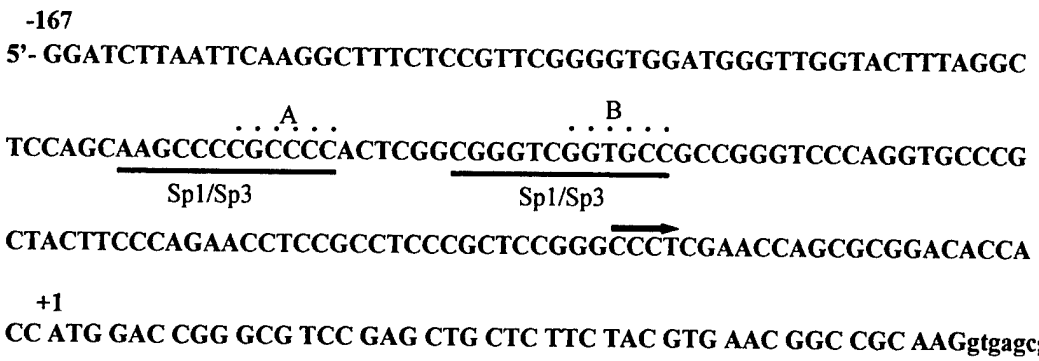

FIG. 11. Summary of the *hAOX* proximal promoter. The 12 bp corresponding to Sp1/Sp3 binding have been underlined. The core hexanucleotide regions of domains A and B are indicated by dots and represent the nucleotides exchanged by substitution mutagenesis. The arrow marks the novel transcription initiation site identified in the present studies. The ATG starting *AOX* translation is indicated by +1.

transcription initiation site not previously detected in human liver. Had the Inr at −298 bp been used in the transfected cells, we would anticipate a dramatic fall in expression from pAO-E2 (5′ terminus at −424) to pAO-E1 (5′ terminus at −167), and this did not occur, consistent with our placement of the initiation site at −25 bp. Proximal transcription initiation sites have also been for cultured HepG2 cells (Terao *et al.*, 1998). Thus, the selection of proximal transcription initiation sites may reflect a common characteristic of cultured cells.

Nuclear protein binding in the proximal promoter did not appear to differ between lung and mammary gland cells. Neither MLE-15 nor HC-11 nuclear proteins revealed binding to the predicted TTF-1 or STAT sites. Instead, Sp1 and Sp3 formed complexes of mobility indistinguishable from that of MLE-15 and HC-11 nuclear proteins. Furthermore, site-directed substitution of the Sp1 domain oligonucleotide revealed the same nucleotides to be essential for Sp1 and Sp3 binding regardless of the cell from which the nuclear proteins were prepared. We draw the unexpected conclusion that lung and mammary gland epithelial cells activate the *hAOX* proximal promoter in very similar, if not identical ways, and that Sp1 and Sp3 are central to this process.

We had anticipated that transcription factors specific for the lung or the mammary gland would be responsible in part for activation of *AOX* in epithelial cells from these tissues. For example, TTF-1 is the best-studied transcription factor mediating lung-specific activation, and the *hAOX* upstream DNA contains sites predicted to bind TTF-1 at −1664, −1523, −1243, −957, −918, −649, and −477 and in the proximal promoter at −163. These sites match the consensus TTF-1 binding site from a low of 91% identity to a high of 100% identity. The TTF-1 was expected to activate the *hAOX* proximal promoter in MLE-15 cells but not in HC-11 cells, as the predicted TTF-1 binding site in the proximal promoter appeared to be quite good (Bruno *et al.*, 1995; Bohinski *et al.*, 1994). Furthermore, *AOX* is dramatically expressed in the lungs of several mammals, and TTF-1 is expressed and functional in the MLE-15 cells used here (Ikeda *et al.*, 1996), whereas it is not expressed in breast epithelia (Holzinger *et al.*, 1996). However, we found no nuclear protein binding in the predicted TTF-1 region of the *hAOX* proximal promoter using conditions in which TTF-1 is known to bind *in vitro* (Ramirez *et al.*, 1997). Thus, TTF-1 does not contribute to activation of the proximal promoter.

Both STAT3 and STAT5 are important mediators of mammary gland development (Philip *et al.*, 1996). Either STAT3 or STAT5 was expected to activate the *hAOX* proximal promoter, because this region contained an excellent match for the consensus binding site for STAT factors, and the HC-11 cells expressing the *hAOX* proximal promoter are mammary gland epithelial cells. Nonetheless, the predicted STAT binding site in the *hAOX* proximal promoter did not appear to contribute to nuclear protein binding under the conditions employed in the present study. Other transcription factors with important specific roles in the mammary gland include YY1 (Meier and Groner, 1994) and MGF (Meier and Groner, 1994; Wakao *et al.*, 1994) that may mediate *AOX* regulation in HC-11 cells outside the proximal promoter.

The Sp1 and Sp3 factors were found to be essential to the formation of all nuclear protein complexes with the *hAOX* proximal promoter *in vitro*. Two sites were active in this region, identified as domains A and B, lying at −96 to −101 (A) and −78 to −83 (B). We observed that binding of Sp factors was cooperative. Independent substitutions in either domain A or domain B resulted in the loss of nuclear protein binding to both sites simultaneously and with equivalent efficiency, whereas substitutions between sites did not diminish competition or preclude nuclear protein binding. Thus, domains A and B functioned cooperatively, not independently. The sequence in domain A corresponds to the consensus Sp1 binding site, whereas the sequence of domain B does not. It will be important to determine how Sp1 and Sp3 occupy these sites, as domain B may represent a novel binding site perhaps related to cooperative binding. We infer that Sp1 and Sp3 cannot be bound simultaneously in complexes CII and CIII, because Sp1 antisera did not affect the Sp3 (CIII) complex and Sp3 antisera did not affect the Sp1 complex (CII). Furthermore, domains A and B were shown to be essential for luciferase expression from the fusion plasmids pAO-E1 and pAO-E4 by substitution mutagenesis. Whereas mutations in domains A and B behaved essentially the same *in vitro*, *in vivo*, the domain A mutation was more sup-

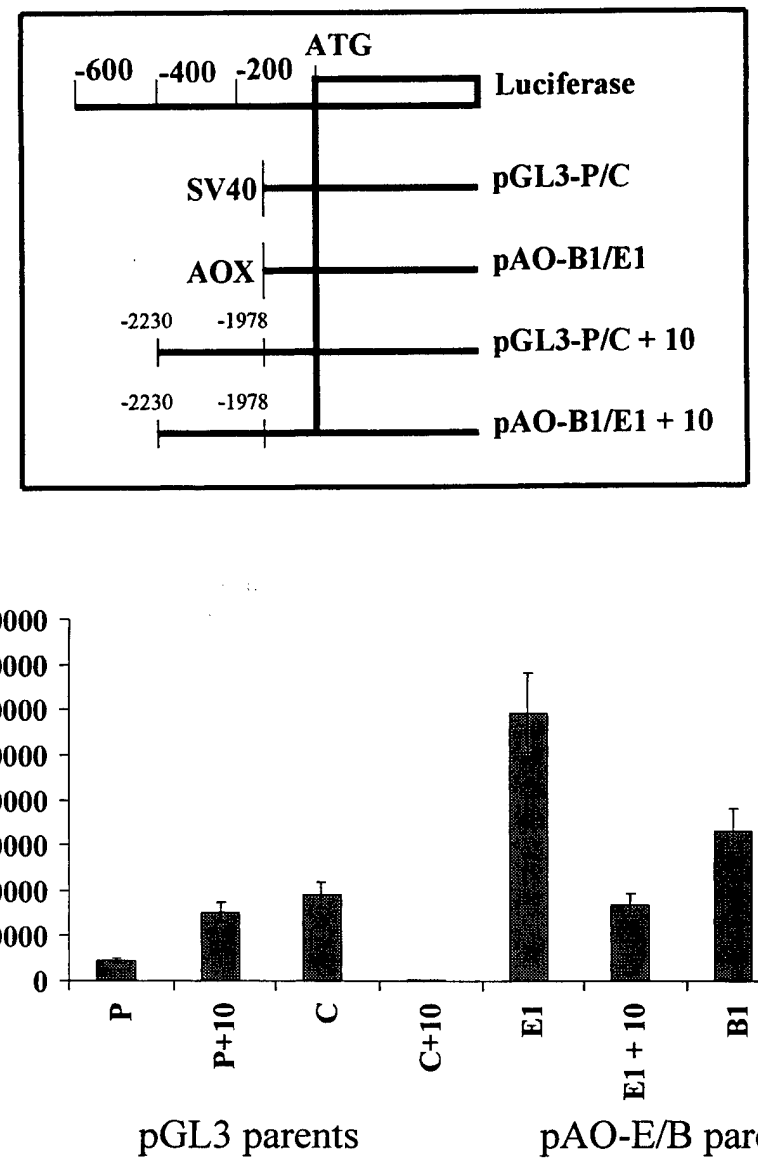

FIG. 12. Functional characterization of an *hAOX* silencer. (**Top**) Structure of the silencer recombinant plasmids. SV40 = SV40 promoter in pGL3-promoter and pGL3-enhancer; AOX = *hAOX* proximal promoter −1/−167 in pAO-E1 or pAO-B1. P, pGL3-promoter, P + 10, pGL3-promoter with silencer (−1978 to −2230) inserted upstream of the SV40 promoter; C, pGL3-control; C + 10, pGL3-control with the silencer domain inserted upstream of the SV40 promoter, B1, pAO-B1; B1 + 10, pAO-B1 with the silencer domain inserted upstream of −167; E1, pAO-E1; E1 + 10, pAO-E1 with the silencer domain inserted upstream of −167. (**Bottom**) Recombinant plasmids in either pGL3 or pAO-B1 or pASO-E1 parents were transfected into HC-11 cells along with pCMV-β-galactosidase. Luciferase activity was quantitated and normalized to β-galactosidase and protein concentration 48 h later.

pressive than the domain B mutation. This may result from the differences in the mutations used or may indicate a potential for more complex protein interactions *in vivo*. In each case, mutations were designed to convert the core Sp1 G:C box into an A:T box consistent with disruption of Sp1 binding (Discher *et al.*, 1998; Hata *et al.*, 1998). The mutations used *in vitro* converted each domain into pure A:T sequences, whereas the *Nde*1 mutations used *in vivo* carry a C and a G residue in the first and sixth positions. Nonetheless, we conclude that Sp1/Sp3 are the critical transcription factors mediating activation of the *hAOX* proximal promoter.

The Sp1 and Sp3 factors are well known to function jointly in the expression of many genes and in many different cell systems (Rajakumar *et al.*, 1998; Discher *et al.*, 1998; Hata *et al.*, 1998; Kida *et al.*, 1999). Thus, Sp1 is frequently found to activate gene expression, whereas Sp3 can function in either activation or repression (Majello *et al.*, 1997; Kennett *et al.*, 1997). Hence, the relative levels of Sp1 and Sp3 can determine

the outcome of their joint participation in the expression of some genes (Apt *et al.*, 1996). On the other hand, the activation function of Sp3 could create a situation with Sp1 in which both proteins served as activators (Noti, 1997; Ihn and Trojanowska, 1997). Complex combinatorial interactions between Sp1/Sp3 and TTF-1 or between Sp1/Sp3 and NF-1 or MZF-1 were found to be necessary for cell-type-specific activation of various genes (Toonen *et al.*, 1996; Bohinski *et al.*, 1994; Kida *et al.*, 1999). Whether related mechanisms operate in the *hAOX* promoter is at present unknown; however, the complex architecture of the *hAOX* upstream DNA suggests the possibility of novel interactions with Sp1/Sp3 in the proximal promoter.

The observation that the domain from −1978 to −2230 contains a silencer element may offer important insight into the mechanism of *AOX* expression and regulation. Although silencer elements regulate the expression of many different genes, a common function appears to be in the control of cell- or tissue-type-specific expression. Epithelial silencer function has been described for platelet-derived growth factor (Liu *et al.*, 1996), transferrin (Sawaya *et al.*, 1996), lipooxygenase (O'Prey and Harrison, 1995), and fibroblast growth factor (Gelfman *et al.*, 1998). It has been proposed that silencer elements stabilize interactions between upstream sequences and activator sites within a proximal promoter (Liu *et al.*, 1996). Cell-type-specific activation of the silencer element, perhaps through specific protein binding or effects on native chromatin structure, could thereby control activation from the proximal promoter. Several nuclear proteins have been reported to activate silencer elements, including Sp1 (Shou *et al.*, 1998), YY1 (Ye *et al.*, 1996), and Oct-1 (Kim *et al.*, 1996). However, the highly A:T-rich nature of the *hAOX* silencer element does not convincingly predict binding by any of these factors, and further localization of the *hAOX* silencer element should clarify potential protein binding sites.

Our goals in the present analysis were to characterize features in the *hAOX* upstream DNA that could confer regulation of expression and to identify transcription factors that mediate activation. This information should allow us to identify regulatory mechanisms not previously recognized. Hence, the observation that Sp1/Sp3 are essential for activation in the proximal promoter is important, because these proteins can be activated by growth factors (Kim *et al.*, 1996; Chen *et al.*, 1998; Li *et al.*, 1995; Greenwel *et al.*, 1997) and by cytokines interleukin-1 and IL-6 (Ray *et al.*, 1999), and they mediate combinatorial interaction with other cell-specific factors (Braun and Suske, 1998). Furthermore, the potential for interaction between the proximal promoter in *hAOX* and an upstream silencer element suggests complex regulatory mechanisms of expression.

ACKNOWLEDGMENTS

The authors are grateful to Dr. Jeffrey Whittset (Cincinnati, OH) for MLE-15 cells and advice on their cultivation and to Dr. Margaret Neville (Denver, CO) for the HC-11 cells and advice on their cultivation.

These studies were supported in part by grants from the National Institutes of Health (HL52509 and HL45582), the Muscular Dystrophy Association, and the Robert and Helen Kleberg Foundation.

REFERENCES

APT, D., WATTS, R.M., SUSKE, G., and BERNARD, H.U. (1996). High Sp1/Sp3 ratios in epithelial cells during epithelial differentiation and cellular transformation correlate with the activation of the HPV-16 promoter. Virology **224,** 281–291.

BEEDHAM, C., CRITCHLEY, D.J., and RANCE, D.J. (1995). Substrate specificity of human liver aldehyde oxidase toward substituted quinazolines and phthalazines: A comparison with hepatic enzyme from guinea pig, rabbit, and baboon. Arch. Biochem. Biophys. **319,** 481–490.

BENDOTTI, C., PROSPERINI, E., KUROSAKI, M., GARATTINI, E., and TERAO, M. (1997). Selective localization of mouse aldehyde oxidase mRNA in the choroid plexus and motor neurons. Neuroreport **8,** 2343–2349.

BERGER, R., MEZEY, E., CLANCY, K.P., HARTA, G., WRIGHT, R.M., REPINE, J.E., BROWN, M., BROWN-STEIN, M., and PATTERSON, D. (1995). Analysis of aldehyde oxidase and xanthine dehydrogenase/oxidase as possible candidate genes for autosomal recessive familial amyotrophic lateral sclerosis. Somat. Cell Mol. Genet. **21,** 121–131.

BOHINSKI, R.J., DILAURO, R., and WHITSETT, J.A. (1994). The lung specific surfactant protein B gene promoter is a target for thyroid transcription factor 1 and hepatocyte nuclear factor 3, indicating common factors for organ specific gene expression along the foregut axis. Mol. Cell. Biol. **14,** 5671–5681.

BONDY, S.C., and OROZCO, J. (1994). Effects of ethanol treatment upon sources of reactive oxygen species in brain and liver. Alcohol Alcoholism **29,** 375–383.

BRAUN, H., and SUSKE, G. (1998). Combinatorial action of HNF3 and Sp family transcription factors in the activation of the rabbit uteroglobin/CC10 promoter. J. Biol. Chem. **273,** 9821–9828.

BRUNO, M.D., BOHINSKI, R.J., HUELSMAN, K.M., WHITSETT, J.A., and KORFHAGEN, T.R. (1995). Lung cell specific expression of the murine surfactant protein A (SP-A) gene is mediated by interactions between the SP-A promoter and thyroid transcription factor-1. J. Biol. Chem. **270,** 6531–6536.

CALZI, M.L., RAVIOLO, C., GHIBAUDI, E., GIOIA, L.D., SALMONA, M., CAZZANIGA, G., KUROSAKI, M., TERAO, M., and GARATTINI, E. (1995). Purification, cDNA cloning, and tissue distribution of bovine liver aldehyde oxidase. J. Biol. Chem. **270,** 31037–31045.

CHEN, S.J., ARLETT, C.M., JIMENEZ, S.A., and VARGA, J. (1998). Modulation of human alpha (I) procollagen gene activity by interaction with Sp1 and Sp3 transcription factors in vitro. Gene **215,** 101–110.

CLARKE, S.E., HARRELL, A.W., and CHENERY, R.J. (1995). Role of aldehyde oxidase in the *in vitro* conversion of famciclovir to penciclovir in human liver. Drug Metabol. Dispos. Biol. Fate Chem. **23,** 251–254.

DIGNAM, J.D., LEBOVITZ, R.M., and ROEDER, R.G. (1983). Accurate transcription initiation by RNA polymerase II in a soluble extract from isolated mammalian nuclei. Nucleic Acids Res. **11,** 1475–1489.

DISCHER, D.J., BISHOPRIC, N.H., WU, X., PETERSON, C.A., and WEBSTER, K.A. (1998). Hypoxia regulates β-enolase and pyruvate kinase M promoters by modulating Sp1/Sp3 binding to a conserved GC element. J. Biol. Chem. **273,** 26087–26093.

FABRE, G., SEITHER, R., and GOLDMAN, I.D. (1986). Hydroxylation of 4-amino antifolates by partially purified aldehyde oxidase from rabbit liver. Biochem. Pharmacol. **35,** 1325–1330.

GELFMAN, C.M., KELLEHER, C.M., and HJELMELAND, L.M. (1998). Differentiation of retinal pigment epithelial cells in vitro uncovers silencer activity in the FGF-5 gene promoter. Exp. Eye Res. **67,** 151–162.

GREENWEL, P., INAGAKI, Y., HU, W., WALSH, M., and

RAMIREZ, F. (1997). Sp1 is required for the early response of α2(I) collagen to transforming growth factor B1. J. Biol. Chem. **272,** 19738–19745.

HATA, Y., DUH, E., ZHANG, K., ROBINSON, G.S., and AIELLO, L.P. (1998). Transcription factors Sp1 and Sp3 alter vascular endothelial growth factor expression through a novel recognition sequence. J. Biol. Chem. **273,** 19294–19303.

HILLE, R., and MASSEY, V. (1985). Molybdenum containing hydroxylases: Xanthine oxidase, aldehyde oxidase, and sulfite oxidase. In *Molybdenum Enzymes*. T.G. Spiro, ed. (Wiley-Interscience Pub., New York NY) pp. 443–518.

HOLMES, R.S. (1979). Genetics, ontogeny, and testosterone inducibility of aldehyde oxidase isozymes in the mouse: Evidence for two genetic loci (AOX-1 and AOX-2) closely linked on chromosome 1. Biochem. Genet. **17,** 517–527.

HOLZINGER, A., DINGLE, S., BEJARANO, P.A., MILLER, M.A., WEAVER, T.E., DILAURO, R., and WHITSETT, J.A. (1996). Monoclonal antibody to thyroid transcription factor-1: Production, characterization, and usefulness in tumor diagnosis. Hybridoma **15,** 49–53.

HUANG, D.Y., FURUKAWA, A., and ICHIKAWA, Y. (1999). Molecular cloning of retinal oxidase/aldehyde oxidase cDNAs from rabbit and mouse livers and functional expression of recombinant mouse retinal oxidase in E. coli. Arch. Biochem. Biophys. **364,** 264–272.

HYNES, N.E., TAVERNA, D., HARWERTH, I.M., CIARDIELLO, F., SALOMON, D.S., YAMAMOTO, T., and GRONER, B. (1990). Epidermal growth factor receptor, but not c-erbB-2, activation prevents lactogenic hormone induction of the beta-casein gene in mouse mammary epithelial cells. Mol. Cell. Biol. **10,** 4027–4034.

IHN, H., and TROJANOWSKA, M. (1997). Sp3 is a transcriptional activator of the human alpha 2(I) collagen gene. Nucleic Acids Res. **25,** 3712–3717.

IKEDA, K., SHAW-WHITE, J.R., WERT, S.E., and WHITSETT, J.A. (1996). Hepatocyte nuclear factor 3 activates transcription of thyroid transcription factor 1 in respiratory epithelial cells. Mol. Cell. Biol. **16,** 3626–3636.

JAVAHERY, R., KHACHI, A., LO, K., ZENZIE-GREGORY, B., and SMALE, S.T. (1994). DNA sequence requirements for transcriptional initiator activity in mammalian cells. Mol. Cell. Biol. **14,** 116–127.

KENNETT, S.B., UDVADIA, A.J., and HOROWITZ, J.M. (1997). Sp3 encodes multiple proteins that differ in their capacity to stimulate or repress transcription. Nucleic Acids Res. **25,** 3110–3117.

KIDA, M., SOURI, M., YAMAMOTO, M., SAITO, H., and ICHINOSE, A. (1999). Transcriptional regulation of cell type specific expression of the TATA-less A subunit gene for human coagulation factor XIII. J. Biol. Chem. **274,** 6138–6147.

KIM, M.K., LESOON-WOOD, L.A., WEINTRAUB, B.D., and CHUNG, J.H. (1996). A soluble transcription factor, Oct-1, is also found in the insoluble nuclear matrix and possesses silencing activity in its alanine rich domain. Mol. Cell. Biol. **16,** 4366–4377.

KISKER, C., SCHINDELIN, H., and REES, D.C. (1997). Molybdenum cofactor containing enzymes: Structure and mechanism. Annu. Rev. Biochem. **66,** 233–267.

KRENITSKY, T.A., NEIL, S.M., ELION, G.B., and HITCHINGS, G.H. (1972). A comparison of the specificities of xanthine and aldehyde oxidase. Arch. Biochem. Biophys. **150,** 585–599.

KUNIEDA, T., KOBAYASHI, E., TACHIBANA, M., and IKADAI, H. (1999). A genetic linkage map of rat chromosome 9 with a new locus for variant activity of liver aldehyde oxidase. Exp. Animals **48,** 43–45.

LI, J.M., NICHOLS, M.A., CHANDRASEKHARAN, S., XIONG, Y., and WANG, X.F. (1995). Transforming growth factor beta activates the promoter of cyclin dependent kinase inhibitor p151NK4B through an Sp1 consensus site. J. Biol. Chem. **270,** 26750–26753.

LIU, B., MAUL, R.S., and KAETZEL, D.M. (1996). Repression of platelet derived growth factor A chain gene transcription by an upstream silencer element: Participation by sequence specific single stranded DNA binding proteins. J. Biol. Chem. **271,** 26281–26290.

MAJELLO, B., DELUCA, P., and LANIA, L. (1997). Sp3 is a bifunctional transcription regulator with modular independent activation and repression domains. J. Biol. Chem. **272,** 4021–4026.

MEIER, V.S., and GRONER, B. (1994). The nuclear factor YY1 participates in repression of the beta casein gene promoter in mammary epithelial cells and is counteracted by mammary gland factor during lactogenic hormone induction. Mol. Cell. Biol. **14,** 128–137.

MIRA, L., MAIA, L., BARREIRA, L., and MANSO, C.F. (1995). Evidence for ROS generation due to NADH oxidation by aldehyde oxidase during ethanol metabolism. Arch. Biochem. Biophys. **318,** 53–58.

MORIWAKI, Y., YAMAMOTO, T., YAMAGUCHI, K., TAKAHASHI, S., and HIGASHINO, K. (1996). Immunohistochemical localization of aldehyde and xanthine oxidase in rat tissues using polyclonal antibodies. Cell. Biol. **105,** 71–79.

NAKAYAMA, H., FUJIHARA, S., NAKASHIMA, T., and KUROGOCHI, Y. (1987). Formation of two major nicotine metabolites in livers of guinea pigs. Biochem. Pharmacol. **36,** 4313–4317.

NOTI, J.D. (1997). Sp3 mediates transcriptional activation of the leukocyte integrin genes CD11C and CD11B and cooperates with c-Jun to activate CD11C. J. Biol. Chem. **272,** 24038–24045.

O'PREY, J., and HARRISON, P.R. (1995). Tissue specific regulation of the rabbit 15 lipoxygenase gene in erythroid cells by a transcriptional silencer. Nucleic Acids Res. **23,** 3664–3672.

PHILIP, J.A.C., BURDON, T.G., and WATSON, C.J. (1996). Differential activation of STATs 3 and 5 during mammary gland development. FEBS Lett. **396,** 77–80.

RAJAKUMAR, R.A., THAMOTHARAN, S., MENON, R.K., and DEVASKAR, S.U. (1998). Sp1 and Sp3 regulate transcriptional activity of the facilitative glucose transporter isoform 3 gene in mammalian neuroblasts and trophoblasts. J. Biol. Chem. **273,** 27474–27483.

RAMIREZ, M.I., RISHI, A.K., CAO, Y.X., and WILLIAMS, M.C. (1997). TGT3, thyroid transcription factor I, and Sp1 elements regulate transcriptional activity of the 1.3 kilobase pair promoter of T1a, a lung alveolar type I cell gene. J. Biol. Chem. **272,** 26285–26294.

RASHIDI, M.R., SMITH, J.A., CLARKE, S.E., and BEEDHAM, C. (1997). In vitro oxidation of famciclovir and 6-deoxypenciclovir by aldehyde oxidase from human, guinea pig, rabbit, and rat liver. Drug Metabol. Dispos. Biol. Fate Chem. **25,** 805–813.

RAY, A., SCHATTEN, H., and RAY, B.K. (1999). Activation of Sp1 and its functional cooperation with serum amyloid A activating sequence binding factor in synoviocyte cells trigger synergistic action on interleukin 1 and interleukin 6 in serum amyloid gene expression. J. Biol. Chem. **274,** 4300–4308.

RUENITZ, P.C., and BAI, X. (1995). Acidic metabolites of tamoxifen: Aspects of formation and fate in the female rat. Drug Metabol. Dispos. Biol. Fate Chem. **23,** 993–998.

SAWAYA, B.E., AUNIS, D., and SCHAEFFER, E. (1996). Distinct positive and negative regulatory elements control neuronal and hepatic transcription of the human transferrin gene. J. Neurosci. Res. **43,** 261–272.

SHAW, S., and JAYATILLEKE, E. (1990). The role of aldehyde oxidase in ethanol induced hepatic lipid peroxidation in the rat. Biochem. J. **268,** 579–583.

SHAW, S., and JAYATILLEKE, E. (1992a). The role of cellular oxidases and catalytic iron in the pathogenesis of ethanol induced liver injury. Life Sci. **50,** 2045–2052.

SHAW, S., and JAYATILLEKE, E. (1992b). Cimetidine as a scavenger of ethanol induced free radicals. Alcohol **9,** 363–367.

SHAW, S., ENG, J., and JAYATILLEKE, E. (1985). Ethanol induced free radical injury to the hepatocyte glucagon receptor. Alcohol **12,** 273–277.

SHOU, Y., BARON, S., and PONCZ, M. (1998). An Sp1 binding silencer element is a critical negative regulator of the megakarocyte specific alpha IIb gene. J. Biol. Chem. **273,** 5716–5726.

SUGIHARA, K., KITAMURA, S., and TATSUMI, K. (1996). Involvement of mammalian liver cytosols and aldehyde oxidase in reductive metabolism of zonisamide. Drug Metabol. Dispos. Biol. Fate Chem. **24,** 199–202.

TAYLOR, S.M., STUBLEY-BEEDHAM, C., and STELL, J.G.P. (1984). Simultaneous formation of 2- and 4-quinolones from quiniolinium cations catalysed by aldehyde oxidase. Biochem. J. **220,** 67–74.

TERAO, M., KUROSAKI, M., DEMONTIS, S., ZANOTTA, S., and GARATTINI, E. (1998). Isolation and characterization of the human aldehyde oxidase gene: Conservation of intron/exon boundaries with the xanthine oxidoreductase gene indicates a common origin. Biochem. J. **332,** 383–393.

TOONEN, R.F.G., GOWAN, S., and BINGLE, C.D. (1996). The lung enriched transcription factor TTF-1 and the ubiquitously expressed proteins Sp1 and Sp3 interact with elements located in the minimal promoter of the rat clara cell secretory protein gene. Biochem. J. **316,** 467–473.

WAKAO, H., GOUILLEUX, F., and GRONER, B. (1994). Mammary gland factor (MGF) is a novel member of the cytokine regulated transcription factor gene family and confers the prolactin response. EMBO J. **13,** 2182–2191.

WIKENHEISER, K.A., VORBROKER, D.K., RICE, W.R., CLARK, J.C., BACHURSKI, C.J., OIE, H.K., and WHITSETT, J.A. (1993). Production of immortalized distal respiratory epithelial cell lines from surfactant protein C simian virus 40 large tumor antigen transgenic mice. Proc. Natl. Acad. Sci. USA **90,** 11029–11033.

WOOTON, J.C., NICOLSON, R.E., COCK, J.M., WALTERS, D.E., BURKE, J.F., DOYLE, W.A., and BRAY, R.C. (1991). Enzymes depending on the pterin molybdenum cofactor: Sequence families, spectroscopic properties of molybdenum and possible cofactor binding domains. Biochim. Biophys. Acta **1057,** 157–185.

WRIGHT, R.M., WEIGEL, L.K., and REPINE, J.E. (1995a). Aldehyde oxidase generates deoxyribonucleic acid single strand nicks in vitro. Redox Report **1,** 349–355.

WRIGHT, R.M., VAITAITIS, G.M., WEIGEL, L.K., REPINE, T.B., MCMANAMAN, J.L., and REPINE, J.E. (1995b). Identification of the candidate ALS2 gene at chromosome 2q33 as a human aldehyde oxidase gene. Redox Report **1,** 313–321.

WRIGHT, R.M., WEIGEL, L.K., VARELLA-GARCIA, M., VAITAITIS, G.M., and REPINE, J.E. (1997). Molecular cloning, refined chromosomal mapping and structural analysis of the human gene encoding aldehyde oxidase (hAOX1), a candidate for the ALS2 gene. Redox Report **3,** 135–144.

WRIGHT, R.M., CLAYTON, D.A., RILEY, M.G., MCMANAMAN, J.L., and REPINE, J.E. (1999). cDNA cloning, sequencing, and characterization of male and female rat liver aldehyde oxidase (rAOX1): Differences in redox status may distinguish male and female forms of hepatic AOX. J. Biol. Chem. **274,** 3878–3886.

YE, J., CIPPITELLI, M., DORMAN, L., ORTALDO, J.R., and YOUNG, H.A. (1996). The nuclear factor YY1 suppresses the human gamma interferon promoter through two mechanisms: Inhibition of AP1 binding and activation of a silencer element. Mol. Cell. Biol. **16,** 4744–4753.

Address reprint requests to:
Dr. Richard M. Wright
The Webb-Waring Institute and Department of Medicine
University of Colorado Health Science Center
4200 E. 9th Ave.
Denver, CO 80262

E-mail: richard.m.wright@uchse.edu

Received for publication October 1, 1999; received in revised form May 11, 2000; accepted May 16, 2000.